N E T C

NEW ENGLAND TRANSPORTATION CONSORTIUM

TIRE CHIPS AS LIGHTWEIGHT BACKFILL FOR RETAINING WALLS - PHASE II

Jeffrey J. Tweedie, Dana N. Humphrey and Thomas C. Sandford

Prepared for
The New England Transportation Consortium

March 11, 1998

NETCR-8

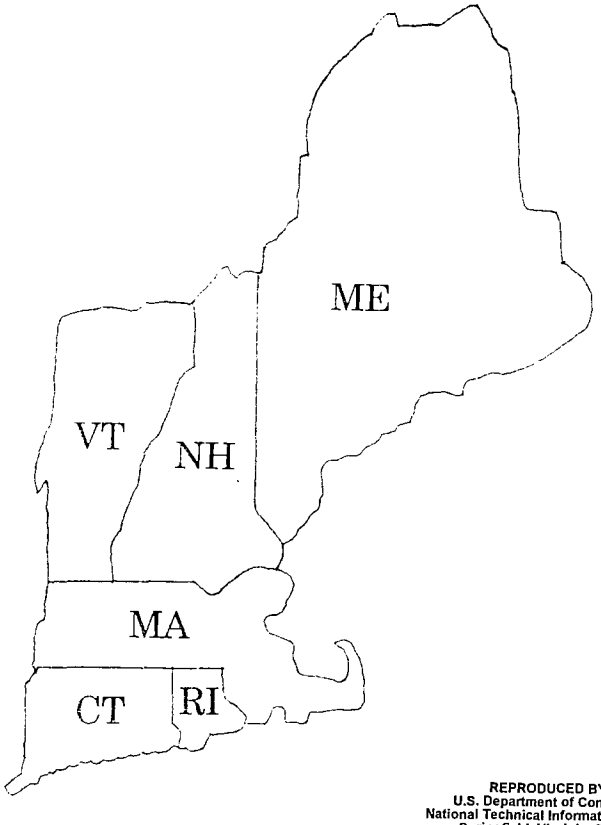

TRANSPORTATION INNOVATIONS AND IMPROVEMENTS FOR THE FUTURE

TIRE CHIPS AS LIGHTWEIGHT BACKFILL FOR RETAINING WALLS - PHASE II

Jeffrey J. Tweedie, Dana N. Humphrey and Thomas C. Sandford

Prepared for
The New England Transportation Consortium

March 11, 1998

NETCR-8

Prepared by:
Department of Civil and Environmental Engineering
University of Maine
Orono, Maine

This report was sponsored by the New England Transportation Consortium, a cooperative effort of the Departments of Transportation and the Land Grant Universities of the six New England States, and the US Department of Transportation's Federal Highway Administration

(BLANK)

Technical Report Documentation Page

1. Report No.	2. Government Accession No.	3. Recipient's Catalog No.
NETCR-8	N/A	N/A

4. Title and Subtitle	5. Report Date
Tire Chips as Lightweight Backfill for Retaining Walls - Phase II	March 11, 1998
	6. Performing Organization Code: N/A

7. Author(s)	8. Performing Organization Report No.
Jeffrey J. Tweedie, Dana N. Humphrey and Thomas C. Sandford	N/A

9. Performing Organization Name and Address	10 Work Unit No. (TRAIS)
Dept. of Civil and Environmental Engineering University of Maine 5711 Boardman Hall Orono, ME 04469-5711	N/A
	11. Contract or Grant No.: N/A
	13. Type of Report and Period Covered: N/A

12. Sponsoring Agency Name and Address	14. Sponsoring Agency Code
New England Transportation Consortium 179 Middle Turnpike University of Connecticut, U-202 Storrs, CT 06269-5202	N/A

15 Supplementary Notes

16. Abstract

Waste tires cut into 25 to 305-mm (1 to 12-in.) pieces yield a material that is coarse grained, free draining, and has a low unit weight, thus offering significant advantages for use as retaining wall backfill. This project is a continuation of Phase I, in which the engineering properties of tire shreds were determined. The purpose of this project was to determine design criteria for using tire shreds as retaining wall backfill. This was done by testing a granular control fill and tire shreds from three suppliers in a full scale retaining wall test facility. Tests were performed for at-rest and active conditions. For the at-rest condition, the horizontal earth pressure, interface shear, and compressibility were measured, at surcharges up to 35.9 kPa (750 psf). As much as 7% strain occurred during surcharge application with an additional 3% occurring due to time-dependent settlement. The majority of time-dependent settlement was completed in 50 days. For the active condition, the horizontal earth pressure and deformation within the backfill were measured; tests were performed at the 35.9 kPa (750 psf) surcharge. The horizontal earth pressure for tire shreds was 35% to 45% less than expected from conventional granular fill. The coefficients of lateral earth pressure (K_o, K_a) were found. K_o for tire shreds decreased with depth and fell within a small range. At the maximum surcharge and a depth of 2 m (6.5 ft), K_o ranged from 0.32 to 0.33. K_a for tire shreds was constant with depth and fell within a small range. At 0.01H of outward wall movement, K_a ranged from 0.22 to 0.25. The interface shear strength between tire shreds and a concrete faced wall ranged from 30° to 32°.

17. Key Words	18. Distribution Statement
tires, tire chips, tire shreds, waste tires, fill material, backfill, retaining walls, earth pressure	

19. Security Classif. (of this report)	20. Security Classif. (of this page)	21. No. of Pages	22. Price
N/A	N/A	314	N/A

(BLANK)

ACKNOWLEDGMENTS

The authors wish to gratefully acknowledge the members of the New England Transportation Consortium research advisory panel. Although the members of the committee have changed since the onset of this study, their contributions and patience throughout the duration of this research project were invaluable.

Thanks goes to the students who helped on all phases the project. They are, in no particular order: Brian Lawrence, Wayne Thompson, Michele Skoorka, Bob Hamilton, Mike McAdams, Joe Howe, Josh Saucier, Sean Dearmont, Mike Diamantopoulos, Rob Grover, Scott Blouin, Tricia Cosgrove, and Paul Kimball. Thanks also goes to Owen J. Folsom Construction and Cianbro Co. for donating materials for the test facility.

Will Manion, Laboratory Coordinator, University of Maine Department of Civil and Environment Engineering, deserves considerable thanks. His help during construction of the test facility was invaluable and he was always available when his skills were needed.

(BLANK)

TABLE OF CONTENTS

LIST OF TABLES

LIST OF FIGURES

LIST OF SYMBOLS

B_0 = initial barometric pressure

B_1 = current barometric pressure

c = cohesion intercept

C = semiempirical value used in Terzaghi, et al. (1996) design procedure

C_a = apparent cohesion

C_f = cohesion intercept in units of force

CF_{lc} = load cell calibration factor

CF_{ps} = pressure cell calibration factor

d = depth of fill

d_h = horizontal distance between bottom hinge and wall face

d_v = vertical distance between bottom and top hinges

d_{wb} = deflection within backfill

D = constrained modules

$D_{0°}$ = dial reading with inclinometer oriented 0°

$D_{180°}$ = dial reading with inclinometer oriented 180°

E = Young's modulus

E_{f_plate} = elevation of settlement plate when facility is full

E_{i_plate} = initial elevation of settlement plate

F = friction force

F_{bottom} = sum of forces measured by the bottom horizontal load cells

F_{lc} = force measured from load cell

F_{result} = resultant force exerted on wall

F_{top} = sum of forces measured by the top horizontal load cells

$F_{vertical}$ = sum of forces measured by vertical load cells

H = height of instrumented wall

H_f = horizontal force

k = inclinometer calibration factor

k_h = semiempirical value used in Terzaghi, et al. (1996) design procedure

K_a = coefficient of active earth pressure

K_o = coefficient of lateral earth pressure at rest

l_r = length of measured interval

L = force due to surcharge

LU = linear reading

LU_0 = initial linear reading

LU_1 = current linear reading

ms_i = initial microstrain reading

ms_n = subsequent microstrain readings

$o.s._{ave\_i}$ = average offset before rotation

$o.s._{ave\_n}$ = average offset after rotation

pq = modifier to horizontal stress when surcharge is applied, used in Terzaghi, et al. (1996) design procedure

P_A = active earth pressure

q = surcharge

T_0 = initial temperature

T_1 = current temperature

T_k = temperature correction factor

V_f = shear force

w = water content

w_{f_bolt} = water elevation measured from anchor bolt when facility is full

w_{f_plate} = water elevation measured from settlement plate when facility is full

w_{ip} = width of instrumented panel

w_{i_bolt} = initial water elevation measured from anchor bolt

w_{i_plate} = initial water elevation measured from settlement plate

W = weight of fill

x = location of resultant force

x_r = distance inclinometer torpedo was raised

x_{r-1} = previous distance inclinometer torpedo was raised

%comp = percent compaction

β = angle wall was rotated

δ = angle of wall friction

ΔDial = change in dial reading

ΔP = change in pressure

ε_v = vertical strain

ϕ = friction angle

ϕ' = effective friction angle

μ = Poisson's ratio

θ = orientation of active wedge with respect to horizontal

ρ_{d_field} = dry field density

ρ_{d_max} = maximum dry density

ρ_{field} = field density

ρ_{w_field} = wet field density

σ_{bottom} = bottom value of horizontal stress distribution

σ_{equiv} = equivalent horizontal stress distribution

σ_h = total horizontal stress

σ'_h = effective horizontal stress

$\sigma_{surcharge}$ = portion of horizontal stress distribution attributed to surcharge

$\sigma_{tire\ chips}$ = portion of horizontal stress distribution attributed to tire chips

σ_{top} = top value of horizontal stress distribution

σ_v = total vertical stress

σ'_v = effective vertical stress

τ = shear stress

(BLANK)

CHAPTER 1. INTRODUCTION

1.1 PROBLEM STATEMENT

In the United States 253 million waste tires are discarded every year, and an estimated 850 million scrap tires are stockpiled throughout the country (Associated Press, 1996). Of the scrap tires generated in 1995 an estimated 72% (approximately 183 million tires) were recovered for another use. Some 136 million of the recovered tires were used for tire derived fuel (TDF), 15 million were used in civil engineering applications, and 8 million were used for fabricated products. Other uses included: applications that use crumb rubber in manufactured products (6 million tires), agricultural applications (2.5 million), and miscellaneous applications (1.3 million). An additional 14 million tires were exported to other countries. Furthermore, if the number of retreaded tires is included in the total number of recovered tires, the percent recovered increased to 80% (Zimmer, 1996).

Of the millions of scrap tires scattered throughout the country, a large concentration is in the New England states. In a 1994 survey performed by the Scrap Tire Management Counsel, Maine had 24.21 to 48.43 tires per capita, the largest per capita concentration of tires in the United States, which corresponds to 30 to 60 million tires. Rhode Island had the next highest with 34 tires per person or 34 million tires. While Connecticut had 1.83 and Vermont had 1.73 tires per capita, which corresponds to 6 and 1 million tires,

respectively. The lowest concentration of tires per capita in New England was reported in Massachusetts, with 0.83 to 1.66 tires per person or 5 to 10 million tires. Data from New Hampshire was not reported (USA Today, 1996).

Although the recovery rate is high for tires (72%) the large number of tires still scattered over the countryside makes it apparent that additional uses for scrap tires are needed. Whole tires occupy a significant amount of space in already overcrowded landfills. Open scrap tire dumps are targets for arson set fires, which release harmful chemicals into the air and groundwater. Discarded tires are also an excellent breeding ground for mosquitoes, rats, and other disease-carrying pests. In addition, scrap tire piles are an eyesore on the landscape.

1.2 CIVIL ENGINEERING USES FOR WASTE TIRES

Civil engineering applications of scrap tires mostly use shredded tires or tire chips. Applications include: road subgrade material, retaining wall backfill, landfill leachate collection systems, landfill cell daily cover, and septic system leach fields. Other applications use whole tires for artificial reefs, breakwaters, and walls (Zimmer, 1996).

Tire chips are pieces of whole tires cut into 25-mm (1-in.) to 305-mm (12-in.) pieces. Construction uses for tire chips include: lightweight fill, insulation beneath roads, and lightweight backfill for retaining walls. Tire chips have a low unit weight (1/3 to 1/2 that of conventional fill), relatively high strength, and high permeability making their use as lightweight fill beneficial. Their use as fill material has been the topic of several studies

(Humphrey and Manion, 1992; Manion and Humphrey, 1992; Eldin and Senouce, 1992; Humphrey and Sandford, 1993; Gharegrat, 1993; Frascoia and Cauley, 1995; Nickels, 1995; Humphrey, 1996a; Humphrey and Nickels, 1997). The thermal properties of rubber make tire chips an attractive insulation material for use beneath roads. A previous study focused on a field trial where tire chips were used as subgrade insulation in Richmond, Maine (Humphrey and Eaton, 1993a, 1993b, 1994, 1995; Humphrey and Nickels, 1994). Chen (1996) and Humphrey, et al. (1997a) presented laboratory results on the thermal conductivity of tire chips. A study by Cosgrove (1995) examined the interface shear between tire chips and geomembrane for use as a drainage layer in landfill covers. The effects on water quality were investigated by Downs (1996) and Humphrey, et al. (1997b). The use of tire chips as retaining wall backfill has been investigated by (Humphrey, et al., 1992, 1993; Gharegrat, 1993; Cecich, et al., 1996).

In 1995, three tire chip fills with thicknesses greater than 7 m (23 ft) experienced an adverse internal heating reaction. The cause of the internal heating is thought to be a combination of chemical and microbial reactions. However, more than 70 thinner fills have been constructed successfully (Humphrey, 1996b). To prevent internal heating from occurring guidelines are now available for fills up to 3 m (10 ft) thick (Ad Hoc, 1997) and are included in Appendix A.

Use of tire chips as lightweight backfill for retaining walls has several potential benefits. They are inexpensive compared to other types of lightweight fill. In areas where the underlying soil is weak or compressible, tire chips, with their low unit weight,

would apply a smaller vertical stress than conventional backfill leading to lower settlement. The horizontal stress and shear stress on a retaining wall would be lower than with conventional backfill, resulting in a less expensive retaining wall design. The insulation qualities of tire chips would reduce frost penetration. Finally, their high permeability would provide good drainage.

The focus of this research is using tire chips as backfill in a full scale test facility. Monitoring of the tire chip behavior was required to fulfill the objectives, as discussed in the following section.

1.3 OBJECTIVE OF THE STUDY

This study is the continuation of a previous New England Transportation Consortium (NETC) study, titled: "Tire Chips As Lightweight Backfill For Retaining Walls-Phase I" (Humphrey, et al., 1992). This laboratory investigation determined the engineering properties of tire chips relative to their use as backfill for retaining walls.

The objective of this study is to determine design criteria for tire chips as lightweight backfill for retaining walls. This includes: horizontal earth pressure for at-rest and active conditions, the interface friction between tire chips and a concrete faced retaining wall, and settlement of the tire chip fill. This was to be done by measuring and monitoring the behavior of a granular control fill and tire chips from three different suppliers in a full scale retaining wall test facility. The facility could accommodate a 4.88-m (16-ft) thickness of backfill for at-rest and active conditions. Measurements for the at-rest

conditions were taken at four different surcharges, ranging from 0 to 35.9 kPa (750 psf). Measurements at the active state were taken at the maximum surcharge of 35.9 kPa (750 psf). Measured behavior was compared to what would have been predicted from Phase I of this study. A secondary objective of this project was to design and build a full scale retaining wall test facility, for this and future retaining wall research.

1.4 ORGANIZATION OF THE REPORT

This report contains ten chapters and two appendices, organized as follows. Chapter 2 includes a brief review of literature of previous studies pertaining to tire chips as backfill for retaining walls. The majority of this review focuses on Phase I of this study by Humphrey, et al. (1992).

The design of the full scale test retaining wall facility is discussed in Chapter 3. Chapter 4 discusses the test protocol, which includes the measurements that were taken and the methodology behind them.

Chapter 5 presents properties of the granular fill used as a control test and the tire chips. The properties determined for the granular control fill included: gradation, maximum dry density, field density, water content, and percent compaction. The properties determined for the three tire chip suppliers were gradation and field densities. Other tire chip properties had been determined previously by Humphrey, et al. (1992).

The measured horizontal earth pressures are discussed in Chapter 6. This includes the change in horizontal stress as the surcharge is increased for the at-rest condition,

horizontal stress for the active condition, and changes in horizontal stress over time for both the at-rest and active states. Design methods and considerations are also discussed.

Chapter 7 presents the interface shear between the backfill and the vertical face of the retaining wall. Settlement of the tire chip backfill is discussed in Chapter 8. This includes the vertical stress-vertical strain relationship and time-dependent settlement.

The horizontal movement within the backfill as the wall was rotated to achieve active conditions are presented in Chapter 9. Chapter 10 summarizes the results of this study and gives conclusions and recommendations for further research.

CHAPTER 2. LITERATURE REVIEW

2.1 INTRODUCTION

Extensive reviews of published literature pertaining to the use of tire chips in highway applications were performed by Humphrey, et al. (1992) and Nickels (1995). The review of literature presented herein will concentrate on the use of tire chips as retaining wall backfill. Most of this chapter will focus on Phase I of this study by Humphrey, et al. (1992). A review of shear strength literature is also included. In addition, the results from a study by Cecich, et al. (1996) will be summarized.

2.2 TIRE CHIPS AS LIGHTWEIGHT BACKFILL FOR RETAINING WALLS - PHASE I

Humphrey, et al. (1992) performed laboratory tests on tire chips from three suppliers. The properties investigated included: basic engineering properties, compressibility, shear strength, and permeability. The three suppliers were: Pine State Recycling, located in Nobleboro, Maine; Palmer Shredding in North Ferrisburg, Vermont; and F & B Enterprises in New Bedford, Massachusetts.

2.2.1 Basic Engineering Properties

The basic engineering properties that were determined included: gradation, specific gravity, compacted unit weight, loose unit weight, and absorption. Each of these properties will be discussed briefly in the following paragraphs.

The gradation tests performed by Humphrey, et al. (1992) showed that F & B Enterprises tire chips were the finest and Palmer Shredding was the coarsest, with Pine State Recycling falling in between. The gradation for the three suppliers is shown on Figure 2.1. In addition, the gradation for tire chips from Sawyer Environmental Recovery in Hampden, Maine, performed by Manion and Humphrey (1992), is included.

The specific gravity tests revealed that tire chips from F & B Enterprises had the lowest specific gravity, with those from Pine State Recycling and Palmer Shredding being slightly higher. Humphrey, et al. (1992) attributed this to the presence of steel belts in the tire chips supplied by Pine State Recycling and Palmer Shredding, while those from F & B Enterprises contained only glass belts. A summary of the specific gravities is shown in Table 2.1. The specific gravity for Sawyer Environmental Recovery tire chips, which contained steel belts, is also included.

Humphrey, et al. (1992) performed compaction tests on air dried samples of tire chips from the three suppliers, using a method similar to AASHTO T 180-86 except that the compaction energy was 60% of standard Proctor. A summary of the results along with those from Sawyer Environmental Recovery is included in Table 2.2. The loose unit weight was determined from samples poured into a compaction mold. These results are given on Table 2.3. Humphrey, et al. (1992) compared the compacted and loose unit weights and showed that compaction increases the unit weight by 25% to 86%.

The absorption for tire chips from the three suppliers and Sawyer Environmental Recovery was determined. The measured values ranged from 2.0% to 4.3%.

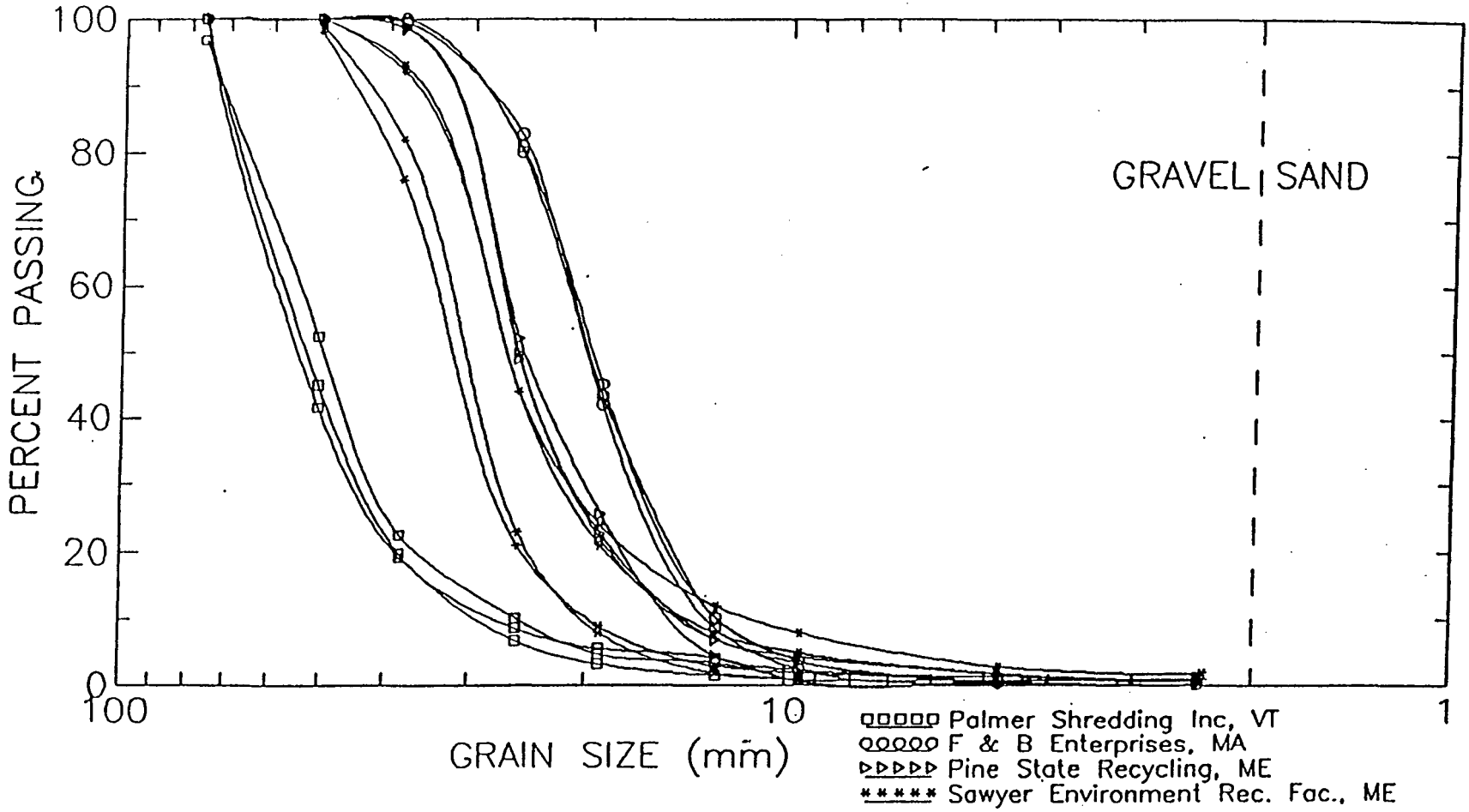

Figure 2.1 Gradation of tire chips from four suppliers (Humphrey, et al., 1992)

Table 2.1 Summary of apparent specific gravity (Humphrey, et al., 1992)

Supplier	Specific gravity
Pine State Recycling	1.24
Palmer Shredding	1.27
F & B Enterprises	1.14
Sawyer Environmental Recovery	1.23

Table 2.2 Summary of compacted unit weights (Humphrey, et al., 1992)

Supplier	Average unit weight (Mg/m^3)	Range of unit weights (Mg/m^3)
Pine State Recycling	0.64	0.62-0.66
Palmer Shredding	0.62	0.60-0.64
F & B Enterprises	0.62	0.61-0.62
Sawyer Environmental Recovery	0.63	0.61-0.63

Table 2.3 Summary of loose unit weights (Humphrey, et al., 1992)

Supplier	Number of samples	Average unit weight (Mg/m^3)	Range of unit weights (Mg/m^3)
Pine State Recycling	3	0.48	0.47-0.49
Palmer Shredding	3	0.34	0.33-0.37
F & B Enterprises	3	0.50	0.49-0.51
Sawyer Environmental Recovery	1	0.41	-----

2.2.2 Short Term Compressibility

Humphrey, et al. (1992) performed compression tests on tire chips from the three suppliers. The short term tests were used to determine compressibility parameters. The tests were performed in a specially constructed testing device, capable of measuring vertical and horizontal stress. The load was applied by a compression machine, at a constant rate of strain. The samples were subjected to three loading/unloading cycles. A typical plot of vertical stress versus vertical strain for Pine State Recycling is shown on Figure 2.2. Humphrey, et al. (1992) noted for the three tire chip suppliers that the initial portion of the loading curves was very steep, which indicates high compressibility. The loading curves then flattened out at higher stresses. The authors also reported that at the subsequent unloading and reloading cycles the slopes were relatively flat, having a slope that was similar to the initial loading curve at higher stresses.

The compressibility parameters determined by Humphrey, et al. (1992) included: the coefficient of lateral earth pressure at rest (K_o), Poisson's ratio (μ), the constrained modulus (D), and Young's modulus (E). These are summarized in Table 2.4, along with values for Sawyer Environmental Recovery.

2.2.3 Time-Dependent Settlement

Humphrey, et al. (1992) performed long term compression tests to examine time-dependent settlement. These tests were performed using the same device used for short term compressibility, as discussed in Section 2.2.2, however, the load was applied with dead weights. For the long term tests, a stress of 48 kPa (1000 psf) was applied for one

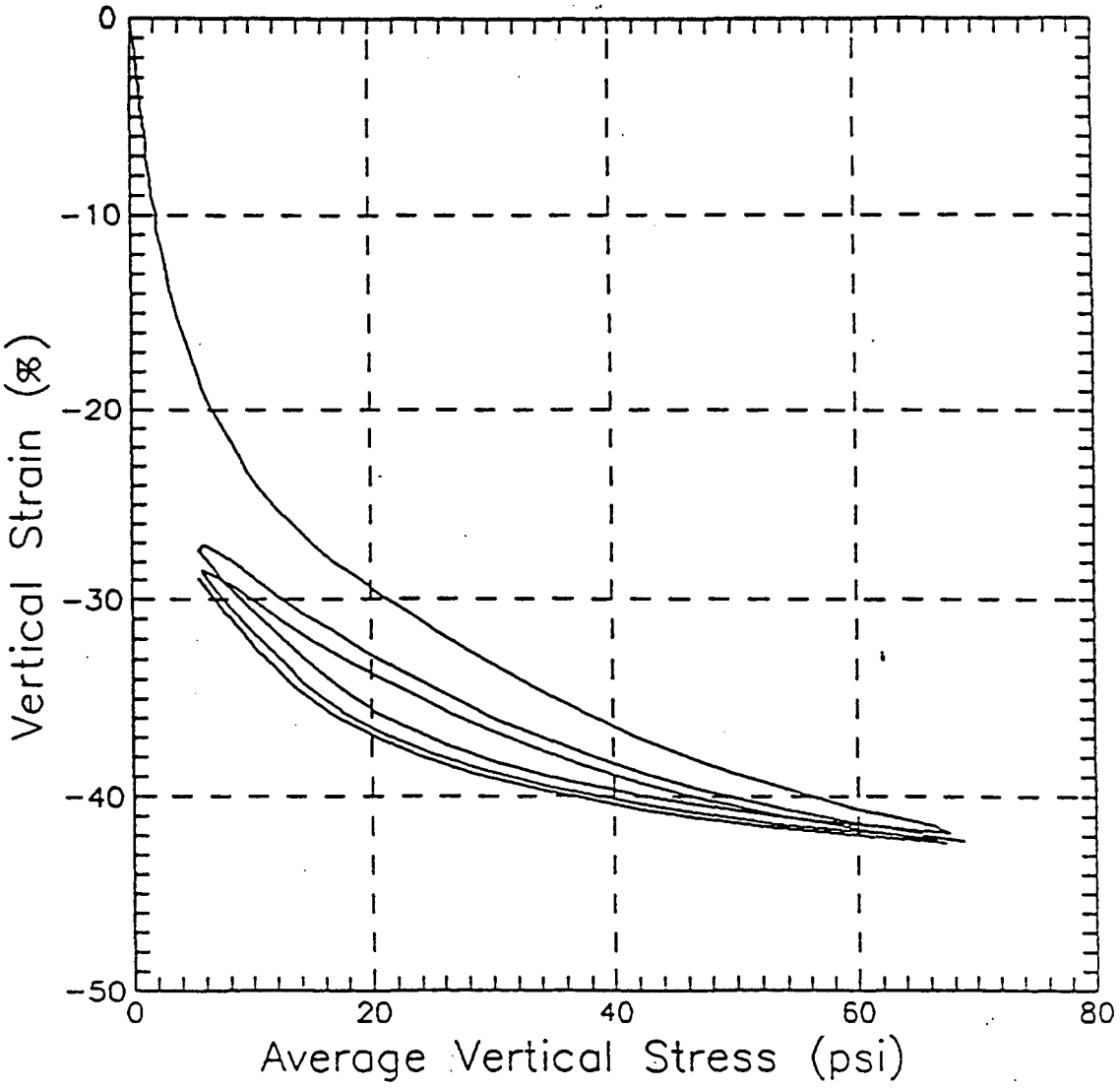

1 psi = 6.89 kPa

Figure 2.2 Typical plot of vertical stress vs. vertical strain for Pine State Recycling (Humphrey, et al., 1992)

Table 2.4 Summary of compressibility parameters (Humphrey, et al., 1992)

Supplier	Test No.	K_o	μ	D (MPa)	E (MPa)
Pine State Recycling*	1	0.55	0.35	1.34	0.83
	2	0.33	0.25	1.69	1.41
	3	0.34	0.25	1.39	1.16
	Average	0.41	0.28	1.48	1.14
Palmer Shredding*	1	0.29	0.22	0.79	0.70
	2	-----	-----	2.51	-----
	3	0.22	0.18	1.74	1.53
	Average	0.26	0.20	1.68	1.11
F & B Enterprises*	1	0.40	0.29	1.04	0.48
	2	0.55	0.36	1.24	0.74
	3	0.45	0.31	1.52	1.10
	Average	0.47	0.32	1.27	0.77
Sawyer Environmental**	301	0.33	0.25	1.81	1.51
	1001	0.65	0.39	2.02	1.01
	1002	0.40	0.29	1.53	1.17
	2001	0.45	0.31	1.57	1.13
	2002	0.35	0.26	1.72	1.41
	Average	0.44	0.30	1.73	1.25

*The values of K_o and μ for Pine State Recycling, Palmer Shredding, and F & B Enterprises were determined at a horizontal stress less than 0.70 MPa (100 psi)

** K_o and μ for Sawyer Environmental was determined at a vertical stress less than 0.17 MPa (25 psi)

month. Humphrey, et al. (1992) reported that these tests suggested that under a constant vertical stress, tire chips tend to continue to settle and the horizontal stress tends to increase with time. However, the authors thought that this could be a function of the testing apparatus and recommended further research.

2.2.4 Shear Strength

Humphrey, et al. (1992) performed direct shear tests using a large scale direct shear testing apparatus. To determine the size of the shear box to use in the testing device, the authors performed tests using Pine State Recycling tire chips with three different size shear boxes: 203-mm (8-in.), 254-mm (12-in.), and 305-mm (16-in.) square dimension. The authors determined, after subsequent tests, that the 203-mm (8-in.) box could not be used and that results from the 254-mm (12-in.) and 305-mm (16-in.) boxes were similar. As a result, subsequent tests with Palmer Shredding and F & B Enterprises were performed using the 254-mm (12-in.) box. Normal stresses ranged from 12.0 kPa (250 psf) to 71.8 kPa (1500 psf). A plot of shear stress versus normal stress for the three suppliers is shown on Figure 2.3. Each line is the average of the results of three trials. From the plots of normal stress versus shear stress Humphrey, et al. (1992) determined the friction angle (ϕ) and the cohesion intercept (c), as summarized on Table 2.5.

2.2.5 Permeability

Humphrey, et al. (1992) built a constant head permeameter capable of measuring high permeabilities. The permeameter was equipped to measure the flow and the hydraulic gradient. With this information and the dimensions of the device, it was possible to

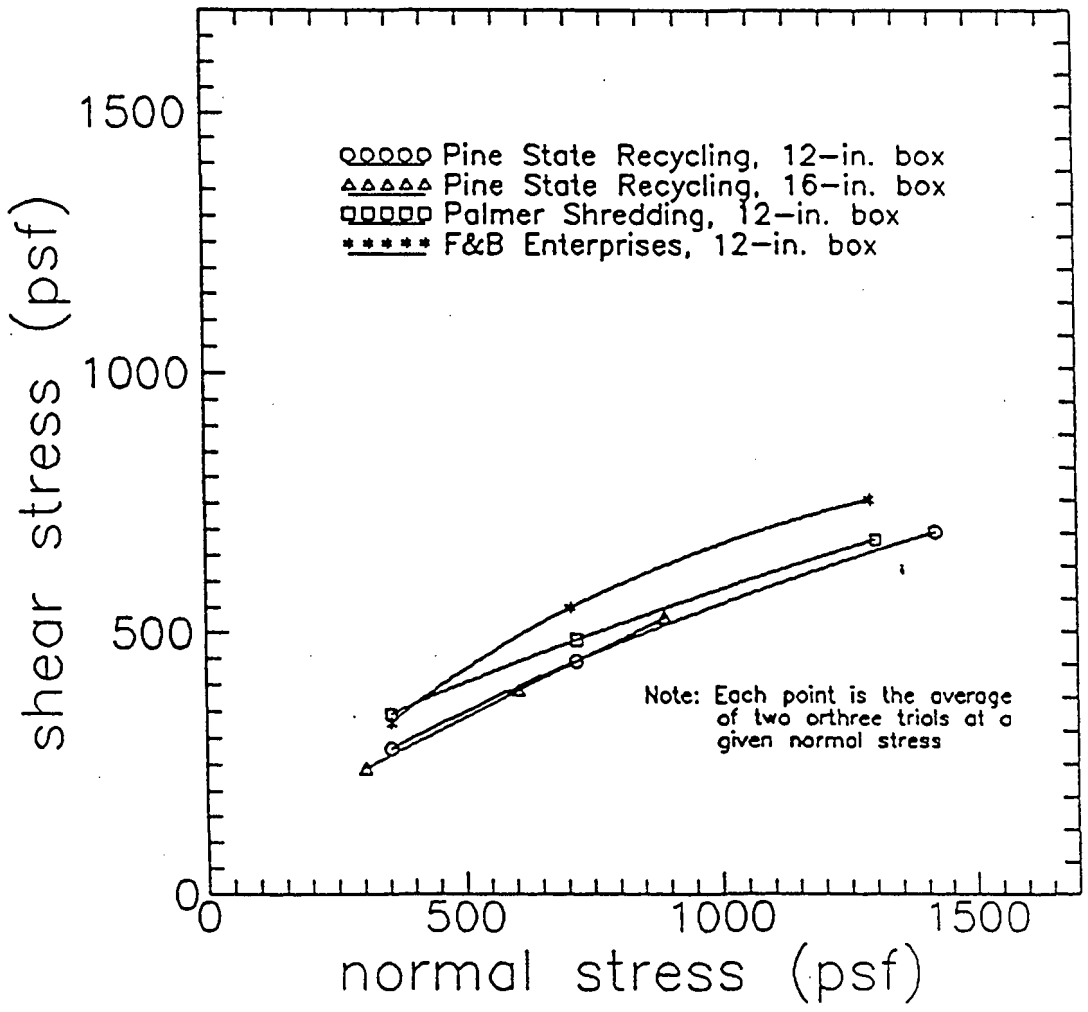

1 psf = 0.0479 kPa

Figure 2.3 Average shear stress vs. average normal stress at failure (Humphrey, et al., 1992)

Table 2.5 Values of ϕ and c from direct shear tests (Humphrey, et al., 1992)

Supplier	ϕ	c (kPa)
Pine State (254-mm box)	21°	7.7
Pine State (305-mm box)	26°	4.3
Palmer Shredding	19°	11.5
F & B Enterprises	25°	8.6

calculate the permeability. In addition, the tire chips could be compressed and the permeability as a function of void ratio could be examined. The permeabilities determined by Humphrey, et al. (1992) are shown on Table 2.6.

2.3 SHEAR STRENGTH

The shear strength of tire chips has been reported by numerous investigators. The shear strength of tire chips has been measured using triaxial tests by Bressette (1984), Ahmed (1993), and Benda (1995); and using direct shear tests by Humphrey, et al. (1992, 1993), Humphrey and Sandford (1993), and Cosgrove (1995). The failure envelopes for tests conducted at low stress levels, less than about 100 kPa (2090 psf) (Humphrey, et al., 1992; Cosgrove, 1995; Benda, 1995), are non-linear and concave down. Ahmed (1993) conducted tests at higher stress levels, greater than 75 kPa (1570 psf), on tire chips with maximum sizes of 13 and 25 mm (0.5 and 1.0 in.). The failure envelopes were approximately linear. Using a failure criteria of 15% axial strain, the cohesion intercepts ranged from 27.4 to 33.0 kPa (572 to 689 psf) with friction angles from 15.9 to 20.3

Table 2.6 Summary of permeability results (Humphrey, et al., 1992)
1 pcf = 0.016 Mg/m^3

Supplier	Compression (%)	Unit Weight (pcf)	Void Ratio	Permeability (cm/s)
Pine State Recycling	0.0	40.2	0.925	7.7
	8.3	43.9	0.761	6.0
	16.6	48.3	0.601	3.4
	22.4	52.0	0.488	2.1
Palmer Shredding	0.0	37.5	1.114	15.4
	8.3	41.0	0.935	12.7
	16.6	45.1	0.758	8.2
	24.9	50.1	0.583	4.8
F&B Enterprises	0.0	38.8	0.833	6.9
	8.3	42.5	0.676	5.0
	16.7	46.7	0.523	2.8
	22.9	50.4	0.414	1.5

degrees. Bressette (1984) tested two samples. One was termed "51-mm square" and it had a cohesion intercept of 26 kPa (543 psf) and a friction angle of 21 degrees. The other was termed "51-mm shredded" and it had a cohesion intercept of 36 kPa (752 psf) and a friction angle of 14 degrees.

2.4 USE OF TIRE CHIPS AS LIGHTWEIGHT BACKFILL FOR RETAINING STRUCTURES

Cecich, et al. (1996) performed a cost comparison of retaining walls using sand as backfill versus tire chips as backfill. This was done by designing hypothetical cantilever retaining walls for three different heights: 3.05 m (10 ft), 6.1 m (20 ft), and 9.14 m (30 ft), using both sand and tire chips as backfill. A cost estimate was then performed for each backfill and retaining wall design. The estimated cost of each wall using tire chips and sand was then compared. Throughout the authors' paper they referred to 12.5-mm (1/2-in.) minus pieces of tires as shredded tires. However, in this review they will be referred to as tire chips.

To perform the cost analysis the authors chose a proposed project site in the Chicago, Illinois area. They used the existing soil conditions as part of the design, that being silty clay which needed to be excavated and replaced with suitable backfill material. Each retaining wall was designed using the properties from the insitu silty clay, a fine to medium sand as backfill, and tire chips. The properties used in design for the insitu silty clay included: cohesion = 58.6 kPa (1224 psf), friction angle = 17°, and unit weight = 2.08 Mg/m^3 (130 pcf). Design properties for the fine to medium sand were as follows: cohesion = 0, friction angle = 38°, unit weight = 2 Mg/m^3 (125 pcf), and wall friction =

20°. The properties for tire chips were determined by the authors in the laboratory, they included: cohesion = 5.75 kPa (120 psf), friction angle = 22°, unit weight = 0.61 Mg/m^3 (38 pcf), and wall friction = 15° (two-thirds of friction angle). The backfill was sloped at 1:4 with no surcharge.

The retaining walls were designed using Coulomb's method to determine the active earth pressure. The passive earth pressure was calculated using the Rankine method. The design for the 3.05-m (10-ft) wall is shown on Figure 2.4. The designs for the 6.1-m (20-ft) and 9.14-m (30-ft) retaining walls are presented in Cecich, et al. (1994).

Cecich, et al. (1996) estimated the cost based on prevailing labor and accounted for other costs including clearing and grubbing, excavation and materials. The material suppliers were also assumed to be somewhat close to the project site. The authors used a cost of \$26.2/m^3 (\$20/yd^3) or \$13.2/tonne (\$12/ton) for sand and a cost of \$6.5/m^3 (\$5/yd^3) or \$11/tonne (\$10/ton^3) for tire chips. The cost of tire chips is lower than experienced in the New England states, where a typical price is \$33/m^3 (\$25/yd^3). Each of the estimates was based on a 30.5-m (100-ft) wall length.

Cecich, et al. (1996) compared the estimated material and total costs of retaining walls using sand and tire chips. They stated that the material costs could be reduced by 81% to 85%, while the total costs could be reduced by 52% to 67% by using tire chips. This is summarized on Table 2.7 and presented graphically on Figure 2.5. In addition, the authors noted that the cost savings would increase with wall height. Because the cost

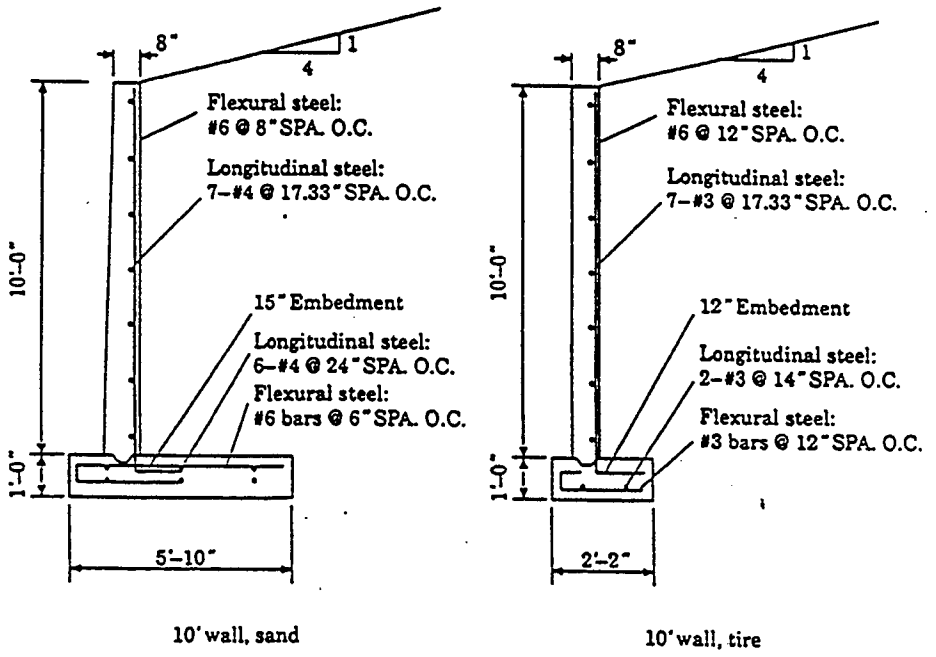

1 ft = 0.3048 m, 1 in. = 25.4 mm

Figure 2.4 Structural design of 3.05-m (10-ft) high retaining wall with sand and tire chips as backfill (Cecich, et al., 1996)

Table 2.7 Comparison of costs for retaining walls with sand vs. tire chip as backfill, 30.5-m (100-ft) long walls (Cecich, et al., 1996)
1 ft = 0.3048 m

Height of wall (ft)	Estimated material cost (U.S. $)			Estimated total cost (U.S. $)		
	Sand backfill	Shredded tire backfill	Savings from shredded tires (%)	Sand backfill	Shredded tire backfill	Savings from shredded tires (%)
10	8000	1300	84	17,900	8600	52
20	29,700	5600	81	53,900	19,700	63
30	82,500	12,400	85	145,800	48,300	67

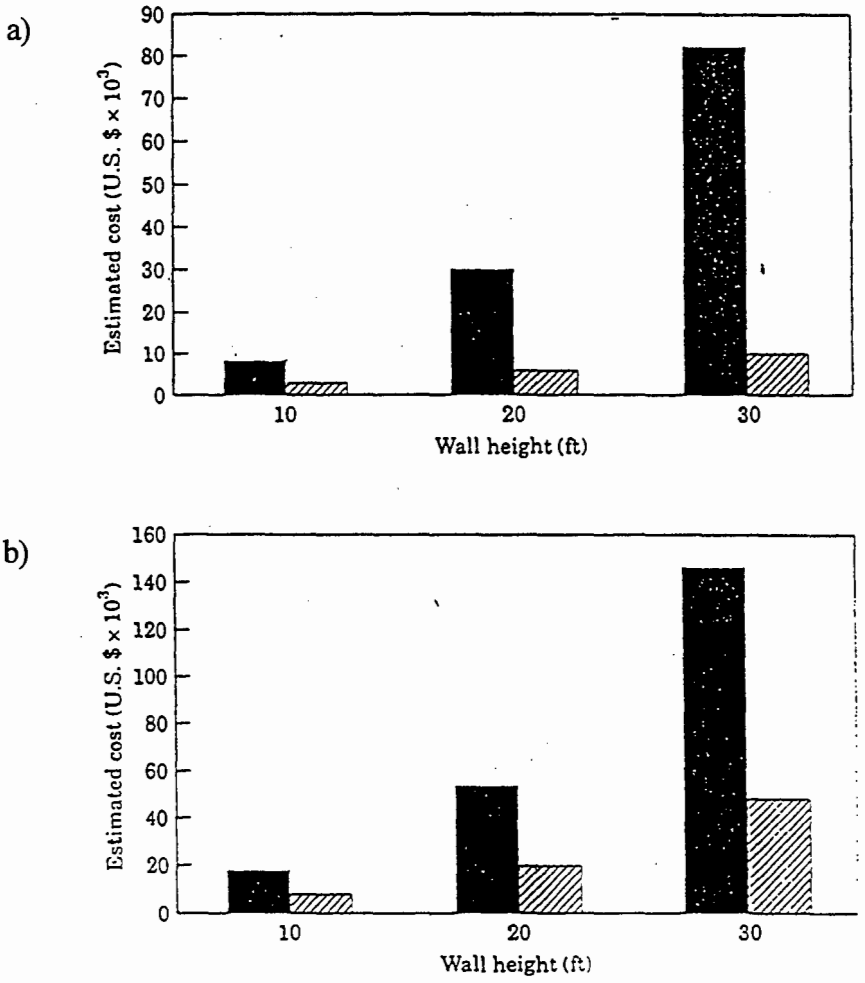

1 ft = 0.3048 m

Figure 2.5 Comparison of cost for retaining walls with sand (solid bars) and tire chips (hatched bars) as backfills, a) material costs, b) total cost (Cecich, et al., 1996)

of tire chips in New England is considerably higher than that used by the authors, the cost savings seems unrealistically optimistic.

CHAPTER 3. DESIGN AND CONSTRUCTION OF FACILITY

3.1 INTRODUCTION

The facility was designed to conduct full scale tests on tire chips and conventional granular soil as retaining wall backfill. The facility can accommodate 4.88 m (16 ft) of backfill with a maximum surcharge of 35.9 kPa (750 psf). The resulting forces and pressures on one face of the facility were measured. This face can be rotated outward about its base to allow the backfill to reach active conditions.

The facility consists of a concrete foundation and four walls. The two side walls are made from concrete. The front wall consists of three panels, with the center panel containing the load cells and pressure cells necessary to measure the forces and pressures. Each of the three panels are equipped with hinge assemblies at their base to allow for the outward rotation necessary to produce active conditions. The three panel construction is needed to minimize the influence of the side walls on the measurements taken on the center panel. The back wall is removable, which allows the backfill to be removed after completion of a test. The facility is also equipped with an overhead crane, attached to the top of the side walls, to assist in facility construction and to hoist backfill and surcharge into the facility. Concrete blocks are used to apply the surcharge.

The controlling condition for designing the facility was granular soil backfill at the maximum surcharge under at-rest conditions. The facility can hold approximately 100 m^3

(130 yd^3) of backfill, and is 4.88 m (16 ft) high and 4.47 m (14.7 ft) by 4.57 m (15 ft) in plan.

3.2 FOUNDATION AND SIDE WALLS

The foundation is reinforced concrete 0.51 m (1.7 ft) thick, as shown on Figure 3.1. At the location of the front wall, the foundation has two different floor elevations, -0.20 m (-0.7 ft) and -0.69 m (-2.0 ft) below the elevation of the facility. This can be seen on a plan view of the facility (Figure 3.2). This was necessary to accommodate the hinge assemblies at the base of the front wall and the load cells at the base of the center panel, as shown on Figures 3.3 and 3.4.

The side walls were constructed from reinforced concrete. They are 5.49 m (18.0 ft) long, 0.51 m (1.7 ft) thick, and 4.88 m (16.0 ft) high, as shown on Figures 3.2 and 3.5. The side walls are also shown on Figure 3.6, which shows the test facility before the front and back walls were erected. To support the timbers used as part of the back wall, as discussed below, a 100-mm (4-in.) wide notch was cast into each side wall, as shown on Figures 3.2 and 3.5. The top of the side walls were fitted with walkways for personnel access during testing, as shown on Figure 3.1.

Friction between the backfill and the concrete side walls was a concern, since it could influence the stress measurements made on the front wall. A large friction force would cause the loads and the pressures acting on the center panel to be lower than those that would occur under normal field conditions. To lessen the potential friction force, 1.2-m

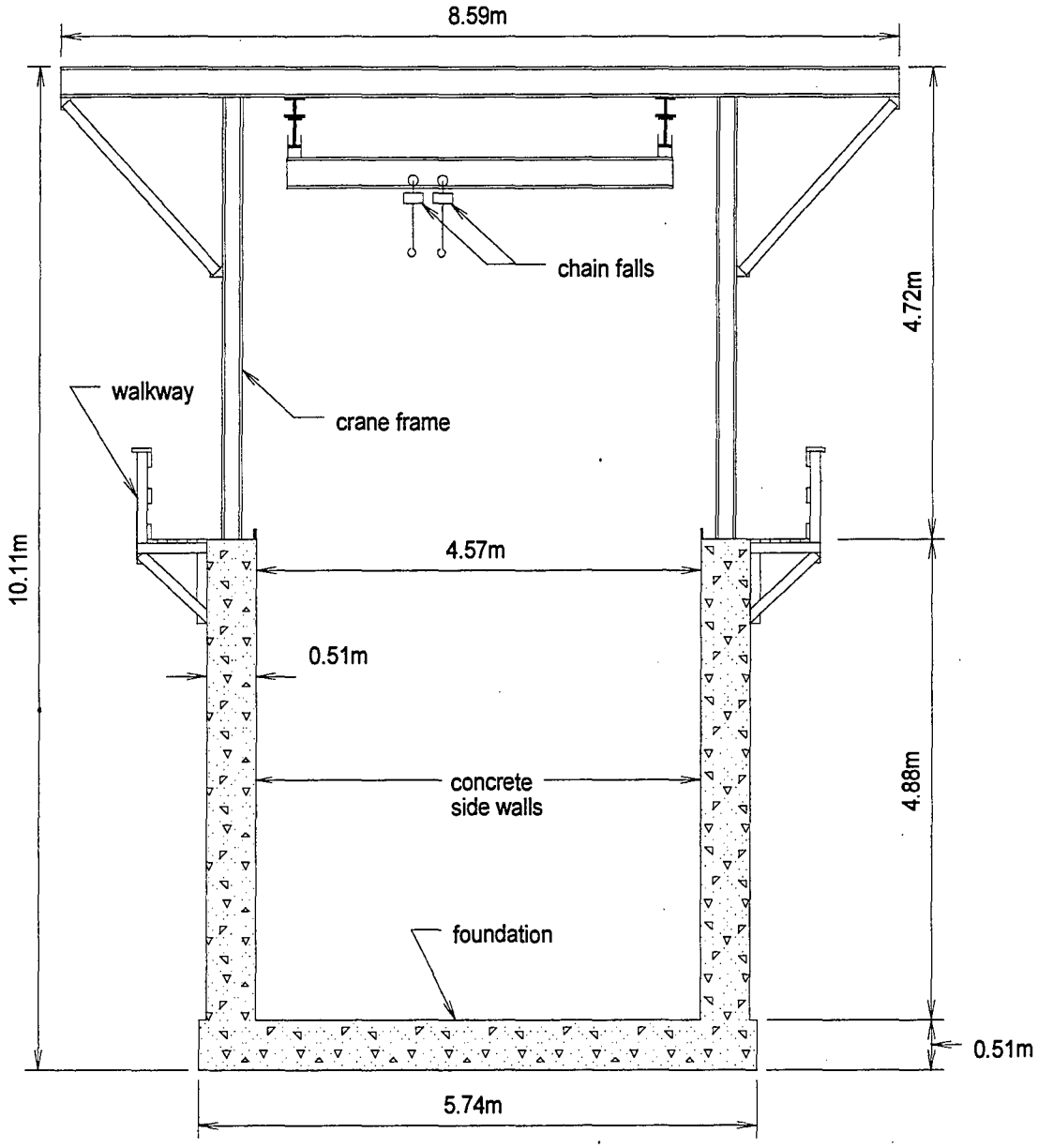

Figure 3.1 Transverse cross-section

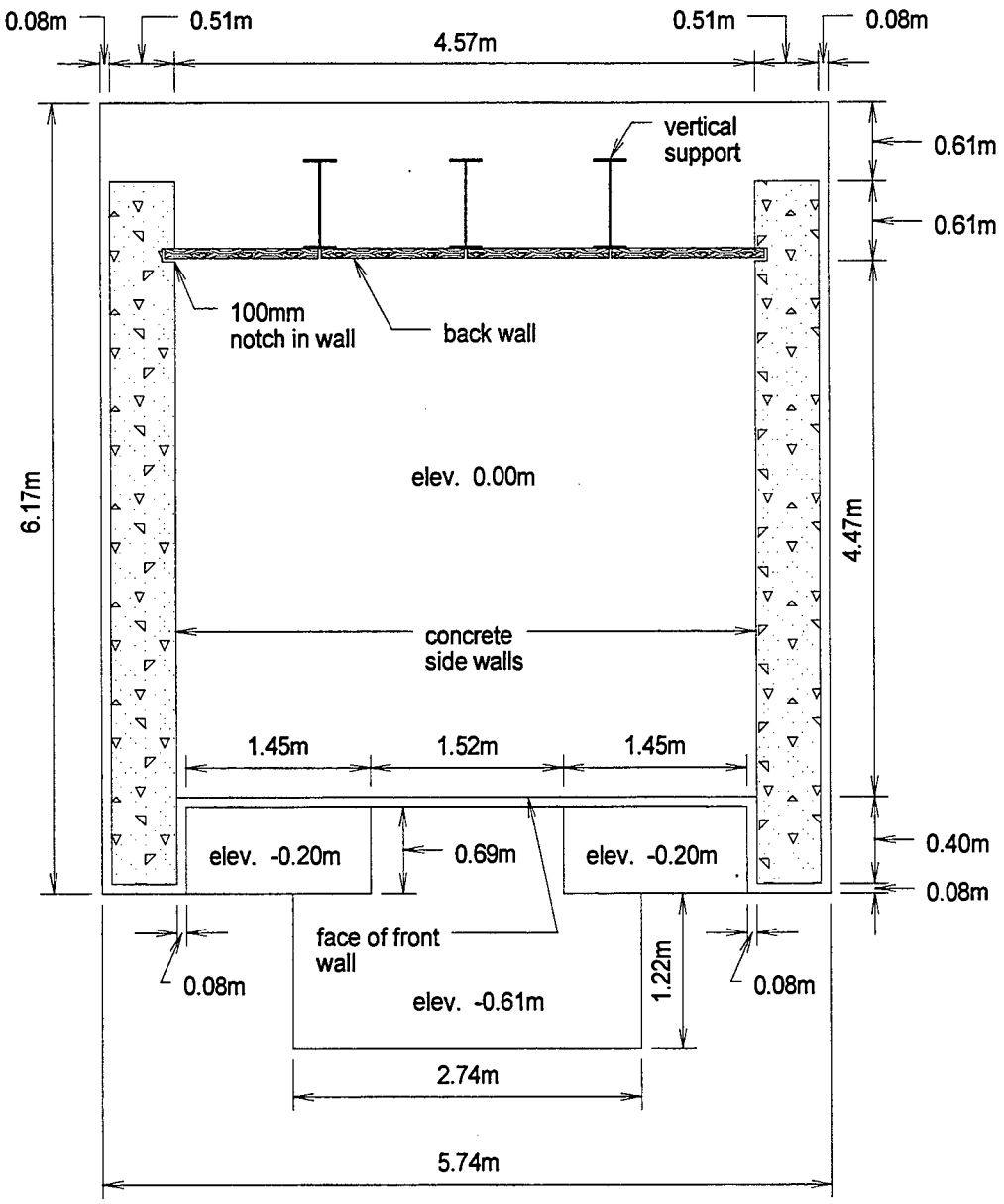

Figure 3.2 Plan view

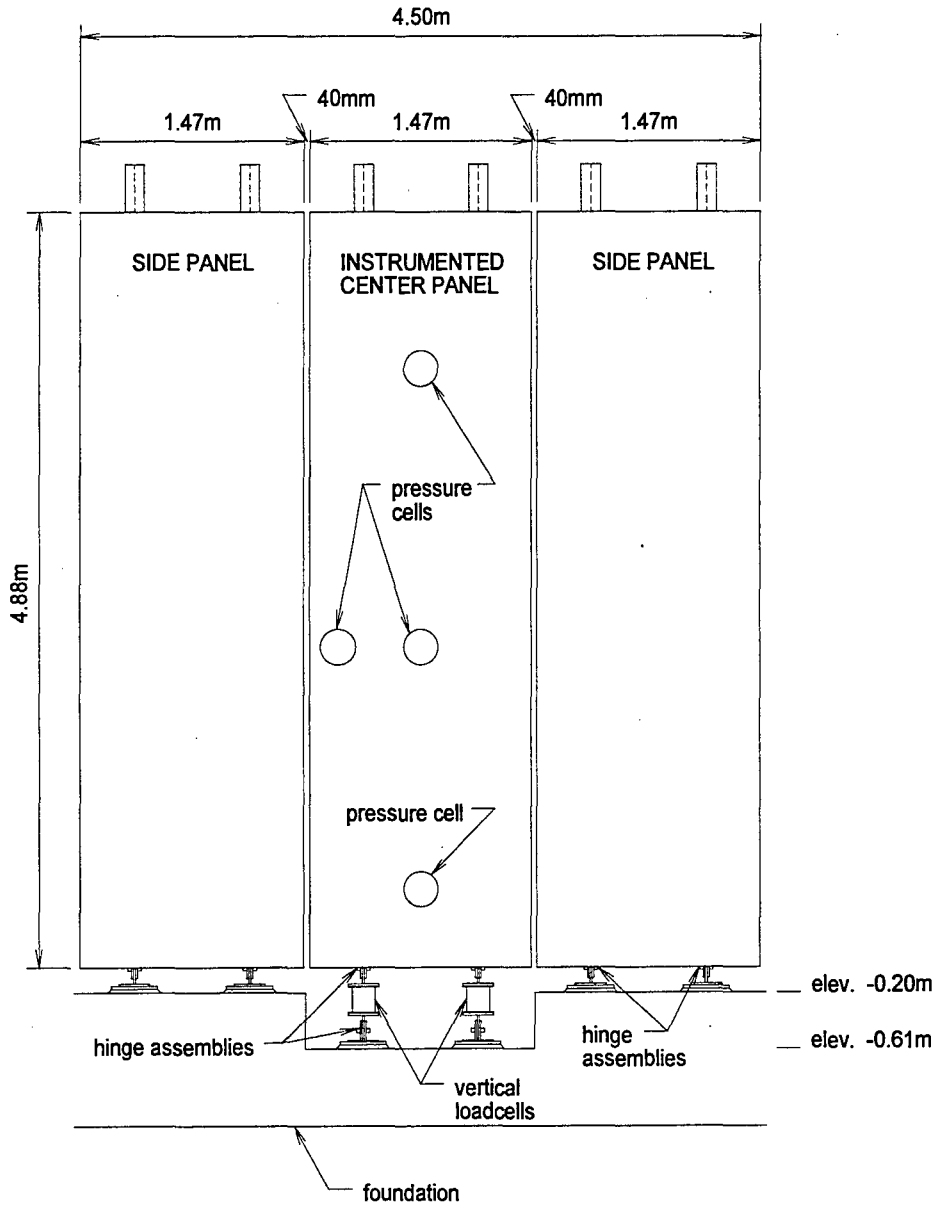

Figure 3.3 Front wall elevation

Figure 3.4 Photograph of front wall

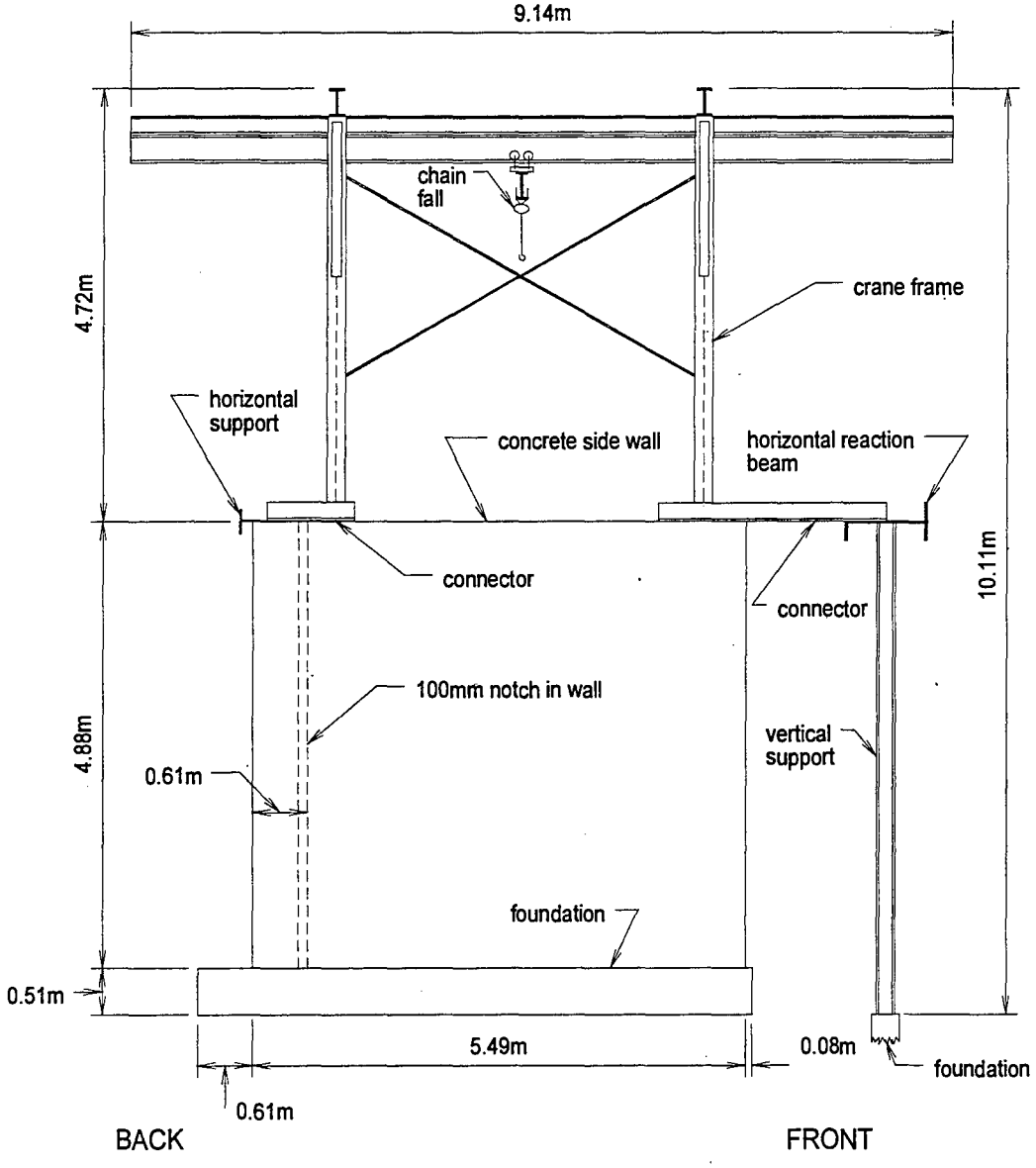

Figure 3.5 Longitudinal section

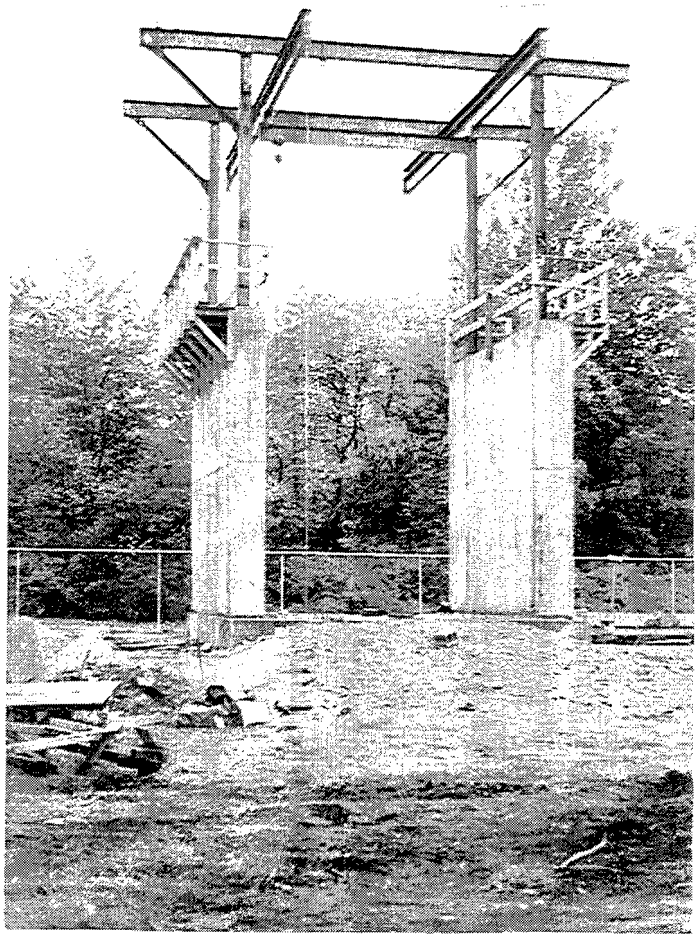

Figure 3.6 Facility before erection of front and back walls

(4-ft) by 2.4-m (8-ft) pieces of 12 gauge sheet metal were anchored to the inside surface of the side walls. Polyethylene plastic was then hung over the sheet metal surface. Thus, as the tire chips moved, either vertically due to compression or horizontally from the movement of the front wall, the two surfaces that would move against each other would be the plastic against the sheet metal, greatly reducing fictional force between the fill and the side walls.

3.3 FRONT WALL

The front wall consists of three separate panels, each 4.88 m (16.0 ft) high, by 1.47 m (4.8 ft) wide. A 40-mm (1.1-in.) space was left between each panel, resulting in a total width of the front wall of 4.50 m (14.8 ft), as shown on Figures 3.3 and 3.4. The three panel construction was used to minimize the effect of friction from the side walls on measurements made on the center panel. As discussed above, friction forces are generated when the tire chips move against the side walls, either vertically or horizontally. However, the influence of friction forces decreases with increasing distance from the side walls. Having the instrumentation located near the centerline of the facility minimizes the effects of friction from the side walls on the force and pressure readings.

Each panel is a structural steel frame consisting of two wide flange sections and angle bracing. The face of the front wall is 100-mm (4-in.) thick reinforced concrete, as shown on Figure 3.7. A concrete face was chosen to duplicate typical field conditions.

To allow for the outward rotation of the front wall, each side panel is equipped with two bottom hinges connected to the base of the structural steel wide flange section and

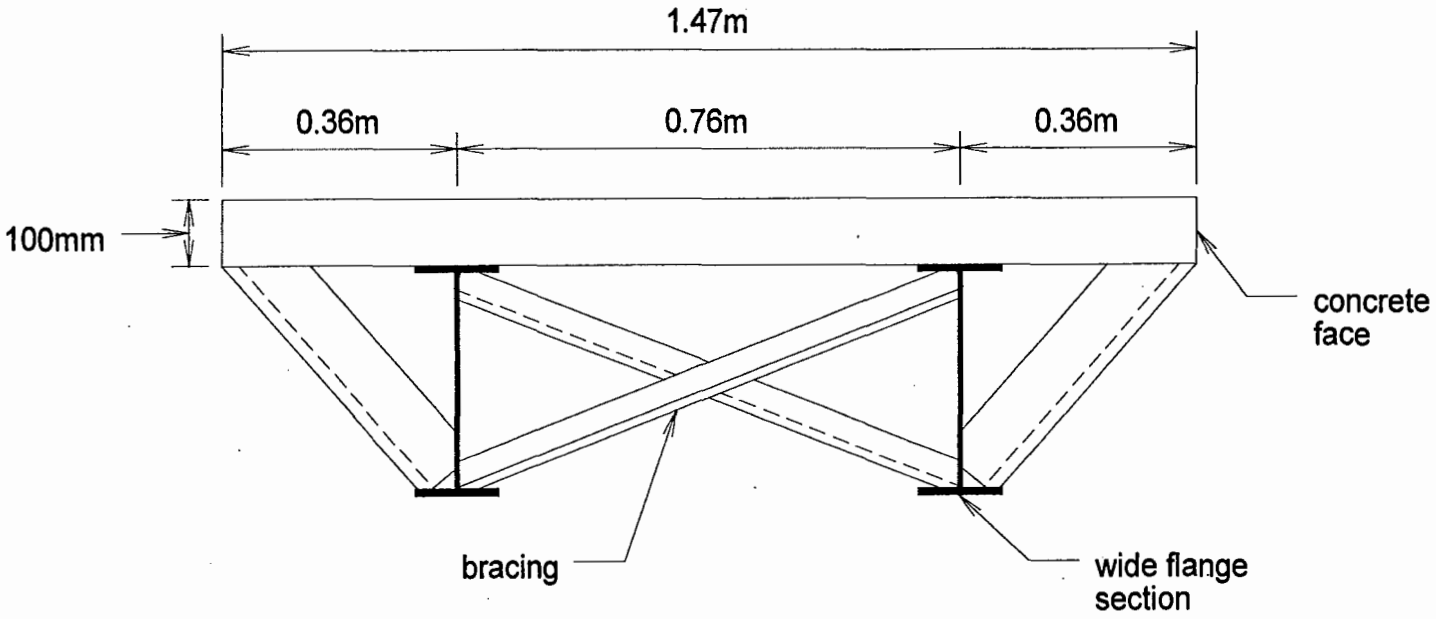

Figure 3.7 Cross-section, front wall panel

the foundation. The center panel is double hinged to accommodate the vertical load cells. One hinge is connected to the wide flange section and the other is anchored to the foundation, with the load cell located between the two, as shown on Figure 3.3. At the top, each panel is fitted with two double hinge assemblies, with one hinge connected to the structural steel of the front wall panels and the other hinge, which consists of a ball joint located on the end of a screw jack, connected to a horizontal reaction beam, as shown on Figure 3.8. The hinge assemblies for the center panel are also fitted with load cells. The horizontal reaction beam provides support for the top of the front wall panels. It is connected horizontally to the crane frame base plates and supported vertically with steel columns, as shown on Figures 3.5 and 3.8. Wall rotation needed to achieve active conditions was obtained by manually turning the screw jacks. This allowed the front wall to pivot on the bottom hinges and move horizontally at the top. This operation was performed with two people, as shown on Figure 3.9.

The center panel is equipped with two horizontal load cells at the top and two horizontal load cells at the bottom. It is also fitted with two vertical load cells at the bottom. The bottom horizontal load cells was double hinged, with the first hinge in common with the vertical load cells, and connected to the bottom of the structural steel wide flange section. The hinge assembly at the other end of the horizontal load cells is connected to a horizontal reaction member, fabricated from a piece of wide flange section reinforced with stiffeners, and anchored to the foundation. The location of the components are shown on Figure 3.10.

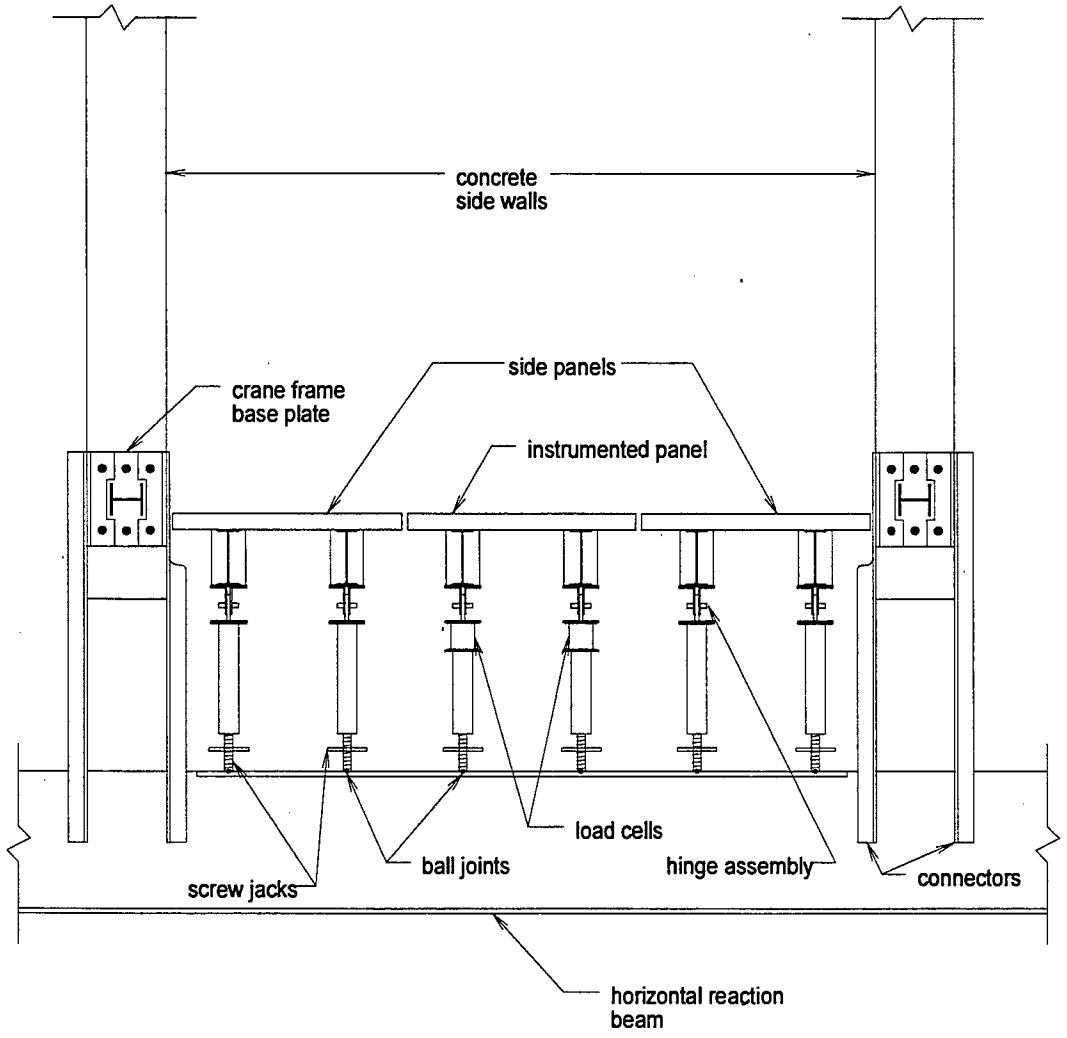

Figure 3.8 Front wall top connection configuration, plan view

Figure 3.9 Rotating front wall

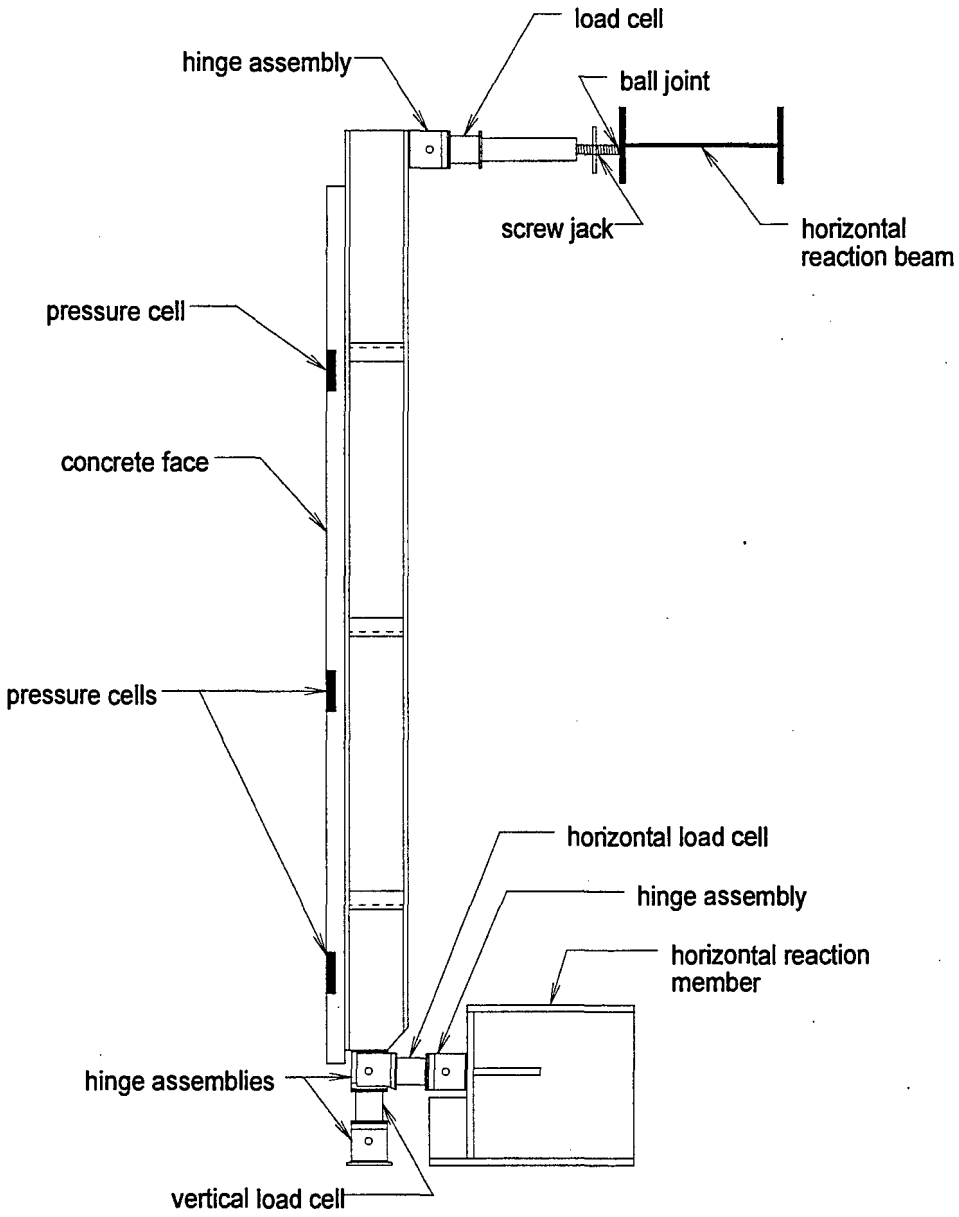

Figure 3.10 Cross-section through front wall center panel

3.4 BACK WALL

The back wall consists of three vertical supports each 4.88 m (16.0 ft) long made from wide flange sections. Each vertical support is bolted at the bottom to the foundation and at the top to a wide flange section, 5.89 m (19.3 ft) long, which functions as a horizontal support, as shown on Figure 3.11. The horizontal support was connected to the crane frame base plates, as shown in Figure 3.5. Timbers were placed against the vertical supports (Figures 3.11 and 3.12) and into the notch cast into the side walls (Figures 3.2 and 3.11). The 75-mm (3-in.) thick timbers were placed as the elevation of the fill increased during backfill placement. The back wall is removable to allow the backfill to be excavated from the facility.

3.5 CRANE

The crane frame is constructed from structural steel. Its overall dimensions are: 9.14 m (30.0 ft) long, 8.59 m (28.2 ft) wide, and 4.72 m (15.5 ft) tall. It is attached to the top of the concrete side walls, as shown on Figures 3.1 and 3.5. It is equipped with two chain falls, a manual chain fall with a capacity of 2.7 metric tons (3.0 short tons), and an electric chain fall with a capacity of 0.91 metric tons (1.0 short tons). The manual chain fall is used to install and remove the front wall panels. The electric chain fall is used to lift backfill into the facility, place surcharge blocks, and remove the back wall. Backfill is brought into the facility with a specially constructed lifting bucket, shown on Figure 3.13.

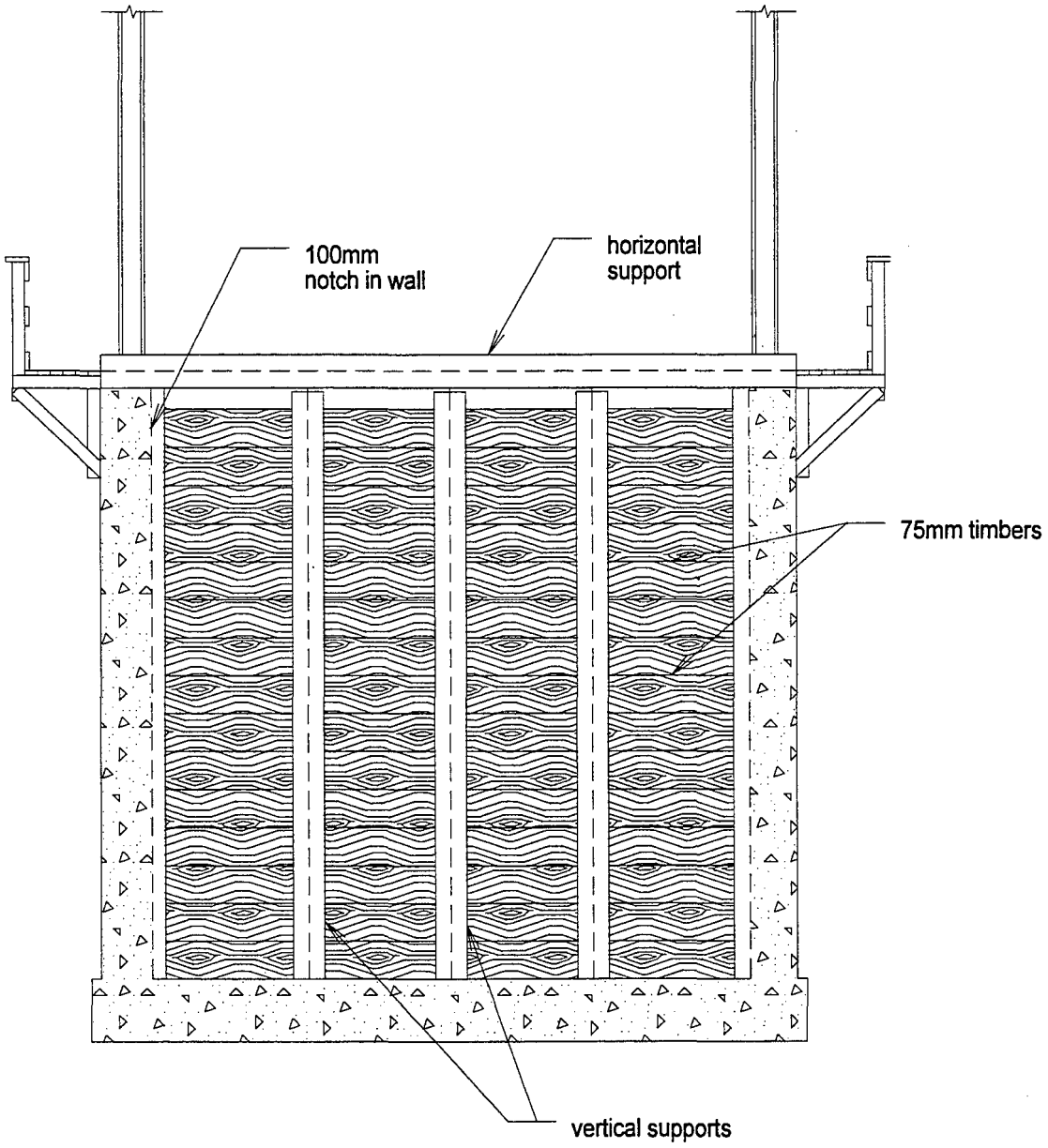

Figure 3.11 Back wall elevation

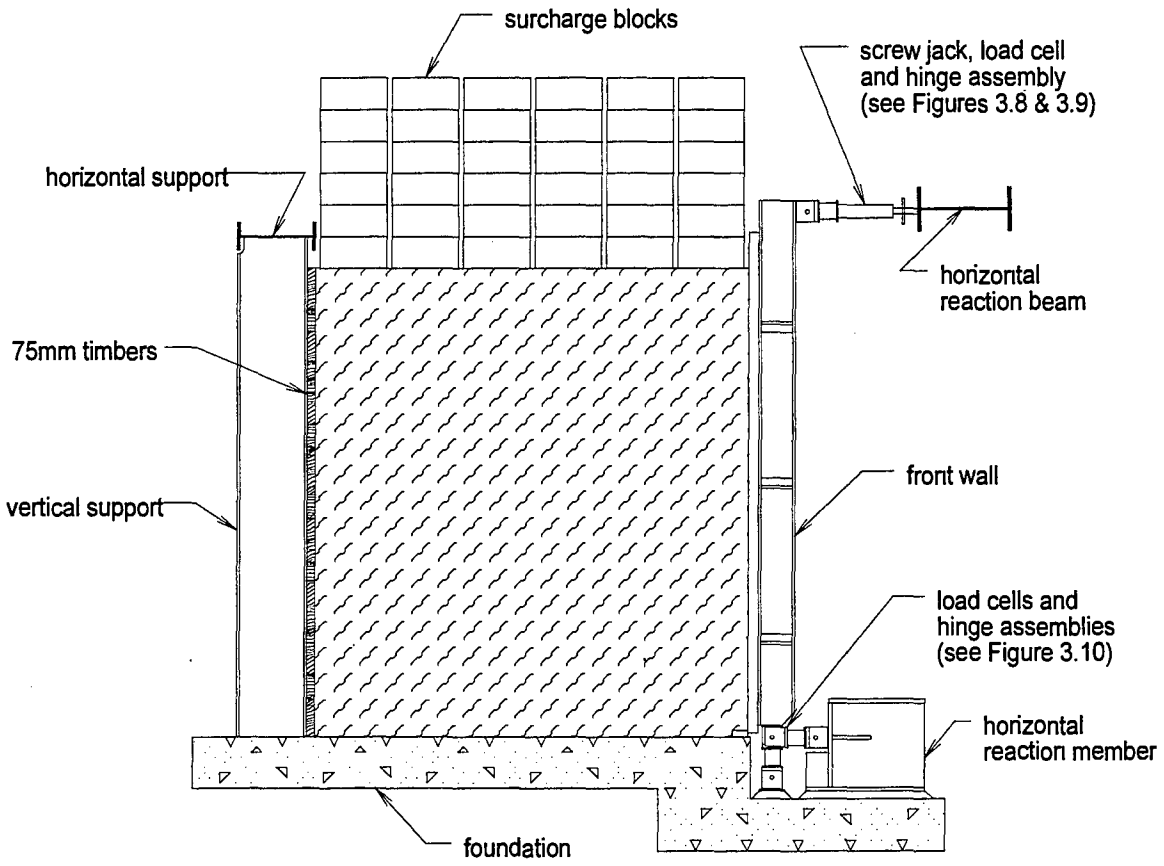

Figure 3.12 Longitudinal cross-section

Figure 3.13 Electric chain fall bringing load of backfill into facility

3.6 SURCHARGE BLOCKS

The surcharge blocks are constructed from concrete. They are 0.70 m (2.3 ft) by, 0.70 m (2.3 ft) in plan, and 0.3 m (1.0 ft) high, as shown in Figure 3.14. Each surcharge block weighs approximately 350 kg (780 lb). A total of 36 blocks are required for one layer, resulting in a stress of 6.0 kPa (125 psf) per layer. Six layers of surcharge blocks are needed to apply the maximum surcharge of 35.9 kPa (750 psf) (216 blocks), as shown on Figure 3.12 and 3.15.

Figure 3.14 Surcharge blocks

Figure 3.15 Facility fully loaded

(BLANK)

CHAPTER 4. TEST PROTOCOL

4.1 INTRODUCTION

The objective of this study was to determine design criteria for using tire chips as backfill for retaining walls. This was done by testing tire chips from three suppliers. The following tire chip suppliers were chosen by the NETC research advisory panel.

Pine State Recycling
Nobleboro, Maine

Palmer Shredding
North Ferrisburg, Vermont

F & B Enterprises
New Bedford, Massachusetts

Pine State Recycling went out of business prior to the completion of this study. Approximately 64 metric tons (70 short tons) of tire chips were needed from each supplier. In addition, a conventional granular soil was tested as a control measure. The order of testing was as follows: granular soil, Pine State Recycling, Palmer Shredding, and F & B Enterprises.

The procedure used during testing is termed the test protocol and is described in this chapter. The test protocol includes the instrumentation, instrument calibration, placement of backfill and surcharge in the test facility, and measurements taken during and after filling. Calibration was necessary for the instruments used to measure the horizontal and

vertical loads, horizontal pressures, and horizontal movement within the backfill. Measurements taken after filling were obtained for the at-rest and active conditions.

Selected properties of the backfill were measured including: gradation and compacted field densities. In addition, the laboratory maximum dry density of the granular fill was measured. The measurements taken during filling were: horizontal load, vertical load, and horizontal pressure on the center panel of the front wall; horizontal displacement of the front wall, and settlement of the fill. Measurements for at-rest conditions were taken at the following surcharges: no surcharge, 12.0 kPa (250 psf), 23.9 kPa (500 psf), and 35.9 kPa (750 psf). The measurements that were taken were the same as listed above for filling. The effects of repeated unloading and reloading were also investigated by removing and reapplying the maximum surcharge a minimum of two times. Measurements for the active condition were taken at a surcharge of 35.9 kPa (750 psf). In addition to the measurements listed above, horizontal movement within the backfill was measured.

Instrumentation, backfilling and loading procedures, and the measurements discussed above will be described in the following sections. The purpose of each measurement will also be discussed.

4.2 INSTRUMENTATION

Some of the instruments used for this research measured the forces and the stresses produced by the backfill. Other instrumentation measured the vertical settlement below and at the fill surface, horizontal displacement within the backfill, and horizontal

displacement of the front wall. Each type of instrumentation will be discussed in the following sections, including a description of the instrument, how the instrument was installed, and if applicable, how the instrument was calibrated.

4.2.1 Forces and Stresses

The front wall of the facility is equipped with both load cells and pressures cells to measure the horizontal and vertical forces, and the stresses produced by backfill. The front wall is made up of three separate panels, with only the center panel containing the load cells and pressure cells. This was done to lessen the effects of friction between the side walls and the backfill on instrument readings, as discussed in Section 3.3.

4.2.1.1 Horizontal and Vertical Forces

The horizontal and vertical forces exerted on the front wall are measured by six load cells, four oriented horizontally and two oriented vertically. Of the four horizontal load cells, two are located at the top of the center panel and two are located at the bottom. The two vertical load cells are located at the bottom of the center panel. The locations of the load cells are shown on Figures 3.3, 3.8, and 3.10. The load cells are model CH20 supplied by APEX Inspections and Engineering, Inc. They are designed to work in compression within the load range of 0 to 89 kN (20,000 lb). The load cells utilize two 90° strain gauge rosettes wired in a full bridge configuration. The output was read by a Measurements Group P-3500 Digital Strain Indicator and was in units of microstrain.

The force was determined by first recording the microstrain from each load cell with the facility empty (zero readings). The microstrain was then recorded for the different loading conditions throughout each test. The force (F_{lc}) could then be determined by subtracting the zero readings from each subsequent reading and multiplying by a calibration factor, unique to each load cell, as shown below,

$$F_{lc} = (ms_n - ms_i)*CF_{lc} \tag{4.1}$$

where ms_i is the reading in microstrain for the initial condition (zero reading), ms_n is the reading in microstrain at subsequent loadings, and CF_{lc} is the calibration factor for the load cell.

The six load cells were calibrated by the supplier and upon receipt the calibration was checked. Calibration utilized an Instron 4202 loading device, which applied a compression load to the load cells. The load was applied at a rate of 1.54 mm/min (0.06 in./min), with a maximum load of approximately 44.5 kN (10 kips). The signal from the load cells (microstrain) was read by a Measurements Group P-3500 Digital Strain Indicator. The output from the load cells and the applied force was recorded at each 2.2 to 4.4-kN (0.5 to 1-kip) increase in applied force as the load cells were being loaded. Once the maximum load was reached the load was removed at the same rate, with the output from the load cells and the testing machine recorded at the same intervals. The signal from the load cells was then plotted verses the applied load, yielding a straight line calibration with the calibration factor (CF_{lc}) equal to the slope of the line.

The load cells were removed from the wall prior to the test with F & B Enterprises tire chips and the calibration was checked, using the same procedure discussed above. Once the calibration was confirmed, the load cells were returned to the facility. The calibration curves and calibration factors are included in Appendix B.

4.2.1.2 Horizontal Stress

The horizontal stress was measured by four total pressure cells. Three pressure cells were installed along the centerline of the center front wall panel at elevations relative to the floor of the facility of 0.51 m (1.7 ft), 2.08 m (6.8 ft), and 3.86 m (12.7 ft). The fourth pressure cell was installed at elevation 2.08 m (6.8 ft) and offset 0.55 m (1.8 ft) from the centerline of the center panel. This was done to examine the variability of pressure measured at the same elevation. The locations of the pressure cells are shown on Figures 3.3 and 4.1.

The pressure cells were ROCTEST model EPC with a capacity of 170 kPa (25 psi). Each 230-mm (9-in.) diameter pressure cell was filled with oil and a vibrating wire transducer measured the pressure in the oil. Each transducer was equipped with a thermistor to measure the temperature change. The output was read initially by a Geologger model DG100F, connected to a personal computer. The readings fluctuated slightly, so a total of ten readings were taken for each measurement and the average was recorded for use in calculating the pressure. For the test with F & B Enterprises tire chips, some of the data was taken with a ROCTEST model MB-6T portable readout unit. The unit gave stable readings, so it was unnecessary to take multiple readings and find the

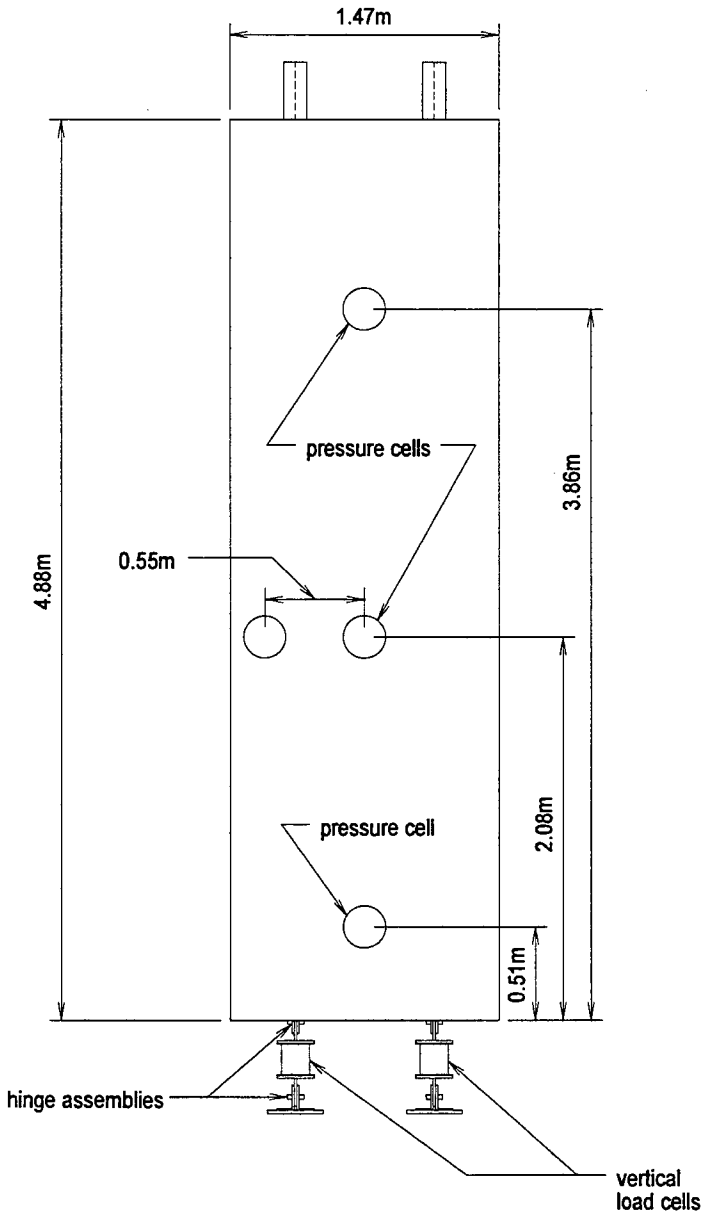

Figure 4.1 Center panel elevation, showing location of pressure cells

average. Output from each pressure cell consisted of the frequency from the vibrating wire transducers (Hz), which was used to find the pressure, and resistance from the thermistor (Ohms), which was used to find the temperature.

Three factors are used to convert the frequency readings from the pressure cells to stress. The first is a calibration factor (CF_{PS}) which converts the output from the vibrating wire transducer into stress. The second is a temperature correction factor (T_k) that corrects the stress for temperature change, while the third is a correction for change in barometric pressure. The readings from the pressure cells was converted into pressure by:

$$\Delta P = CF_{ps}(LU_o - LU_1) - T_k(T_o - T_1) + 0.133(B_o - B_1) \qquad (4.2)$$

where: ΔP = change in pressure in kPa

CF_{ps} = calibration factor in kPa/linear unit

LU_o, LU_1 = initial and current linear reading

T_k = temperature correction factor in kPa/°C

T_o, T_1 = initial and current temperature readings in °C

0.133 = barometric pressure factor in kPa/mm of mercury (Hg)

B_o, B_1 = initial and current barometric pressure readings in millimeters of Hg

The linear reading (LU) is found from the frequency using the following equation:

$$LU = 0.001016(Hz)^2 \quad (4.3)$$

The resistance given by the thermistor must be converted from Ohms to temperature (°C), using the following equation:

$$T(°C) = 56.303 - 2.1393x10^{-2}(Ohms) + 3.4327x10^{-6}(Ohms)^2 - 2.8527x10^{-10}(Ohms)^3 + 9.1285x10^{-15}(Ohms)^4 \quad (4.4)$$

This type of pressure cell is usually used in applications where it is installed in an embankment and surrounded by earth material on all sides. However, for this application it was necessary to have one side bear against the concrete front wall while the other side was exposed to the backfill. The pressure cells were installed by casting a bed of mortar which conformed to the back side of each pressure cell. Each bedding was then cast into the center front wall panel at its appropriate elevation, then each pressure cell was secured into each bedding.

The pressure cells needed to be able to measure the stress produced by the tire chips. Tire chip pieces are considerably larger than the grain sizes of typical embankment soils, with some tire chip pieces in excess of 80 mm (3 in.). The number of particles in contact with the face of the pressure cell would be less than for most soils. Because of this and the method of installation discussed above, the pressure cells were calibrated for conditions similar to those expected in the field. This included finding CF_{ps} and T_k for each pressure cell. The barometric pressure factor was the same for each pressure cell and determined by the manufacturer. For the calibration procedures discussed below, the

center panel was removed and placed horizontally on the facility floor as shown on Figure 4.2.

The calibration factor for stress, CF_{ps}, was determined in two ways. The first method used a 230-mm (9-in.) diameter, 80-mm (3-in.) deep cylinder with no top or bottom. The cylinder was placed over the pressure cell and tire chips were placed inside of the cylinder. A load was then applied by stacking 16-kg (35.3-lb) weights on top of the tire chips. The second method used a 1.52-m (5.0-ft) by 1.52-m (5.0-ft) by 0.5-m (1.6-ft) deep box with no top or bottom. Tire chips were compacted into the box and a variable load was applied by the 350-kg (780-lb) surcharge blocks. For both methods, a correlation between the applied stress and the pressure cell frequency readout was obtained. The frequency was converted to LU using Equation 4.3. This was then used to find CF_{ps} in units of kPa/LU. The values of CF_{ps} for each of the pressure cells are shown in Appendix C.

The correction factor for temperature, T_k, was determined by two different trials. Each trial used a 230-mm (9-in.) diameter, 80-mm (3-in.) deep cylinder with no top or no bottom. The cylinder was placed over the pressure cell and tire chips were placed inside of the cylinder. A constant load was then applied by stacking six 16-kg (35.3-lb) weights on top of the tire chips, resulting in an applied stress of 22.9 kPa (3.3 psi). During calibration the temperature and pressure cell readout were typically recorded for 24 hours. A correlation between the temperature and pressure cell frequency readout was then obtained. The correlation was then converted into units of LU/°C using Equations 4.3 and 4.4. T_k for each trial was then determined by multiplying by CF_{ps} determined by the

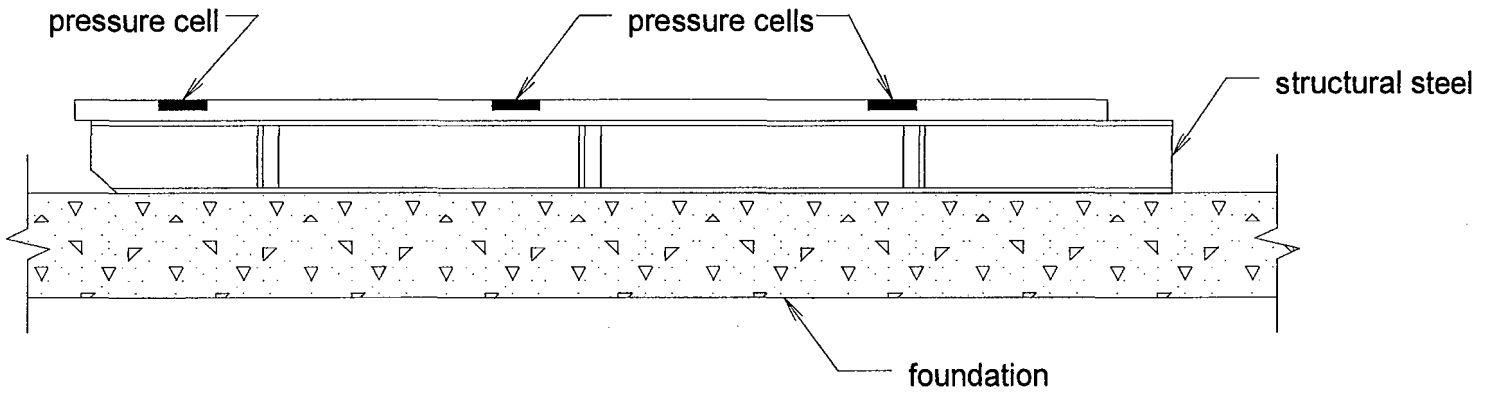

Figure 4.2 Orientation of center panel during pressure cell calibration

two methods discussed above. This resulted in four values of T_k for each pressure cell, as shown in Appendix C.

4.2.2 Settlement

Vertical settlement was measured below and at the fill surface. The vertical settlement below the fill surface was measured with two settlement plates. The surface settlement was determined from the change in elevation of fixed points, called the settlement grid, located on the surface of the fill.

4.2.2.1 Settlement Plates

The settlement plates were installed at approximately the 1/3 and 2/3 depth of the backfill, at elevations of 1.63 m (5.3 ft) and 3.25 m (10.7 ft). They were offset 1.14 m (3.7 ft) from the face of the front wall. Throughout this report these will be referred to as the 1.63-m (5.3-ft) and 3.25-m (10.7-ft) settlement plates, respectively. Each settlement plate consisted of a 0.61-m (2-ft) by 0.61-m (2-ft) by 19-mm (3/4-in.) thick plywood base plate. Attached to the base plate was a length of 25-mm (1-in.) diameter pipe to serve as a riser. The length of the riser for the 1.6-m (5.3-ft) settlement plate was approximately 5.5 m (18 ft) and 4.0 m (13 ft) for the 3.25-m (10.7-ft) settlement plate. PVC pipe with a nominal diameter of 38 mm (1.5 in.) was used as a sleeve around the riser to prevent friction between the backfill and the riser from affecting the readings.

The settlement plates were installed during filling of the facility. When the fill elevation corresponded with the desired elevation of the settlement plate, the plate was

placed on top of the compacted fill surface at the appropriate location. Filling of the facility then continued. The locations of the settlement plates are shown on Figures 4.3 and 4.4.

The settlement of each settlement plate was obtained by measuring the elevation of the top of the riser with respect to a stationary point. The stationary point was one of the anchor bolts for the crane frame, located at the top of one of the concrete side walls. This particular anchor bolt was marked with orange paint and used throughout the duration of the study. The elevation was measured with a water level, which consisted of a one gallon water-filled jug with a long clear plastic tube coming out of the bottom. The elevation was determined by first placing the water jug at a fixed point, then by putting the zero end of a standard tape measure on the end of the riser. The elevation of the water with respect to the top of the riser could be read by holding the clear tube against the tape measure and recording the reading at the bottom of the meniscus. The water elevation with respect to the anchor bolt was measured in a similar manner. The elevation of the settlement plate with respect to the anchor bolt was then determined by subtracting the settlement plate reading from the anchor bolt reading. An initial elevation of the settlement plate was taken prior to placing the first lift of fill over the plate. The elevation of the settlement plate was then measured after each subsequent two lifts of fill were placed. The settlement was calculated by subtracting each subsequent elevation from the initial reading.

An example using the water level is shown on Figure 4.5. The left side of the figure shows the conditions when the zero reading was determined. The sign convention used

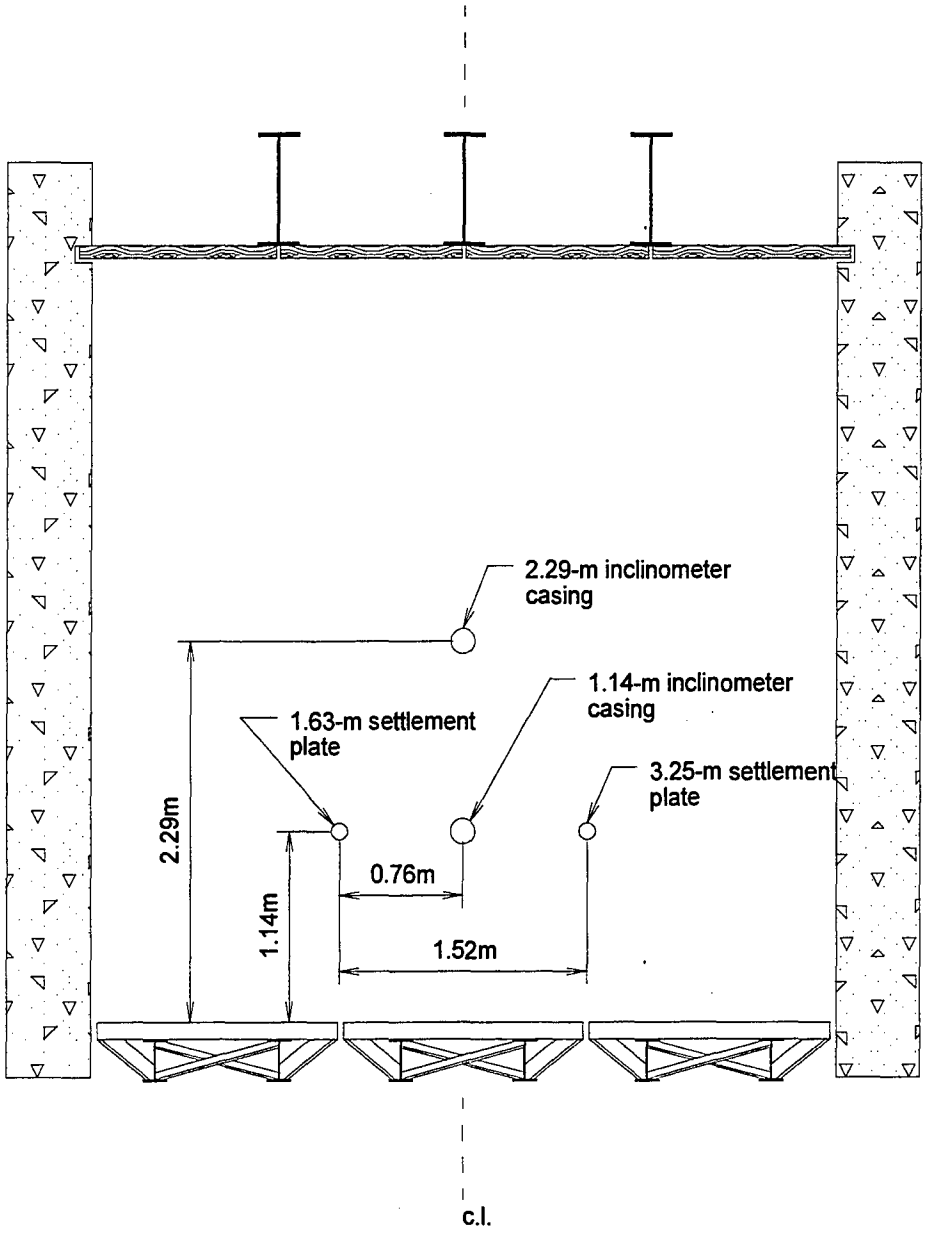

Figure 4.3 Plan view of facility showing location of settlement plates and inclinometer casings

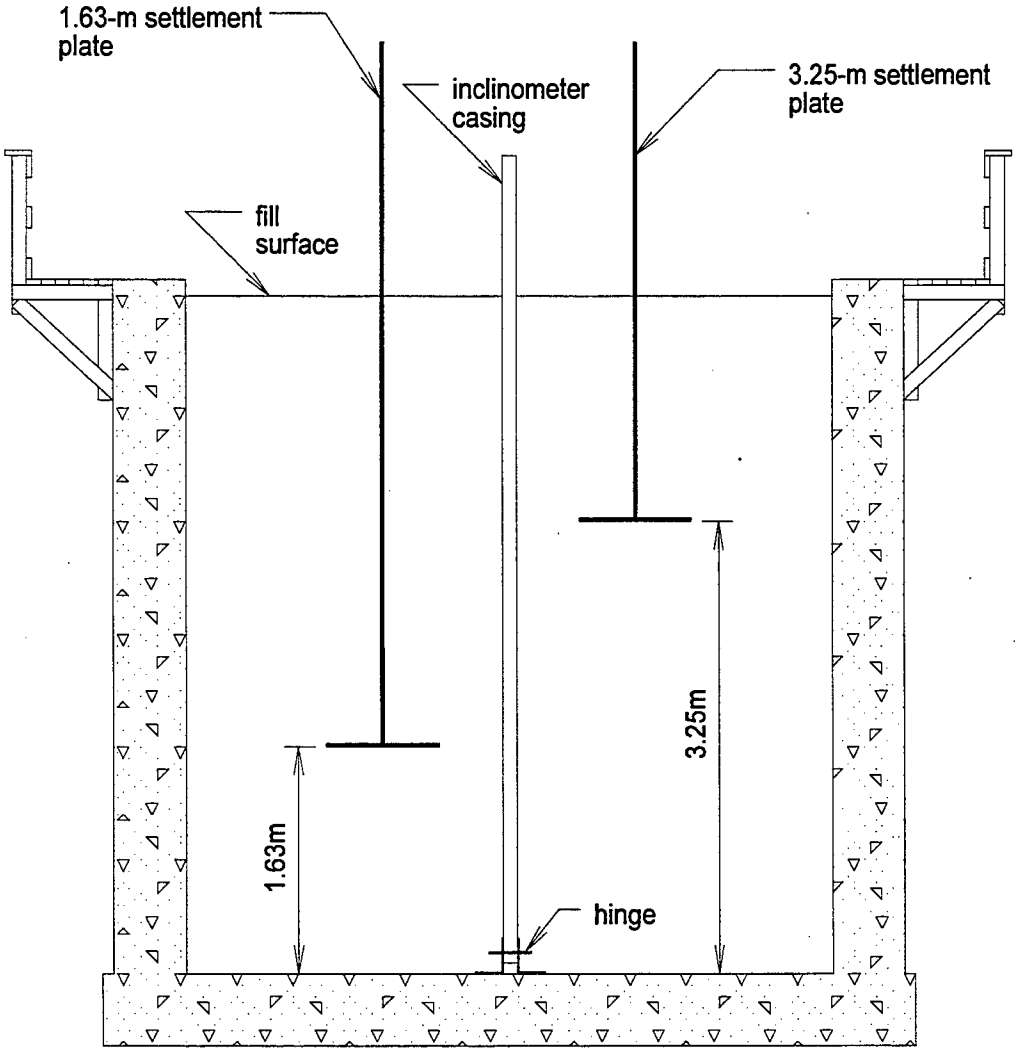

Figure 4.4 Cross-section of facility showing location of settlement plates and inclinometer casings

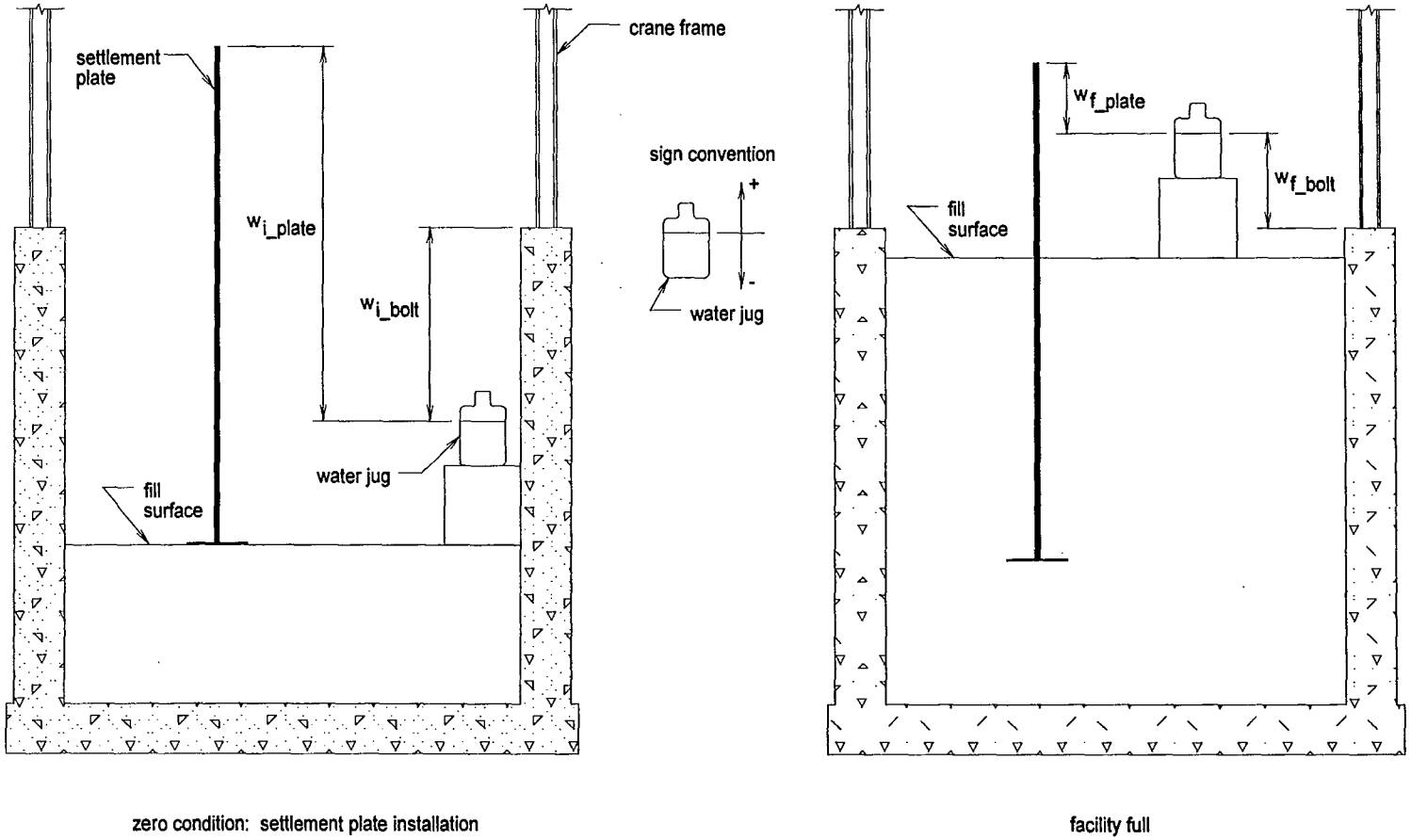

Figure 4.5 Elevation determination for settlement plates

throughout the test is shown in the middle of the figure. Elevations measured from below the water level were designated as negative and those above were positive. So the initial elevation of the settlement plate with respect to the anchor bolt is given by the equation:

$$E_{i\_plate} = w_{i\_plate} - w_{i\_bolt} \tag{4.5}$$

where w_{i_plate} is the initial water elevation measured from the top of the settlement plate riser and w_{i_bolt} is the initial water elevation measured from the anchor bolt. The right side of Figure 4.5 shows conditions when the facility was full. The elevation of the settlement plate for this condition is:

$$E_{f\_plate} = w_{f\_plate} - w_{f\_bolt} \tag{4.6}$$

where w_{f_plate} and w_{f_bolt} are the water levels measured from the settlement plate and the anchor bolt when the facility is full, respectively. The settlement can then be found by subtracting the initial from the full elevation.

4.2.2.2 Settlement Grid

Vertical displacement of the fill surface was found by measuring the change in elevation of points at the surface of the fill, referred to as the settlement grid. The settlement grid consisted of 19 points spaced 0.76 m (2.5 ft) apart. Seven points down the centerline of the facility and two rows of seven points extending from side wall to side wall across the facility at distances of 0.76 m (2.5 ft) and 2.29 m (7.5 ft) from the front wall, as shown on Figure 4.6. Squares of plywood, 150 mm by 150 mm (6 in. by 6 in.) in size, were placed at each grid point to provide a solid base from which to measure

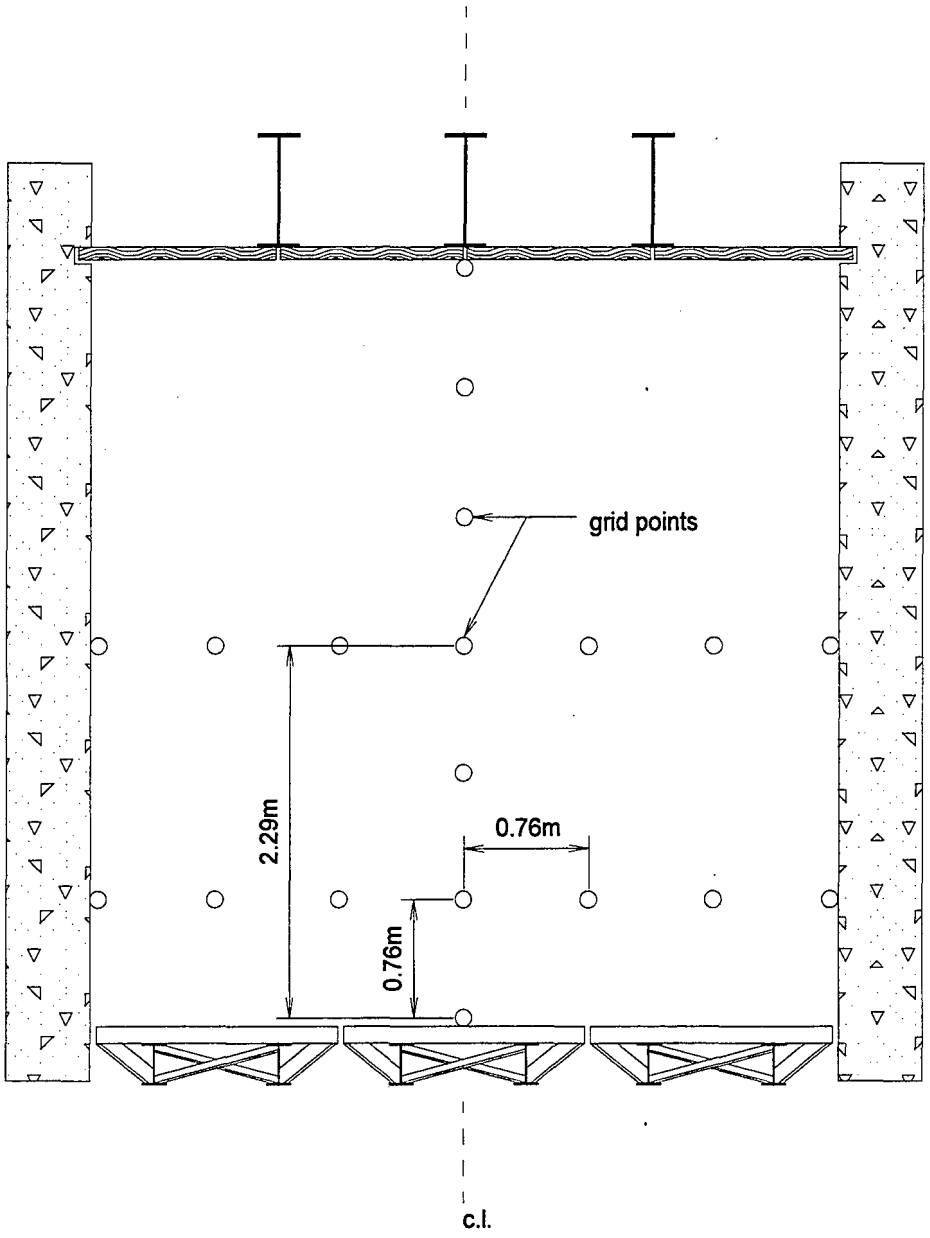

Figure 4.6 Plan view of facility showing settlement grid

elevations. The squares were installed when the first layer of surcharge blocks was applied. This was done by placing each square on the fill surface, then positioning the blocks on the corners of the square. This prevented shifting of the squares during testing. The initial reading of the settlement grid was taken just after the first layer of blocks was applied, which corresponds to a surcharge of 6.0 kPa (125 psf). The settlement was measured using a water level, as discussed in Section 4.2.2.1 for the settlement plates.

4.2.3 Horizontal Movement

Horizontal displacement within the backfill and of the front wall was measured. The horizontal displacement within the backfill was measured using an inclinometer. The front wall displacement was measured using the distance between reference beams and fixed points on the front wall.

4.2.3.1 Movement Within the Backfill

Measurement of horizontal displacement within the backfill was accomplished using an inclinometer. The deformation for the granular fill, Pine State Recycling, and Palmer Shredding was determined by using a Slope Indicator Co. series 200-B inclinometer. For F & B Enterprises a Slope Indicator Co. model #50300940 inclinometer was used. Calibration of the inclinometers was performed at the factory. The inclinometers worked in conjunction with inclinometer casings which passed through the depth of the fill. The inclinometer casings were installed along the centerline of the facility, at offsets of 1.14 m (3.7 ft) and 2.29 m (7.5 ft) from the front wall face, as shown on Figures 4.3 and 4.4.

Throughout this report, these will be referred to as the 1.14-m (3.7-ft) and 2.29-m (7.5-ft) casings, respectively.

Installation of the inclinometer casings started when the facility was empty. The first segment of casing was connected to a hinge anchored to the facility floor, as shown on Figure 4.4. The hinge was oriented so that the casing could rotate toward the front wall. When enough fill was added to support the casing laterally, it was brought into plum manually and checked with a 1.2-m (4-ft) level. Subsequent casing lengths were added as the elevation of the fill increased until the facility was full. During filling, the verticality of the casings was checked after each lift, and when necessary was manually adjusted.

To use the inclinometer, it was first lowered down the casing until it reached the bottom. It was then raised through the fill, stopping every 0.2 m (0.7 ft) to 0.8 m (2.5 ft) so that the reading could be recorded. In the case of the series 200-B instrument data acquisition was manual, while for the model #50300940 readings were taken by a computer. The inclinometer was then removed and rotated 180° and the procedure was repeated. Measurements were recorded in the planes parallel and perpendicular to the front wall. Readings were taken before the front wall was tilted (zero reading) and at subsequent rotations of the front wall.

The output from the series 200-B instrument was in dial readings. It was converted to deflection at each elevation (stopping point) using the following formula:

$$d_{wb} = \left(\frac{l_r}{2k}\right) * \Delta\text{Dial} \qquad (4.7)$$

where k is a unitless instrument calibration factor, equal to 1934. l_r is the length of the measured interval, found by:

$$l_r = \frac{x_{r-1} + x_r}{2} \tag{4.8}$$

where x_r is the distance the inclinometer was raised and x_{r-1} is the previous distance the inclinometer was raised. This is shown graphically on Figure 4.7. ΔDial is found from the dial readings and is given by the following equation:

$$\Delta Dial = (D_{0°} - D_{180°})_n - (D_{0°} - D_{180°})_i \tag{4.9}$$

where: $D_{0°}$ = dial reading with inclinometer oriented 0°

$D_{180°}$ = dial reading with inclinometer oriented 180°

n = readings taken at subsequent rotations of the front wall

i = readings taken before rotation (zero reading)

Output from the model #50300940 was given in inches offset from vertical. The deflection was determined by first taking two sets of readings before rotation and then taking three sets of readings after rotation. The average of the before and after readings was computed. The deflection at each elevation was determined by taking the difference between the averages using the formula:

$$d_{wb} = o.s._{ave\_n} - o.s._{ave\_i} \tag{4.10}$$

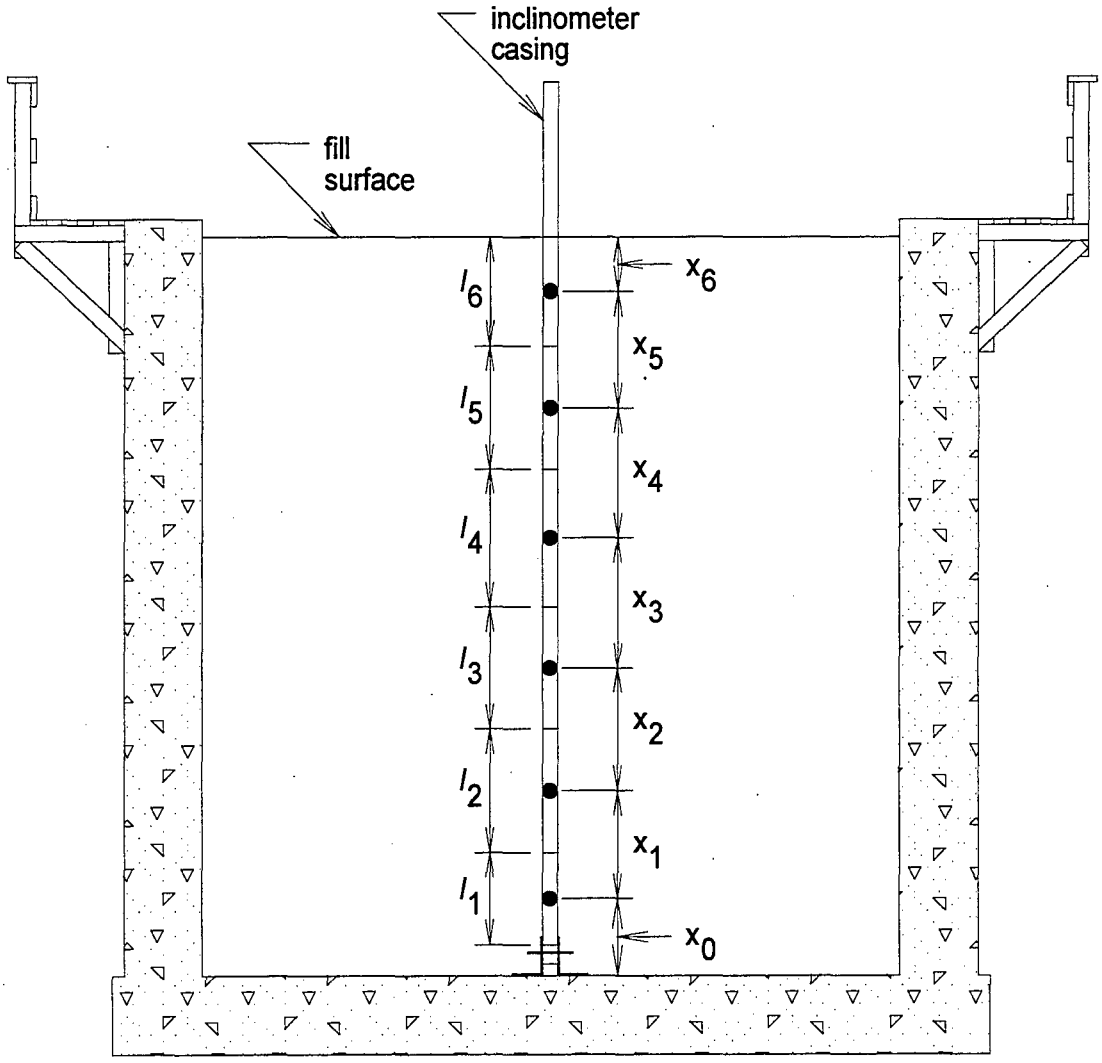

Figure 4.7 Determination of inclinometer measured interval

where $o.s._{ave\_n}$ and $o.s._{ave\_i}$ are the average of the offsets after and before rotation of the front wall, respectively.

4.2.3.2 Movement of Front Wall

Horizontal movement of the front wall was determined by measuring the change in horizontal distance at six points on each of the three panels that make up the front wall. On each panel, a pair of points were located at each of three elevations. The elevation of the reference points, with respect to the facility floor, are as follows: 0.38 m (1.25 ft), 2.29 m (7.50 ft), and 4.60 m (15.09 ft). The movement of the reference points was measured with respect to three reference beams. The reference beams were connected to the ends of the concrete side walls at elevations corresponding to the reference points. Each beam was made from two 4.87-m (16-ft) by 51-mm (2-in.) by 254-mm (10-in.) pieces of lumber screwed together to form a 90° angle. The reference beams at 0.38 m (1.25 ft) and 2.29 m (7.50 ft) were bolted directly to the ends of the concrete side walls. The reference beam at 4.60 m (15.09 ft) was bolted to a scrap peace of wide flange section 203 mm (8 in.) deep, which was then bolted to the ends of the concrete side walls. This was necessary to accommodate the outward rotation of the top of the front wall. The reference points and reference beams are shown on Figure 4.8.

The distance between the reference points and reference beams was measured with dial calipers accurate to 0.025 mm (0.001 in.). The initial distance between the reference points and the reference beam was measured when the facility was empty (zero reading).

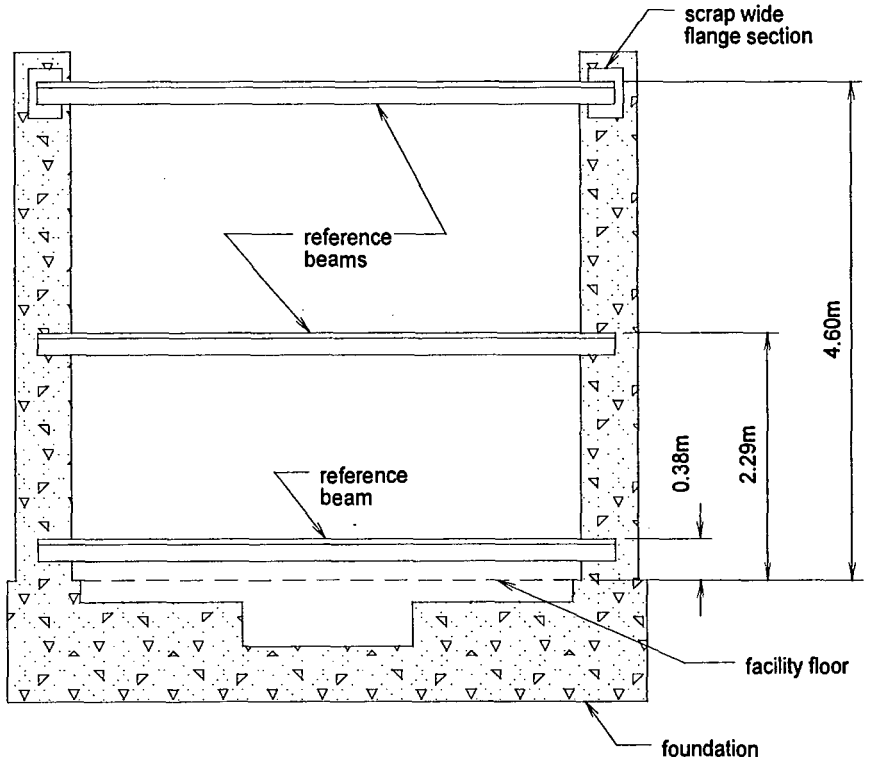

plan view of front of facility, showing location of reference beams
note: the front wall panels are not shown

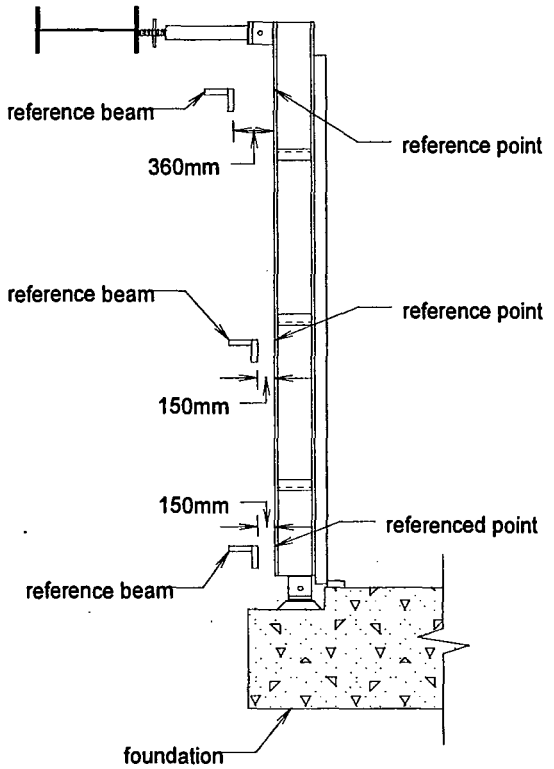

cross section through sidepanel, showing approximate
initial reference beam offsets before the start of a test

Figure 4.8 Reference points and reference beams

The deflection was then calculated by subtracting subsequent readings from the zero reading.

4.3 BACKFILL AND SURCHARGE PLACEMENT

4.3.1 Backfill

Granular and tire chip backfill was placed by filling a specially constructed skip bucket with fill and raising it over the back wall using the electric chain fall, as shown on Figure 3.13. The skip bucket was then lowered into the facility and emptied. Shovels and garden rakes were then used to spread the load. This process was repeated until sufficient fill was brought into the facility to complete a 200-mm (8-in.) lift, the lift was then compacted. The methods of compaction differed for the granular soil and the tire chips, as discussed below. Lifts were added until the facility was full. After filling the facility the resulting elevations differed slightly for each backfill type. The resulting elevations were as follows: granular, 4.57 m (15 ft); Pine State Recycling, 4.67 m (15.3 ft); Palmer Shredding, 4.88 m (16 ft); and F & B Enterprises, 4.88 m (16 ft).

The granular backfill was spread in layers of not more than 200 mm (8 in.) loose measure. Each lift was compacted with a 272-kg (600-lb) vibratory plate compactor.

Before the first test with tire chips, the method of compaction, lift thickness, and number of passes with a compactor was determined. Compaction of the tire chips was initially attempted with a 272-kg (600-lb) vibratory plate compactor. This method was ineffective, because the tire chips provided a base that was too soft to allow the

compactor to be moved forward and back. As a result, an alternate method of compaction was chosen. The compactor used for all tire chip tests was a walk-behind vibratory tamping foot roller (Stone Bulldog model BD33) with a static weight of 1180 kg (2600 lb).

In selecting the lift thickness and number of compactor passes, the goal was to produce the highest density that could reasonably be obtained with the compactor. This was investigated by constructing a box 0.61 m (2 ft) high by 3.05 m (10 ft) long by 1.02 m (3.3 ft) wide, with no top or bottom. A layer of Pine State chips was then spread onto the floor of the test facility to approximate a layer of preexisting tire chips. A piece of clear plastic was then put over the tire chips and the box was placed on the plastic. The plastic was required to maintain a boundary between the previously placed tire chips and the current lift. Then 100 mm (4 in.) of loose tire chips was put into the box. The compactor was lowered into the box with the chain fall and two passes were made. The compactor was then lifted out of the box and the resulting density was calculated.

The density was calculated by first determining the volume of tire chips. This was done by measuring the thickness of the compacted tire chips from the surface to the layer of plastic. This along with the dimensions of the box made it possible to determine the volume of tire chips. Then the contents of the box were removed and weighed. With this information the density could be determined. Subsequent trials with 100 mm (4 in.) and four and six passes of the compactor were performed. These were followed by trials with 200-mm (8-in.) and 300-mm (12-in.) lifts with two, four, and six passes of the compactor.

The optimum number of passes determined was four with a lift thickness of 200 mm (8 in.). Subsequent trials were not performed for Palmer Shredding and F & B Enterprises.

4.3.2 Surcharge

The surcharge was applied by 350-kg (780-lb) surcharge blocks, described in Section 3.6. The surcharge blocks were applied using a lifting arm capable of picking up two blocks simultaneously. The blocks were lifted by the electric chain fall and physically manipulated into position. A total of 36 surcharge blocks was required to complete one layer of blocks, resulting in a surcharge of 6.0 kPa (125 psf). To apply the maximum surcharge of 35.9 kPa (750 psf) six layers of blocks were required, for a total of 216, as shown on Figures 3.12 and 3.15.

4.4 MEASUREMENTS

The measurements taken during this research included those to determine the backfill material properties and backfill behavior. The backfill behavior was measured as the test facility was being filled and after filling. Measurements taken after filling were obtained for at-rest and active conditions.

4.4.1 Material Properties

For each backfill type, the gradation and field density was determined. For the granular fill the maximum laboratory compacted dry density was also determined.

4.4.1.1 Granular Fill

The granular fill to be used for the control test was to meet Maine Department of Transportation (MDOT) requirements for "gravel borrow" used for backfilling major structures. These requirements state that the gravel borrow shall consist of well-graded granular material having no particles with a dimension over 76 mm (3 in.) and with not more than 10 percent passing the No. 200 mesh sieve. In addition, the dry density of the compacted fill shall be at least 90% of the modified Proctor maximum density.

A total of five gradations were performed on the granular soil. The tests were performed in accordance with AASHTO T 146-88, Method B, "Wet Preparation of Disturbed Soil Samples for Test" and AASHTO T 88-90, "Particle Size Analysis of Soils" (AASHTO, 1990). The following sieve openings were used: 50.8-mm (2-in.), 25.4-mm (1-in.), 12.7-mm (1/2-in.), 6.4-mm (1/4-in.), standard #4, standard #20, standard #40, and standard #200.

The density in the field (ρ_{field}) for the granular soil was determined in accordance with AASHTO T 191-86 "Density of Soil In-Place by the Sand-Cone Method" (AASHTO, 1990). Field density measurements were taken at seven different locations during filling of the facility. Water contents (w) were also determined for samples obtained from the field density tests.

The maximum dry density (ρ_{d_max}) for the granular soil was determined in accordance with AASHTO T 180-90, Method D, "Moisture-Density Relationships of Soils Using a 10 lb [4.54 kg] Rammer and an 18 in. [457 mm] Drop" (AASHTO, 1990). Two tests

were performed. Results from the field density tests and the maximum dry density were used to determine the percent compaction.

4.4.1.2 Tire Chips

Gradation tests were performed on tire chips from each supplier. The gradations were determined in accordance with AASHTO T 27-88, "Sieve Analysis of Fine and Coarse Aggregates" (AASHTO, 1990). The following sieve openings were used for Pine State Recycling and Palmer Shredding: 76.2-mm (3-in.), 50.8-mm (2-in.), 38.1-mm (1-1/2-in.), 25.4-mm (1-in.), 19.1-mm (3/4-in.), 12.7-mm (1/2-in.), and standard #4. The same sieve openings were used for F & B Enterprises except that the 76-mm (3-in.) was omitted. A total of six tests were performed for Pine State Recycling and F & B Enterprises, and three for Palmer Shredding.

The field density (ρ_{field}) for tire chips was determined by putting a piece of clear plastic on the surface of a previously compacted lift. A box, 0.61 m (2 ft) high by 3.05 m (10 ft) long by 1.02 m (3.3 ft) wide with no top or bottom, was then placed on top of the plastic. The plastic was required to maintain a boundary between the previously lift and the current lift. The box was then filled with loose tire chips equal to one 200-mm (8-in.) thick lift. The compactor was lowered into the box with the chain fall and four passes were made. The compactor was then lifted out of the box and ρ_{field} was calculated. The field density was calculated using the method discussed in Section 4.3. Test frequency was approximately one test for every 19 m^3 (25 yd^3) of backfill placed, resulting in five tests for each tire chip type.

4.4.2 Measurements During Filling

The field density was determined for each backfill type during filling, as discussed in Section 4.4.1. Other measurements were also taken, including: settlement, front wall deflections, and force and stress measurements. A set of measurements was taken after every two lifts of backfill were placed. The settlement from the settlement plates, as discussed in Section 4.2.2.1, was measured to determined compression during filling. The front wall deflections, as discussed in Section 4.2.3.2, were monitored during filling of the facility to confirm that no substantial movements were taking place. The horizontal and vertical forces and horizontal stress were monitored by the load cells and pressure cells, as discussed in Sections 4.2.1.1 and 4.2.1.2. Readings from each pressure cell were initiated once the fill reached the elevation of the cell.

4.4.3 Measurements for At-Rest Conditions

Several measurements were made to monitor behavior for the at-rest condition under each of the following surcharges: no surcharge, 12.0 kPa (250 psf), 23.9 kPa (500 psf), and 35.9 kPa (750 psf). To investigate the effects of creep on the measurements, the maximum surcharge was left in place for several days and additional readings were taken. The effect of repeated loadings on the at-rest condition and the amount of rebound/compression that would occur on unloading/reloading was investigated. This was done by removing the maximum surcharge and then reapplying it a minimum of two times. In cases where the surcharge was left in place for a day or more, several readings were taken at periodic time intervals.

The measurements taken for the at-rest condition included horizontal and vertical forces, and horizontal pressures. Settlement was also measured with the settlement plates and the settlement grid. In addition, the deflection of the front wall was measured. The following paragraphs discuss each of the measurements and its contribution to developing design recommendations.

The load cell readings (Section 4.2.1.1) and the pressure cell readings (Section 4.2.1.2) were used to determine the horizontal stress distribution. The horizontal stress along with the vertical stress were used to calculate the coefficient of lateral earth pressure at rest (K_o). Measurements of the vertical and horizontal force on the wall were used to determine the interface friction angle between the backfill and the front wall.

Vertical settlement was measured using the settlement plates (Section 4.2.2.1) and settlement grid (Section 4.2.2.2). The measurements allowed for the vertical compressibility and material density to be determined for each surcharge and each tire chip supplier. Measurements were recorded for the granular control fill, however, no substantial settlement occurred and settlement results for the granular soil are not presented.

The front wall deflections were determined using methods discussed in Section 4.2.3.2. The movement of the front wall was monitored to confirm that movements were small. In dense cohesionless soils the amount of movement at the top of the wall caused by outward rotation about the base needed create active conditions is 0.001 to 0.002H

(Bowles, 1988), where H is the height of the wall. The front wall movements were measured for each surcharge and all tests.

4.4.4 Measurements for Active Conditions

The active earth pressure condition was investigated with the maximum surcharge of 35.9 kPa (750 psf) applied. The front wall was rotated outward about its base in increments, as discussed in Section 3.3. To investigate the effects of creep, the wall was left at varying angles of rotation for a few days, during which measurements were taken at periodic time intervals. For the granular fill, Pine State Recycling, and Palmer Shredding, the front wall was rotated until the surcharge blocks nearest the wall started to lean forward at an ominous angle. For F & B Enterprises, a smaller amount of rotation was used. At each increment, the measurements discussed in Section 4.4.3 for the at-rest condition were taken. In addition, the horizontal movement within the backfill was measured using inclinometers (Section 4.2.3.1). The significance of each measurement to the design criteria is discussed below.

Measurements of the horizontal and vertical forces (Section 4.2.1.1), and horizontal stress (Section 4.2.1.2) on the wall were used to determine the distribution of horizontal stress versus elevation. With this and knowledge of the vertical stress in the backfill, the coefficient of active earth pressure (K_a) was determined. Measurements of vertical settlement using surface measurements from the settlement grid, as discussed in Section 4.2.2.2, combined with measurements of the horizontal movement within the backfill

measured with inclinometers, as discussed in Section 4.2.3.1, made it possible to estimate the pattern of movement in the backfill as the wall was rotated outward.

4.5 SUMMARY

The test protocol was developed to determine the data necessary for a design criteria for using tire chips as lightweight backfill for retaining walls. This was done by testing tire chips from three suppliers, along with a conventional granular backfill. The test protocol included instrumentation, backfill and surcharge placement, and measurements.

The instrumentation included load cells and pressure cells to measure the horizontal and vertical forces acting on the instrumented wall, and horizontal stress produced by the backfill. Settlement plates embedded in the fill and a settlement grid located on the surface of the fill were used to measure the vertical settlement of the tire chips. Inclinometers were installed to measure horizontal displacement within the backfill. Reference beams and reference points were used to measure the horizontal movement of the front wall.

Backfill was brought into the facility by way of a skip bucket and an electric chain fall. Lifts of granular backfill were compacted with a vibratory plate compactor. Tire chips were compacted with a walk-behind vibratory tamping foot roller. The elevations of the backfills ranged from 4.57 m (15 ft) to 4.88 m (16 ft). The surcharge was applied with 350-kg (780-lb) concrete blocks. The surcharge blocks were placed on the backfill using the electric chain fall. The maximum surcharge was 35.9 kPa (750 psf).

Measurements taken included those to determine backfill material properties, such as gradations and the maximum dry density for the granular soil. Other measurements were recorded during filling of the facility and after filling. The measurements taken after filling were obtained for the at-rest and active conditions. During filling of the facility, measurements included field density, settlement, horizontal displacement of the front wall, and the force and stress acting on the front wall.

For the at-rest condition, the forces and stresses acting on the front wall, settlement, and horizontal displacement of the front wall were measured. The force and stress measurements made it possible to determine the change in horizontal stress with depth and the coefficient of lateral earth pressure at rest. The angle of wall friction was calculated from the vertical and horizontal forces. Measurement of the settlement allowed for examination of the compressibility characteristics. The horizontal displacement of the front wall was measured to confirm that the amount of movement of the front wall was small enough to maintain at-rest conditions.

Active state measurements consisted of those taken for the at-rest condition, with the addition of the horizontal movement within the backfill. Measurement of the forces and stress allowed for the horizontal stress distribution and the coefficient of active earth pressure to be determined. The settlement of the fill surface coupled with measurement of horizontal movement within the backfill were used to estimate the pattern of fill movement.

(BLANK)

CHAPTER 5. SOIL AND TIRE CHIP PROPERTIES

5.1 INTRODUCTION

Material properties were determined for the granular fill used as a control test and the three tire chip suppliers: Pine State Recycling, Palmer Shredding, and F & B Enterprises. The properties determined for the granular fill included: gradation, modified Proctor maximum dry density, field density, field water content, and percent compaction. The properties determined for the tire chips were gradation and field densities.

5.2 GRANULAR FILL

5.2.1 Gradation

The gravel backfill used for the control test met Maine Department of Transportation (MDOT) requirements for "gravel borrow" used for backfilling major structures. These requirements state that the gravel borrow shall consist of well-graded granular material having no particles with a dimension over 76 mm (3 in.) and with not more than 10 percent passing the No. 200 mesh sieve. Gradations were found using AASHTO T 146-88 and AASHTO T 88-90, as discussed in Section 4.4.1.1.

Results from the gradation analysis are presented in Figure 5.1. As required by the MDOT specifications, the gradation shows that there are no particles over 76 mm (3 in.) and less than 10% passed the #200 sieve.

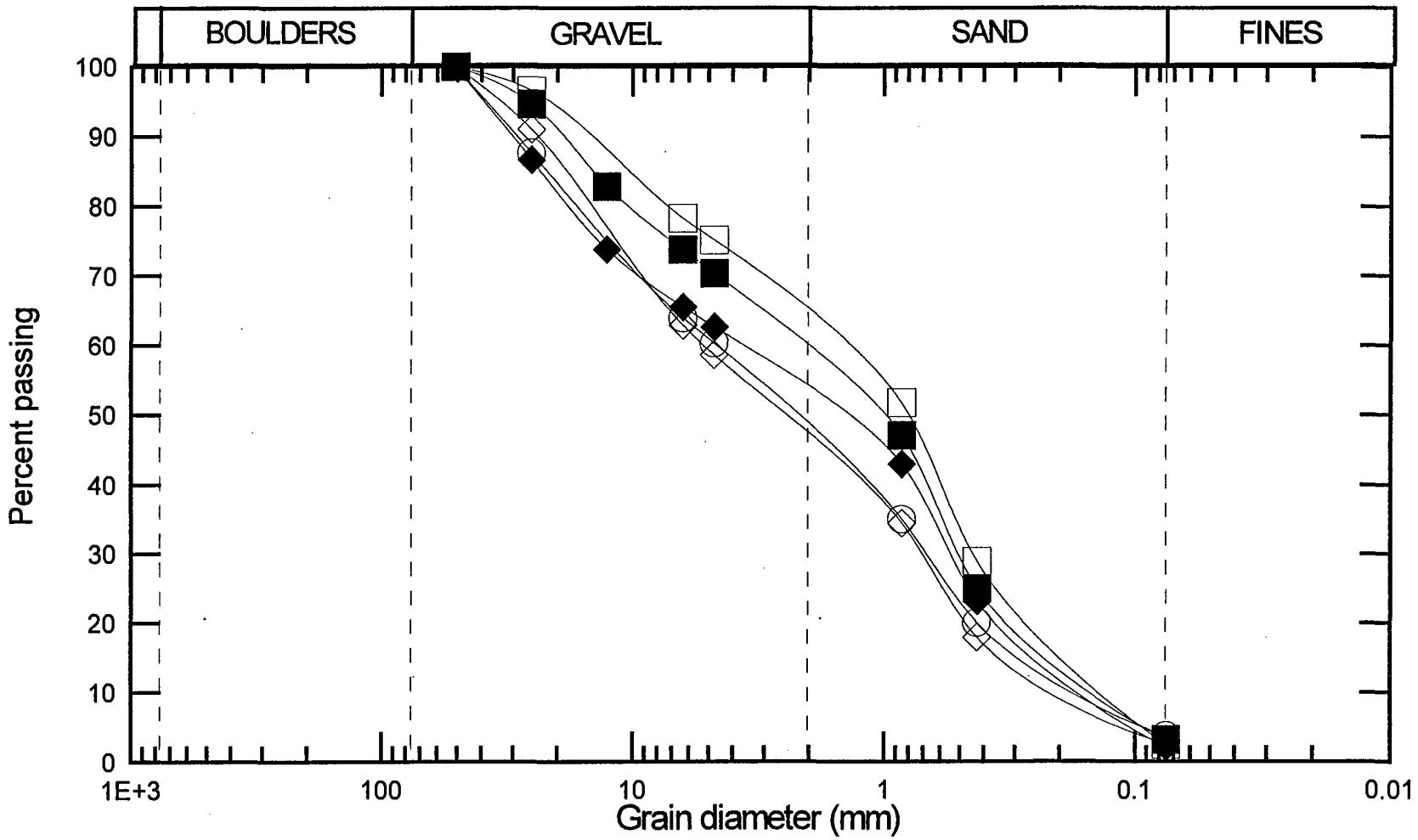

Figure 5.1 Gradation, granular fill

5.2.2 Maximum Dry and Field Densities

The maximum dry density (ρ_{d_max}) was determined using AASHTO T 180-90, as discussed in Section 4.4.1.1. A total of two tests were performed. The compaction curves are shown on Figure 5.2. This shows that for the two compaction tests, the maximum dry densities were 2.083 Mg/m^3 (130.2 pcf) and 2.056 Mg/m^3 (128.5 pcf) and the optimum water contents were 9.0% and 9.7%, respectively.

The dry density in the field (ρ_{d_field}) was determined using AASHTO T 191-86, as discussed in Section 4.4.1.1. Seven field density measurements were taken at random locations during filling of the facility. The water content (w) was also determined from the samples used from the field density tests.

The requirements for this study were based on Maine Department of Transportation requirements for structural backfill. They stated that the granular fill shall be compacted to a minimum of 90% of the maximum dry density. To determine the percent compaction it was necessary to estimate the maximum dry density using the values from the two tests described above. The maximum dry density was taken to be 2.066 Mg/m^3 (129.0 pcf), which is between the values determined from the laboratory compaction tests. Using the maximum dry density and the values obtained from the field density tests the percent compaction can be determined using the following equation:

$$\%comp = \left(\frac{\rho_{d\_field}}{\rho_{d\_max}} \right) * 100 \qquad (5.1)$$

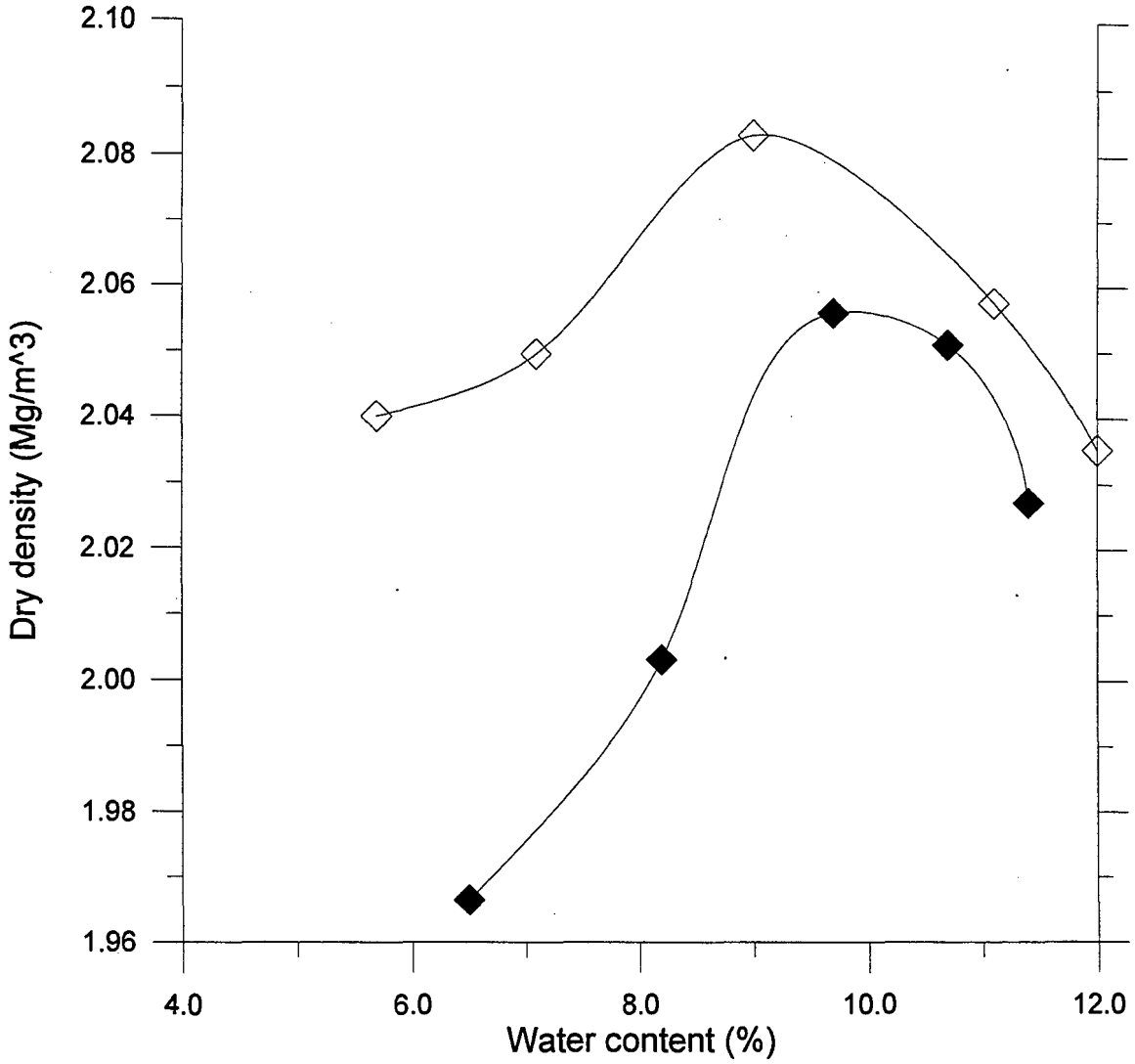

Figure 5.2 Compaction tests results, granular fill

A summary of the field densities, water contents, and the percent compaction is shown on Table 5.1

Table 5.1 Dry field densities, water contents, and percent compaction for granular fill

Dry field density (Mg/m^3)	Water content (%)	Percent compaction (%)
1.941	3.6	94
1.989	3.7	96
1.913	2.9	93
1.916	3.5	93
1.985	3.6	96
2.046	3.6	98
1.885	3.8	91

5.3 TIRE CHIPS

Visual inspection of the tire chips from the three suppliers showed that Pine State Recycling and Palmer Shredding tire chips contained significantly more steel belts than tire chips from F & B Enterprises. F & B Enterprises tire chips contained few steel belts.

5.3.1 Gradations

The gradations were found using AASHTO T.27-88, as discussed in Section 4.4.1.2. The results are shown on Figures 5.3 through 5.5 for Pine State Recycling, Palmer

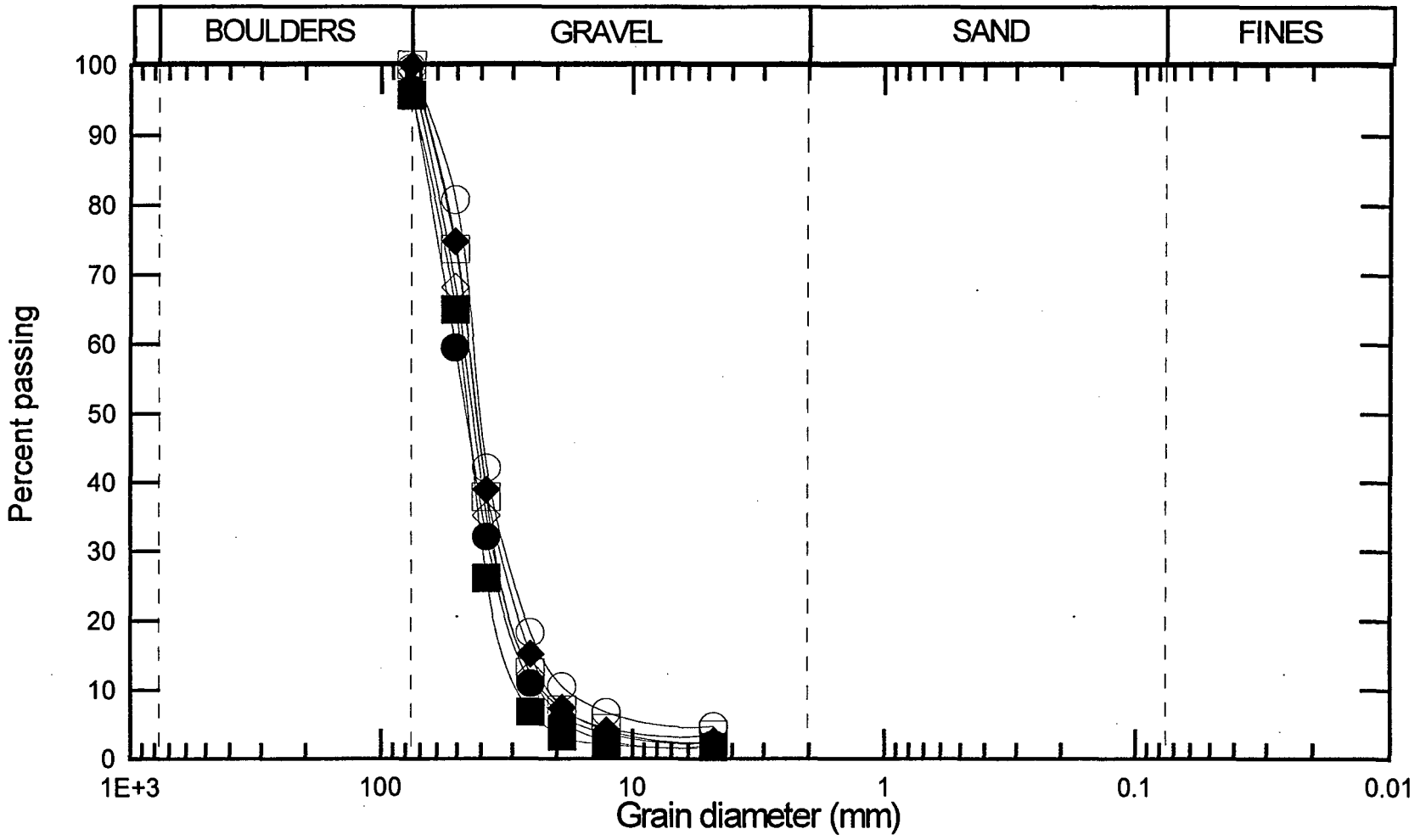

Figure 5.3 Gradation, Pine State Recycling

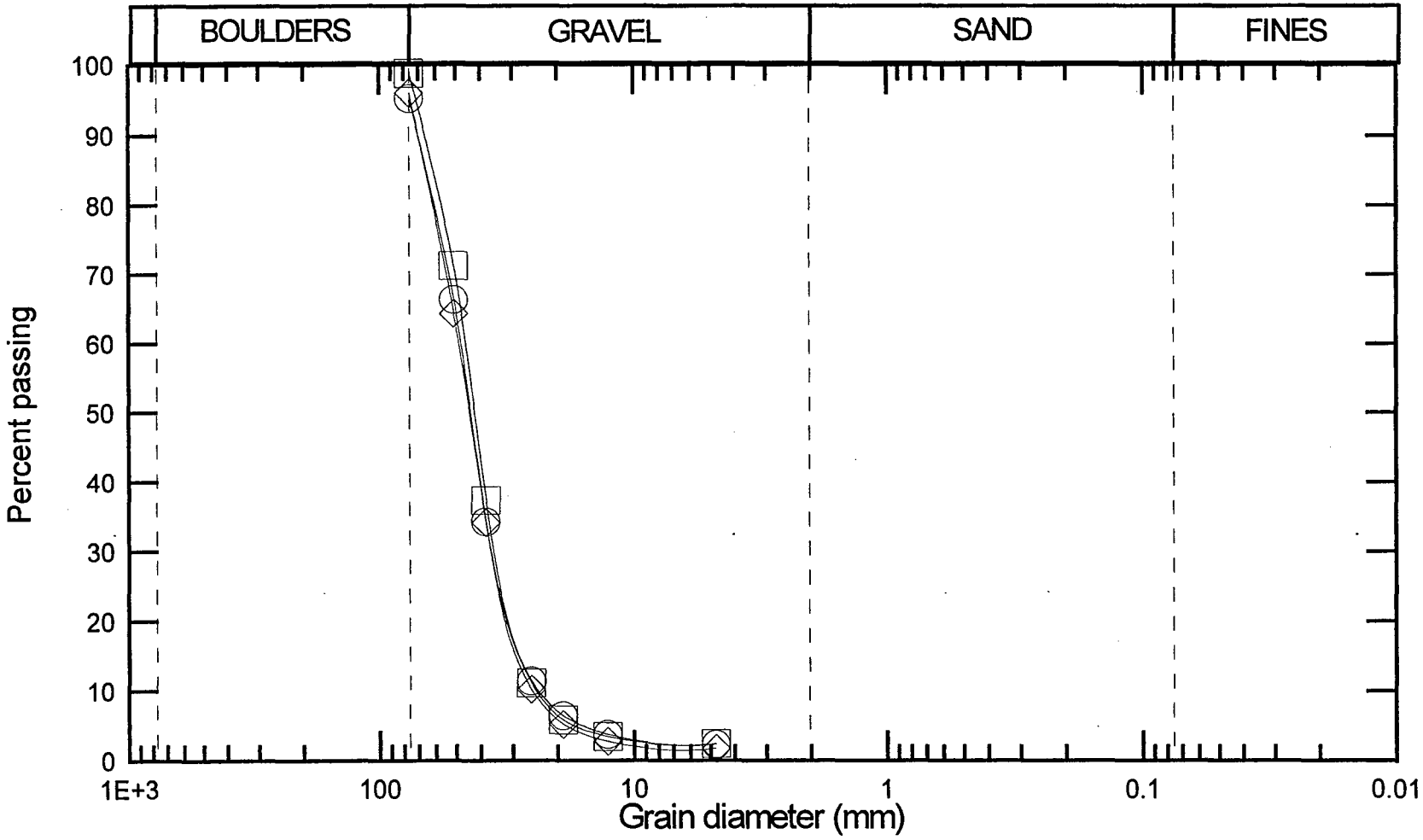

Figure 5.4 Gradation, Palmer Shredding

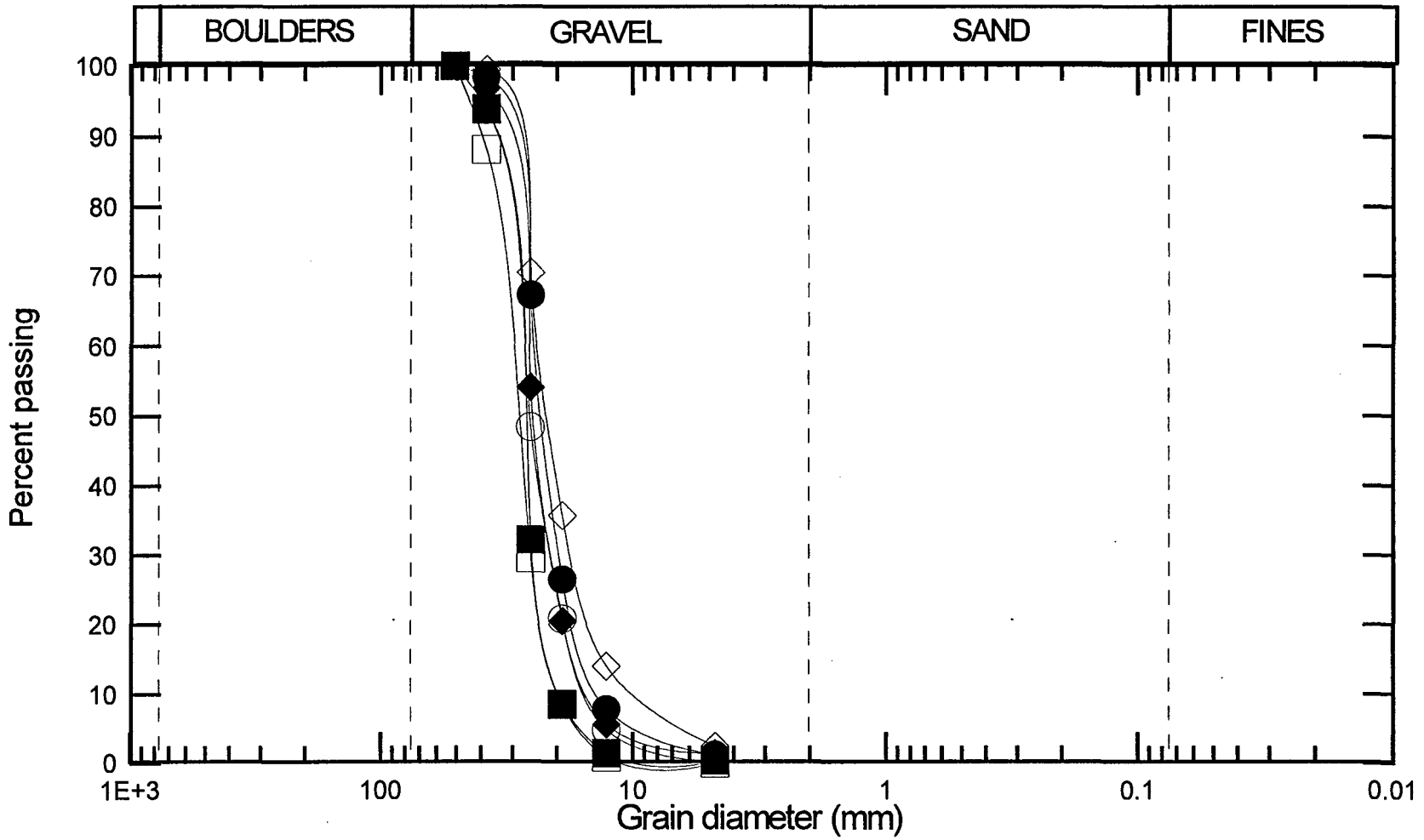

Figure 5.5 Gradation, F & B Enterprises

Shredding, and F & B Enterprises, respectively. Pine State Recycling and Palmer Shredding have similar gradations. Examination of Figures 5.3 and 5.4 shows 25% to 40% pass the 38.1-mm (1-1/2-in.) sieve for Pine State Recycling, while about 35% pass for Palmer Shredding. Between 5% and 12% fall between the 25.4-mm (1-in.) and 12.7-mm (1/2-in.) sieves for Pine State Recycling, with about 8% for Palmer Shredding. Figure 5.5 shows the F & B Enterprises samples are the finest with 88% to 100% passing the 38.1-mm (1-1/2-in.) sieve and 30% to 55% falling between the 25.4-mm (1-in.) and 12.7-mm (1/2-in.) sieves.

The gradation analysis can be compared to Humphrey, et al. (1992) who performed gradations on tire chips from the same suppliers. These gradation analyses are shown on Figure 2.1, along with gradation results for tire chips from Sawyer Environmental Recovery performed by Manion and Humphrey (1992). Examination of Figures 5.3 and 2.1 show that the Pine State Recycling tire chips tested by Humphrey, et al. (1992) were finer than the ones used for this study. Comparison of Figures 5.4 and 2.1 shows that the Palmer Shredding tire chips used for both studies were similar in their grain size distribution, although the ones used for this project were slightly finer than those tested by Humphrey, et al. (1992). When Figures 5.5 and 2.1 are compared, they show that the F & B Enterprises tire chips from this study are slightly coarser.

5.3.2 Field Densities

Due to the large particle size and large volume of voids of tire chips, conventional methods of measuring the density in the field could not be utilized. As a result, an

alternative method was developed, as discussed in Section 4.4.1.2. The tire chips at the time of weighing were at the field water content, thus the computed density is the wet field density (ρ_{w_field}). Test frequency was no less than one test for every 19 m^3 (25 yd^3) of backfill placed, resulting in five tests for each tire chip supplier. A summary of the field densities is shown on Table 5.2.

Table 5.2 Summary of wet field densities for tire chips

Pine State Recycling	**Palmer Shredding**	**F & B Enterprises**
Wet field density (Mg/m^3)		
0.73	0.67	0.69
0.73	0.67	0.70
0.75	0.70	0.68
0.66	0.66	0.77
0.66	0.76	0.72
Average wet field density (Mg/m^3)		
0.71	0.69	0.71

Examination of the values in Table 5.2 show that the field densities for the three types of tire chips are very similar. These values can be compared to the dry densities reported by Humphrey, et al. (1992). Humphrey, et al. (1992) performed compaction tests on tire chips from the same suppliers, finding densities of 0.64 Mg/m^3 (40.1 pcf) for Pine State Recycling, 0.62 Mg/m^3 (38.7 pcf) for Palmer Shredding, and 0.62 Mg/m^3 (38.6 pcf) for F & B Enterprises. These are also shown on Table 2.2. These densities are less than those

found for this project. This can be partially explained by the fact that the tire chips used in Humphrey, et al. (1992) were air dried tire chips, while those in this study were wet. The field water content of the tire chips used it this study was not measured. However, if a value of 3% is assumed for the water content, the dry field densities can the determined from the average wet field densities using the following:

$$\gamma_{d\_field} = \gamma_{w\_field}(1 + w) \tag{5.2}$$

The resulting dry field densities would be 0.69 Mg/m^3 (43.0 pcf) for Pine State Recycling, 0.67 Mg/m^3 (41.8 pcf) for Palmer Shredding, and 0.69 Mg/m^3 (43.0 pcf) for F & B Enterprises. These are larger than those determined by Humphrey, et al. (1992) by 7% to 10%.

(BLANK)

CHAPTER 6. HORIZONTAL EARTH PRESSURE

6.1 INTRODUCTION

The primarily goal of this research was to examine the horizontal pressures exerted by tire chips on a retaining wall. This was done by measuring the horizontal pressures and horizontal forces on the front wall center panel of the test facility, for both at-rest and active conditions. The methods used to obtain these measurements were discussed in Section 4.2.1. The results obtained from the test measurements will be discussed for each backfill type for both at-rest and active conditions. In addition, selected results from tire chips will be compared to a finite element analysis by Gharegrat (1993). In the next section, earth pressure parameters are developed. The final section discusses considerations for design.

6.2 MEASUREMENT AND CALCULATION PROCEDURES

The horizontal stresses and forces were recorded for at-rest conditions, for the following surcharges: no surcharge, 12.0 kPa (250 psf), 23.9 kPa (500 psf), and 35.9 kPa (750 psf). In addition, measurements were taken with a surcharge of 35.9 kPa (750 psf) and the front wall rotated outward away from the fill, to simulate active conditions. The number of readings for each loading condition and backfill type varied. The horizontal stress distribution was determined for each loading condition using measurements from the load cells and pressure cells.

6.2.1 Load Cells

To determine the horizontal stress distribution, the forces were measured at the top and bottom of the center panel by the horizontal and vertical load cells (Figures 3.3, 3.8, and 3.10). The horizontal stress distribution was determined by analysis of a free body diagram of the center panel, as shown on Figure 6.1. It was assumed that the horizontal stress exerted by the backfill and surcharge on the wall varied linearly with depth. The sum of the forces measured by the two horizontal load cells located at the top is shown as F_{top}. The sum of the forces measured by the two horizontal load cells located at the bottom is F_{bottom} and the sum of the forces measured by the two vertical load cells is shown as $F_{vertical}$. The magnitude of the resultant force exerted on the wall by the backfill is equal to the sum of F_{top} and F_{bottom}, shown as F_{result}. The location of F_{result} can be determined by summation of the moments about the bottom hinge, given by:

$$x = \frac{\left(F_{top} d_v + V_f d_h\right)}{F_{result}} \tag{6.1}$$

where d_v is the vertical distance from the bottom hinge to the top hinge, 4.98 m (16.3 ft), and d_h is the horizontal distance from the bottom hinge to the wall face, 0.22 m (0.71 ft). The shear force is shown as V_f on Figure 6.1 and Equation 6.1, and is equal to $F_{vertical}$.

Once the location of the resultant is determined and the depth of fill (d) is known, the top value of the horizontal stress distribution can be determined by:

$$\sigma_{top} = \left(\frac{6F_{result}x}{d^2} - \frac{2F_{result}}{d}\right) * \frac{1}{w_{ip}} \tag{6.2}$$

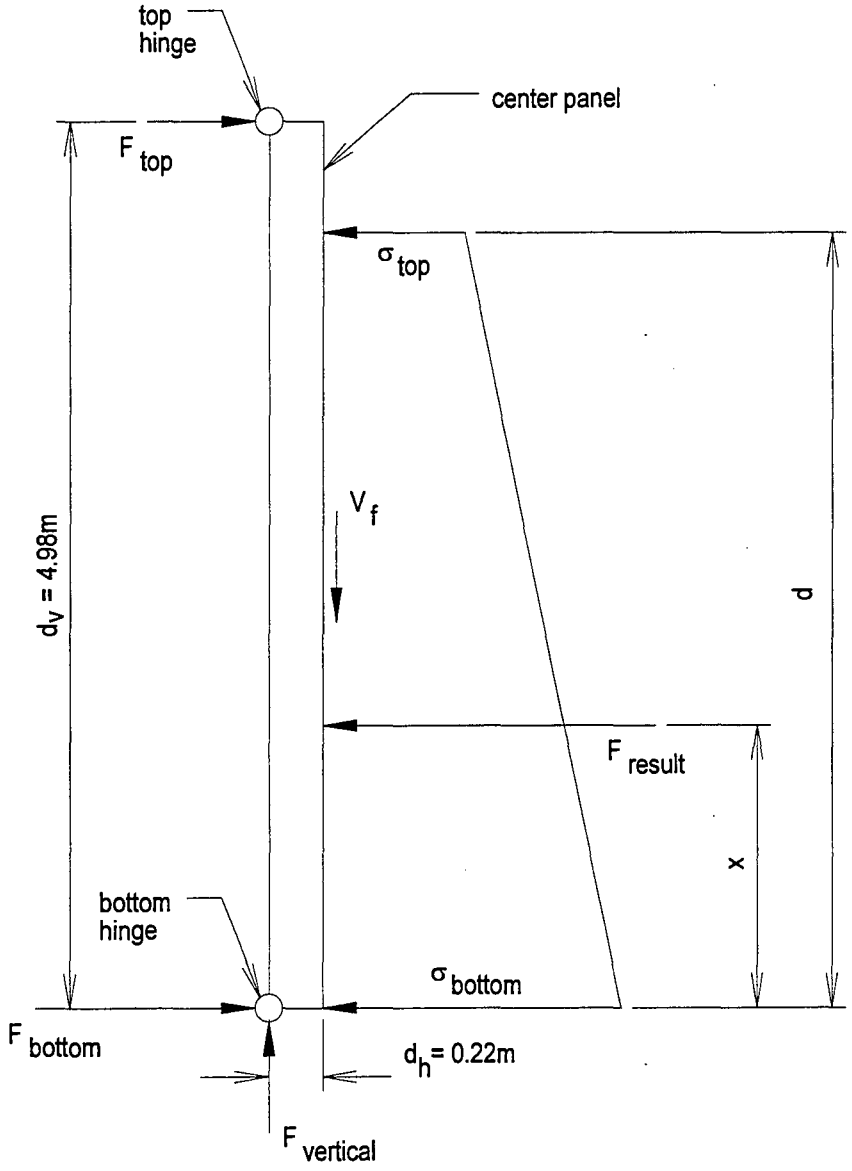

Figure 6.1 Free-body diagram of center panel

where w_{ip} is the width of the center panel, 1.47 m (4.82 ft). Once σ_{top} is known the horizontal stress at the bottom of the fill can be determined by the following equation:

$$\sigma_{bottom} = \frac{2F_{result}}{dw_{ip}} - \sigma_{top} \tag{6.3}$$

6.2.2 Pressure Cells

The horizontal pressures acting on the wall were measured by the four pressure cells located as shown on Figures 3.3 and 4.1. The pressure cells were only calibrated for tire chips so only results for tire chips are presented. Three correction factors are used to convert the readings from the pressure cells to the applied stress. The first factor converts the reading to an uncorrected applied stress. The other two factors correct the applied stress for temperature change relative to the initial reading and barometric pressure. The calibration factor for stress, CF_{ps}, was determined in two ways, as discussed in Section 4.2.1.2. In method one the stress was applied to the pressure cell using a 230-mm (9-in.) diameter container filled with tire chips, while in method two a 1.52-m by 1.52-m (5.0-ft by 5.0-ft) container filled with tire chips was used. The correction factor for temperature, T_k, was determined by two trials using a 230-mm (9-in.) diameter container filled with tire chips, as discussed in Section 4.2.1.2. The correction for changes in barometric pressure was performed using the factor recommended by the manufacturer.

Results from the pressure cells are presented in four ways using the calibration combinations summarized below.

calibration combination #1: CF_{ps} from method one, T_k from trial one

calibration combination #2: CF_{ps} from method one, T_k from trial two

calibration combination #3: CF_{ps} from method two, T_k from trial one

calibration combination #4: CF_{ps} from method two, T_k from trial two

The correction factor for barometric pressure recommended by the manufacturer was used for all four calibration combinations. Calibration of the pressure cells, procedures used to determined the correction factors, and the correction factor values were discussed in Section 4.2.1.2.

6.3 AT-REST CONDITIONS

The horizontal stresses for the at-rest condition were examined for the following surcharges: no surcharge, 12.0 kPa (250 psf), 23.9 kPa (500 psf), and 35.9 kPa (750 psf). The effects of repeated unloading and reloading were examined by removing and reapplying the maximum surcharge of 35.9 kPa (750 psf) a minimum of two times. Changes in stress with time were also investigated by examining Palmer Shredding chips during the Winter of 1994-95.

6.3.1 Initial Loading

When a surcharge was left in place for periods of time ranging from one day to several months it was possible to collect more than one set of readings. It was observed that the stresses did not tend to increase or decrease with time. However, the readings did tend to fluctuate somewhat about a central value. Consequently, the results presented in

this section were obtained by taking the average of the values determined from the load cells and the pressure cells from all of the readings at each surcharge during the initial loading. Tire chips results were compared to a finite element analysis by Gharegrat (1993).

6.3.1.1 Granular Fill

The horizontal stress versus fill elevation as determined by the load cells for the granular fill is shown in Figure 6.2. This shows that the horizontal stress increases with increasing surcharge. It also shows that the stress distribution for all four loading conditions is trapezoidal in shape, with the value at the base of the fill being lower than at the top of the fill. This deviates considerably from the distribution expected from classical earth pressure theory, namely, horizontal stress increasing linearly with depth. One possible explanation for the horizontal stress decreasing with depth is presence of apparent cohesion, which may have developed in this well graded, partially saturated soil, resulting in a temporary increase in strength and reduction in horizontal stress. The horizontal stress at the surface may also be larger due to an increase in the horizontal pressure caused by compaction. Compaction of backfill behind a wall can increase the horizontal stress in the upper elevation of the fill (Ingold, 1979). In addition, the high angle of wall friction (discussed in Section 7.2.1), and arching between the concrete side walls may have contributed to the lower pressures. This will be discussed more fully in Chapter 9, where data on the location of the active failure surface is discussed.

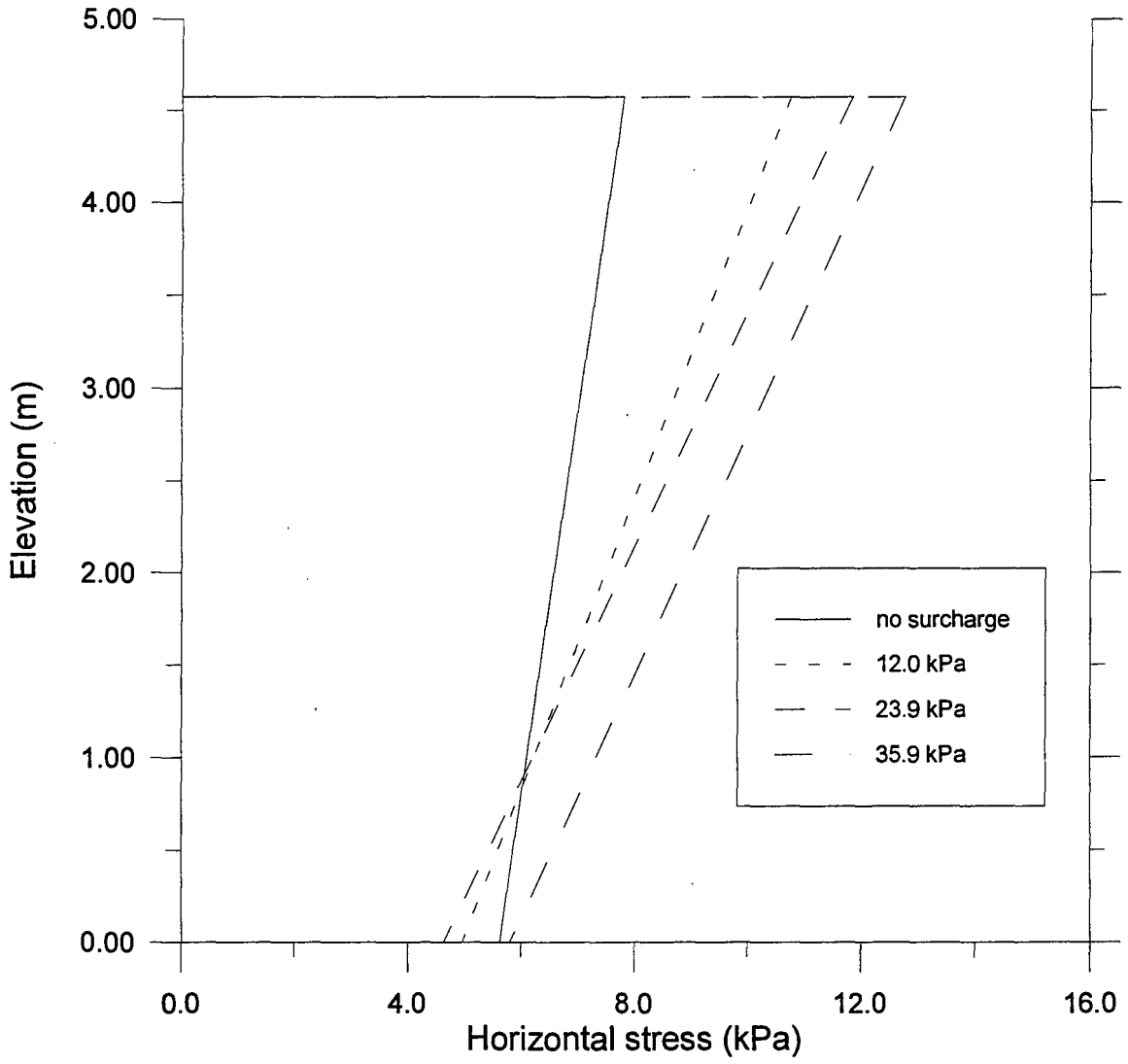

Figure 6.2 Horizontal stress vs. elevation, at-rest conditions (loading), granular fill

Variations in the vertical load cell readings were observed as the temperature increased during the day. However, these variations had little influence on the horizontal stress distribution at different surcharges. Their influence is greater for the unload/reload cycles, as discussed in Section 6.3.2.1. The magnitude of the variations in vertical load cell readings is discussed in Section 7.2.1.

6.3.1.2 Tire Chips

The horizontal stress versus fill elevation for initial application of surcharge, as determined by the load cells, for Pine State Recycling, Palmer Shredding, and F & B Enterprises are shown in Figures 6.3, 6.4 and 6.5, respectively. These figures show that the horizontal stress increases with increasing surcharge. In each case at the lower surcharges, the horizontal stress increases with depth; but at the higher surcharges, the horizontal stress becomes almost constant with depth.

For each of the tire chip types, the shape of the horizontal stress distributions and the magnitude of the horizontal stresses are similar for no surcharge and the 12.0 kPa (250 psf) surcharge. However, for Palmer Shredding (Figure 6.4) the stress at the top of the fill is slightly larger for the 23.9 kPa (500 psf) and 35.9 kPa (750 psf) surcharges than for Pine State Recycling and F & B Enterprises. Also, the horizontal stress for Palmer Shredding chips increases less with depth at the intermediate surcharge, and at the maximum surcharge the horizontal stress actually decreases somewhat with depth.

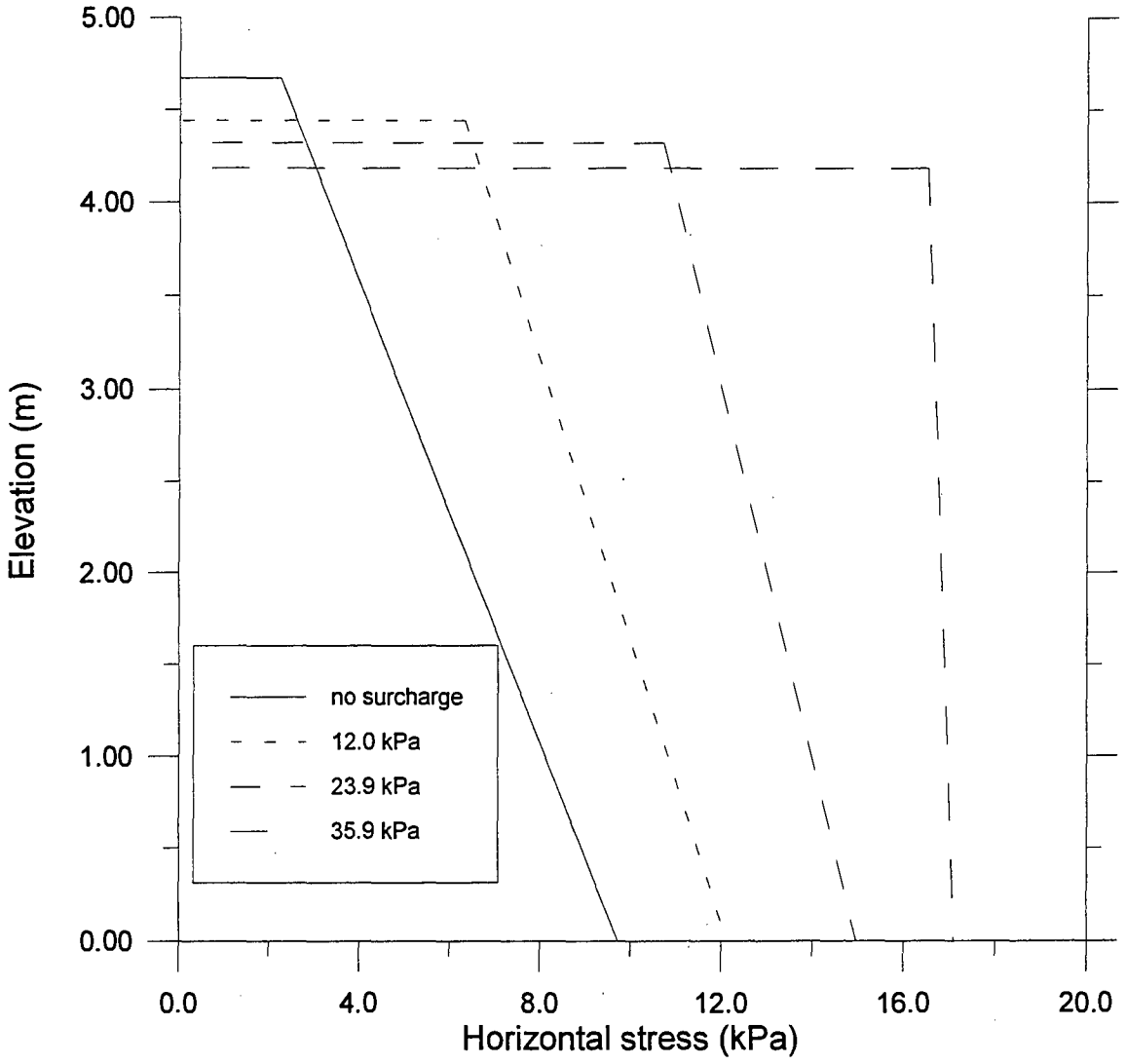

Figure 6.3 Horizontal stress vs. elevation, at-rest conditions (loading), Pine State Recycling

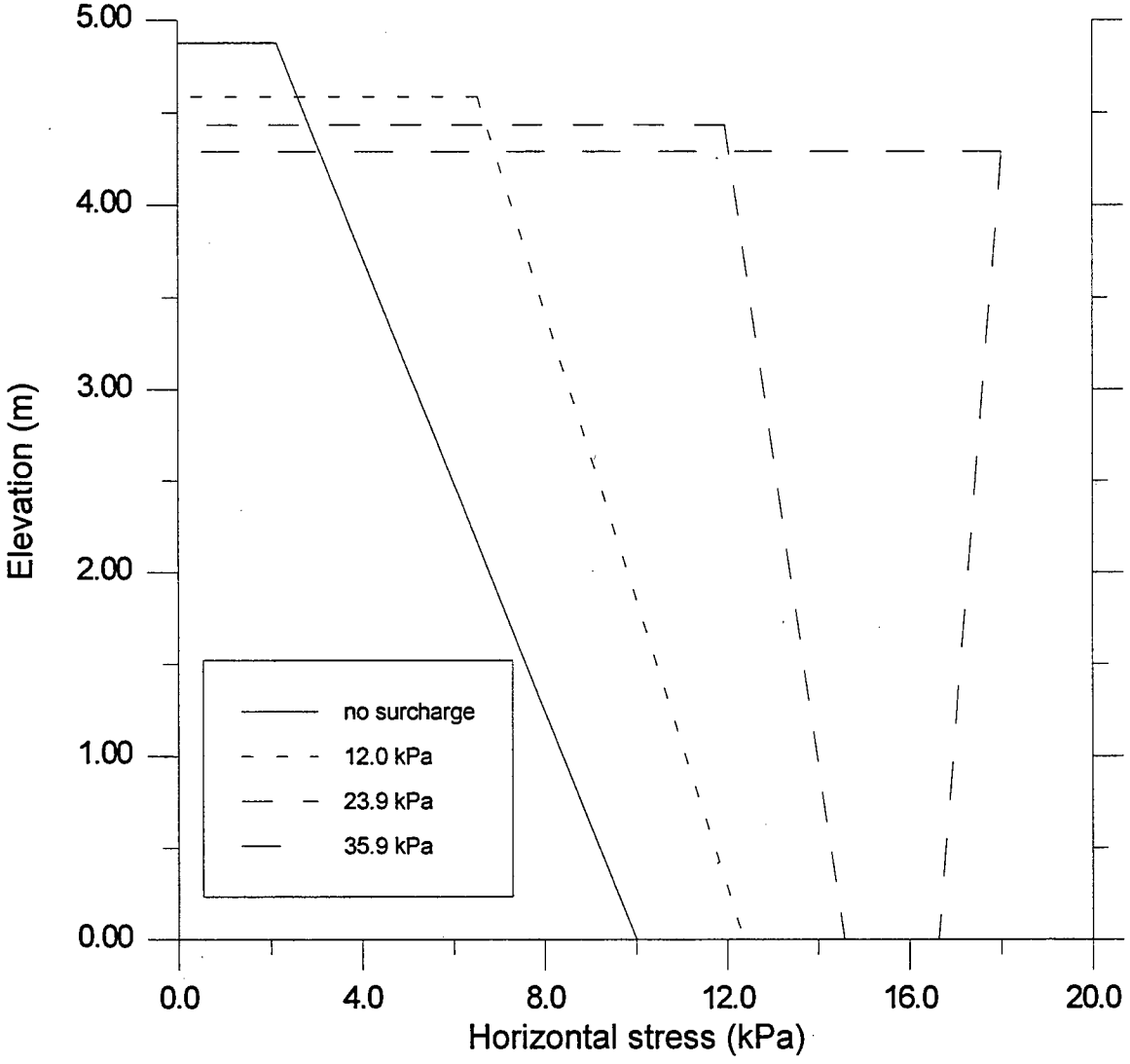

Figure 6.4 Horizontal stress vs. elevation, at-rest conditions (loading), Palmer Shredding

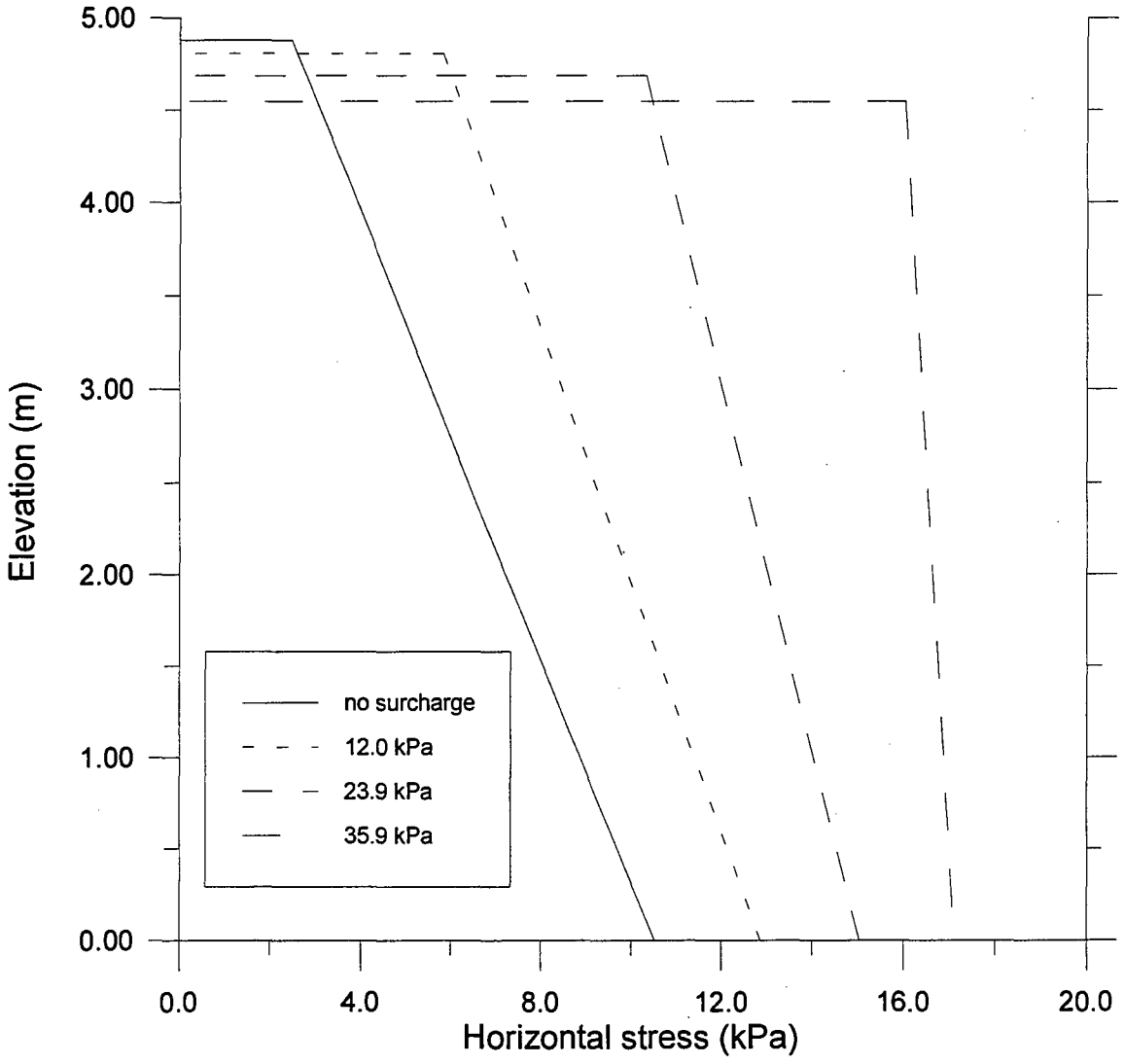

Figure 6.5 Horizontal stress vs. elevation, at-rest conditions (loading), F & B Enterprises

Further examination of the horizontal stress distribution can be done by including the pressure cells, as shown in Figures 6.6 through 6.8. In each of the cases only the loading conditions of no surcharge and the maximum surcharge of 35.9 kPa (750 psf) are shown. The results at the intermediate surcharges were similar. Pressure cell values are shown for each of the four calibration combinations described in Section 6.2.2. Locations of each of the pressure cells is shown on Figures 3.3 and 4.1. The corresponding horizontal stress distributions from the load cells are included for comparison. Examination of Figures 6.6 through 6.8 shows that calibration combinations #3 and #4 tend to be higher than #1 and #2. The difference between calibration combinations #1 and #2 and between #3 and #4 tends to be small. This indicates that there is little difference between the two temperature correction factors. Further examination of Figures 6.6 through 6.8 shows that the pressures for the offset pressure cell are lower for Palmer Shredding and F & B Enterprises and higher for Pine State Recycling. Thus, there is no consistent pattern of higher or lower stresses at greater distances from the centerline of the facility. Moreover, the magnitude of the difference between the centerline and offset pressure cells indicates that there is large scatter in the data.

Figures 6.6 through 6.8 show that there are differences between the pressure cell results and the load cell results. Possible explanations for these discrepancies are given in the following: 1) The initial system used to read the pressure cells was powered by a portable generator. This cause a significant amount of electronic noise that caused fluctuations in the readings. The generator was grounded to reduce the noise and ten readings, taken at 10 to 40 second intervals, were averaged, which partially eliminated the

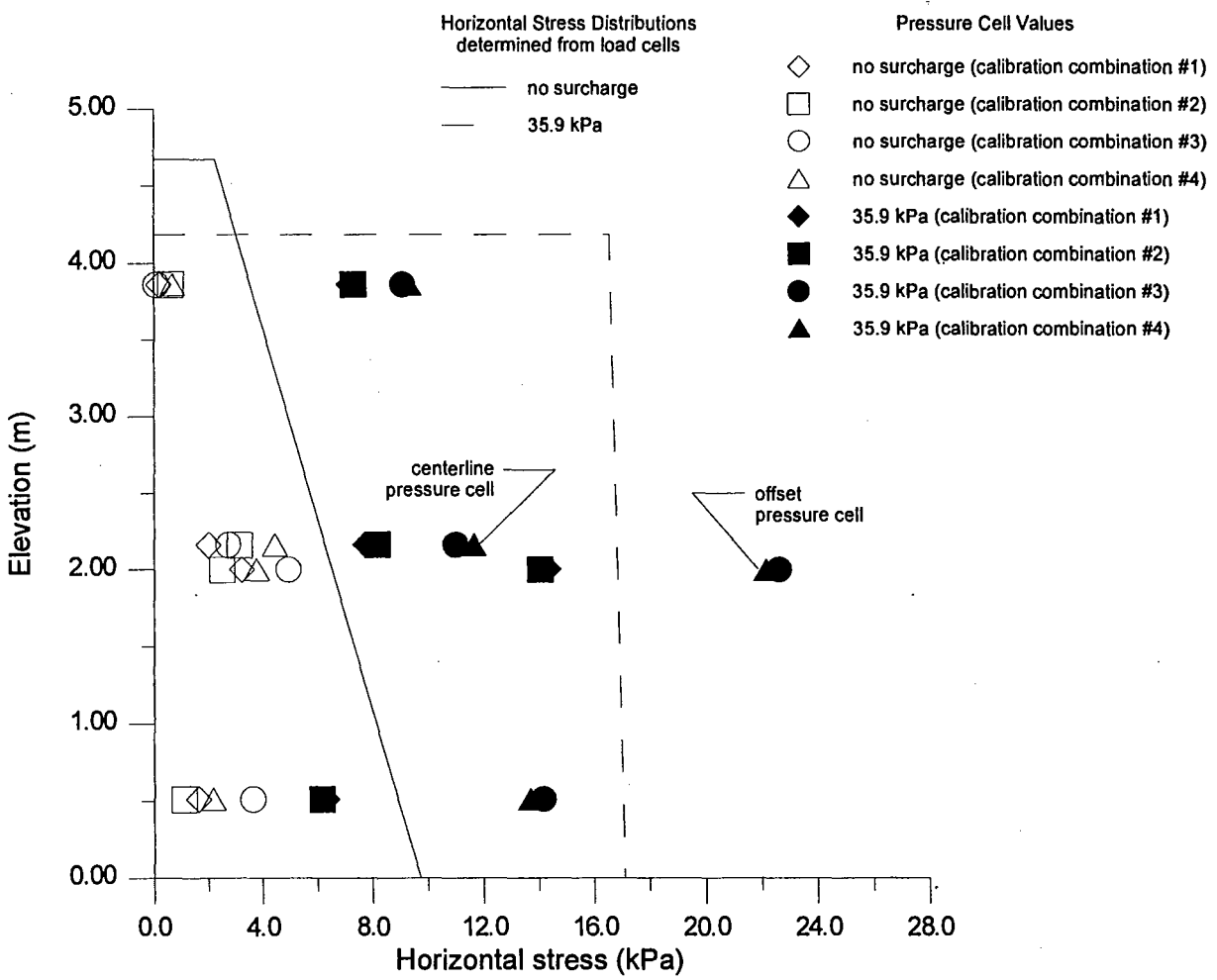

Figure 6.6 Horizontal stress vs. elevation, at-rest conditions (loading), with pressure cell values, Pine State Recycling

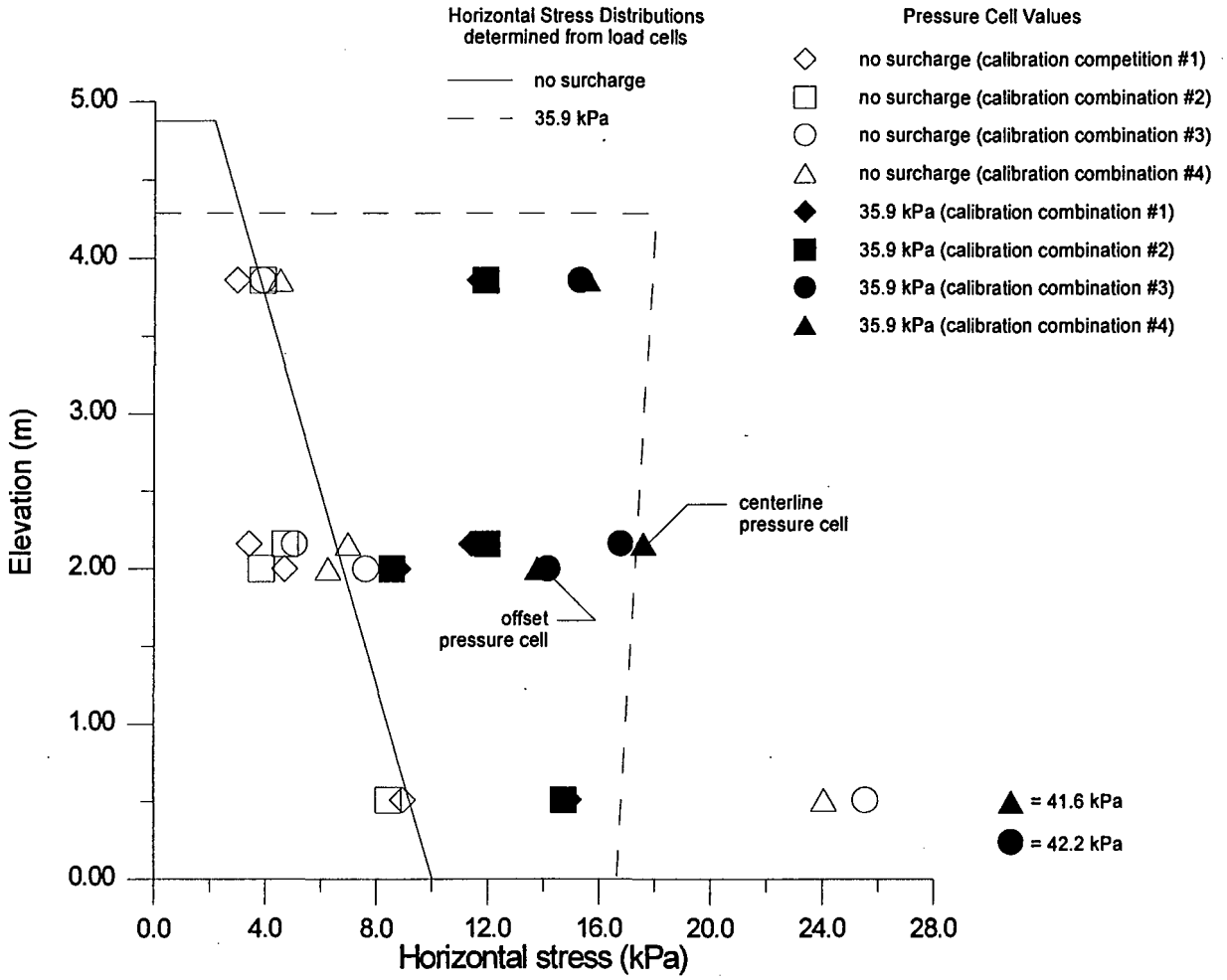

Figure 6.7 Horizontal stress vs. elevation, at-rest conditions (loading), with pressure cell values, Palmer Shredding

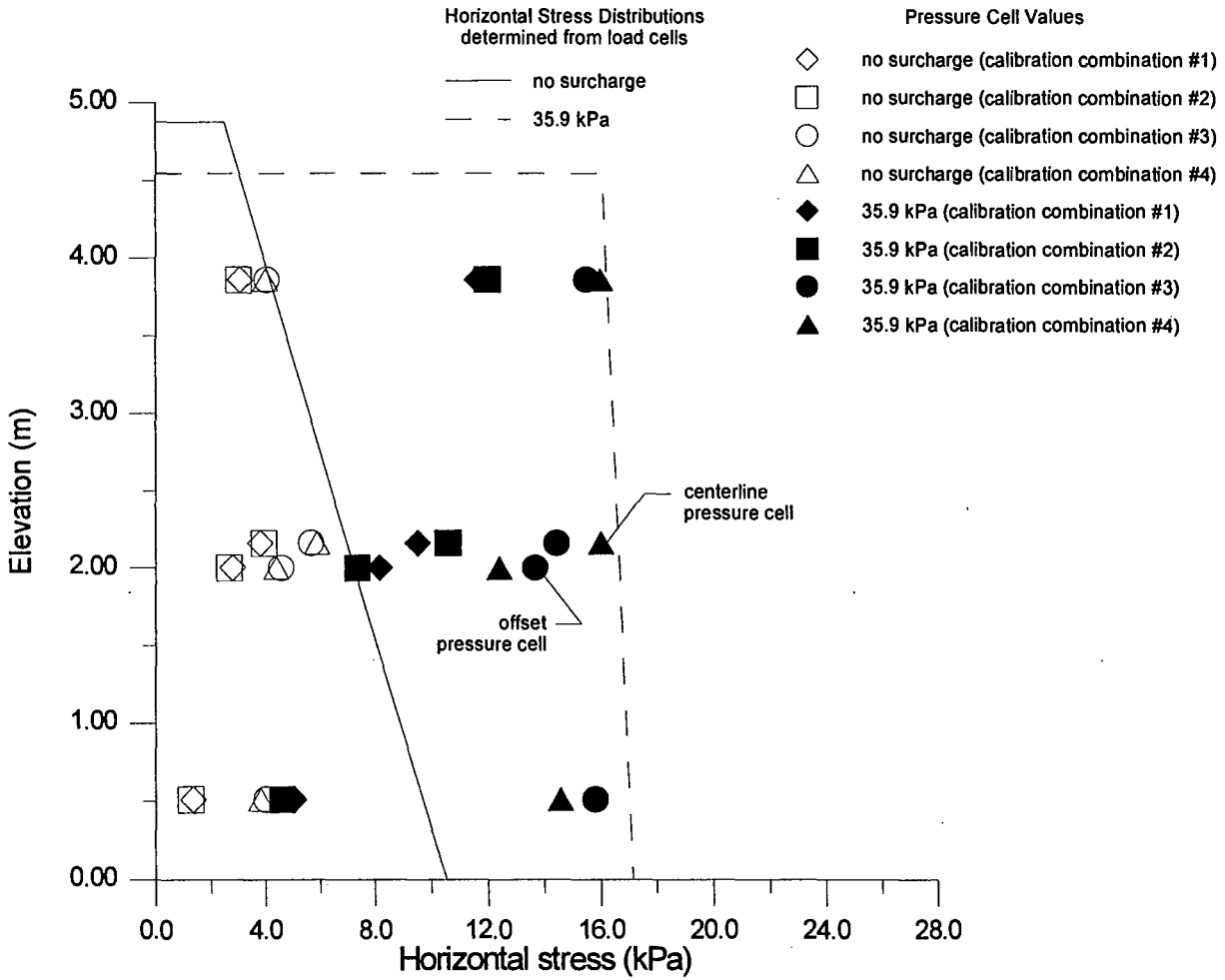

Figure 6.8 Horizontal stress vs. elevation, at-rest conditions (loading), with pressure cell values, F & B Enterprises

random fluctuation of the readings. After the test with Palmer Shredding, this system was replaced with a manual, battery operated system, that reduced electronic noise (discussed in Section 4.2.1.2). 2) The pressure cells used for this study (ROCTEST model EPC) consisted of an oil filled pressure plate and a pressure transducer. They are generally embedded in earth fills, which have only minor temperature variations. However, for this application the transducers were on the exterior of the front wall and thus subjected to changes of the air temperature. The pressure plate was on the inside of the wall, as shown on Figure 6.9, and would not necessarily be at the same temperature as the transducer. This was particularly true when the late afternoon sun hit the outside of the wall. It was not possible to completely overcome this problem, although a dark plastic tarp was erected for the trials with tire chips to shade the outside of the wall from the direct sunlight. For the last trial with F & B Enterprises tire chips the transducers were surrounded with an insulated box. 3) The pressure cells used in this study are commonly used for earth materials. Due to the nature of tire chips, some of the pieces being in excess of 80 mm (3 in.), the number of particles in contact with the face of the pressure cell would be less than for most soils. An example of this is illustrated on Figure 6.10, which shows the vertical face of tire chips revealed after the back wall was removed upon completion of the test with Pine State Recycling. It was possible to examine this vertical surface because once the surcharge was reduced to zero and the back wall was removed, the vertical surface of the tire chips remained intact. This is discussed further in Section 6.4.2. Figure 6.10 shows that the cut edges of the tire chips tended to bear against the face of the back wall, and presumably the front wall pressure cells. This was more evident at approximately 200 mm (8 in.) intervals, which coincided

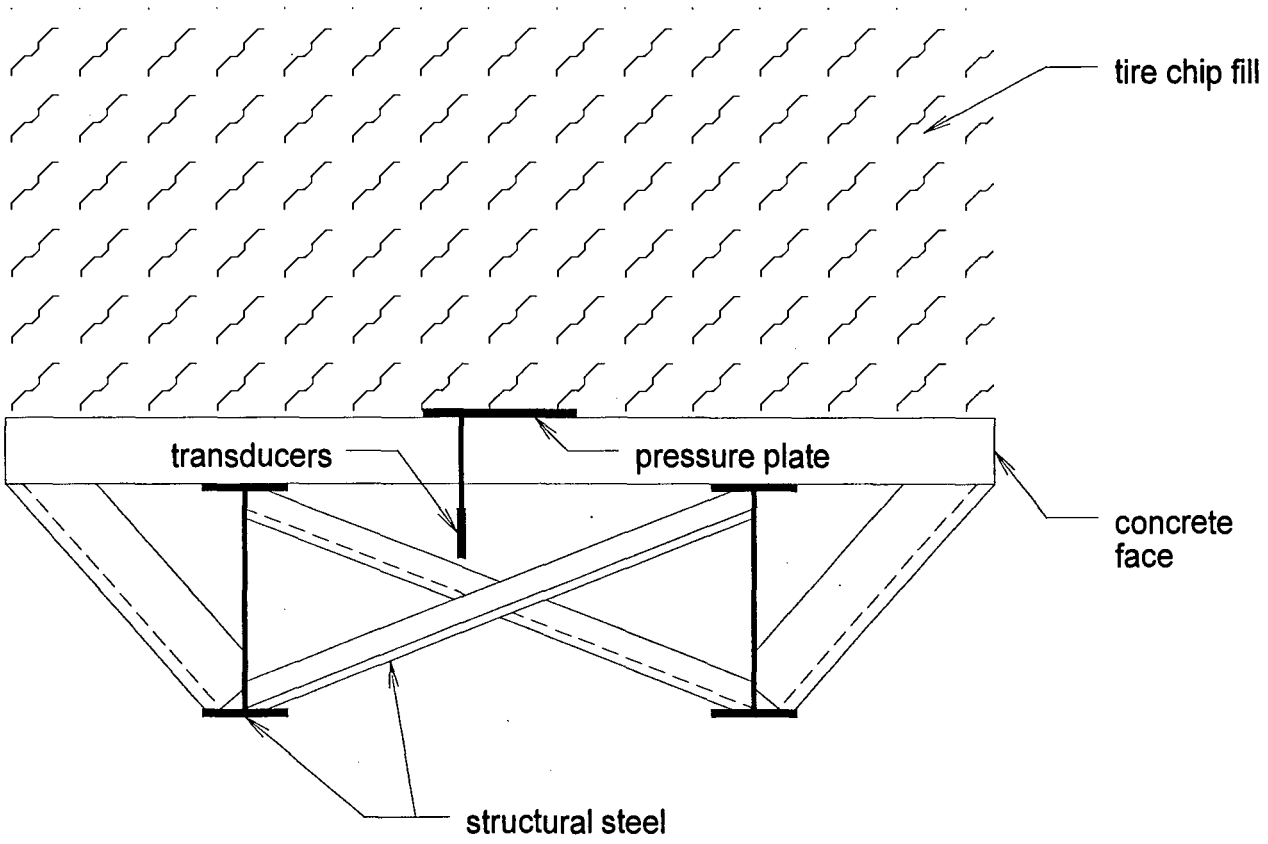

Figure 6.9 Center panel with pressure cell

Figure 6.10 Tire chip orientation after completion of test with Pine State Recycling

with the depth of each lift as the tire chips were placed. This was partially accounted for by calibrating the pressure cells with tire chips placed against the face of the cell, as discussed in Section 4.2.1.2.

Overall, the stress from the pressure cells tended to be less than from the load cells, although in some cases they were about the same. This suggests that the horizontal stresses are no higher than measured by the load cells.

The at-rest horizontal stress distributions for tire chips during loading can be compared to a finite element (FE) analysis using tire chips as backfill by Gharegrat (1993). Gharegrat (1993) performed a FE analysis carried out on a 4.57-m (15-ft) high retaining wall with tire chips as the backfill using the FE program CANDE (FHWA, 1989). The modeled wall was hinged at the bottom, supported at the top, and rested on a concrete pad. Analysis was performed for at-rest and active conditions. The tire chip properties used in the analysis were determined from Humphrey, et al. (1992) for Pine State Recycling tire chips. The at-rest FE analysis simulated conditions under the following surcharges: no surcharge, 12.0 kPa (250 psf), 23.9 kPa (500 psf), and 35.9 kPa (750 psf). The horizontal stress versus fill elevation by Gharegrat (1993) for at-rest condition is shown on Figure 6.11.

Comparison of Figures 6.3 through 6.5 with Figure 6.11 shows differences in the shape of the stress distributions. For the FE distributions, the stress value at the fill surface is equal to zero, whereas the value at the top for the stress distributions on Figures 6.3 through 6.5 start at some value greater than zero. One reason for this is the

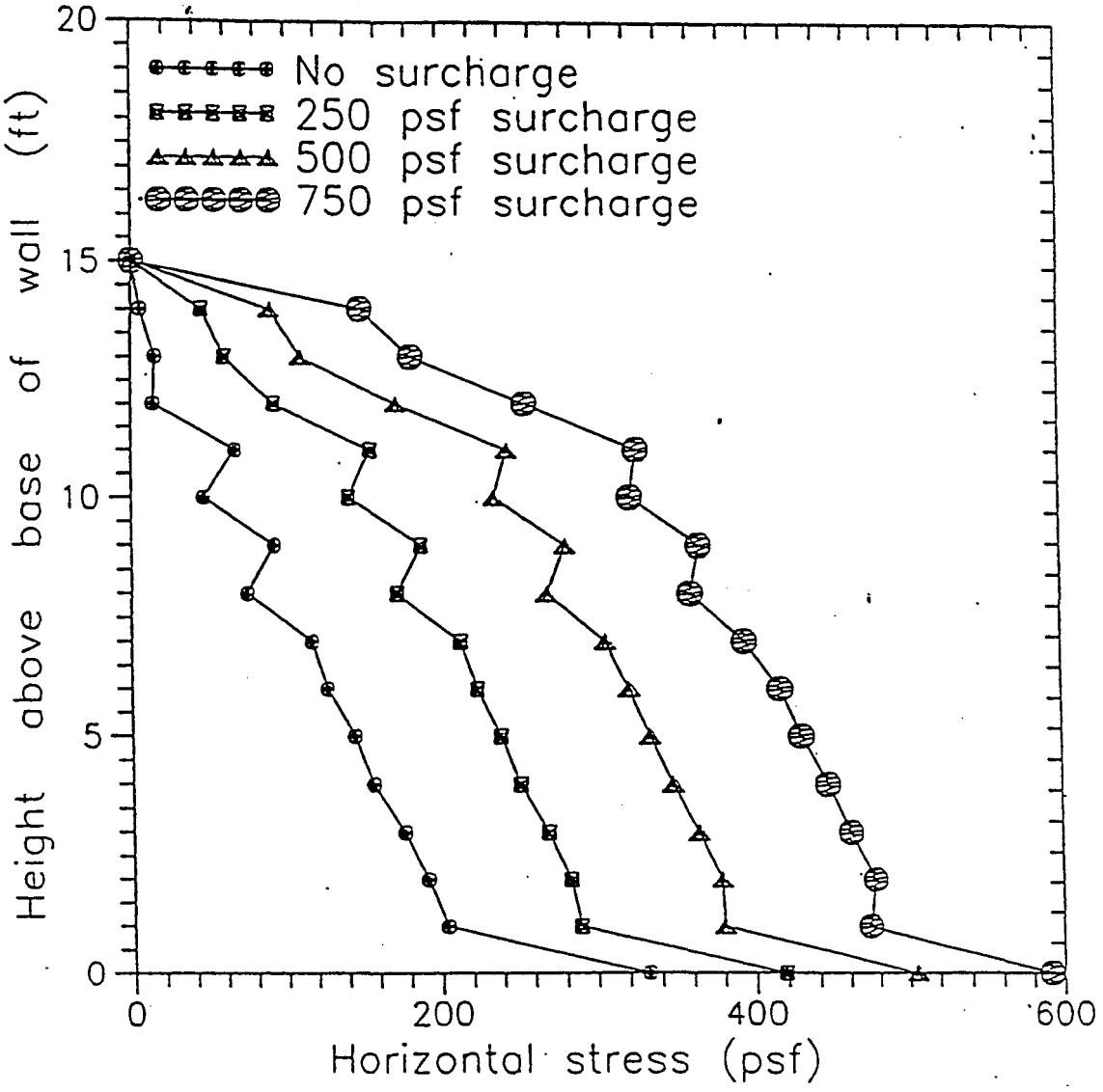

1 psf = 0.0479 kPa

Figure 6.11 At-rest horizontal stress from finite element analysis (Gharegrat, 1993)

approximate method used by the FE analysis to calculate stresses at a boundary. Another is the method used to calculate the stress distribution from the load cells. The distributions determined from the load cell were assumed to vary with depth, as discussed in Section 6.2.1. However, the variation of stress with depth may in fact be nonlinear. When the resultant horizontal forces determine at each surcharge from Figures 6.3 through 6.5 are compared to the resultants determined from the Figure 6.11, there is little difference in the magnitude. However, the location of the resultant is 14% to 31% lower than measured by the load cells. Thus, the finite element analysis gives a reasonable prediction of the magnitude of the horizontal force, but a greater concentration of the horizontal stress nearer the base of the wall than measured by the load cells.

6.3.2 Unloading/Reloading

The effects of reducing the surcharge from 35.9 kPa (750 psf) to the intermediate surcharge of 23.9 kPa (500 psf), and then reapplying the 35.9 kPa (750 psf) surcharge were investigated. The sequence of the loading/unloading, starting with the initial loading, was: 23.9 kPa (initial loading), 35.9 kPa (initial loading), 23.9 kPa (1st unload), 35.9 kPa (1st reload), 23 kPa (2nd unload), 35.9 kPa (2nd reload). The horizontal stress distributions presented in this section were determined by taking the average of the load cell values at each loading condition.

6.3.2.1 Granular Fill

The plots for unloading/reloading for granular fill are shown on Figure 6.12. The left side of the figure shows the horizontal stress versus elevation for the intermediate

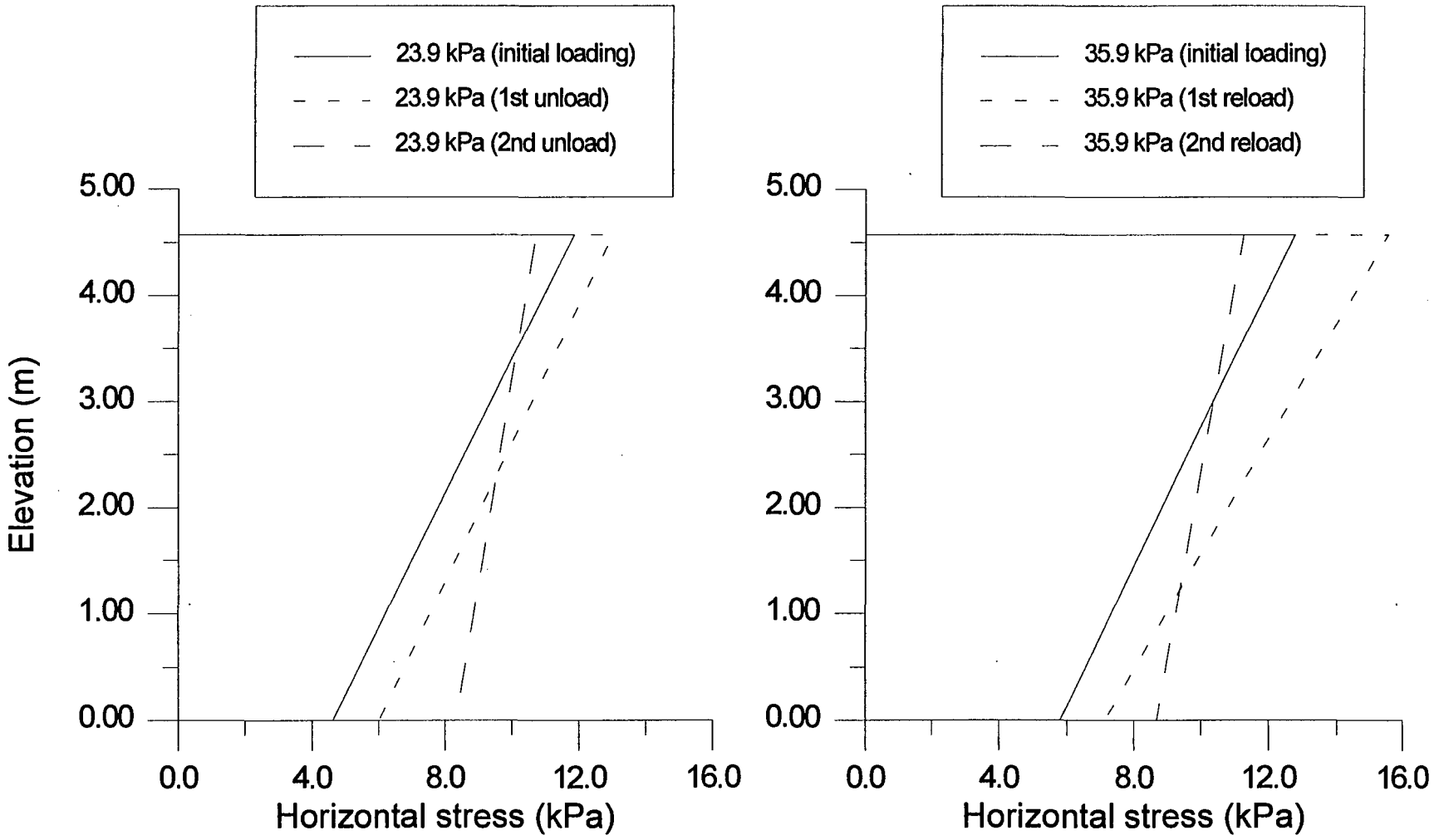

Figure 6.12 Horizontal stress vs. elevation, at-rest conditions (unload/reload cycles), granular fill

surcharge, while the right side of the figure shows the maximum surcharge. Here, as with the initial loading, the horizontal stress distributions deviate considerably from classical earth pressure theory. Examination of Figure 6.12 shows that the horizontal stress does not change significantly from 35.9 kPa (initial loading) to 23.9 kPa (1st unload). The stress then increases once the maximum surcharge is reapplied for the first time, 35.9 kPa (1st reload), to levels greater than the initial loading with 35.9 kPa (750 psf), resulting in a 22% increase in the total horizontal force. During the application of the first reload to 35.9 kPa (750 psf), the electric chain fall used to place the surcharge blocks on top of the fill malfunctioned. This resulted in a surcharge of 28.2 kPa (590 psf) left on for 12 days while the chain fall was being repaired. Plots of the horizontal stress during this time give insight into the possible reasons for the greater stress measured on 35.9 kPa (1st reload) than on 35.9 kPa (initial loading).

Plots of horizontal stress distributions on the first day with 28.2 kPa (590 psf) (7/22/94), a day in the middle (7/29/94), and the last day (8/3/94), are shown on Figure 6.13. This shows a general increase in the horizontal stress during this time, with the distribution for 7/29/94 decreasing more with depth, similar to 35.9 kPa (1st reload) (Figure 6.12). One possible explanation for the increase in stress after 28.2 kPa (7/22/94) and the one observed on 35.9 kPa (1st reload) is a reduction in apparent cohesion, as discussed Section 6.3.1.1. A reduction in apparent cohesion could be caused by drying of the soil or the soil becoming nearly saturated during a rain event.

The reason for the similar shapes of the stress distributions for 28.2 kPa (7/29/94) and 35.9 kPa (1st reload), as shown on Figures 6.13 and 6.12, respectively, can be explained

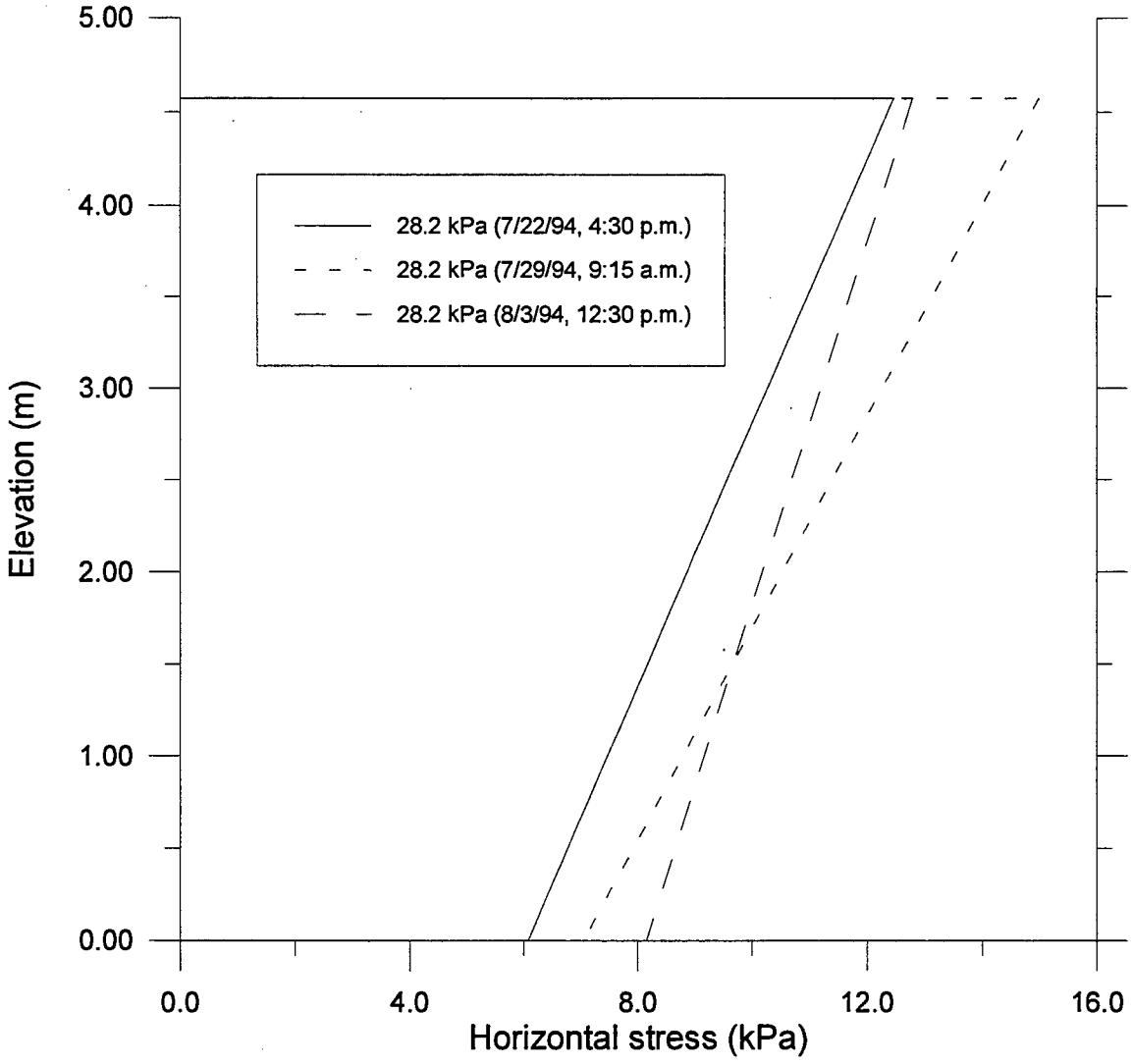

Figure 6.13 Horizontal stress distributions during 12 day period that electric chain fall was being repaired

by the time of day the measurements were taken. On Figure 6.13, the stress distribution for 28.2 kPa (7/29/94) was determined from measurements taken at 9:15 a.m., while those for 28.2 kPa (7/22/94) and 28.2 kPa (8/3/94) were taken at 4:30 p.m. and 12:30 p.m., respectively. The shape of the stress distribution on 7/29/94 and the slightly greater magnitude than on 8/3/94 is attributed to variations in the vertical load cell readings with temperature. Measurements from the vertical load cells were lower in the morning than in the afternoon. As a result, the measured horizontal forces are slightly greater in the morning, resulting in slightly greater horizontal stress distribution with a different shape than from one determined from measurements taken in the afternoon. The variation in load cell readings with time of day is discussed in detail in Section 7.2.1. Similarly, the stress distribution for 35.9 kPa (1st reload) was determined from the average of two sets of readings, the first reading was taken at 5:30 p.m. and the second at 7:30 a.m. Thus, the stress distribution shape and magnitude may have been influenced by the measurements taken at 7:30 a.m. This effect was reduced by shielding the front wall from direct sun with dark plastic for the remaining three tests with tire chips.

When the maximum surcharge is removed for the second time (23.9 kPa (2nd unload)), Figure 6.12, the horizontal stress at the bottom increases while decreasing at the top. Resulting in a stress distribution that decreases only slightly with depth, with a resultant force only slightly greater than the stress distribution for 23.9 kPa (1st unload). It is possible that this occurred as a result of the reduction in apparent cohesion. When 35.9 kPa (750 psf) was removed for the second time, after the reduction in apparent cohesion, the soil mass reoriented itself, resulting in a change in the shape of the stress

distribution. This is also supported by the similar shape of the stress distribution for 35.9 kPa (2nd reload), where the magnitude of the resultant force is 5% greater than 23.9 kPa (2nd unload) and approximately equal to the initial loading with 35.9 kPa (750 psf).

6.3.2.2 Tire Chips

The unloading/reloading horizontal stress distributions for Pine State Recycling, Palmer Shredding, F & B Enterprises are shown on Figures 6.14, 6.15, and 6.16, respectively. These figures show that when the maximum surcharge was removed for the first time, the horizontal stress for the intermediate surcharge, 23.9 kPa (1st unload), was larger than when the facility was first loaded, 23.9 kPa (initial loading). The larger horizontal stress after unloading to 23.9 kPa (500 psf) may be a result of the tire chips rebounding to an elevation less than for the initial loading with 23.9 kPa (500 psf). This is seen on Figures 6.14 through 6.16. This is analogous to a normally consolidated soil. When the vertical stress is reduced on a normally consolidated soil, the horizontal and vertical stress do not decrease by the same amount, resulting in a greater K_o for an overconsolidated soil than for a normally consolidated soil (Mitchell, 1993). It is theorized that similar behavior from the tire chips contributed to the horizontal stress being greater after unloading than during initial loading. When the facility was reloaded and unloaded a second time, 23.9 kPa (2nd unload), the horizontal stress increased slightly for Pine State Recycling and Palmer Shredding, while decreasing slightly for F & B Enterprises. This shows that there is no significant change between the first and second unloadings.

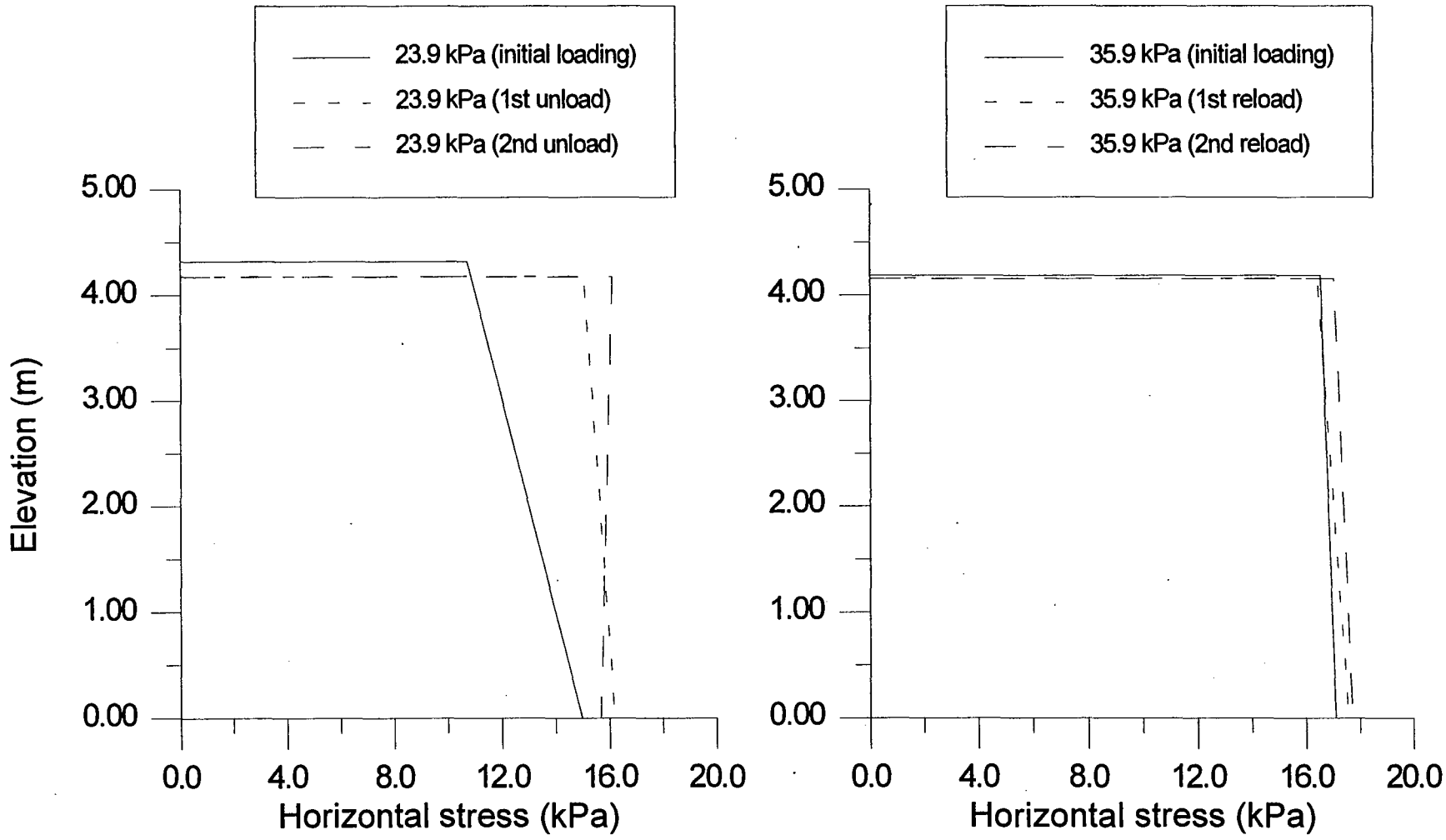

Figure 6.14 Horizontal stress vs. elevation, at-rest conditions (unload/reload cycles), Pine State Recycling

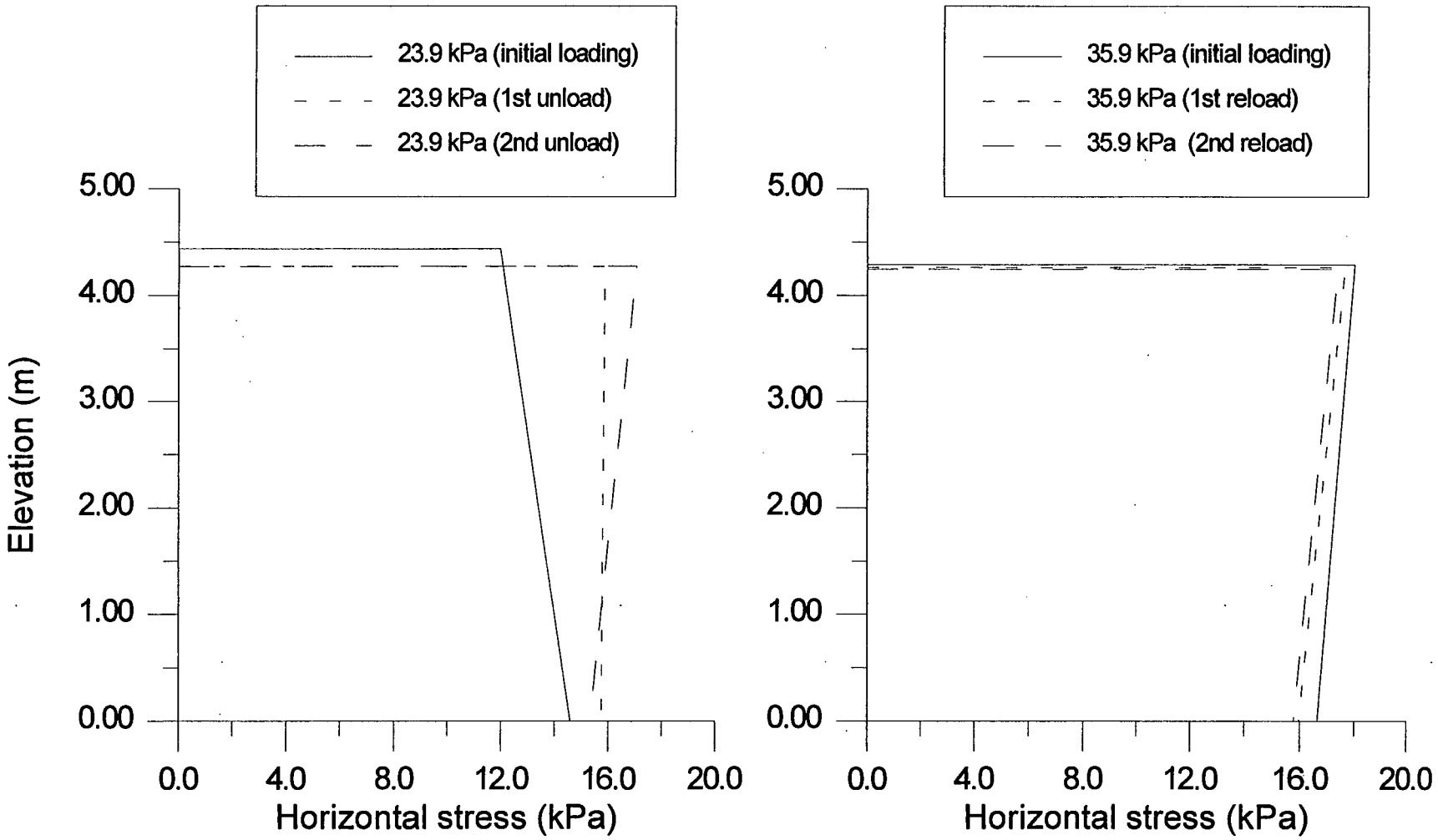

Figure 6.15 Horizontal stress vs. elevation, at-rest conditions (unload/reload cycles), Palmer Shredding

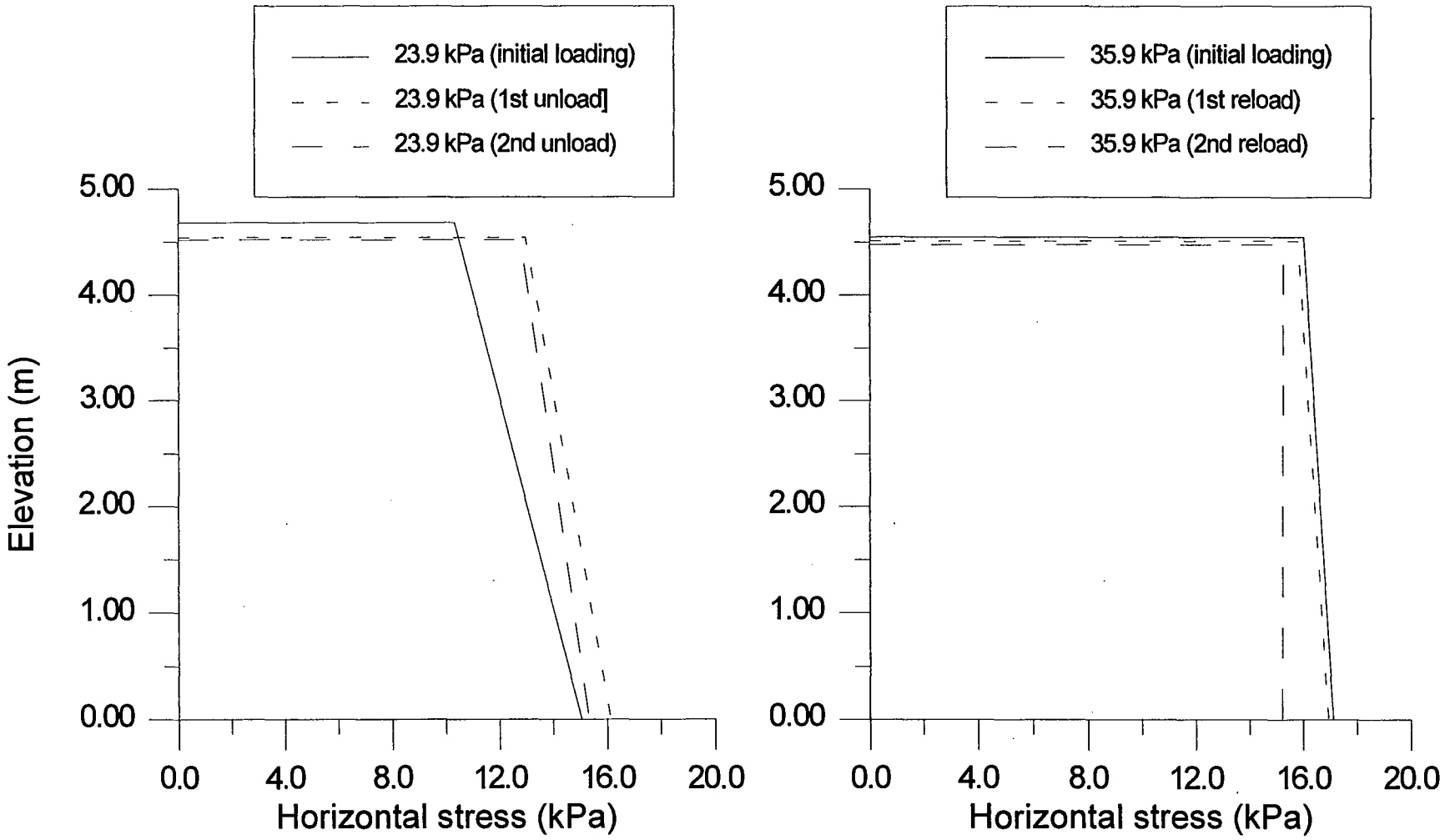

Figure 6.16 Horizontal stress vs. elevation, at-rest conditions (unload/reload cycles), F & B Enterprises

Further examination of Figures 6.14 through 6.16 shows that the horizontal stress decreases slightly as the surcharge is lowered from 35.9 kPa (750 psf) to 23.9 kPa (500 psf). Comparison can be made by examining the change in the horizontal stress at the mid-elevation as the surcharge (vertical stress) is reduced from 35.9 kPa (750 psf) to 23.9 kPa (500 psf). For Pine State Recycling the horizontal stress decreased 1.2 kPa (25 psf) for first and second unloads. This is a 7% reduction in horizontal stress, corresponding to 33% reduction in vertical stress. Similarly, the horizontal stress decreased 1.5 to 0.6 kPa (32 to 13 psf), 9 to 4%, during the two unload cycles for Palmer Shredding. For F & B Enterprises during the first unload cycle, the horizontal stress decreased 2.0 kPa (42 psf) or 12%, and 2.3 kPa (48 psf), 14%, during the second unload cycle. The larger reduction in horizontal stress experienced by F & B Enterprises may be a function of the size of the chips and the quantity of steel belts. Palmer Shredding and Pine State Recycling tire chips are larger with more steel belts compared to F & B Enterprises, as discussed in Section 5.3. Because F & B Enterprises contains fewer steel belts, which tend to hold the tire chips together, the tire chips may have rebounded more during unloading, resulting in a larger decrease in the horizontal stress.

Further examination of Figure 6.14 shows that for Pine State Recycling the horizontal stress increases slightly with each subsequent reload of the maximum surcharge. While Figures 6.15 and 6.16 show that the horizontal stress decreases slightly with each subsequent reload for Palmer Shredding and F & B Enterprises. Thus, the horizontal stress does not appear to increase with repeated reloading.

6.3.3 Time-Dependent Change in Stress

After the second unload/reload cycle was completed with Palmer Shredding, the tire chips were left in the facility during the Winter of 1994-95, with the maximum surcharge, to examine any changes in stress with time. In the Spring of 1995 a third unload/reload cycle was performed.

The pattern of the changing stress is described in the following. After the second unload/reload cycle, 11/21/94, no change in stress was observed until 1/18/95. This stress level remained the same until 4/28/95. No readings were taken between 4/28/95 and the start of the third unload/reload cycle. On 5/31/95 the third unload/reload cycle was started when the maximum surcharge was reduced to 23.9 kPa (500 psf). This surcharge was left in place until 6/5/96 when the maximum surcharge was reapplied and left in place until 6/13/95. Figure 6.17 shows the horizontal stress distributions for the period before the change in load was observed (11/21/94 to 12/28/94), the period after the change in load was observed, from 1/18/95 until 4/28/95 (winter), and the third unload/reload cycle. The stress distributions were determined by taking the average of the values from the load cells during each loading time period. Examination of Figure 6.17 shows that shape of the horizontal stress distribution changed during the winter. The total horizontal force during this time increased 13%. When the third unload/reload cycle was completed, the shape of the horizontal stress distribution resembled that of before winter, however, the horizontal stress had increased 4.0 kPa (84 psf) with depth. This results in a total increase of 14% in horizontal force from the before winter (2nd reload)

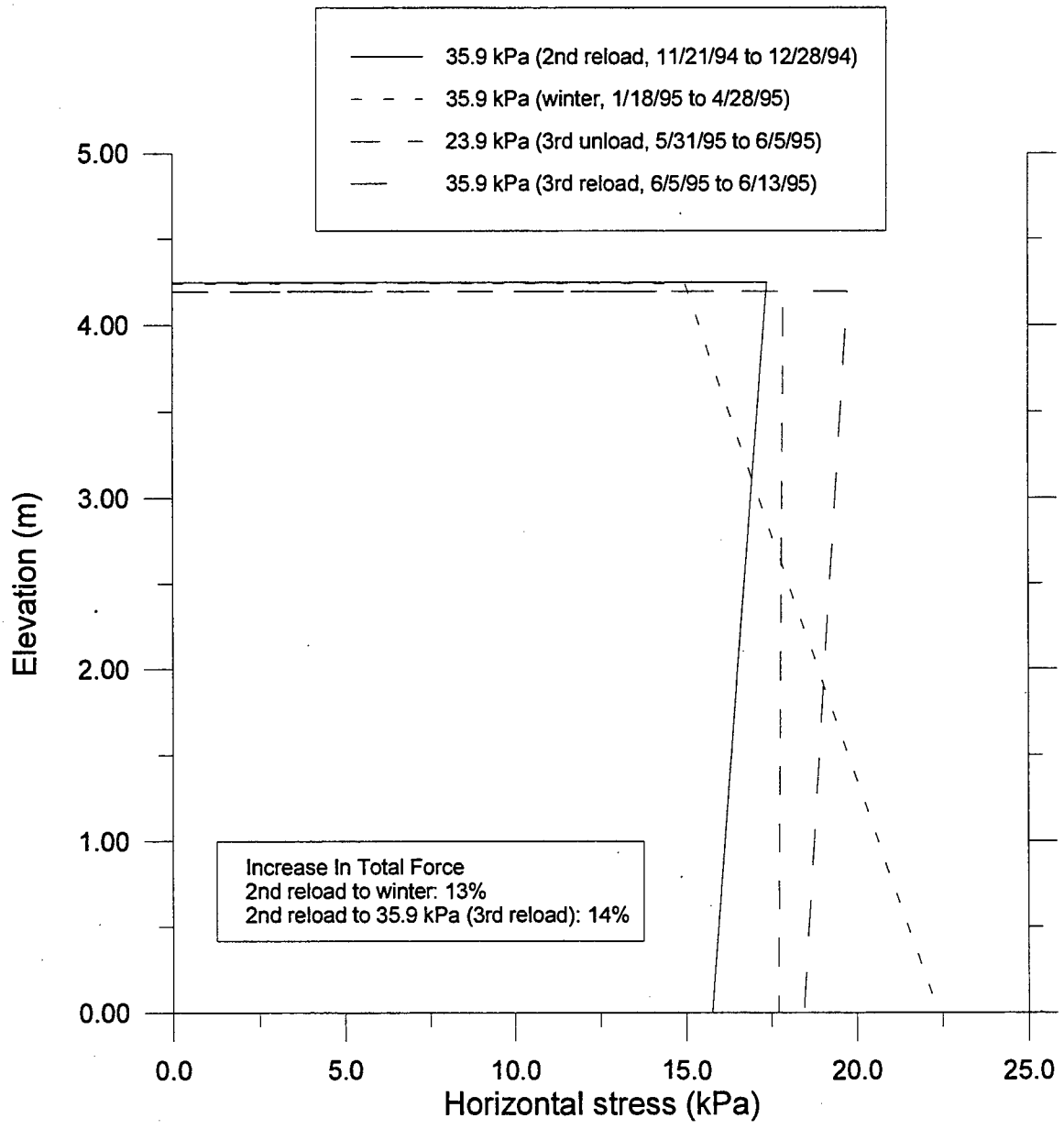

Figure 6.17 Measured horizontal stress before and after winter, Palmer Shredding

to the end of the third unload/reload cycle. It appears that the tire chips underwent some time dependent increase in horizontal stress sometime after 12/28/94.

The change in distribution shape from 1/18/95 to 4/28/95 may be due to cold weather. At very cold temperatures the steel frame of the front wall contracts, causing the wall face to move down relative to the backfill. This would cause a decrease in the vertical force and an increase in the horizontal force. As a result, the horizontal stress at the top would decrease and the bottom stress would increase, as shown on Figure 6.17. This is supported by results presented in Section 7.2.2.3. One possible reason for the shape of the stress distribution after the third unload/reload cycle to resembling that before winter (2nd reload), is that unloading the chips caused the vertical stress to reestablish its pre-winter value, resulting in a stress distribution similar to before winter.

6.3.4 Granular Fill Versus Tire Chips

The horizontal stress distributions for each of the tire chip suppliers under the 35.9 kPa (750 psf) surcharge, as shown Figures 6.3 through 6.5, can be compared to the horizontal stress distribution that would typically be used for granular fill. This was done by plotting the horizontal stress distributions at the 35.9 kPa (750 psf) surcharge for each of the tire chip suppliers, as shown on Figure 6.18. The horizontal stress distribution for the granular fill was determined for the maximum surcharge and an elevation of 4.34 m (14.2 ft), which is the average of the three tire chip elevations at the same surcharge. The properties used to determine the horizontal stress were the average density, 2.023 Mg/m^3 (126.3 pcf), and the friction angle (ϕ), 38°, determined from triaxial tests. The friction

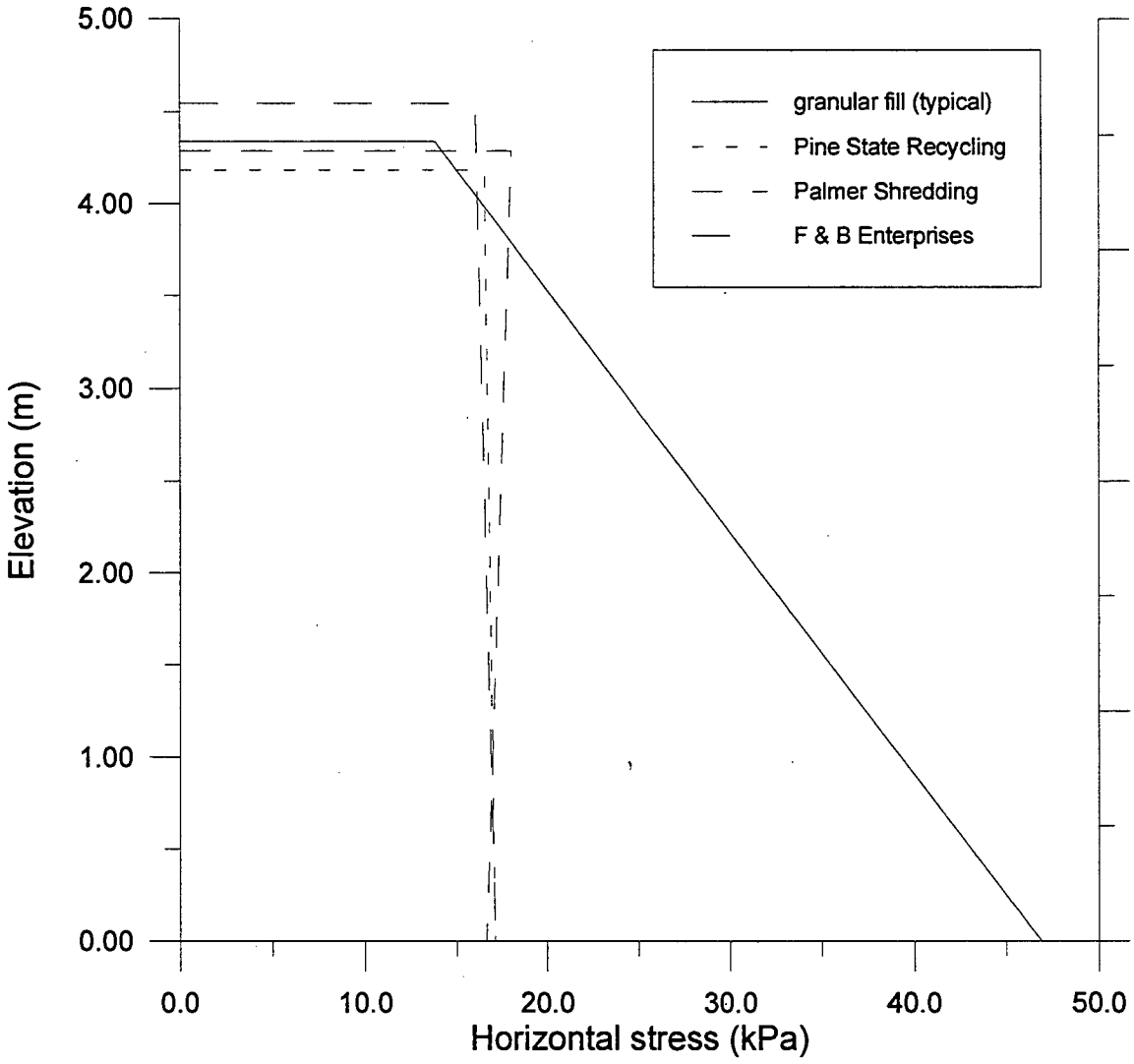

Figure 6.18 Typical at-rest horizontal stress distribution for granular fill compared with those measured from three tire chip suppliers (35.9 kPa (750 psf) surcharge)

angle was used to find the coefficient of lateral earth pressure at rest (K_o) using (Jaky, 1948; Mesri and Hayat, 1993):

$$K_o = 1\text{-}\sin\phi \tag{6.4}$$

The resulting K_o is 0.38.

Examination of Figure 6.18 shows that the horizontal stress for the granular soil is considerably larger than for the tire chips. The resultant of the horizontal stress from the tire chips is approximately 45% less than for granular fill. This is due, at least in part, to the density of tire chips being approximately 1/3 to 1/2 that of conventional granular backfill.

6.4 ACTIVE CONDITIONS

After each of the fills had stabilized under the full surcharge, the front wall was rotated about its base to attain active conditions. After the wall was rotated about its base, it was observed that the load cell and pressure cell values continued to change with time. Therefore, results in this section are based on one set of readings, corresponding to a particular time, so that the change in stress with time can be observed. Tire chip results were compared to a finite element analysis by Gharegrat (1993).

6.4.1 Granular Fill

The horizontal stress versus elevation for the granular fill, based on load cell readings, is shown in Figure 6.19. The front wall was rotated in increments until a maximum of 0.7 degrees, or about 0.01H, where H is the height of the wall, was reached. For

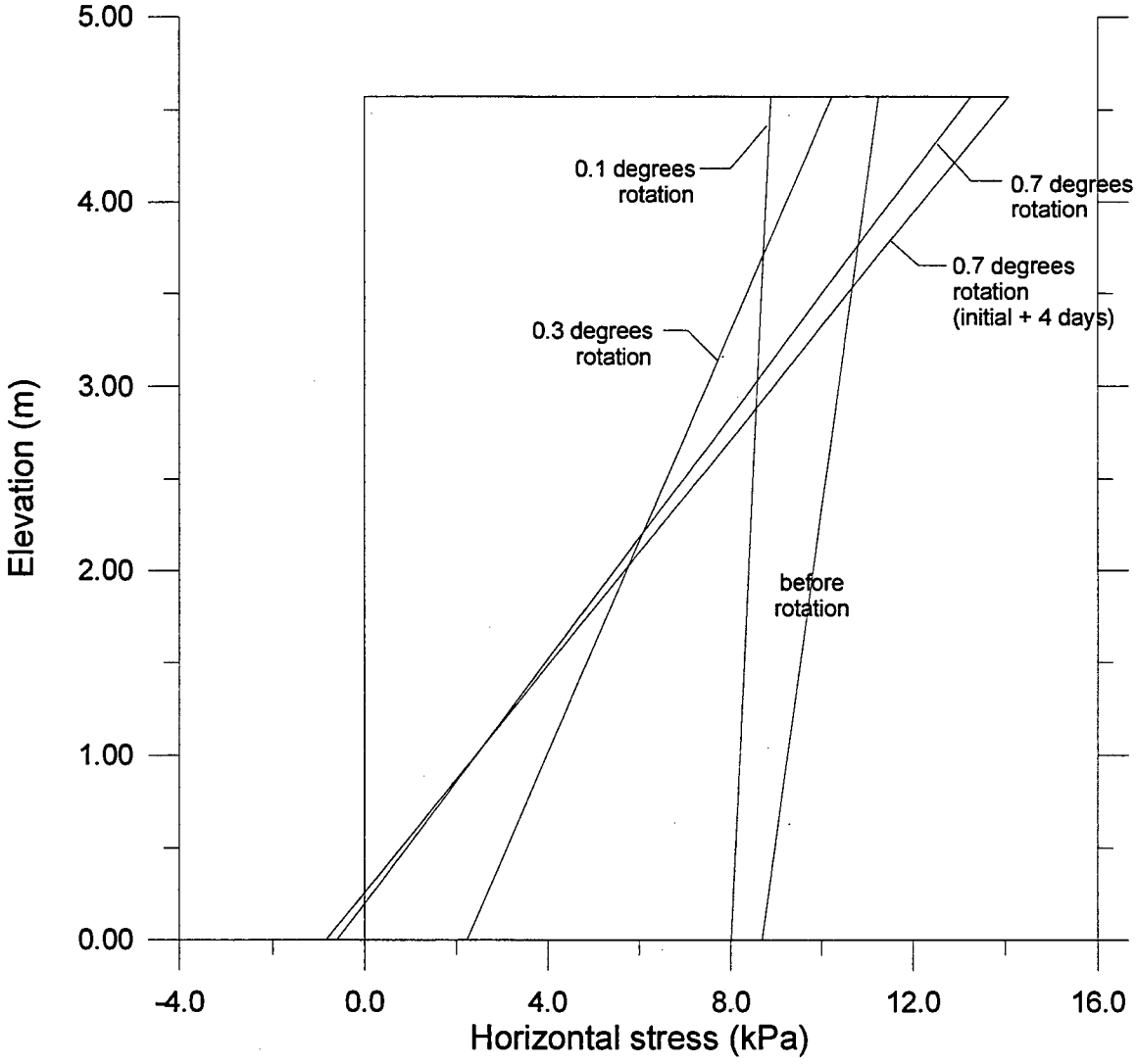

Figure 6.19 Horizontal stress vs. elevation, active conditions, granular fill

comparison, the amount of rotation needed to produce active conditions for dense, cohesionless soils is reported in the literature as 0.001 to 0.002H (Bowles, 1988). Figure 6.19 shows that as the wall is rotated outward, past 0.1 degrees (0.002H), the stress continues to decrease up to the maximum rotation. Thus, based on the literature the rotation was sufficient to attain active conditions. However, since the stress continued to decrease, true active conditions were not achieved. Further rotation was not attempted, as the row of surcharge blocks adjacent to the front wall face were leaning outward at an ominous angle, due to settlement of the fill behind the front wall. As a result, the conditions measured at 0.7 degrees will be used when discussing movement within the fill and the orientation of the failure plane, as discussed in Chapter 9.

Further examination of Figure 6.19 shows that the stress decreased at the top and bottom up to 0.1 degrees, then as the wall is rotated further the stress is reduced at the base of the fill and increased at the top. The resulting stress at the maximum rotation, decreased with depth and the values were much lower than would be expected based on classical earth pressure theory. In fact, the calculated stress at 0.7 degrees was slightly negative at the base of the wall. One possible explanation for this is the presence of a high angle of wall friction. As the wall is rotated outward, the fill moves down relative to the wall face, mobilizing the interface shear strength between the concrete face and the granular fill. This would result in a decrease in the horizontal stress. In addition, the influence of apparent cohesion and arching could play a role, as discussed further in Section 9.4.1. Figure 6.19 also shows only a slight change in the horizontal stress over a

four day period at 0.7 degrees, indicating that no apparent time-dependent change in stress occurred.

6.4.2 Tire Chips

The horizontal stress versus elevation for Pine State Recycling, Palmer Shredding, and F & B Enterprises are shown on Figures 6.20 through 6.22, respectively. The wall was rotated outward approximately 0.01H. The actual rotation was 0.8 degrees for Pine State Recycling, 0.8 degrees for Palmer Shredding, and 0.6 degrees for F & B Enterprises. Readings were taken for several days at this rotation. Then, for Pine State Recycling and Palmer Shredding, the wall was rotated further until the front row of surcharge blocks was leaning outward at an ominous angle, resulting in maximum rotations of 2.2 degrees or 0.04H for Pine State Recycling and 1.7 degrees or 0.03H for Palmer Shredding. Figures 6.20 through 6.22 show that horizontal stress decreases as the wall is rotated outward away from the fill. In each case when the angle of rotation is held constant for one hour to several days, the horizontal stress increases, with the value at the top of the fill increasing more than the value at the bottom. This suggests that tire chips experience some time-dependent creep after being displaced by movement of the wall.

The existence of time-dependent creep can be explained as follows. With the maximum surcharge applied and the front wall rotated outward away from the tire chips, part of the fill, known as the active wedge, has a tendency to move forward towards the wall, as shown on Figure 6.23. The active wedge moves because the tire chip backfill continued to settle and undergo shear strain after the initial rotation due to the surcharge,

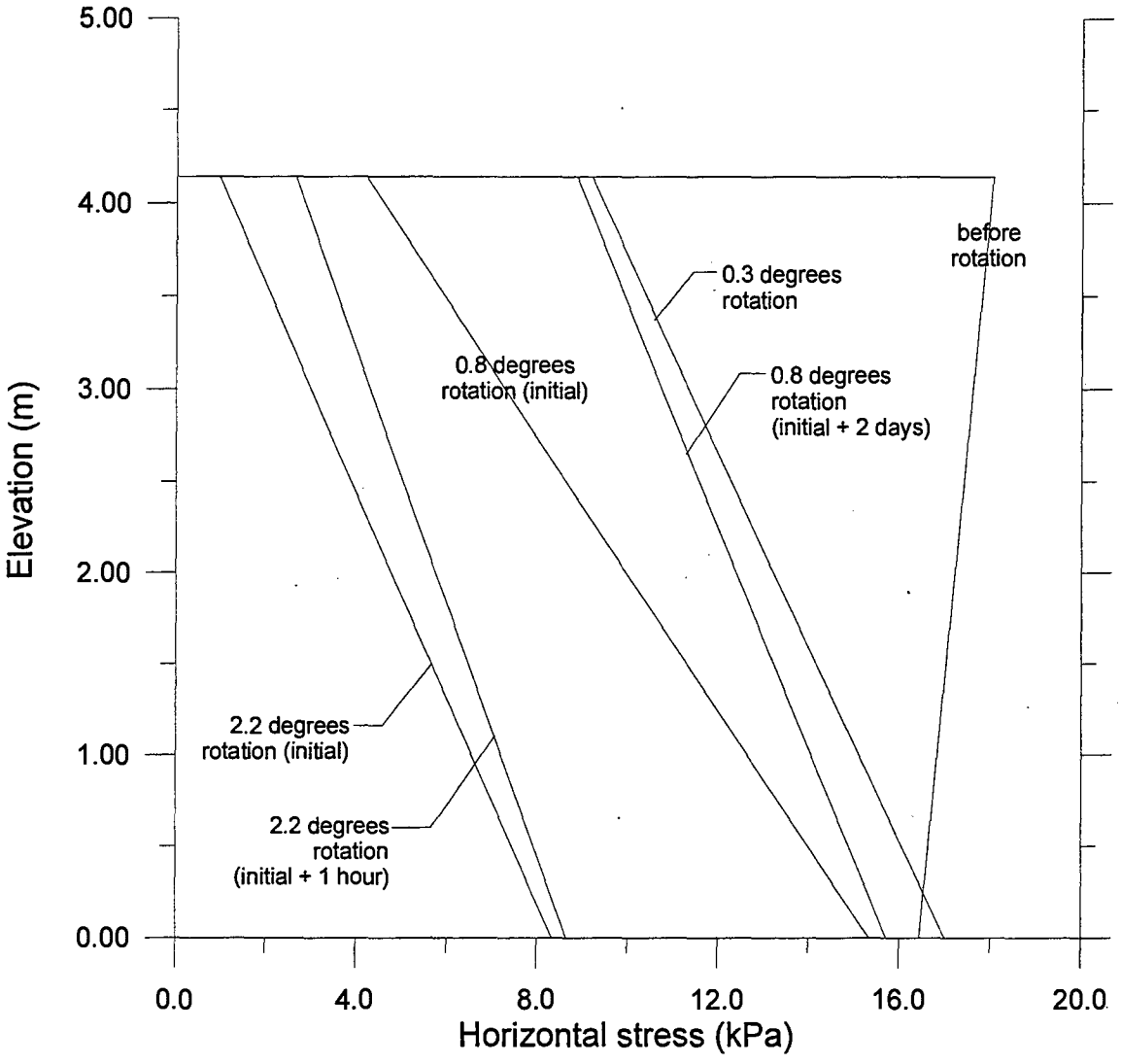

Figure 6.20 Horizontal stress vs. elevation, active conditions, Pine State Recycling

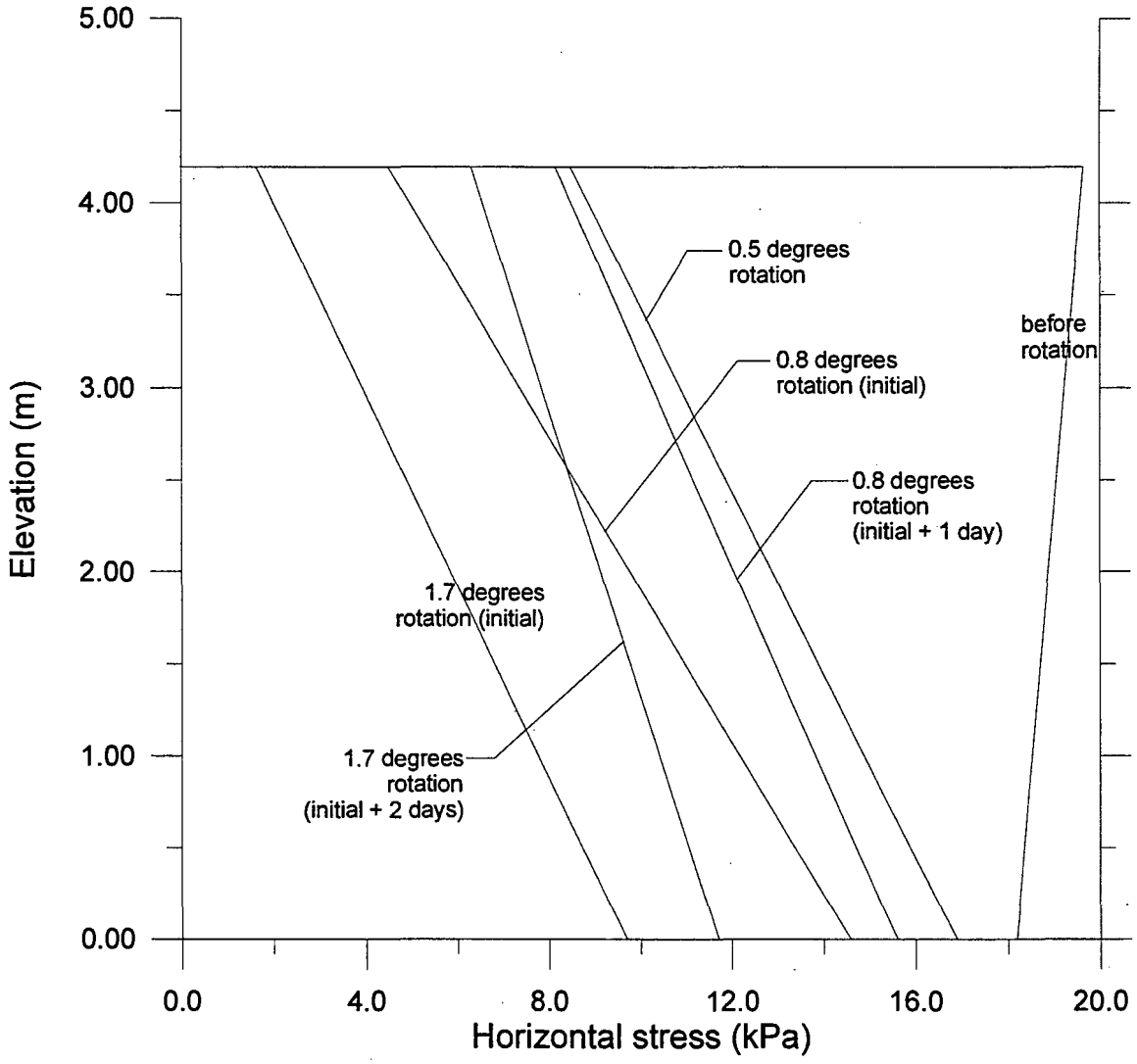

Figure 6.21 Horizontal stress vs. elevation, active conditions, Palmer Shredding

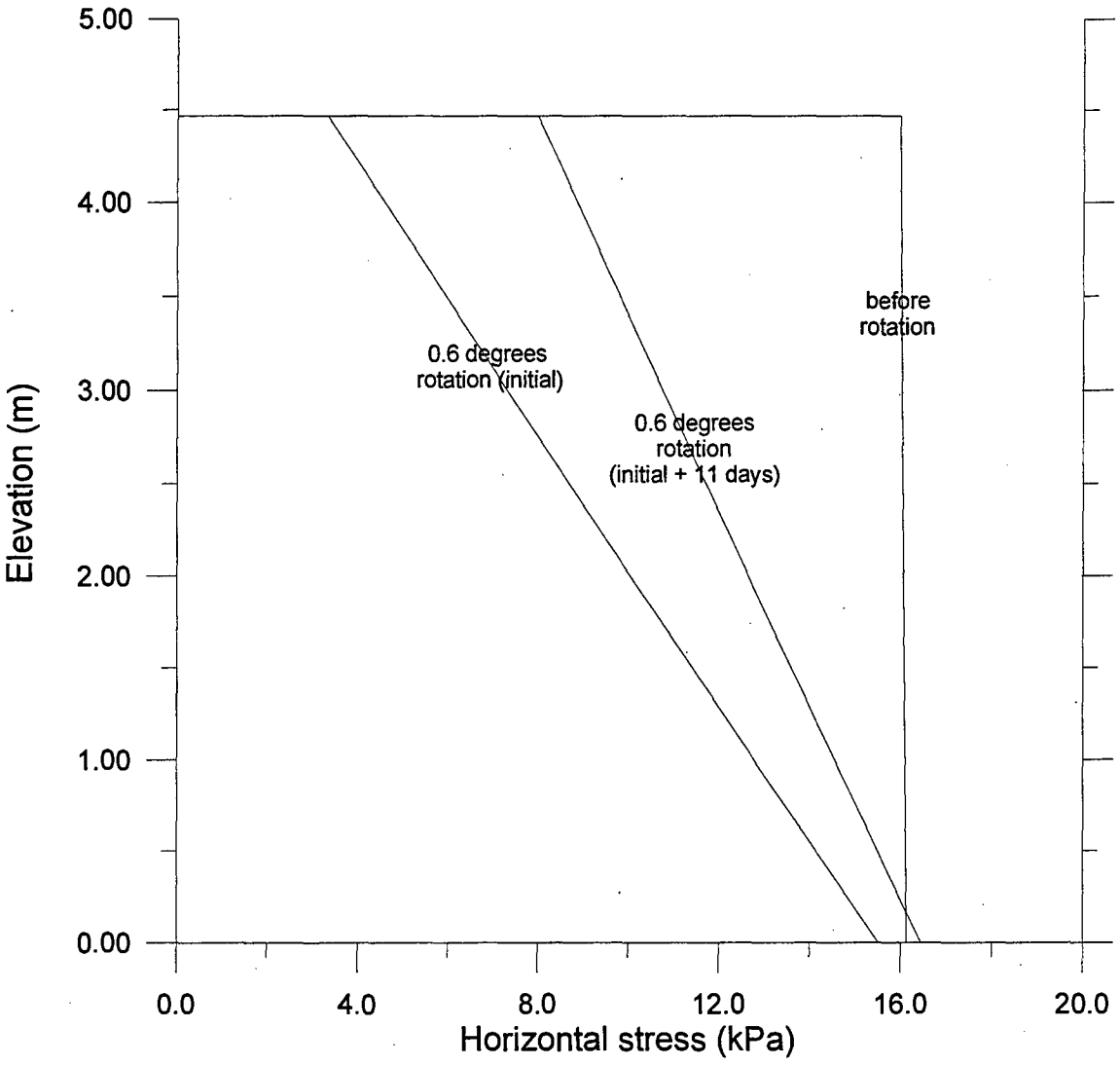

Figure 6.22 Horizontal stress vs. elevation, active conditions, F & B Enterprises

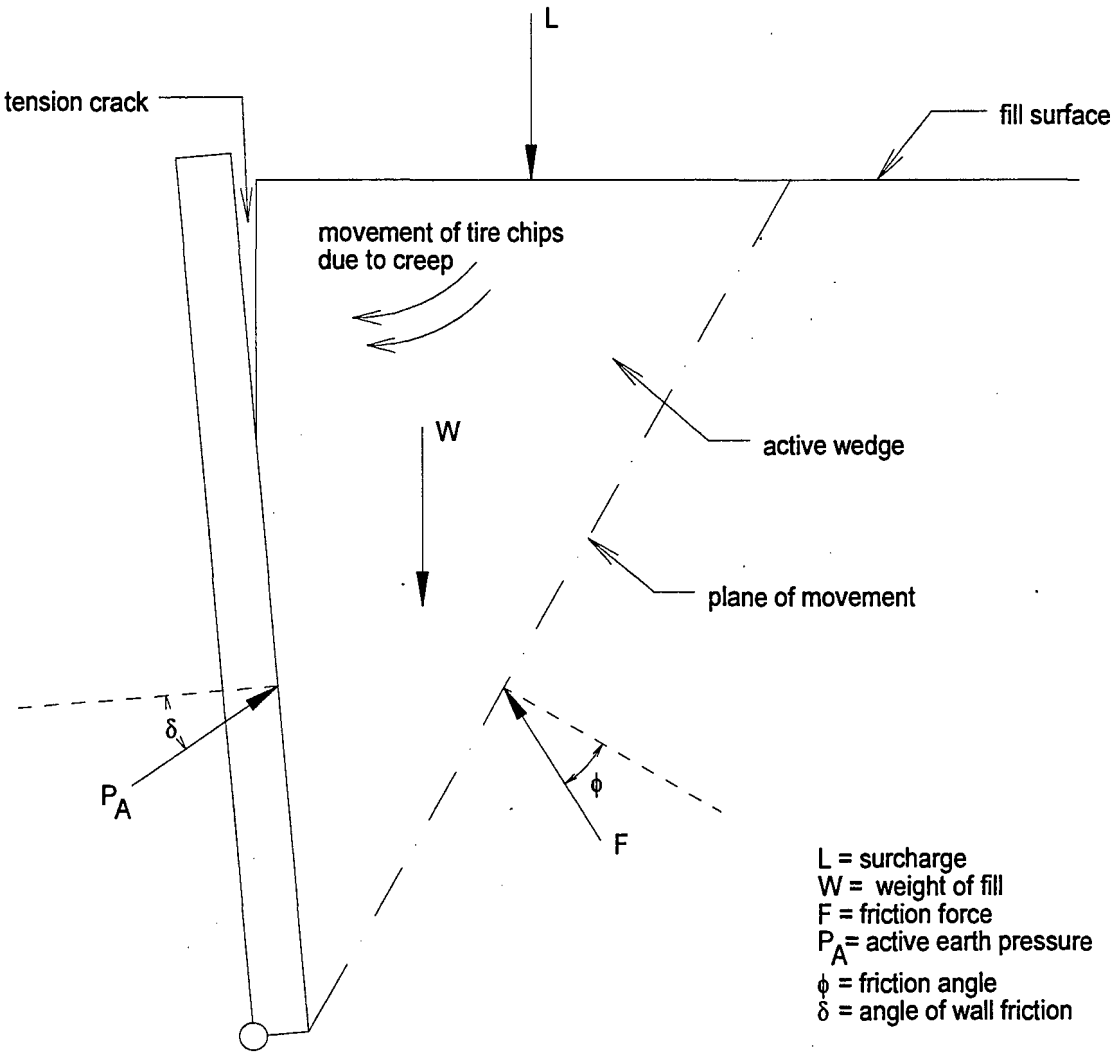

Figure 6.23 Active wedge

weight of the tire chips, and shear stress created when the wall was rotated away from the backfill. This phenomenon is caused by time-dependent creep between tire chips, the interface between the tire chips and the wall, or the rubber itself. One possible explanation for the larger increase of horizontal stress at the top of the fill is the presence of the tension crack. As the wall is tilted outward away from the fill, the shear strength of the tire chips keeps it away from the wall, causing a crack along the tire chip-wall interface, similar to what is shown on Figure 6.23. As creep overcomes the fictional force and active earth pressure the wedge may move into the wall, decreasing the size of the tension crack and increasing the contact area at the top of the wall, causing a larger increase in stress.

Compacted tire chips with no surcharge can stand on a vertical face for short periods of time, raising the possibility the lower bound of active earth pressures could approach zero. An example of this can be seen in Figure 6.24 where the back wall has been removed after a test. This shows a 4.57 m (15.0 ft) vertical face of tire chips, with no surcharge load applied.

Active conditions are achieved when the amount of wall movement is sufficient to produce the minimum horizontal stress. This occurs when the wall moves away from the tire chips and deforms the mass sufficiently to fully mobilize the shear strength. Examination of Figures 6.20 (Pine State Recycling) and 6.21 (Palmer Shredding) shows that the horizontal stress continued to decrease up to the maximum rotations of 2.2 degrees and 1.7 degrees. Thus, it is felt that the rotation was insufficient to achieve true active conditions. However, since the large movements necessary to achieve active

Figure 6.24 Vertical wall of tire chips after completion of test with Pine State Recycling

conditions using tire chips (greater than 2.2 degrees) would seldom be acceptable, it is felt that sufficient information was gathered relative to the decrease in horizontal stress with wall movement.

The horizontal stress distribution for the intermediate rotation with F & B Enterprises and maximum rotation with Pine State Recycling and Palmer Shredding were examined further using the pressure cells, as shown in Figures 6.25 through 6.27. The pressure cell values were computed using four calibration combinations, as described in Section 6.2.2. In each case, the pressure cell yields a range of possible horizontal stresses. Figures 6.25 through 6.27 also show that the values obtained using the pressure cells vary from about the same to values lower than obtained using the load cells. The reasons for differences between stresses from the load cells and pressure cells were discussed in Section 6.3.1.2.

The horizontal stress distributions shown on Figures 6.20 through 6.22 can be compared to a FE analysis by Gharegrat (1993), as discussed in Section 6.3.1.2. Gharegrat (1993) performed FE analysis for four rotations of a retaining wall with tire chip backfill at a surcharge of 35.9 kPa (750 psf). The four rotations were as follows: 0.03 m (0.10 ft), 0.08 m (0.25 ft), 0.11 m (0.35 ft), and 0.15 m (0.50 ft). For a wall height of 4.57 m (15 ft), the wall movements range from approximately 0.01H to 0.03H. The horizontal stress versus fill elevation by Gharegrat (1993) for active condition is shown on Figure 6.28.

Examination of Figure 6.28 shows that the horizontal stress at the backfill surface is zero, while for the distributions on Figures 6.20 through 6.22 the stress at the surface is

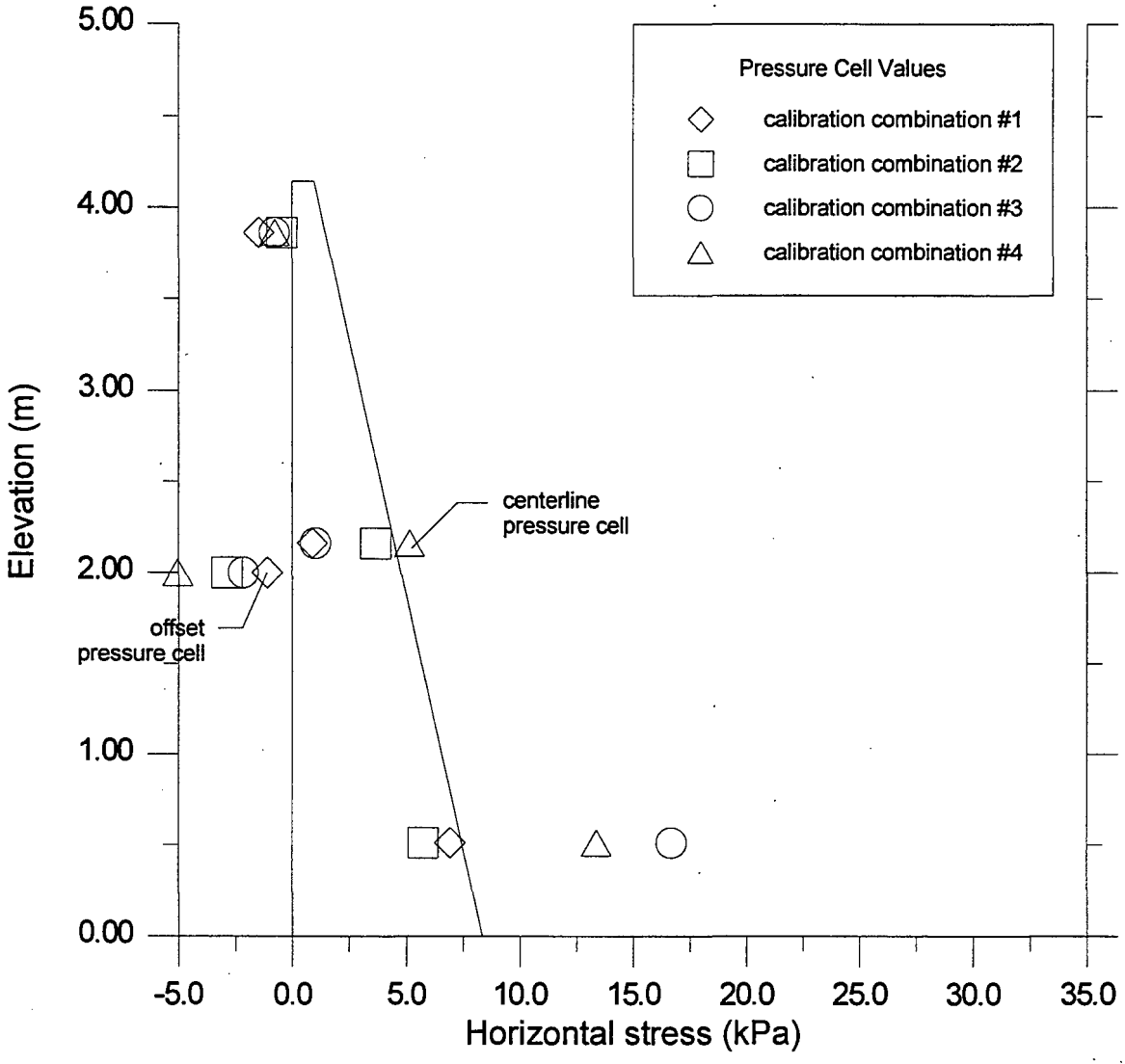

Figure 6.25 Horizontal stress vs. elevation, active conditions, with pressure cell values, Pine State Recycling (2.2 degrees, initial)

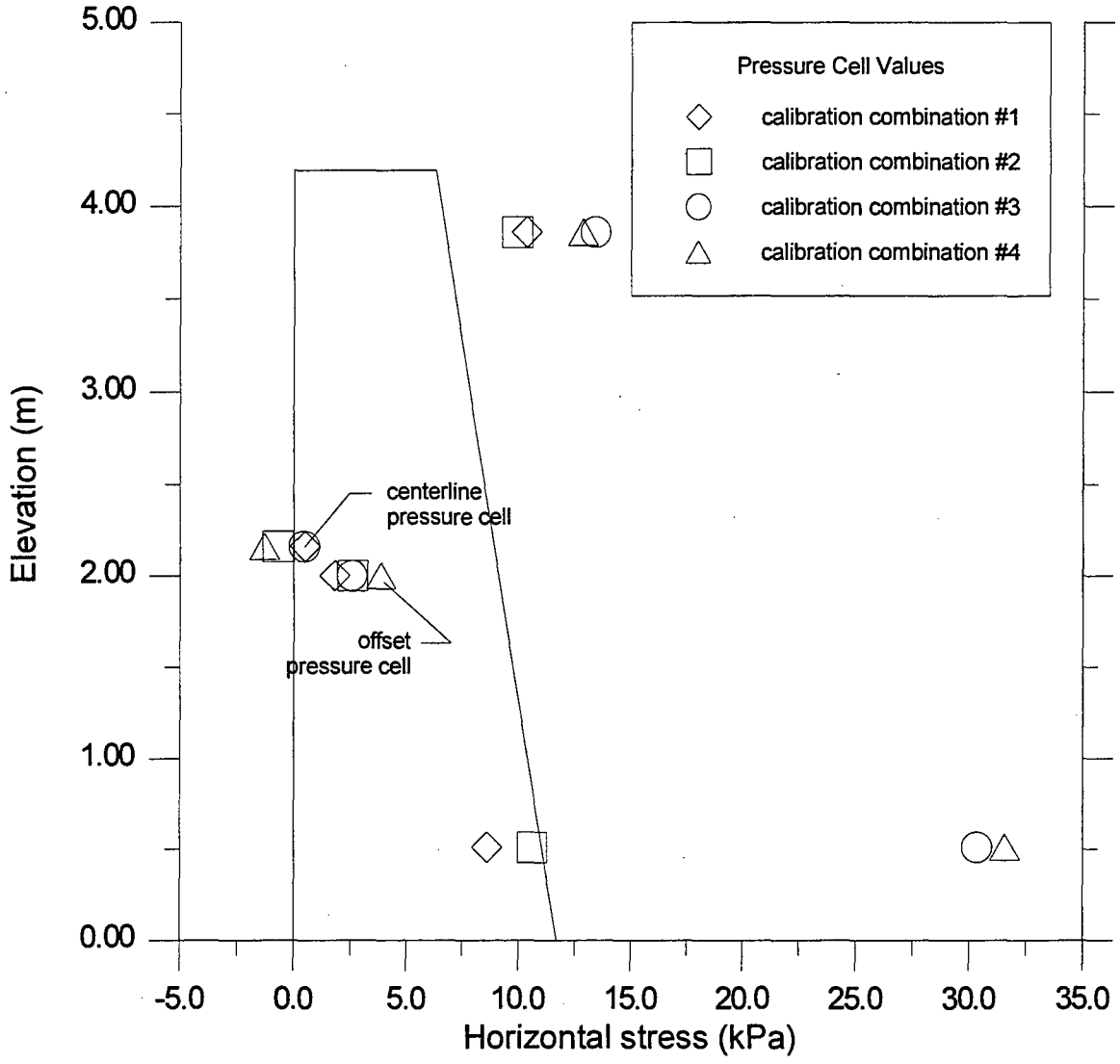

Figure 6.26 Horizontal stress vs. elevation, active conditions, with pressure cell values, Palmer Shredding (1.7 degrees, initial + 2 days)

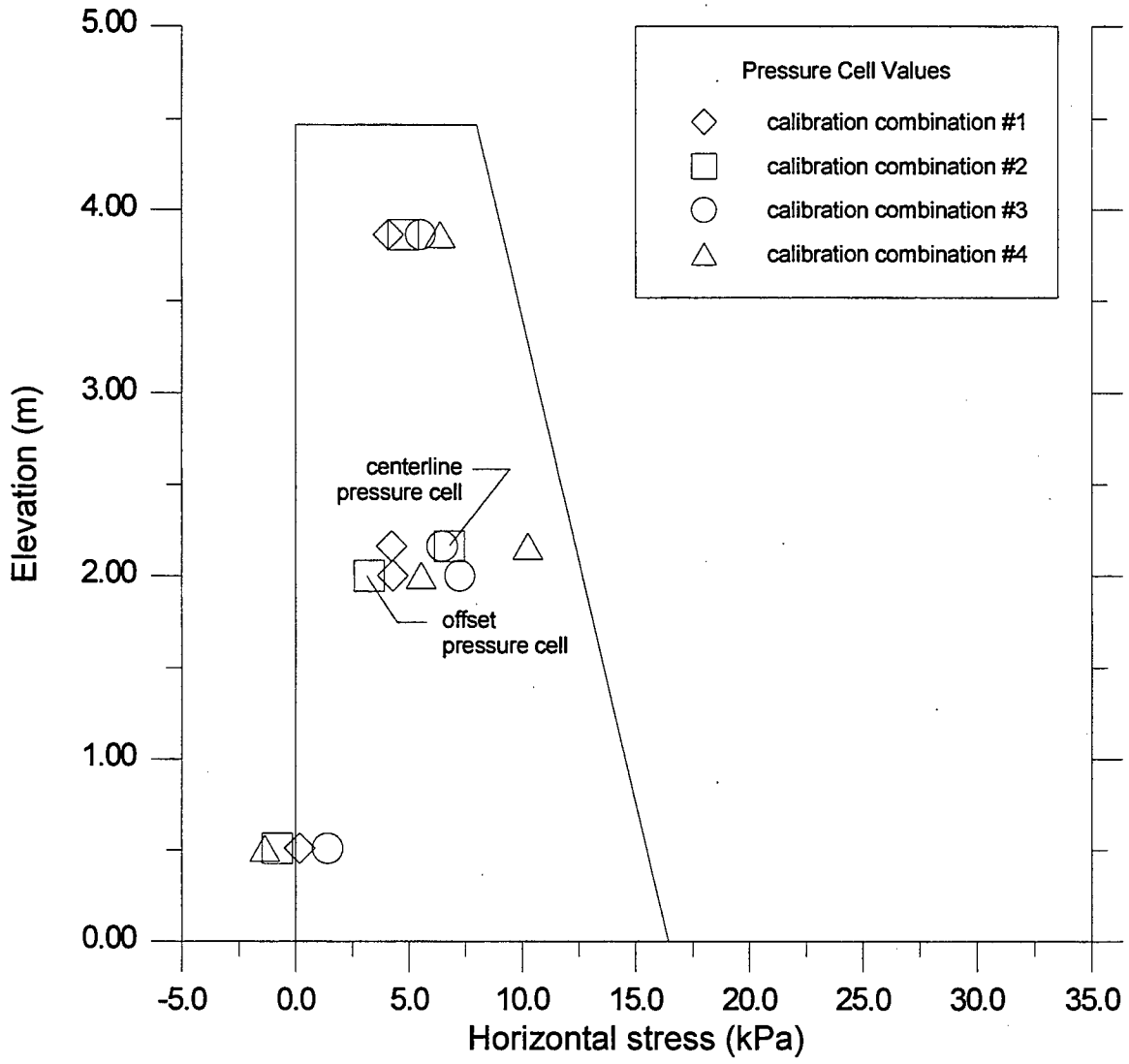

Figure 6.27 Horizontal stress vs. elevation, active conditions, with pressure cell values, F & B Enterprises (0.6 degrees, initial + 11 days)

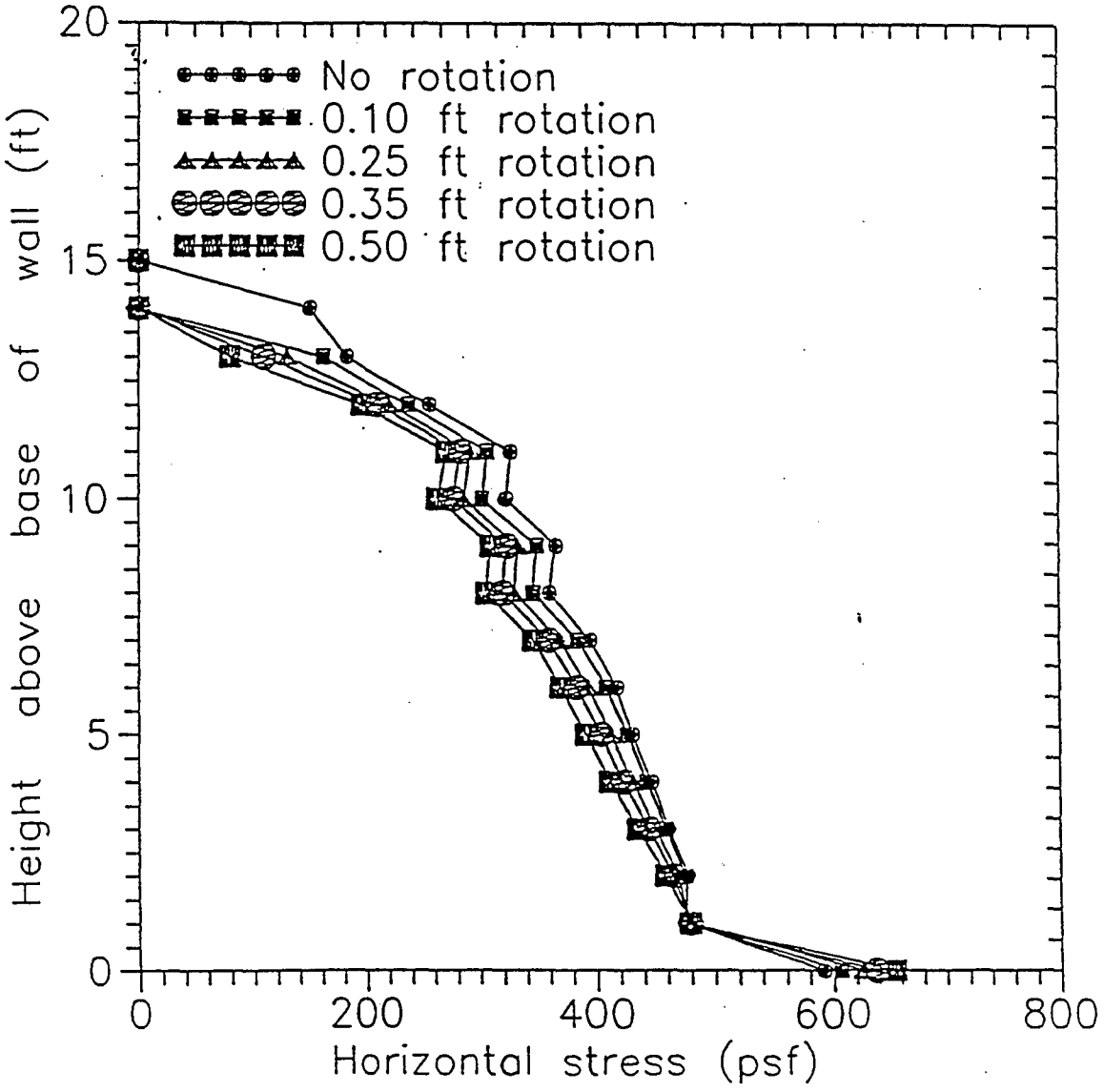

1 psf = 0.0479 kPa

Figure 6.28 Active horizontal stress from finite element analysis (Gharegrat, 1993)

greater than zero. This is similar for the FE comparison for the at-rest state (Section 6.3.1.2). This is due to, at least part, to the method used in the FE analysis to calculate stress at a boundary and the assumed linear variation of horizontal stress with depth for stresses calculated from the load cells.

Further comparison can be made by examining the resultant horizontal forces. The resultant determined from the 0.03-m (0.10-ft) plot from Gharegrat (1993), which corresponds to a rotation of approximately 0.01H, can be compared to the resultants from Figures 6.20 through 6.22 for the rotation of approximately 0.01H. The readings corresponding to the maximum amount of time passed after the initial rotation were used: Pine State Recycling, 0.8 degrees (initial + 2 days); Palmer Shredding, 0.8 degrees (initial + 1 day); F & B Enterprises, 0.6 degrees (initial + 11 days). This shows that the FE resultant force is approximately 30% greater than those measured in the field from the three suppliers. A similar comparison can be made for rotations of approximately 0.03H from Gharegrat (1993) and Palmer Shredding. This shows that the FE resultant for the 0.15-m (0.50-ft) rotation is 44% greater than Palmer Shredding, at a rotation of 1.7 degrees (initial + 2 days). Thus, the finite element analysis by Gharegrat (1993) over estimated the active horizontal stress that occurred in the field. One reason for this is that Gharegrat (1993) used an interface friction angle (δ) of 14°. This is less than half of the δ measured in this study, as will be discussed in Chapter 7. Had Gharegrat (1993) used a higher δ, the resulting horizontal stress would have been lower.

6.4.3 Granular Fill Versus Tire Chips

The horizontal stress distributions for each of the tire chip suppliers at the rotation of 0.01H, as shown on Figures 6.20 through 6.22, can be compared to the horizontal stress distribution that would have been expected for the granular fill. This was done by plotting the horizontal stress distributions for a rotation of approximately 0.01H, with the maximum amount of elapsed time since rotation, for each of the tire chip suppliers, as shown on Figure 6.29. The active earth pressure for the granular fill was determined using the average of the elevations of the tire chips and the maximum surcharge. The properties used were the average density, 2.023 Mg/m^3 (126.3 pcf), and a friction angle (ϕ) of 38°. The friction angle was used to calculate K_a from the Rankine active earth pressure coefficient using:

$$K_a = \tan^2(45 - \phi/2) \tag{6.5}$$

The resulting K_a is 0.24.

Examination of Figure 6.29 shows that the granular stress distribution is considerably larger than from the three tire chip suppliers, with the resultant of the horizontal stress from the tire chips approximately 35% less than that of the granular fill.

6.5 DESIGN PARAMETERS

The results discussed above were used to obtain parameters to be used in design. First, the coefficients of lateral earth pressure will be discussed. Then, semiempirical methods based on the material property and behavior will be discussed.

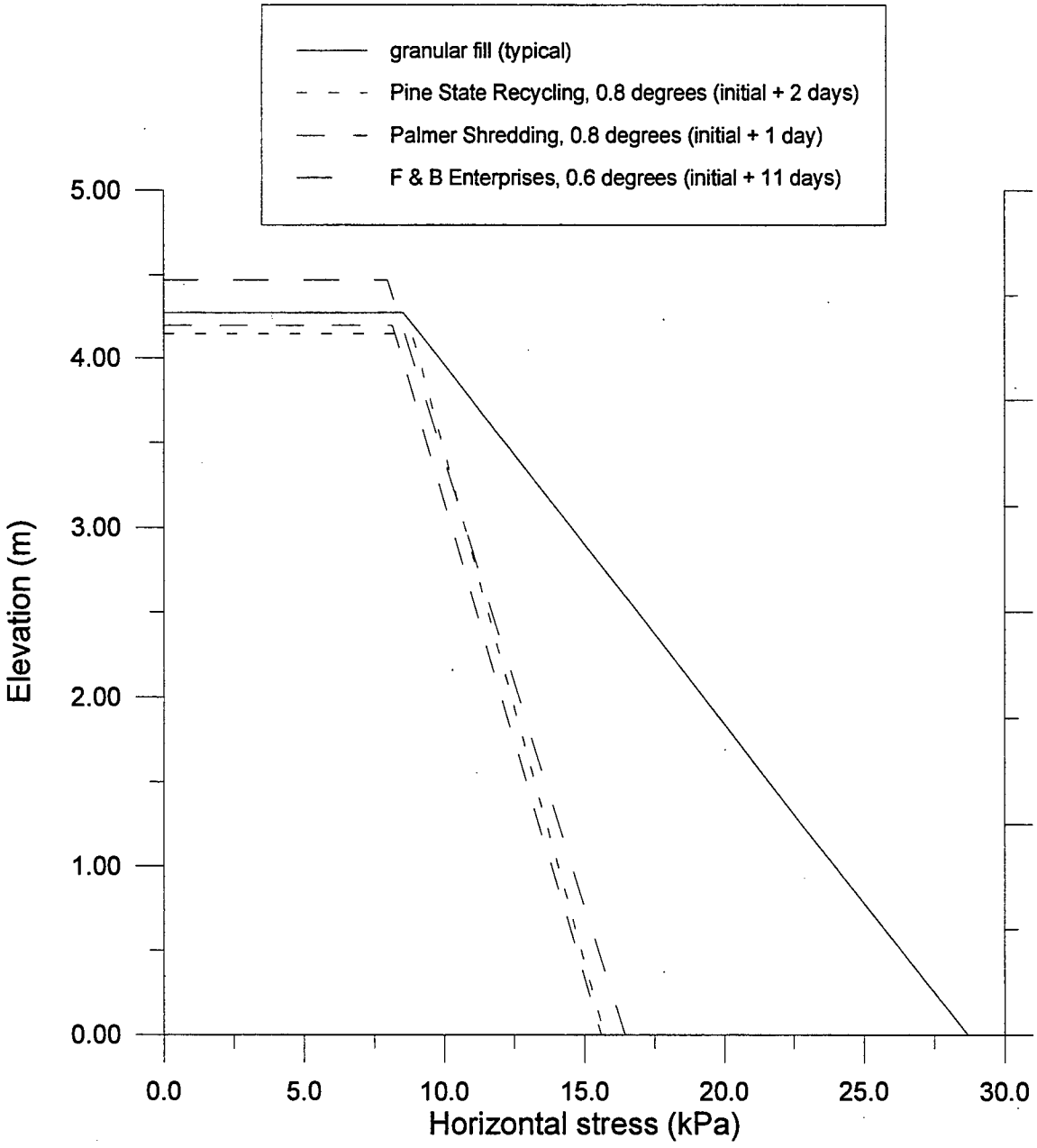

Figure 6.29 Typical active horizontal stress distribution for granular fill and those measured from three tire chip suppliers (0.01H of outward wall movement)

6.5.1 Coefficient of Lateral Earth Pressure

6.5.1.1 Coefficient of Lateral Earth Pressure At Rest, K_o

The relationship between the vertical stress and the horizontal stress is defined by

$$\sigma'_h = K_o \sigma'_v \tag{6.6}$$

where σ'_h is the horizontal effective stress, σ'_v is the vertical effective stress, and K_o is known as the coefficient of lateral earth pressure at rest.

To determine the coefficient of lateral earth pressure at rest it was necessary to determine the vertical stress versus elevation in the fill for each tire chip supplier. Previous studies by Humphrey, et al. (1992) measured the compressibility and percent increase in density versus vertical stress for tire chips from the same suppliers as used in this study. A typical plot for Pine State Recycling is shown on Figure 6.30. Knowing the depth of fill and the maximum surcharge, the maximum vertical stress at the base of the fill could be estimated at 68.9 kPa (10 psi). If the initial loading curves (as shown on Figure 6.30) are assumed to be linear between the stress values of 0 and 68.9 kPa (10.0 psi) a direct correlation can be made between density and vertical stress. These values are shown in Table 6.1.

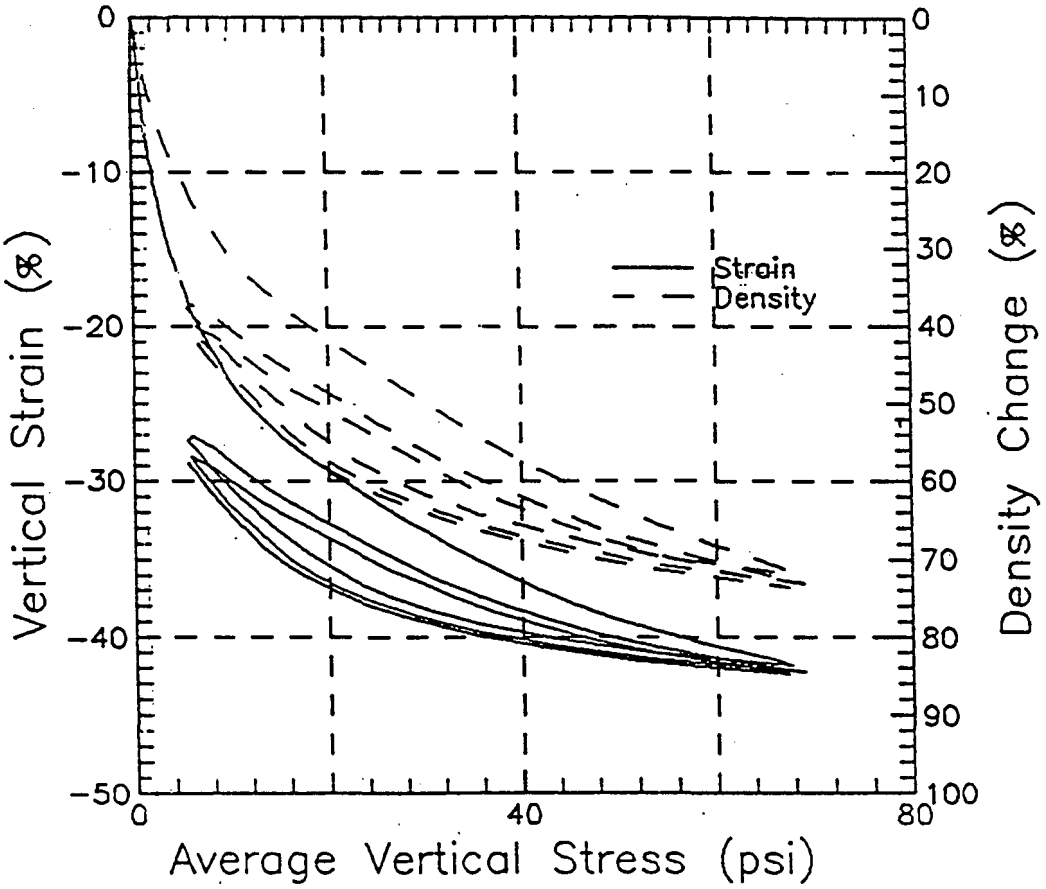

1 psi = 6.89 kPa

Figure 6.30 Vertical strain and density change vs. average vertical stress, Pine State Recycling (Humphrey, et al., 1992)

Table 6.1 Normalized percent change in density for vertical stress range of 0 to 68.9 kPa (10.0 psi)

Supplier	Density Change (%) / Vertical Stress (kPa)
Pine State Recycling	0.62
Palmer Shredding	0.69
F & B Enterprises	0.45

As the fill elevation increases, the vertical stress increases at the base of the fill, resulting in an increase in density. Thus, a direct correlation can be made between vertical stress and fill elevation. A typical plot for Pine State Recycling is shown on Figure 6.31.

The coefficient of lateral earth pressure at rest, K_o, was determined using the relationship between vertical stress and fill elevation, and the horizontal stress distributions during initial filling, as shown on Figures 6.3 through 6.5. K_o was determined for the following surcharges: no surcharge, 12.0 kPa (250 psf), 23.9 kPa (500 psf), and 35.9 kPa (750 psf). For the minimum, intermediate, and maximum surcharges, K_o was determined at the depths of 0 m, 2.0 m (6.6 ft), and 4.0 m (13.1 ft). For no surcharge, it was necessary to determine K_o just below the fill surface, because σ'_v is zero at the fill surface; so, K_o is undefined. Thus, K_o was determined at the depths of 0.5 m (1.6 ft), 2.0 m (6.6 ft), and 4.0 m (13.1 ft) for the no surcharge case. The values for K_o are summarized in Table 6.2.

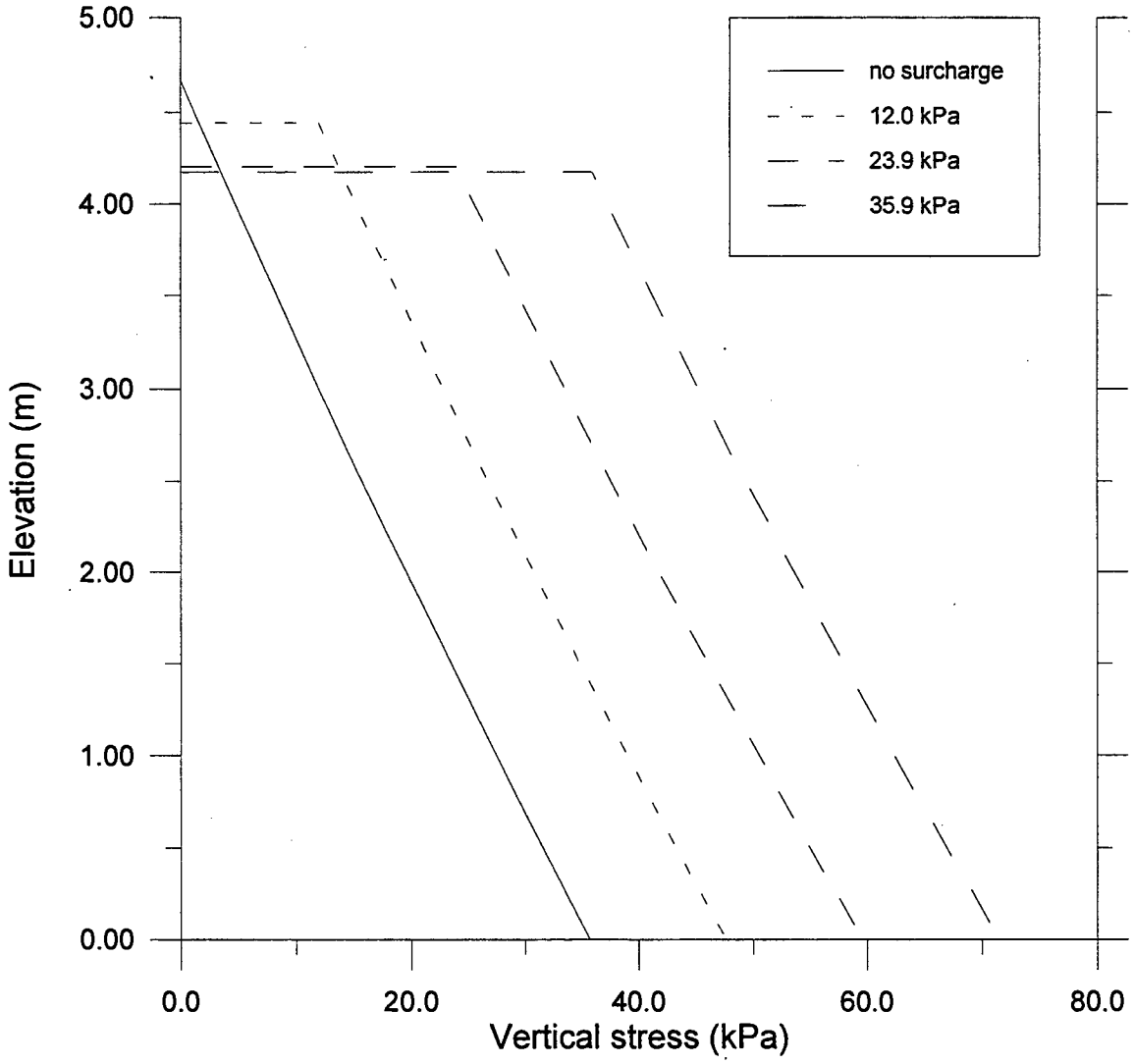

Figure 6.31 Vertical stress vs. elevation, determined from values in Table 6.1 for Pine State Recycling

Table 6.2 Coefficient of lateral earth pressure at rest, K_o

No surcharge			
Depth (m)	**Pine State Recycling**	**Palmer Shredding**	**F & B Enterprises**
0.5	0.93	0.94	0.99
2.0	0.37	0.37	0.39
4.0	0.28	0.29	0.31
12.0 kPa surcharge			
0.0	0.55	0.58	0.51
2.0	0.32	0.33	0.33
4.0	0.26	0.27	0.28
23.9 kPa surcharge			
0.0	0.46	0.51	0.44
2.0	0.32	0.27	0.32
4.0	0.26	0.17	0.26
35.9 kPa surcharge			
0.0	0.47	0.51	0.45
2.0	0.32	0.33	0.32
4.0	0.25	0.24	0.25

Table 6.2 shows that the coefficient of lateral earth pressure at rest decreases with depth for all four loading conditions. The values for K_o at the surface decrease from no surcharge to 23.9 kPa (500 psf). K_o then remains approximately constant from 23.9 kPa (500 psf) to 35.9 kPa (750 psf). For no surcharge, K_o at the depth of 0.5 m (1.6 ft) is slightly larger for F & B Enterprises than for the other two tire chips. For the other three surcharges the value at the fill surface is slightly larger for Palmer Shredding. However, for surcharges of 12.0 kPa (250 psf), 23.9 kPa (500 psf), and 35.9 kPa (750 psf), the values for K_o at depths of 2.0 m (6.6 ft) and 4.0 m (13.1 ft) are similar for the three suppliers, the one exception is for the intermediate surcharge of 23.9 kPa (500 psf). At this surcharge K_o is slightly lower for Palmer Shredding.

Comparison of K_o at the 35.9 kPa (750 psf) surcharge for the three suppliers shows that the range of values is small. At the fill surface, K_o ranges from 0.51 to 0.45, with Palmer Shredding being the largest and Pine State Recycling the smallest. K_o varies from 0.33 to 0.32 at 2.0 m (6.6 ft) and 0.24 to 0.25 at 4.0 m (13.1 ft). The differences between the high and low values of K_o are small for the other three surcharges, which shows that K_o differs only slightly for the range of tire chip types tested in this study.

The values in Table 6.2 can be compared to K_o measured in the laboratory by Humphrey, et al. (1992) for the same tire chip suppliers. Their results, along with some from this study, are given in Table 6.3.

Table 6.3 shows that the K_o measured in the laboratory for Pine State Recycling and F & B Enterprises is higher than measured in the field at both the 2.0-m (6.6-ft) and 4.0-m

Table 6.3 Comparison of K_o with values measured in the laboratory by Humphrey, et al. (1992)

Supplier	Average K_o*	K_o at 2.0-m depth**	K_o at 4.0-m depth**
Pine State Recycling	0.41	0.32	0.25 to 0.26
Palmer Shredding	0.26	0.27 to 0.33	0.17 to 0.27
F & B Enterprises	0.47	0.32 to 0.33	0.25 to 0.28

*Humphrey, et al. (1992)

**Range of K_o measured in this study for surcharges of 12.0 kPa (250 psf), 23.9 kPa (500 psf), and 35.9 kPa (750 psf)

(13.1-ft) depths. However, K_o measured by Humphrey, et al. (1992) for Palmer Shredding tire chips is within the range of values measured from this study at both depths. It is noted the K_o for Palmer Shredding determined by Humphrey, et al. (1992) is lower than those determined for the other two tire chip suppliers. Thus, K_o determined by Humphrey, et al. (1992) for Pine State Recycling and F & B Enterprises are higher than measured for field conditions.

The coefficient of lateral earth pressure at rest for tire chips can also be compared to the value for granular material. For granular material, K_o can be estimated by Equation 6.4 (Jaky, 1948; Mesri and Hayat, 1993). Using the angle of internal friction measured from triaxial tests K_o is 0.38. This is higher than the K_o for tire chips measured in this study at the 2.0-m (6.6-ft) and 4.0-m (13.1-ft) depths. This suggests that the lower at-rest pressures produced by the tire chips are due both to the lower K_o and lower density of tire chips.

6.5.1.2 Coefficient of Active Earth Pressure, K_a

Active conditions are reached when the wall is rotated outward and the horizontal stress reaches a minimum value. The relationship between the vertical stress for active conditions is

$$\sigma'_h = K_a \sigma'_v \tag{6.7}$$

where K_a is the coefficient of active earth pressure.

The coefficient of active earth pressure was determined using the relationship between vertical stress and fill elevation, as discussed in Section 6.5.1.1, and the active horizontal stress distributions shown on Figures 6.20 through 6.22. K_a was determined for each tire chip supplier at an intermediate rotation, approximately 0.01H. It was also determined at the maximum rotations for Pine State Recycling and Palmer Shredding. For both the intermediate and maximum rotations, K_a was determined from the horizontal stress distribution corresponding with the longest period of time after the initial rotation. The values for K_a are shown in Tables 6.4.

Table 6.4 shows that for the intermediate rotation (0.01H), K_a is very similar for the three suppliers at each depth, with values ranging from 0.22 to 0.25. Thus, K_a does not vary significantly with tire chips type and depth. At the maximum rotation, K_a ranged from 0.16 to 0.18 for Palmer Shredding at a rotation of 0.03H and 0.08 to 0.12 for Pine State Recycling for a larger rotation of 0.04H. This shows that K_a may decrease with outward movement.

Table 6.4 Coefficient of active earth pressure, K_a

Intermediate rotation			
Depth (m)	**Pine State Recycling (0.8 degrees, 2 days)**	**Palmer Shredding (0.8 degrees, 1 day)**	**F & B Enterprises (0.6 degrees, 11 days)**
0.0	0.25	0.23	0.23
2.0	0.23	0.22	0.23
4.0	0.22	0.22	0.23

Maximum rotation		
Depth (m)	**Pine State Recycling (2.2 degrees, 1 hour)**	**Palmer Shredding (1.7 degrees, 2 days)**
0.0	0.08	0.18
2.0	0.11	0.17
4.0	0.12	0.16

As discussed in Section 6.4.2, it is felt that more rotation of the front wall was necessary to achieve active conditions for the tire chip backfills. Consequently, K_a for the tire chips reported in this study is not truly the coefficient of active earth pressure. It is, rather, the ratio of horizontal stress to vertical stress somewhere in between at-rest and active conditions. However, since the large movements necessary to achieve active conditions using tire chips would rarely, if ever, be designed for, the values in Table 6.4 are considered to be applicable for typical conditions.

The coefficient of active earth pressure for tire chips can be compared to the value typically used for granular material. Comparison can be made to the Rankine active

earth pressure coefficient given in Equation 6.5. Using the measured friction angle of 38° K_a is 0.24, which is slightly larger than the tire chip values at the intermediate rotation and significantly larger than those for the maximum rotation. As with the at-rest case, this suggests that the lower active pressures produced by tire chips are due both to the lower K_a and lower density of tire chips.

6.5.2 Semiempirical Design Parameters

Semiempirical design parameters were developed following the methods presented in Terzaghi, et al. (1996) for soils. This method allows the horizontal stress acting on the vertical wall face to be estimated from the soil type and the inclination of the backfill surface. The key parameter is a semiempirical value, k_h, with units of weight per unit volume. The method can be thought of as replacing the soil with a fluid of density k_h. The value k_h can then be used to determine the resultant force acting on the wall, as shown on Figure 6.32a, and the horizontal stress. The horizontal stress can be determined by the following equation:

$$\sigma_h = k_h H \tag{6.8}$$

where H is the depth below the top of the wall.

In cases where a surcharge is applied and the surface of the backfill is horizontal the horizontal stress at any depth is increased by the amount

$$p_q = Cq \tag{6.9}$$

a)

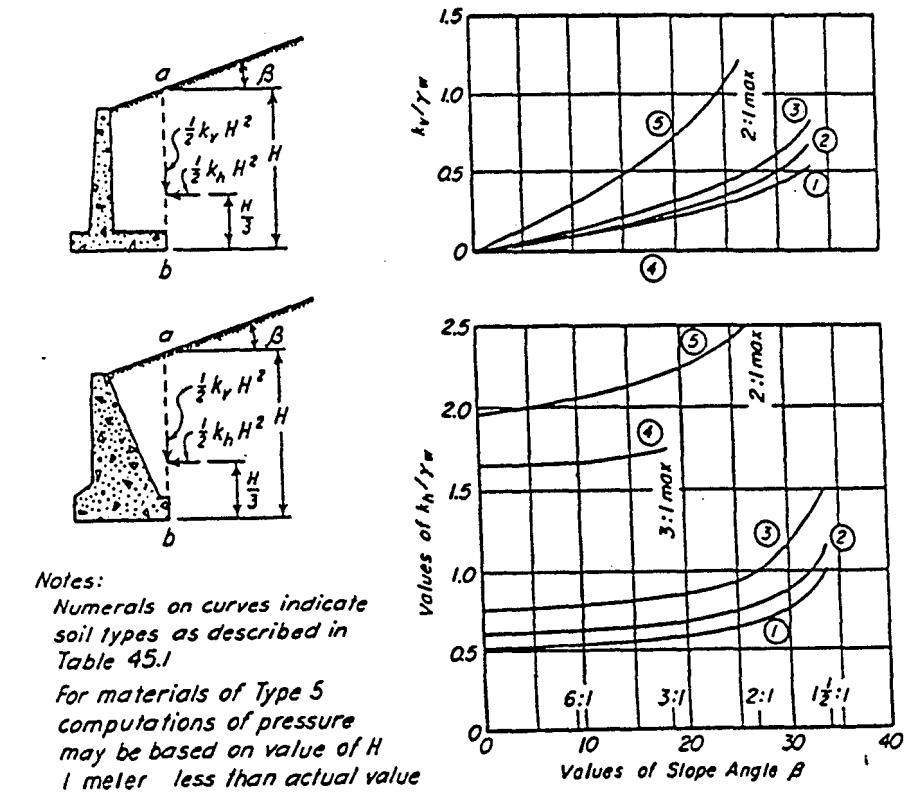

Notes:
Numerals on curves indicate soil types as described in Table 45.1
For materials of Type 5 computations of pressure may be based on value of H 1 meter less than actual value

b)

Type of Soil	C
1	0.27
2	0.30
3	0.39
4	1.00
5	1.00

c)

1. Coarse-grained soil without admixture of fine soil particles, very permeable (clean sand or gravel).
2. Coarse-grained soil of low permeability due to admixture of particles of silt size.
3. Residual soil with stones, fine silty sand, and granular materials with conspicuous clay content.
4. Very soft or soft clay, organic silts, or silty clays.
5. Medium or stiff clay.

Figure 6.32 Semiempirical design method: a) k_h, b) C, c) soil types (Terzaghi, et al., 1996)

where C is a coefficient dependent on the soil type, and q is the surcharge in units of load per unit area. The combination of the stress due to the soil and the surcharge results in a trapezoidal distribution, as shown on Figure 6.33. Values of k_h and C for soil are shown on Figures 6.32a and 6.32b, respectively. The semiempirical values k_h and C were determined for the three tire chip suppliers for the at-rest and active conditions, as discussed in the following paragraphs.

For the at-rest conditions, k_h was found for the following surcharges: no surcharge, 12.0 kPa (250 psf), 23.9 kPa (500 psf), and 35.9 kPa (750 psf). With no surcharge, k_h was determined by resolving the trapezoid shaped distribution obtained from the load cells into an equivalent triangle shaped distribution, as shown on Figure 6.34. k_h was then determined from the horizontal stress at the base of the equivalent triangle shaped distribution, given by the equation:

$$\sigma_{equiv} = \sigma_{top} + \sigma_{bottom} \tag{6.10}$$

where σ_{top} and σ_{bottom} are the top and bottom values of the horizontal stress distribution obtained from the load cells. k_h could then be determined by

$$k_h = \frac{\sigma_{equiv}}{d} \tag{6.11}$$

where d is the fill depth.

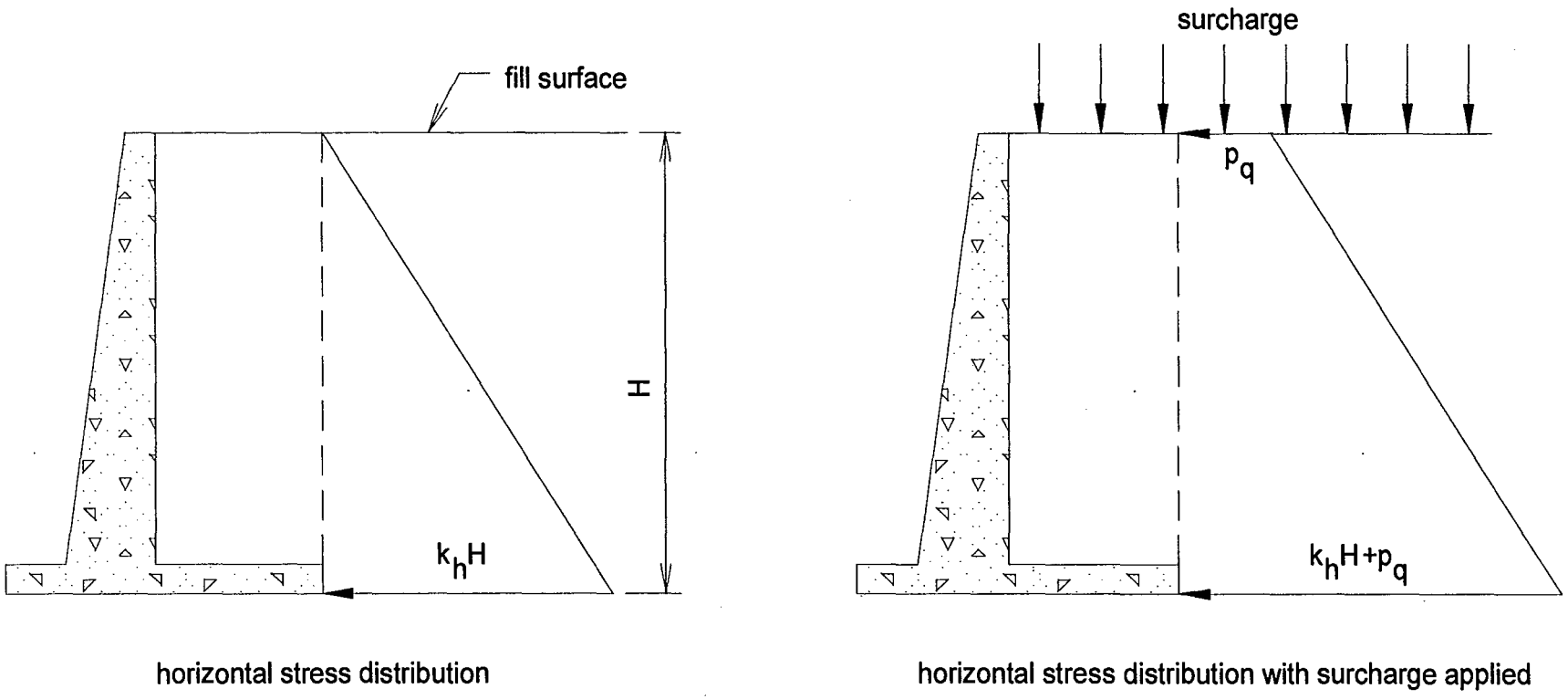

Figure 6.33 Horizontal stress distributions using Terzaghi, et al. (1996)

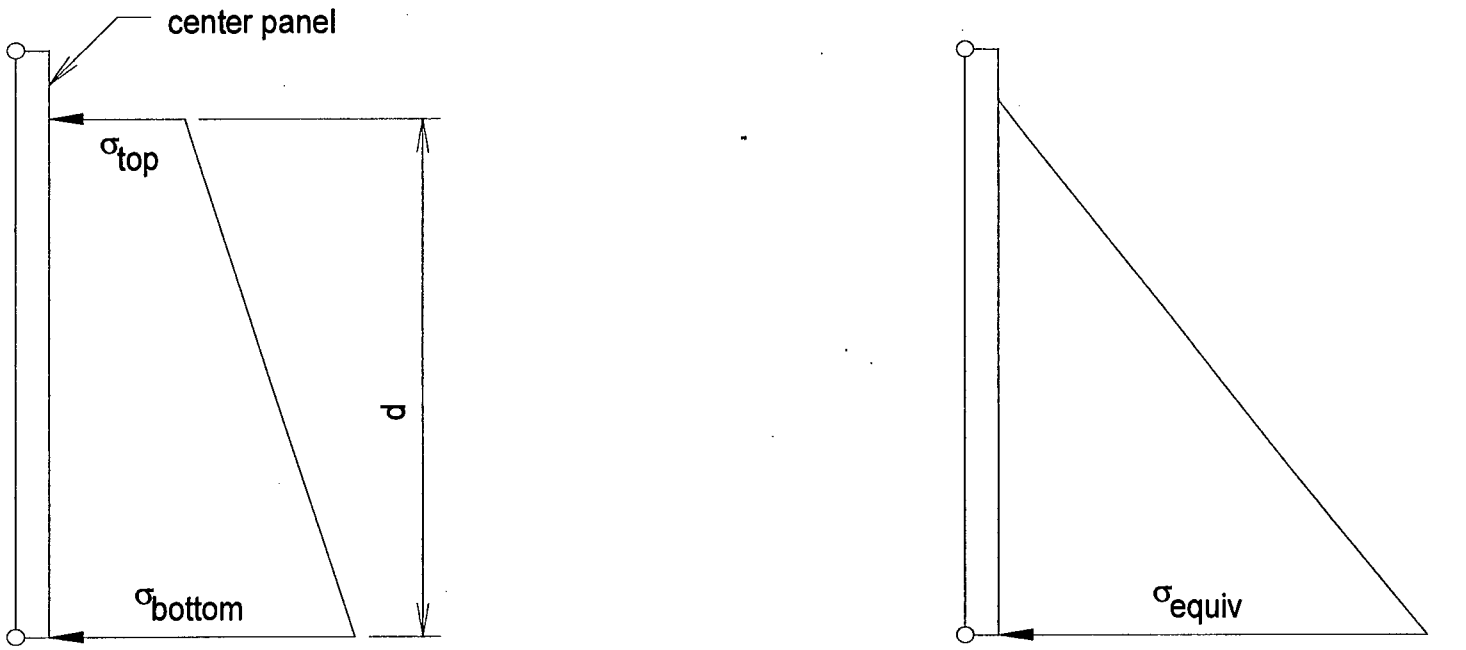

Figure 6.34 Determination of equivalent triangle-shaped distribution for no surcharge

For the minimum, intermediate, and maximum surcharges, k_h and C were determined by dividing the trapezoid shaped distributions shown on Figures 6.3 through 6.5 into two parts, as shown on Figure 6.35. The contribution to the horizontal stress from the tire chips was taken to be the trianglular portion of the distribution, shown as $\sigma_{\text{tire chips}}$. The remainder of the horizontal stress was assigned to the $\sigma_{\text{surcharge}}$. k_h and C were determined using $\sigma_{\text{tire chips}}$ and $\sigma_{\text{surcharge}}$, respectively, and the following equations:

$$k_h = \frac{\sigma_{\text{tire chips}}}{d} \tag{6.12}$$

where d is the fill depth

$$C = \frac{\sigma_{\text{surcharge}}}{q} \tag{6.13}$$

where q is the surcharge

For the active case k_h and C were determined from the horizontal stress distributions shown on Figures 6.20 through 6.22. k_h and C were found by dividing the trapezoidal shaped horizontal stress distributions in Figures 6.20 through 6.22 into $\sigma_{\text{tire chips}}$ and $\sigma_{\text{surcharge}}$, as shown on Figure 6.31, and utilizing Equations 6.12 and 6.13. The values were determined for each tire chip supplier at an intermediate rotation, approximately 0.01H, and at the maximum rotations for Pine State Recycling and Palmer Shredding. For both the intermediate and maximum rotations, k_h and C were determined from the horizontal stress distribution corresponding with the longest period of time after the initial rotation.

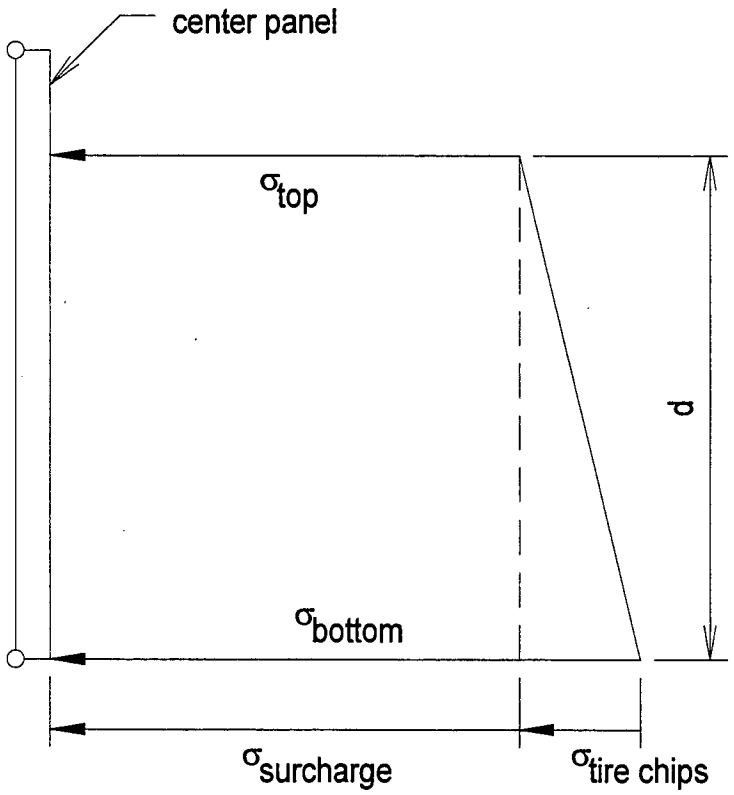

Figure 6.35 Division of horizontal stress distribution at minimum, intermediate, and maximum surcharges

The values for k_h are given in units of density and are presented in Tables 6.5 and 6.6 for the at-rest and active conditions, respectively.

Table 6.5 Semiempirical value, k_h, for the at-rest condition

Surcharge (kPa)	k_h (Mg/m^3)		
	Pine State Recycling	**Palmer Shredding**	**F & B Enterprises**
0	0.26	0.25	0.27
12.0	0.13	0.13	0.15
23.9	0.10	0.06	0.10
35.9	0.01	-0.03	0.02

Table 6.6 Semiempirical value, k_h, for the active condition

k_h (Mg/m^3)		
Immediate rotation		
Pine State Recycling (0.8 degrees, 2 days)	**Palmer Shredding (0.8 degrees, 1 day)**	**F & B Enterprises (0.6 degrees, 11 days)**
0.17	0.18	0.19
Maximum rotation		
Pine State Recycling (2.2 degrees, 1 hour)	**Palmer Shredding (1.7 degrees, 2 days)**	
0.15	0.13	

Table 6.5 shows that the values for k_h decreases as the surcharge is increased, with k_h near zero for the surcharge of 35.9 kPa (750 psf). This shows that the contribution from

the tire chips to the horizontal stress decreases with increasing surcharge. The negative value for Palmer Shredding at 35.9 kPa was caused by the negative slope of the horizontal stress distribution shown in Figure 6.4. Table 6.6 shows that the values for k_h generally decrease with rotation. Table 6.6 also shows that the values at each rotation are similar.

Comparing the values in Tables 6.5 and 6.6 with that for type 1 soil, as described by Terzaghi, et al. (1996) in Figure 6.32c, the value for k_h is 0.51 Mg/m^3 (31.8 pcf). This value is twice that for tire chips with no surcharge and approximately 50 times greater than that for the maximum surcharge. While for the active case, k_h for type 1 soil is approximately 3 times greater than for tire chips.

The semiempirical value, C, was determined for all three surcharges in the at-rest condition and for the intermediate rotation and the maximum rotation in the active state. The values for C are dimensionless and are presented in the Tables 6.7 and 6.8 for the at-rest and active conditions, respectively.

Table 6.7 Semiempirical value, C, for the at-rest condition

Surcharge (kPa)	**Pine State Recycling**	**Palmer Shredding**	**F & B Enterprises**
12.0	0.53	0.54	0.49
23.9	0.45	0.50	0.43
35.9	0.46	0.50	0.45

Table 6.7 shows that the values for C decrease as the surcharge increases from 12.0 kPa (250 psf) to 23.9 kPa (500 psf). C does not show a significant change from 23.9 kPa (250 psf) to 35.9 kPa (750 psf). The values for Palmer Shredding are slightly higher than those for Pine State Recycling and F & B Enterprises. Table 6.7 also shows that the value for C for all three surcharges fall in the range from 0.43 to 0.54.

Table 6.8 Semiempirical value, C, for the active condition

Immediate rotation		
Pine State Recycling (0.8 degrees, 2 days)	**Palmer Shredding (0.8 degrees, 1 day)**	**F & B Enterprises (0.6 degrees, 11 days)**
0.25	0.23	0.22
Maximum rotation		
Pine State Recycling (2.2 degrees, 1 hour)	**Palmer Shredding (1.7 degrees, 2 days)**	
0.07	0.18	

Table 6.8 shows that the values for C decreases as the wall is rotated outward away from the fill. This corresponds with the decrease in horizontal stress as the wall is rotated outward, as shown on Figures 6.20 through 6.22.

The C values for tire chips in Tables 6.7 and 6.8 can be compared with those of type 1 soil in Figure 6.32b. C for type 1 soil, as described by Terzaghi, et al. (1996) is 0.27. This value is nearly half that for tire chips in the at-rest condition; however, Terzaghi, et al. (1996) assumed active conditions, so this is not a valid comparison. At the

intermediate rotation (approximately 0.01H), C from Terzaghi, et al. (1996) is slightly more than the value for tire chips.

Further examination can be done by comparing the resultant horizontal force for type 1 soil with Pine State Recycling tire chips, at both at-rest and active conditions using the methods discussed above. For comparison purposes, the resultant horizontal force will be computed at the maximum surcharge of 35.9 kPa (750 psf) with a 4-m (13.1-ft) depth of fill. For type 1 soil using a C = 0.27 and k_h = 0.51 Mg/m^3 (31.8 pcf), the resultant horizontal force is calculated to be 120 kN (30 kips). For at-rest conditions using Pine State Recycling tire chips and an elevation of 4 m (13.1 ft), the measured horizontal resultant is 102 kN (23 kips), 18% lower than type 1 soil. For the active conditions using Pine State Recycling tire chips, 0.8 degrees (initial + 2 days), and an elevation of 4 m (13.1 ft), the measured horizontal resultant is 75 kN (17 kips), 60% lower than type 1 soil.

6.6 DESIGN CONSIDERATIONS

The design parameters discussed above only apply to retaining walls approximately 4.57 meters (15 feet) in height and with surcharges of 35.9 kPa (750 psf) or less. The backfill material must be tire chip fill with the properties similar to those discussed in Chapter 5. The design considerations were consolidated from the results discussed above.

6.6.1 Coefficient of Lateral Earth Pressure

When using the coefficient of lateral earth pressure for design it is recommended that the vertical stress be determined using criteria in Humphrey, et al. (1992). For fills that are about 4 m (13 ft) thick, the vertical stress from Figure 6.31 may be used.

Examination of the values in Table 6.2 show that K_o decreases with depth for each tire chip supplier at all of the surcharges, while only varying slightly from supplier to supplier. Thus, different recommended values of K_o are suggested for use at the surface and base of tire chip backfills, depending on the surcharge. Moreover, since K_o differs only slightly between tire chips suppliers, the recommended design values were determined from the average from the three suppliers.

The trend of K_o as the surcharge is increased can be seen on Figure 6.36, where the average K_o from the three suppliers is plotted versus depth. This shows that as surcharge increases, K_o tends to approach a constant value. Further examination of Figure 6.36 shows that K_o actually increases slightly from 23.9 kPa (500 psf) to 35.9 kPa (750 psf). This increase is shown to be greater at depths greater than 2 m (6.6 ft). This can be partially attributed to the lower values of K_o for Palmer Shredding at the 2.0 and 4.0-m (6.6 and 13.1-ft) depths at the intermediate surcharge, as shown on Table 6.2. The difference in average K_o from 23.9 kPa (500 psf) to 35.9 kPa (750 psf) is slight and the general trend is to approach a constant value. Thus, the design values for surcharges greater than 23.9 kPa (500 psf) and less than 35.9 kPa (750 psf) were chosen to be the same.

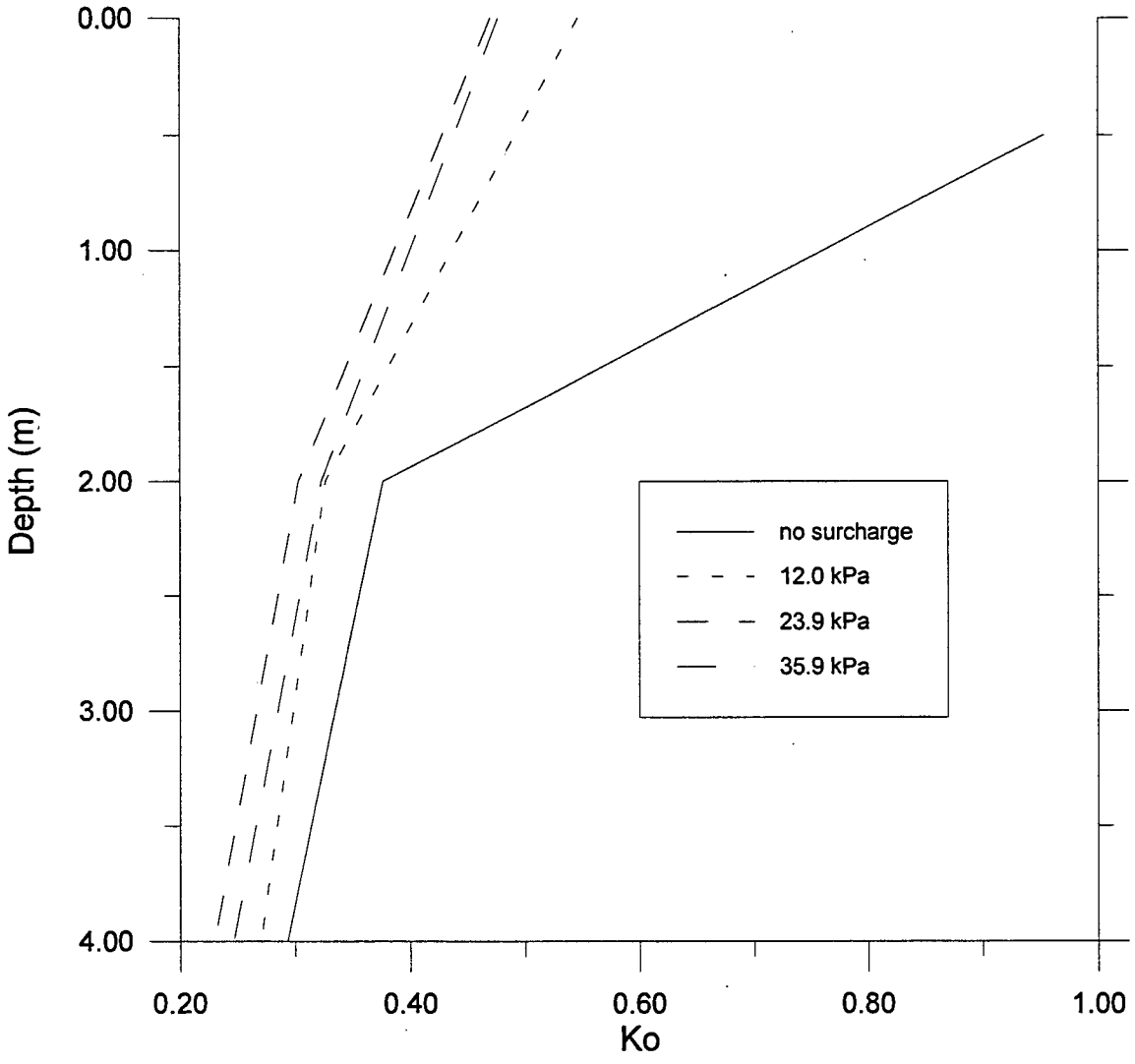

Figure 6.36 Average K_o vs. depth

Table 6.9 shows recommended values of K_o for the following surcharges: no surcharge, 12.0 kPa (250 psf), and 23.9 kPa (500 psf) to 35.9 kPa (750 psf). In situations where the surcharge is between those given in Table 6.9 the coefficient of lateral earth pressure at rest may be interpolated.

Table 6.9 Recommended design values for K_o

Surcharge (kPa)	backfill surface	backfill base
no surcharge	0.95	0.29
12.0	0.55	0.27
23.9 to 35.9	0.47	0.24

Examination of the values in Table 6.4 show that K_a is relatively constant for the intermediate rotation, ranging from 0.22 to 0.25. Therefore, it is recommended that a value of 0.25 for K_a be used for design. Substantial wall movements like those for the maximum rotation of Pine State Recycling and Palmer Shredding are seldom, if ever, designed for. However, in those instances where large wall movements are expected, a conservative approach is recommended, by using the same K_a of 0.25 for all design cases.

6.6.2 Semiempirical Design Parameters

Examination of values of k_h in Table 6.5 for the at-rest condition show little difference between values from the three tire chip suppliers. Thus, when using the semiempirical value, k_h, for design the average value determined from the three tire chip suppliers should be used. In situations where the surcharge is between the given values,

k_h may be interpolated. The recommended values for k_h for the at-rest condition are shown in Table 6.10.

Table 6.10 Recommended semiempirical values for k_h for the at-rest condition

Surcharge (kPa)	k_h (Mg/m^3)
0	0.26
12.0	0.14
23.9	0.09
35.9	0.00

When taking the contribution of the surcharge into account, the value C must be added to the horizontal stress determined using the value k_h. It is shown in Table 6.7 that the value C for the three tire chip suppliers at all of the surcharges is relatively constant, ranging from 0.43 to 0.54. Therefore, it is recommended that a value of 0.50 for C be used for of all surcharges greater than 12.0 kPa (250 psf) and less than 35.9 kPa (750 psf), for at-rest conditions.

For the active case, k_h ranges from 0.17 to 0.19 Mg/m^3 (10.6 to 11.9 pcf) for the intermediate rotation, as shown on Table 6.6. Thus, a value of 0.19 Mg/m^3 (11.9 pcf) is recommended for k_h for the active condition. Examination of Table 6.8 shows that the value C ranges from 0.22 to 0.25 for the intermediate rotation. So, a value of 0.25 is recommended for the active case.

CHAPTER 7. INTERFACE SHEAR

7.1 INTRODUCTION

One of the goals of this research was to measure the interface shear between the tire chips and a smooth faced concrete retaining wall. Concrete was chosen for the front wall face since this is the material used to construct most retaining walls. The interface shear was determined by measuring horizontal and vertical forces on the center panel in the at-rest condition. The methods for measuring these forces were discussed in Section 4.2.1.1. The results obtained from the test measurements will be discussed for each backfill type. The final section of the chapter will discuss considerations for design.

7.2 ANGLE OF WALL FRICTION

Downward movement of the backfill relative to the retaining wall develops an upward friction force that causes the resultant with the horizontal force from the backfill to be inclined at an angle δ with respect to the normal to the wall. This angle is known as the angle of wall friction. For the research presented in this report, the angle of wall friction was determined by plotting the total shear force (total vertical force) versus the total horizontal force acting on the center panel. For each backfill tested, the shear force versus horizontal force was plotted as the test facility was being filled and as the surcharge was applied. The first data point was plotted when the fill elevation was 2.03 meters (6.7 feet), because there was considerable scatter in the data below this elevation.

The unload/reload portion of the tests were also plotted. Changes in the shear and horizontal forces with time were investigated for Palmer Shredding tire chips during the Winter of 1994-95.

7.2.1 Granular Fill

The shear force versus horizontal force for granular fill is shown in Figure 7.1. This shows that for the filling/loading portion of the plot the shear force generally increases as the horizontal force increases. Triaxial tests performed on the granular fill showed an effective angle of internal friction (ϕ') of 38 degrees. This failure envelope is shown on Figure 7.1. It is a reasonable approximation of the angle of wall friction for the initial loading with surcharges between 12.0 kPa (250 psf) and 35.9 kPa (750 psf). The angle of wall friction is somewhat lower when the facility is half full to full with no surcharge. A $\delta = 30$ degrees would be a reasonable approximation, as shown on Figure 7.1. For the unload/reload cycles $\delta = 23$ degrees would be a reasonable estimate, as shown on Figure 7.1.

In comparison, for concrete walls where forms are used, δ is typically estimated from the friction angle (ϕ). Bowles (1988) recommends $\delta = 0.6$ to 0.8ϕ. This results in an estimated angle of wall friction of 23 to 30 degrees. Values of δ tabulated by Bowles (1988) show values ranging from 22 to 26 degrees for gravel and sand against formed concrete. The δ obtained from this study for the surcharges of 12.0 kPa (250 psf) to 35.9 kPa (750 psf) is 21% to 42% greater than values from Bowles (1988). However, the δ obtained from 1/2 full to full and for the unload/reload cycles is within the range of

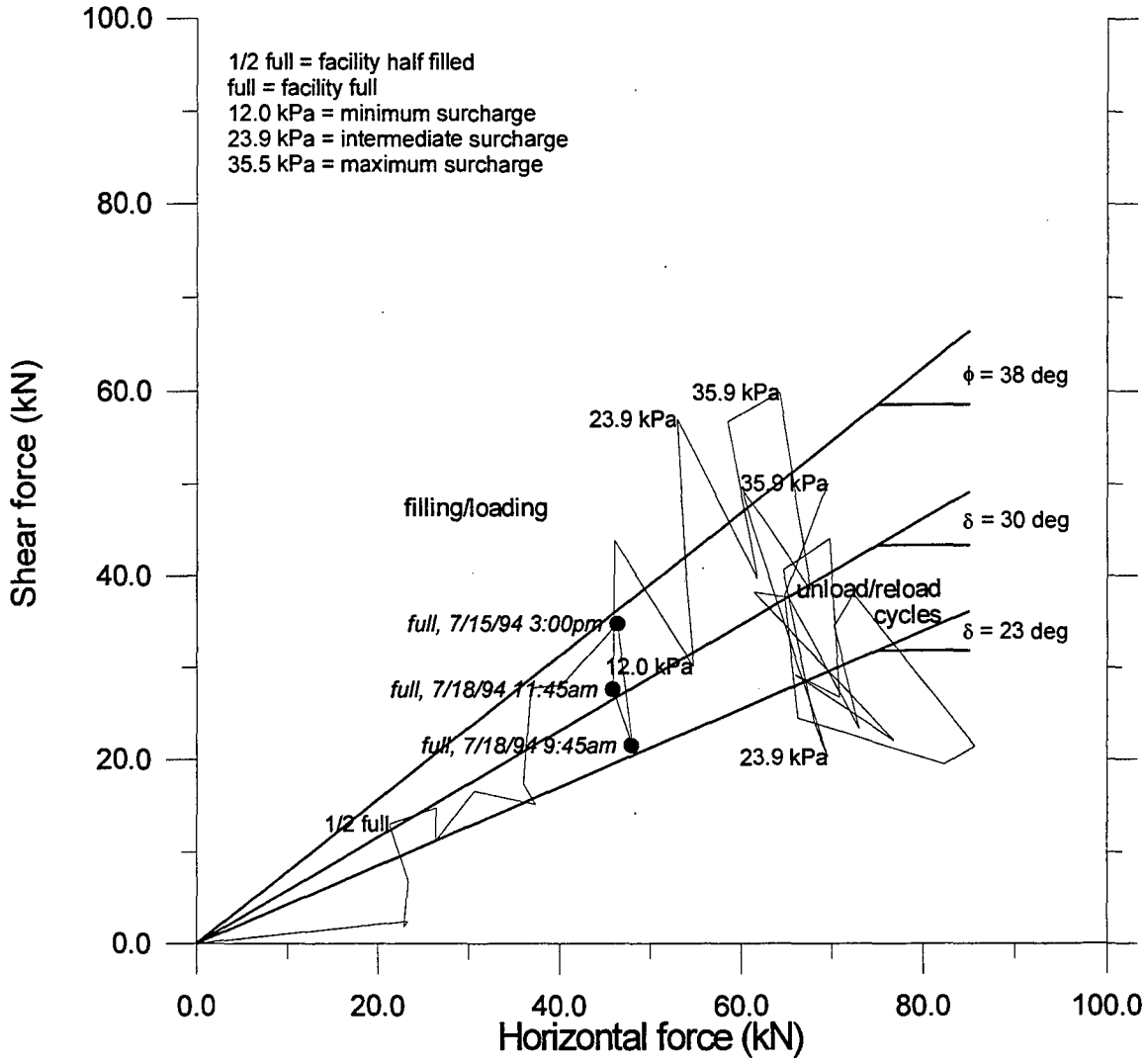

Figure 7.1 Shear force vs. horizontal force, granular fill

values from Bowles (1988). One possible reason for δ from 12.0 kPa (250 psf) to 35.9 kPa (750 psf) being larger than from Bowles (1988), is that the values are recommended for formed concrete, whereas the instrumented wall of the test facility was smoothed with concrete hand tools. This resulted in a finish that was slightly rougher than a formed face; this would result in a higher δ. However, δ from 1/2 full to full and for the unload/reload cycles is within the range of the typical values. This suggests that the effects of roughness of the test wall may be small. Examination of the unload/reload cycles in Figure 7.1 shows that the forces vary over a large range for an individual cycle, and tend to slope in the negative direction.

Further examination of Figure 7.1 shows a large amount of scatter in the values for shear force. One possible explanation for this is the variation of temperature during the day. Figure 7.1 shows the times for several readings taken when the facility was full. It can be seen that the shear forces determined later in the day, when the sun warms the front wall, are higher than those in the morning hours. This may be caused by expansion of the steel in the frame of the front wall. Expansion of the steel would cause the wall face to move upward relative to the backfill, resulting in an increase in force on the vertical load cells. The effect would not be as significant on the horizontal load cells because the amount of steel along their axes is less. Diagrams of the front wall and load cells are shown on Figures 3.3, 3.8, and 3.10. To lessen the effects of temperature on the load cells, dark colored plastic was used to shade the exposed steel from direct sunlight for subsequent tests. The effectiveness of this scheme was verified by measuring relatively no fluctuation in the vertical load cell readings for subsequent tests with tire

chips. Moreover, expansion of the face of the wall would have less effect on the vertical shear force for tire chips which have a lower shear modulus than the relatively stiff compacted granular soil.

7.2.2 Tire Chips

7.2.2.1 Filling/Loading

The shear force versus horizontal force for Pine State Recycling, Palmer Shredding, and F & B Enterprises are shown in Figures 7.2, 7.3, and 7.4, respectively. These figures show that for the filling/loading portion of the plots, the shear force increases as the horizontal force increases. The data suggests that there is no adhesion intercept between the backfill and the wall, so a best fit line passing through the origin was fit through the filling/loading portion of the plots to find the angle of wall friction, as shown on Figure 7.2 through 7.4. The values for δ for filling/loading are shown on Table 7.1. These values may be slightly higher than for a poured concrete wall since the finish on the face of the wall was slightly rougher than the face of a typical poured concrete wall.

Table 7.1 Angle of wall friction (δ), filling/loading

Supplier	δ
Pine State Recycling	31°
Palmer Shredding	32°
F & B Enterprises	30°

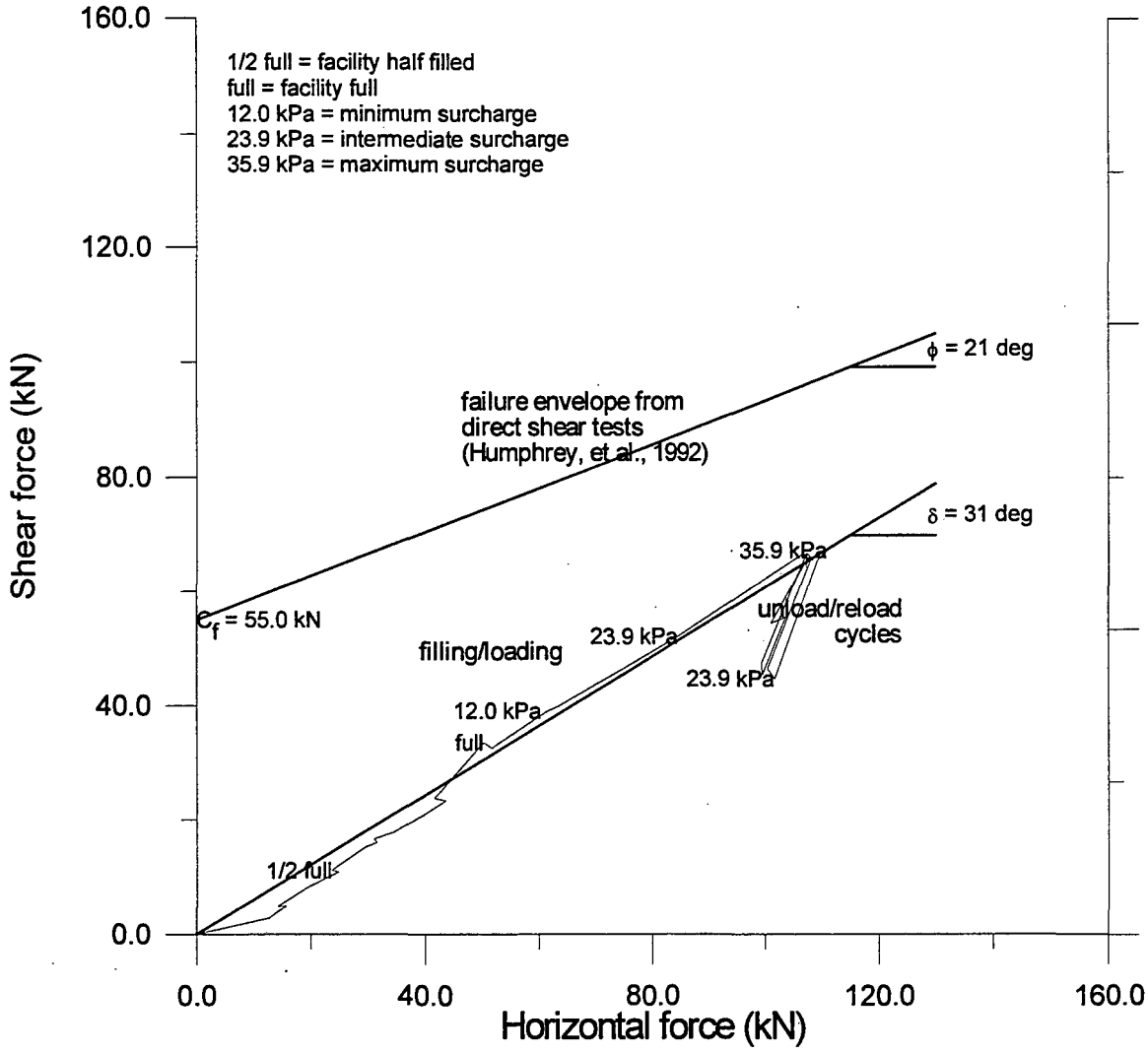

Figure 7.2 Shear force vs. horizontal force, Pine State Recycling

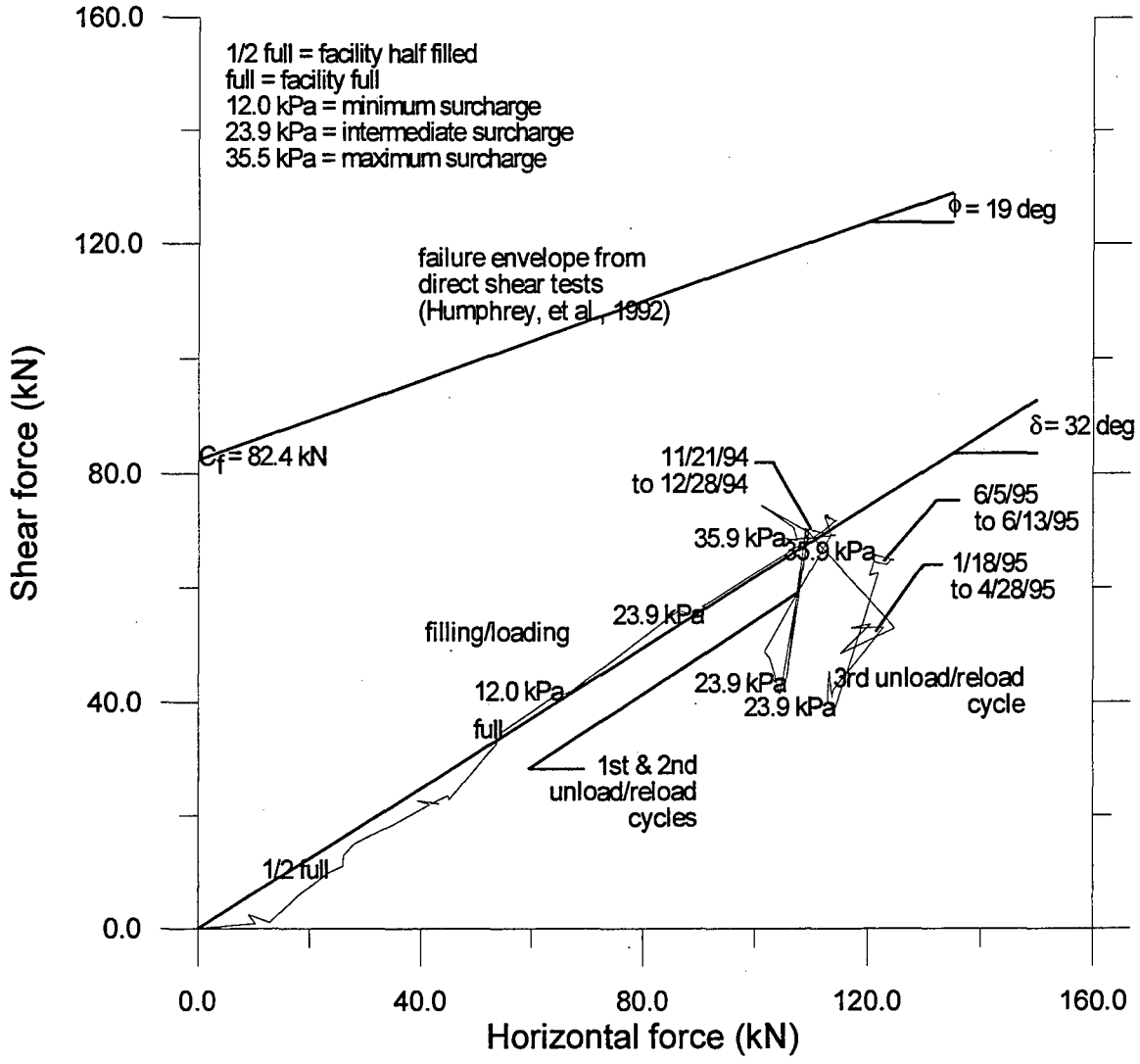

Figure 7.3 Shear force vs. horizontal force, Palmer Shredding

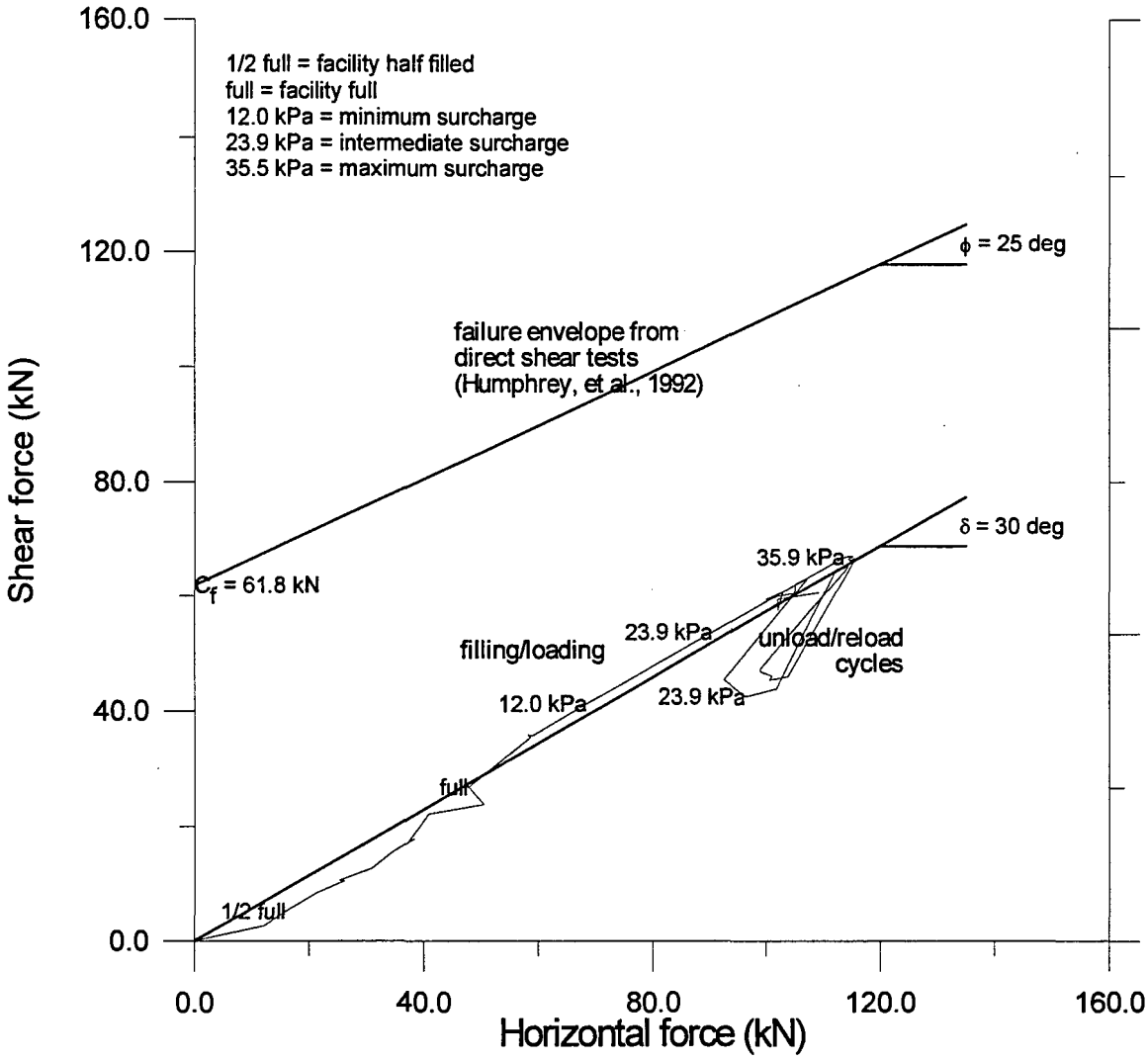

Figure 7.4 Shear force vs. horizontal force, F & B Enterprises

The values of δ in Table 7.1 are very similar for the three types of tire chips. These values can be compared to the friction angles (ϕ) and cohesion intercepts (c) reported by Humphrey, et al. (1992) as determined by direct shear tests using a 254-mm (12-in.) shear box, as discussed in Section 2.2.4. Their fiction angles ranged between 25 to 19 degrees for the same three tire chip suppliers, while the cohesion intercept ranged from 7.7 to 11.5 kPa (160 to 240 psf). The failure envelope for each tire chip type is plotted on Figures 7.2 through 7.4, where the cohesion is shown as C_f and is in units of force. It is seen that the failure envelopes plot above the interface friction angles. This shows that the shear strength between tire chips is greater than the interface shear strength between the concrete wall and tire chips. The values of δ in Table 7.1 are at the upper bound or slightly larger than those for granular backfill from Bowles (1988).

The angles of wall friction in Table 7.1 can be compared to tire-concrete pavement interface friction angles. Tabulated values from Pline (1992) show the interface friction angle between Portland cement concrete and tires to be between 34° to 37°. For the three suppliers the angles of wall friction in Table 7.1 are slightly below the range from Pline (1992).

7.2.2.2 Unloading/Reloading

Each test with tire chips was subjected to two unload/reload cycles, with the exception of Palmer Shredding, which underwent three unload/reload cycles. Figures 7.2 through 7.4 also shows the shear force versus horizontal force for the unload/reload portion of each test for each tire chip supplier. These figures show that after unloading to

the intermediate surcharge of 23.9 kPa (500 psf), the shear force is lower and the horizontal force is higher than for the initial loading with the same surcharge. Comparison can be made by examining the shear and horizontal forces at the intermediate surcharge during initial filling/loading and the average of these forces during unloading of the unload/reload cycles. Comparing the average forces during the first and second unload/reload cycles at the 23.9 kPa (500 psf) surcharge to the forces during initial filling/loading with 23.9 kPa (500 psf) for Pine State Recycling shows that the average shear force during the unload/reload cycles is 12% lower and the average horizontal force is 19% greater. The same comparison for F & B Enterprises yields an average shear force during both unload/reload cycles that is 15% less and a horizontal force that is 10% greater than the forces recorded during initial filling/loading.

To compare the total forces for Palmer Shredding it was necessary to calculate the average forces during initial filling/loading for the intermediate surcharge because four readings were taken. These were compared separately to the average forces for the first and second unload/reload cycles and the third unload/reload cycle. This was done because the magnitude of the forces from third unload/reload cycle were significantly different than the first and second cycles. This analysis showed that during first and second unload/reload cycles the average shear and horizontal forces were 19% less and 17% greater, respectively, than those of initial filling/loading. Moreover, the vertical force was 26% less and the horizontal force was 27% greater during the third unload/reload cycle than during initial filling/loading. The reason for the larger difference during the third unload/reload cycle is attributed to the magnitude of the forces

at the surcharge of 35.9 kPa (750 psf) at the start of the unload/reload cycle, as discussed Section 7.2.2.3.

One possible reason for the shear force being consistently lower and the horizontal force always being larger after unloading, deals with the compressive nature of rubber. The decrease in shear force is caused by rebound of the tire chips when the maximum surcharge is removed. When the tire chips rebound they move up relative to the wall, causing a decrease in the shear force. This results in a lower shear force than during the initial filling/loading with 23.9 kPa (500 psf). The larger horizontal force after unloading to 23.9 kPa (500 psf) is similar to an overconsolidated soil having a larger K_o than a normally consolidated soil. When a normally consolidated soil is unloaded the horizontal stress decreases by a smaller amount than the vertical stress (Mitchell, 1993), as discussed in Section 6.3.2.2. It is theorized that similar behavior from tire chips contributed to the horizontal force being greater after unloading than during initial filling/loading.

The angle of wall friction for the unload/reload portions of each test was determined by calculating δ at each set of readings by:

$$\delta = \tan^{-1}\left(\frac{V_f}{H_f}\right) \tag{7.1}$$

where V_f and H_f are the shear and horizontal force at individual readings. δ was then found for the unload and reload conditions, by averaging the δ's at 23.9 kPa (500 psf) and 35.9 kPa (750 psf) for all unload/reload cycles. The values are summarized in Table 7.2.

Table 7.2 Angle of wall friction (δ), unload/reload

Supplier	δ	
	unload	**reload**
Pine State Recycling	25°	31°
Palmer Shredding	22°	29°
F & B Enterprises	25°	30°

Table 7.2 shows that the angle of wall friction is greater at the reload surcharge (35.9 kPa; 750 psf) than at the unload surcharge (23.9 kPa; 500 psf) by 19% for Pine State Recycling, 24% for Palmer Shredding, and 17% F & B Enterprises. The values of δ for reload are similar to δ for initial filling/loading (Table 7.1). The lower value at unload can be attributed to the decrease in shear force and increase in horizontal force discussed above. The values of δ for unload and reload are similar to those used for granular material (22° to 30°), with δ unload closer the lower bound of values and δ reload similar to a upper bound. However, the values in Table 7.2 could be slightly high due to roughness of the front wall.

7.2.2.3 Time-Dependent Change in Force Distribution

After the second unload/reload cycle was completed for Palmer Shredding, the tire chips were left in the facility during the Winter of 1994-95 with the maximum surcharge applied, to examine changes in force distribution with time. In the Spring of 1995 a third unload/reload cycle was performed. The pattern of change in force distribution is described in the following.

The second unload/reload cycle was completed on 11/21/94. Their was no significant change in the measured forces through 12/28/94, as shown on Figure 7.3. However, the shear force decreased and the horizontal force increased by the next reading, which occurred on 1/18/95. This magnitude of forces remained about the same until 4/28/95, as shown on Figure 7.3. No readings were taken between 4/28/95 and 5/31/95, at which time the third unload/reload cycle was started by removing 12.0 kPa (250 psf), leaving a surcharge of 23.9 kPa (500 psf). This surcharge remained on the tire chips until 6/5/95, then the maximum surcharge of 35.9 kPa (750 psf) was reapplied and left in place until 6/13/95. The measured forces during this time were different than those recorded after the second unload/reload cycle (11/21/94 to 12/28/94) and before the third unload/reload cycle (1/18/95 to 4/28/95), as shown on Figure 7.3. A summary of the average forces for the periods of time discussed above is shown in Table 7.3.

Table 7.3 Summary of average forces at 35.9 kPa (750 psf) surcharge for specified time periods

Date	Average vertical force (kN)	Average horizontal force (kN)
11/21/94 to 12/28/94	69.9	107.3
1/18/95 to 4/28/95	52.5	120.7
6/5/95 to 6/13/95	64.5	122.1

Examination of Table 7.3 shows the magnitude of the change from 12/28/94 to 1/18/95 resulted in a 24% decrease in the average shear force and a 13% increase in the horizontal force. The average shear force from 6/5/95 to 6/13/95 was 8% less than the

average from 11/21/94 to 12/28/94 and 18% greater than from 1/18/95 to 4/28/95. Also, the average horizontal force from 6/5/95 to 6/13/95 was 12% greater than from 11/21/94 to 12/28/94, with only a slight difference compared to 1/18/95 to 4/28/95.

One possible explanation for these observations is that from the time period from 12/28/94 to 1/18/95 the tire chips underwent some time-dependent settlement which could have included some reorientation of the chips. Another possible explanation for the decrease in shear force and increase in horizontal force between 12/28/94 and 1/18/95 is related to the temperature. At very cold temperatures the steel frame of the front wall would contract, causing the wall face to move down relative to the backfill. This would cause a decrease in the vertical force. A decrease in the vertical force would result in more vertical stress carried by the tire chips and an increase in the horizontal force. The change in the magnitude of the shear and horizontal forces measured from 6/5/95 to 6/13/95 may have occurred as a result of the third unload/reload cycle. Unloading the tire chips could have slightly reoriented them again. Thus, resulting in another redistribution of the forces.

7.3 VERTICAL STRESS VERSUS SHEAR STRESS

For all four of the backfill types tested, the vertical stress at the base of the fill (σ_v) versus the shear stress (τ) on the center panel face was plotted. This was done to show the extent of increase in shear stress on the wall as the vertical stress increases. The vertical stress at the base of fill versus shear stress was plotted as the test facility was being filled and as the surcharge was applied. The first data point was plotted when the

fill elevation reached 2.03 meters (6.7 feet). This was necessary because there was considerable scatter in the data for lower fill elevations. The unload/reload portions of the tests were also plotted.

The vertical stress at the base of the fill versus shear stress for the granular backfill is shown on Figure 7.5. This shows that the shear stress increases as the vertical stress at the base of the fill increases. Further examination of Figure 7.5 shows a large amount of scatter in the shear stress data. This can be attributed to the reasons discussed in Section 7.2.1.

The vertical stress at the base of the fill versus shear stress for Pine State Recycling, Palmer Shredding, and F & B Enterprises are shown in Figures 7.6, 7.7, and 7.8, respectively. These show that the shear stress increases as the vertical stress at the base of fill increases. The vertical stress was determined using the methods discussed in Section 6.5.1.1. However, the effects of repeated unloading/reloading that caused small increases in density (Humphrey, et al., 1992) were not accounted for when determining the vertical stress at the base of the fill during the unload/reload cycles.

Comparison of Figures 7.5 through 7.8 shows a more rapid increase in shear stress for the three types of tire chips as compared to the granular fill over the same range of applied vertical stresses.

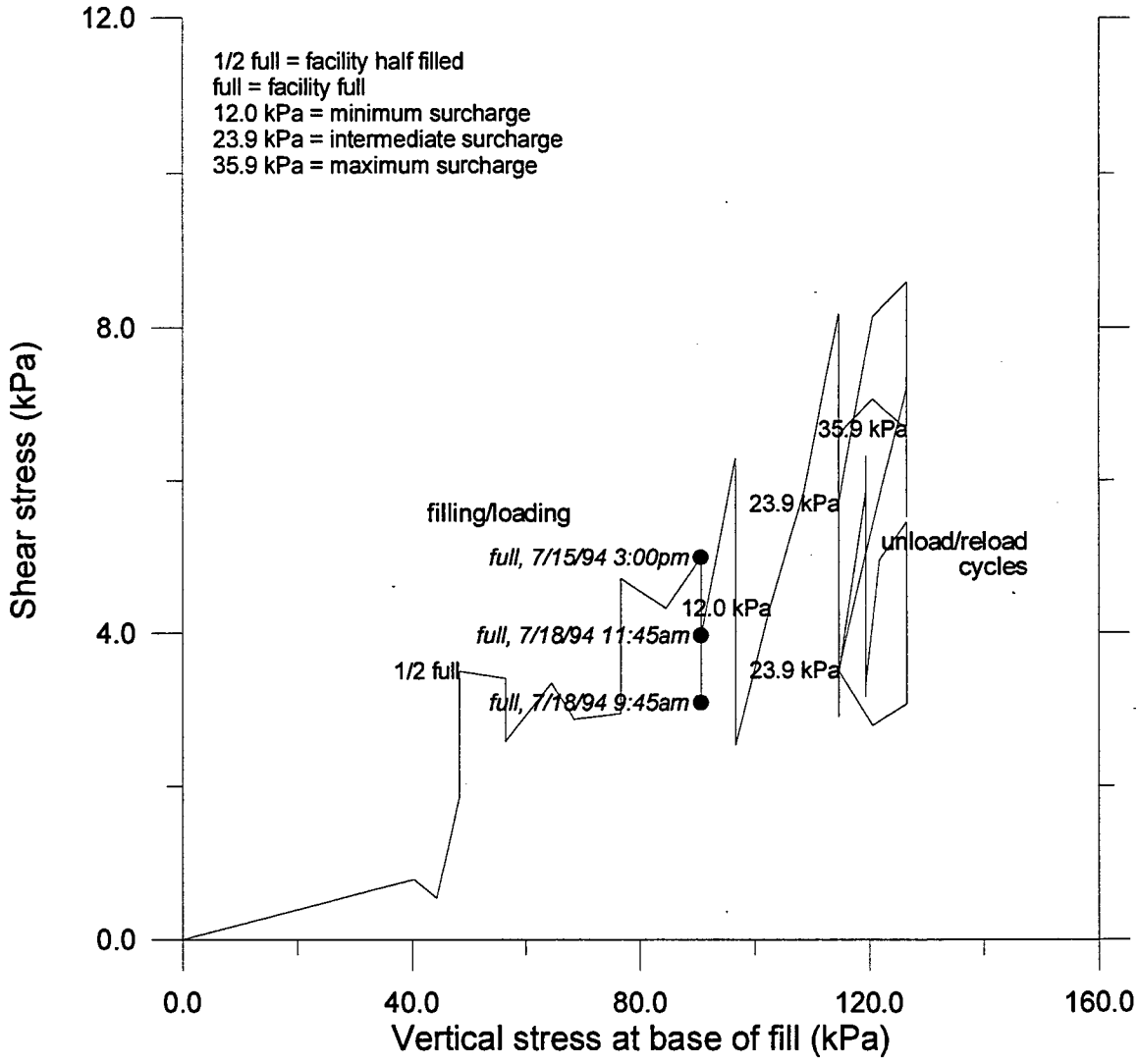

Figure 7.5 Shear stress vs. vertical stress at base of fill, granular fill

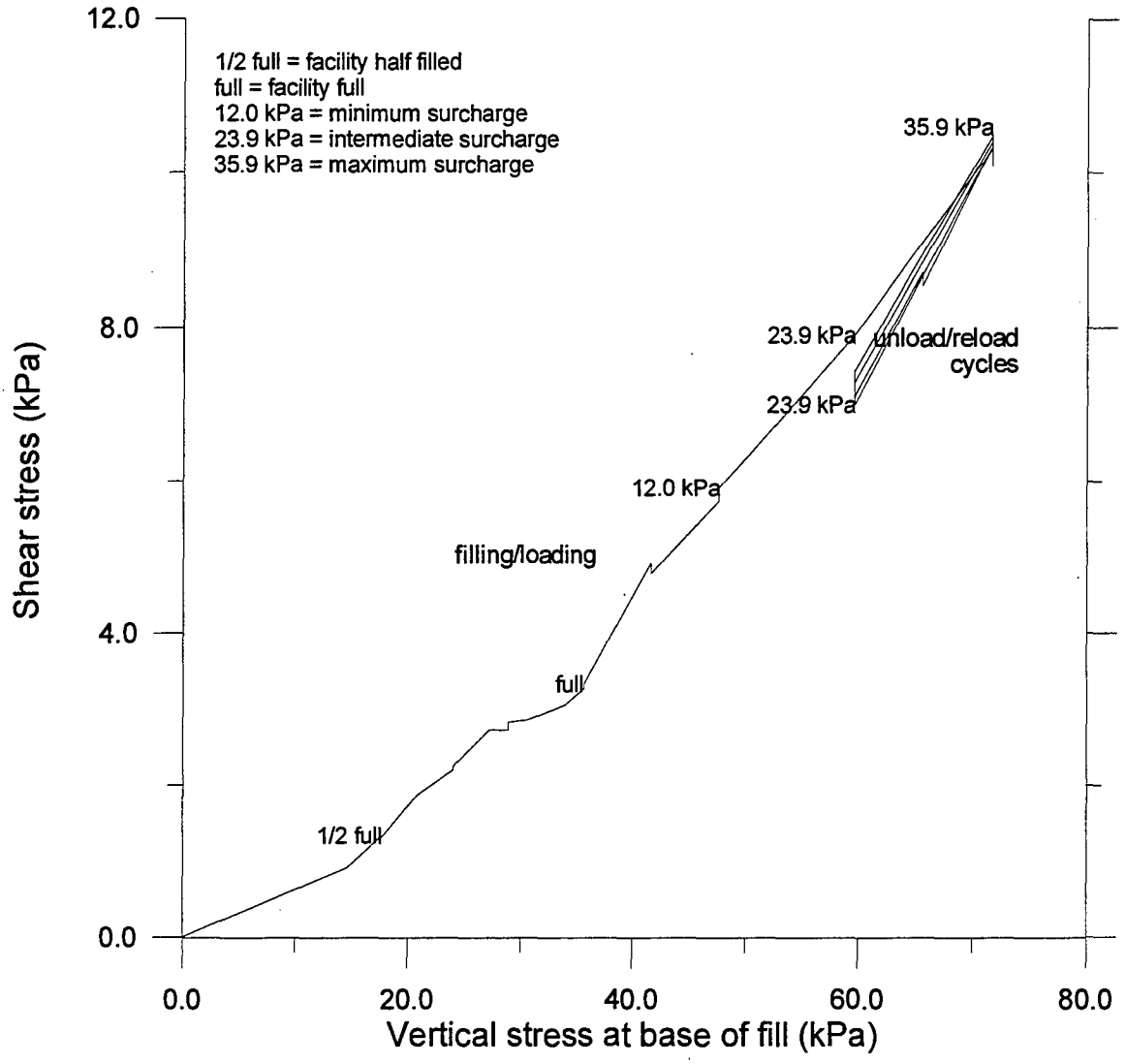

Figure 7.6 Shear stress vs. vertical stress at base of fill, Pine State Recycling

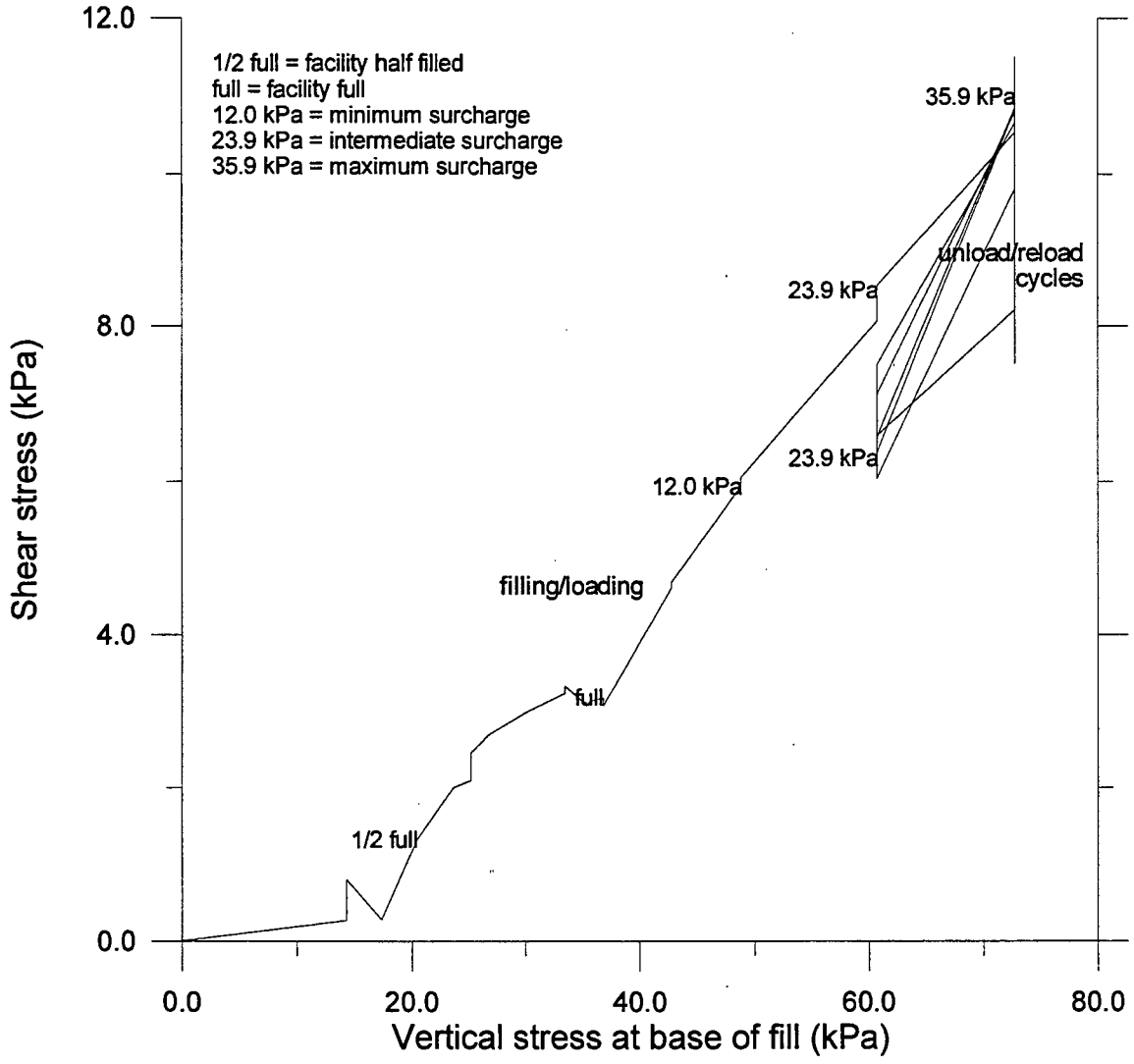

Figure 7.7 Shear stress vs. vertical stress at base of fill, Palmer Shredding

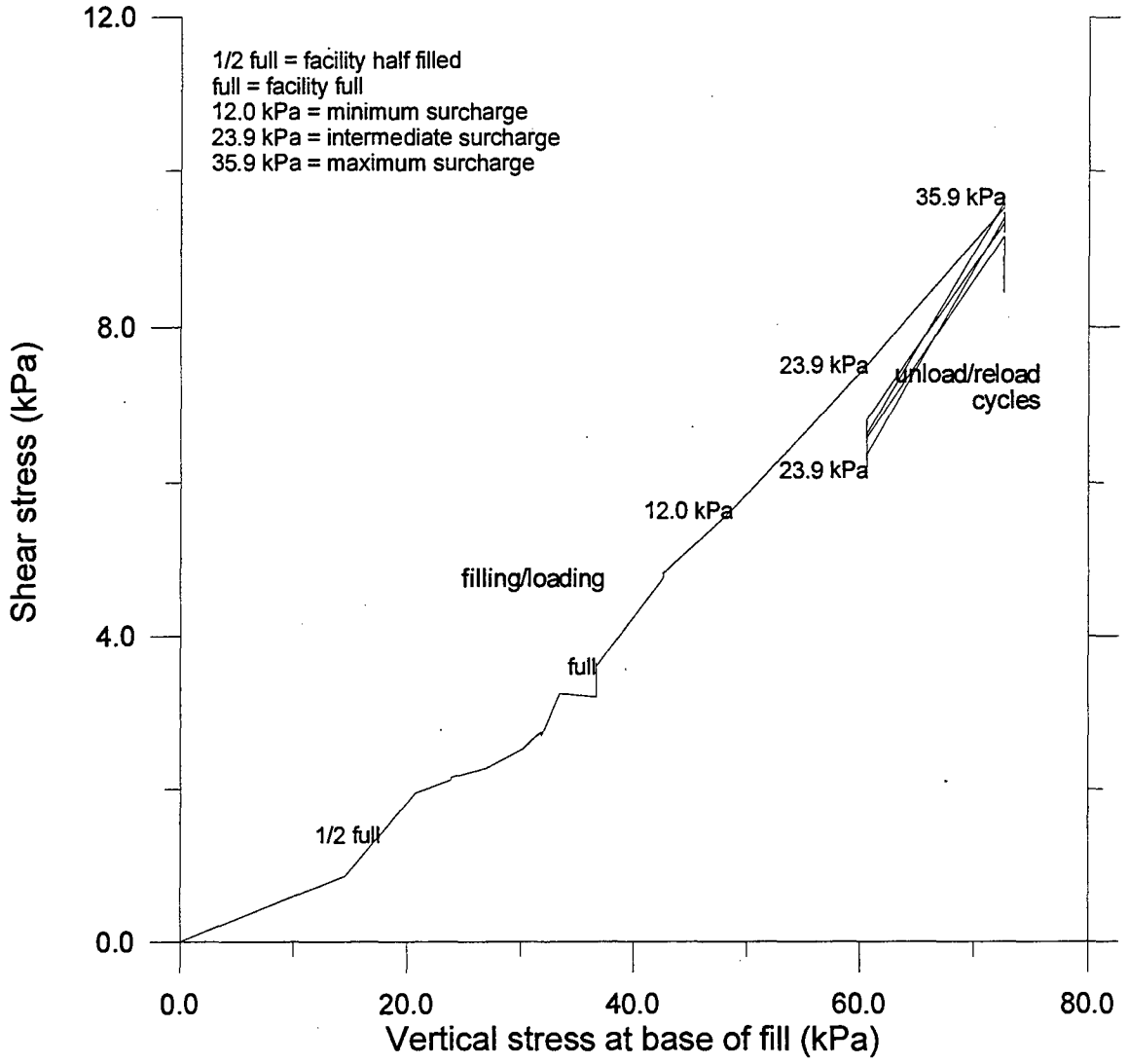

Figure 7.8 Shear stress vs. vertical stress at base of fill, F & B Enterprises

7.4 DESIGN CONSIDERATIONS

The angle of wall friction for design of retaining walls with conventional soil backfills placed against a formed concrete face is typically taken to be 0.6 to 0.8ϕ or tabulated values, such as those given by Bowles (1988), are used. If the same criteria of 0.6 to 0.8ϕ is used for tire chips and using the friction angle determined by Humphrey, et al. (1992), the resulting δ would range from 20 to 11 degrees. These are considerably lower than the δ found in this study. Since the results for initial filling/loading were consistently around 30 degrees, this value may be used for design when tire chips are placed against concrete retaining walls.

CHAPTER 8. COMPRESSIBILITY AND SETTLEMENT

8.1 INTRODUCTION

One of the goals of this research was to determine the compression and settlement characteristics for the at-rest condition. Vertical deformation data was obtained in two ways. The first was settlement and compression below the fill surface as measured with settlement plates. The second was settlement of the fill surface. Settlement below the fill surface was determined by measuring the change in elevation of settlement plates originally placed at elevations of 3.25 m (10.7 ft) and 1.63 m (5.3 ft), termed the 3.25-m (10.7-ft) and 1.63-m (5.3-ft) settlement plates, respectively. Their locations are shown on Figures 4.3 and 4.4. Settlement of the fill surface was determined by measuring the elevation of 19 points, referred to as the settlement grid, located on the fill surface, as shown on Figure 4.6. Details of the methods used to take the measurements are discussed in Section 4.2.2.

The first section of this chapter discusses the vertical stress-vertical strain relationship. Included in this section are comparisons of the measured change in strain from this study to that expected from laboratory results by Humphrey, et al. (1992). The next section discusses the time-rate of settlement under the maximum surcharge. The final section presents considerations for design. It was observed during testing that the

settlement of the granular fill was less than 10 mm (0.4 in.) and no usable results were obtained.

8.2 STRESS-STRAIN RELATIONSHIP

The vertical stress (σ_v) versus vertical strain (ε_v) for each of the tire chips was determined with the 3.25-m (10.7-ft) and 1.63-m (5.3-ft) settlement plates, and the settlement grid. The stress-strain relationship was investigated during filling and initial loading of the test facility. In addition, the effects of repeated unloading and reloading were investigated by removing the maximum surcharge and reapplying it a minimum of two times. The unload/reload cycles were only examined at the fill surface using the settlement grid. This was necessary because results from the settlement plates showed some scatter in the data, which had greater impact on the unloading and reloading results than during filling/loading. The scatter in the data is discussed in Sections 8.2.1.1 and 8.2.2. In all cases the vertical stress was determined by the methods discussed in Section 6.5.1.1.

8.2.1 Filling/Loading

Settlement results during filling were determined from the settlement plates. Data from the settlement plates was taken after every two lifts (400 mm; 16 in.) of tire chips were added after the initial installation of the settlement plates. Settlement data was acquired during surcharge placement from both the settlement plates and settlement grid at the following surcharges: 6.0 kPa (125 psf), 12.0 kPa (250 psf), 23.9 kPa (500 psf), and 35.9 kPa (750 psf). Settlement readings were taken at 6.0 kPa (125 psf), which

corresponds to one layer of surcharge blocks, because this surcharge corresponded to the initial reading for the settlement grid, as discussed in Section 4.2.2.2. When a surcharge was left on for more than a day, readings were taken at selected times.

8.2.1.1 Settlement Plates

The vertical stress versus vertical strain for each tire chip supplier was determined for both the 3.25-m (10.7-ft) and 1.63-m (5.3-ft) settlement plates. Data acquisition and measurements procedures were discussed in Section 4.2.2.1. The vertical stress was calculated at the elevation of the base plate of the settlement plate, and was determined after every other lift was placed, commencing with initial plate installation, and as each surcharge was applied. The vertical strain was calculated by taking the elevation at which the settlement plate was installed as the zero reading, strain was then determined from measuring the change in elevation of the plate. The results for the settlement plates during filling/loading showed some scatter of the data, the details of which will be discussed below. Results from each settlement plate, along with a comparison with Humphrey, et al. (1992), are discussed in the following paragraphs.

The vertical stress versus vertical strain determined from the 3.25-m (10.7-ft) settlement plate for Pine State Recycling, Palmer Shredding, and F & B Enterprises are shown on Figures 8.1, 8.2, and 8.3, respectively. Examination of these figures shows vertical line segments at some of the surcharges. This is a result of time-dependent settlement that occurred when the same surcharge was left on the backfill for a day or more. This is particularly apparent on Figure 8.2 for Palmer Shredding, where the 6.0

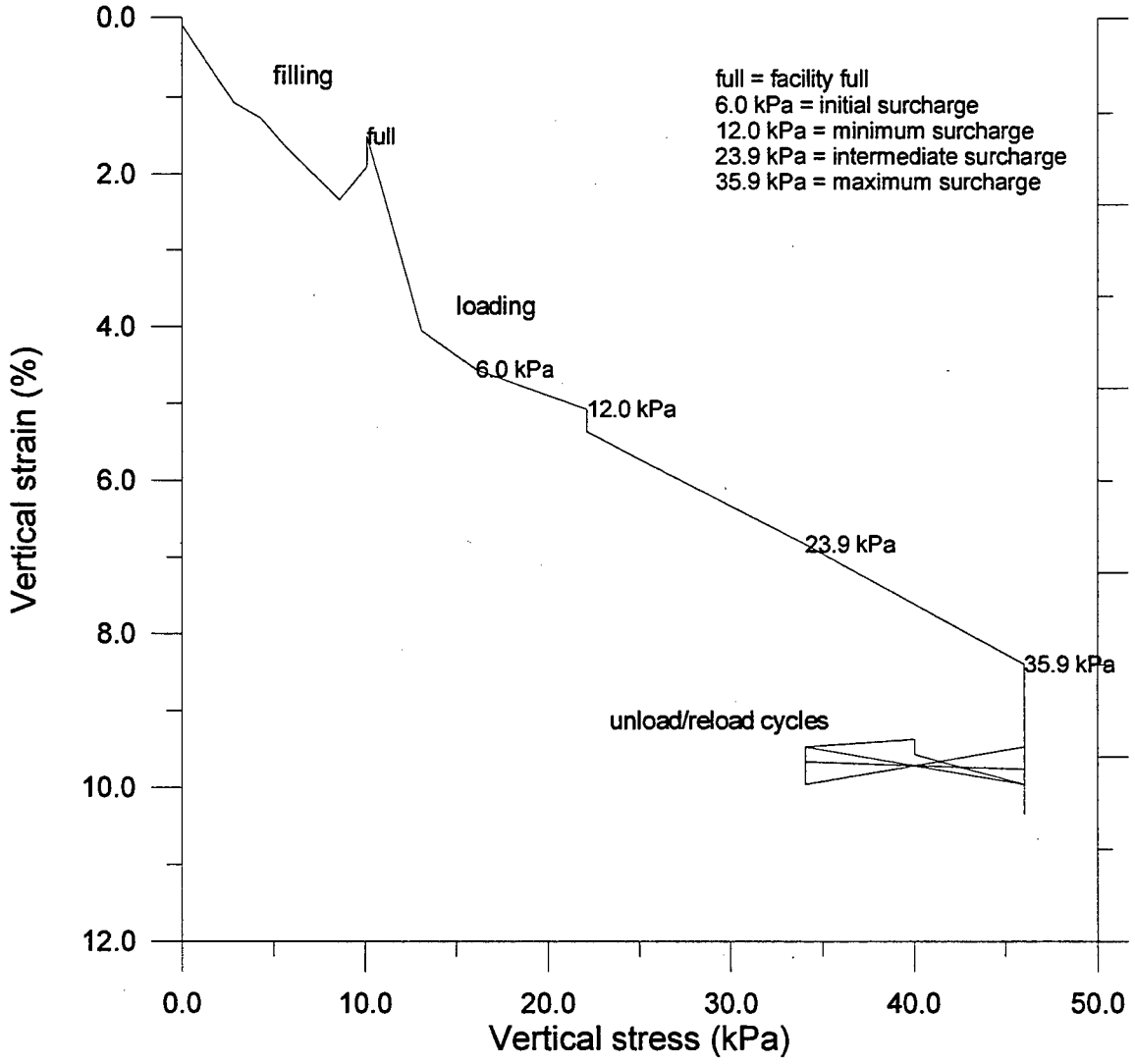

Figure 8.1 Vertical stress vs. vertical strain, Pine State Recycling, 3.25-m (10.7-ft) settlement plate

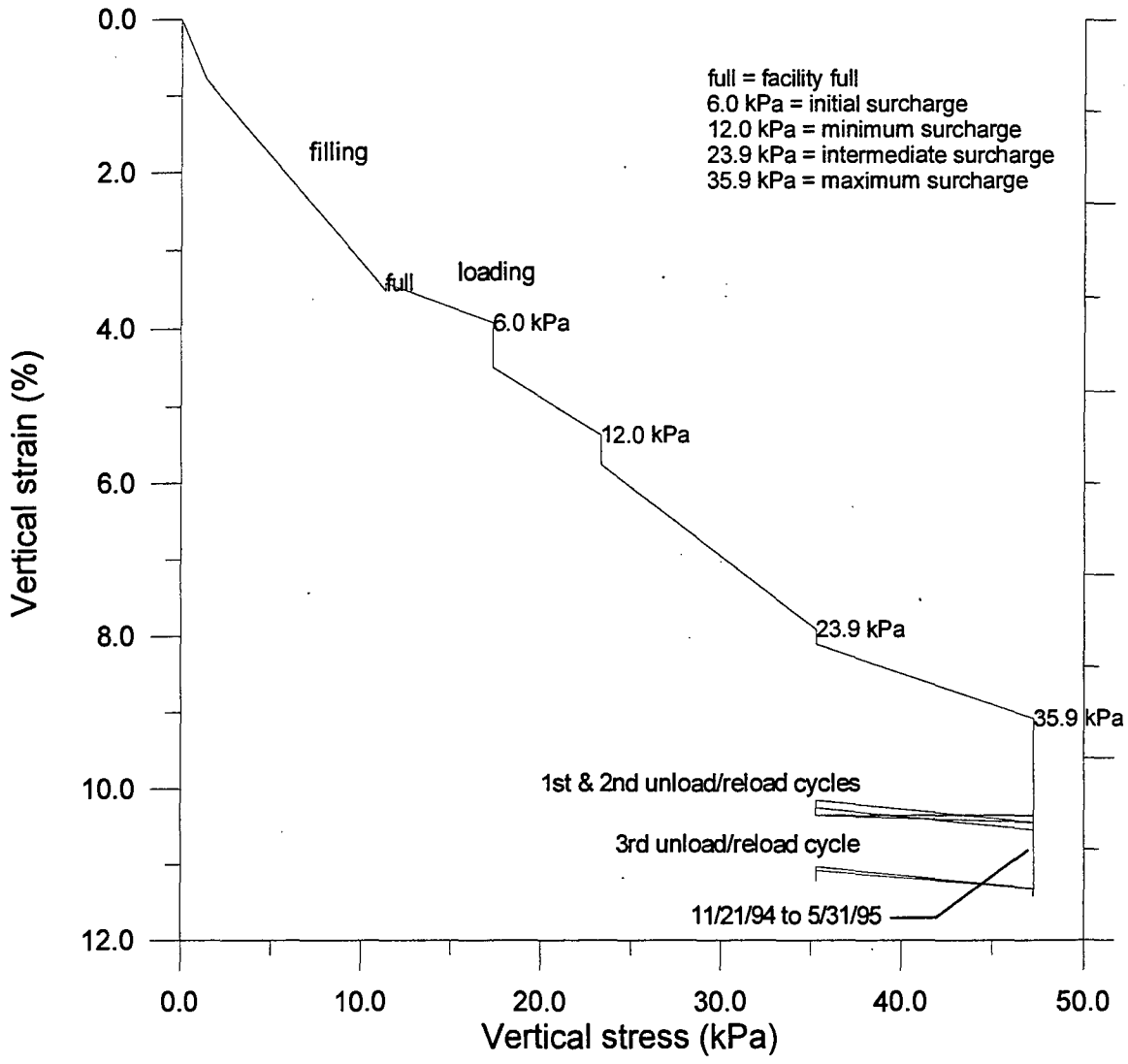

Figure 8.2 Vertical stress vs. vertical strain, Palmer Shredding, 3.25-m (10.7-ft) settlement plate

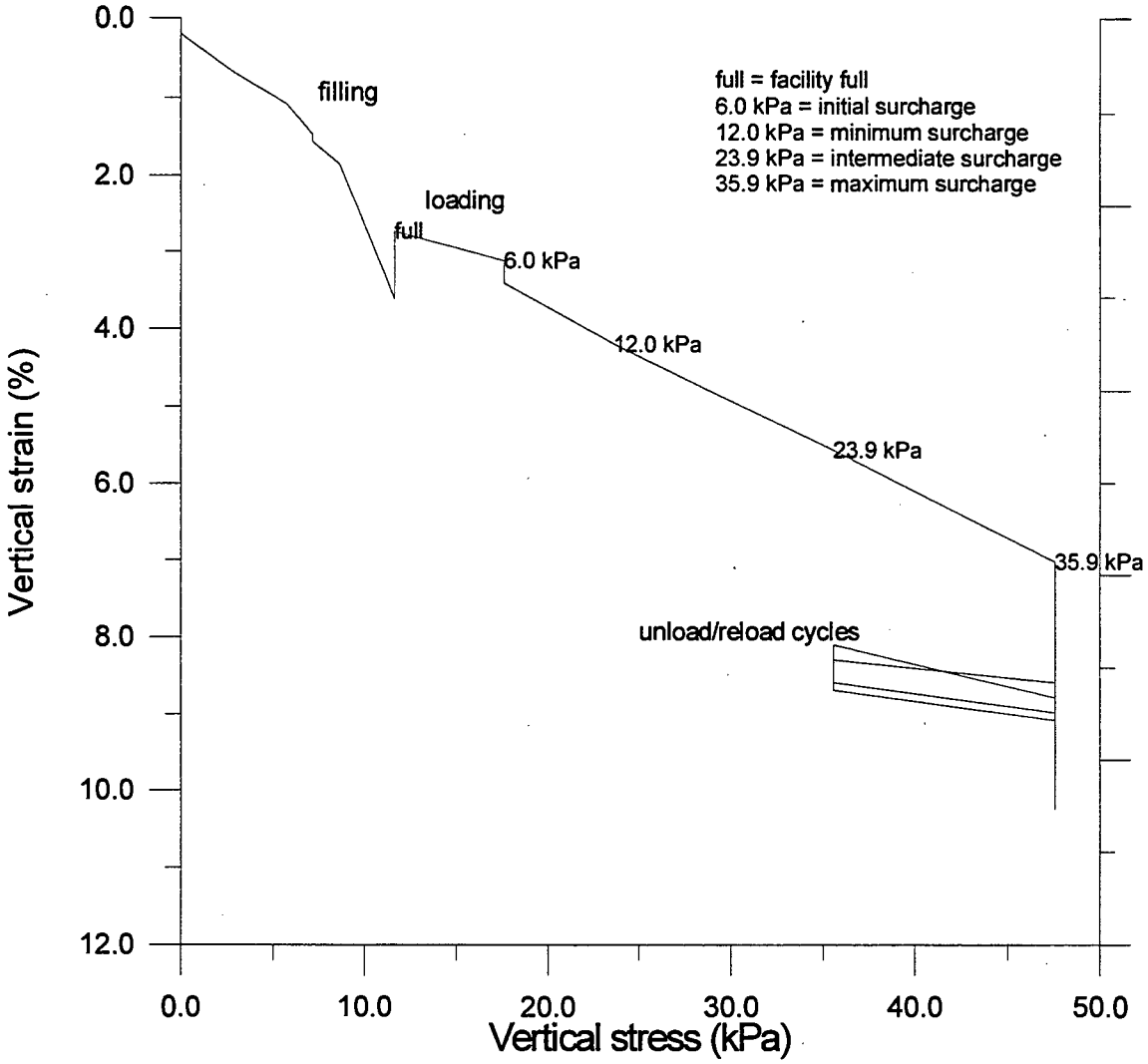

Figure 8.3 Vertical stress vs. vertical strain, F & B Enterprises, 3.25-m (10.7-ft) settlement plate

kPa (125 psf) surcharge was left for 4 days, 12.0 kPa (250 psf) for 1 day, and 23.9 kPa (500 psf) for 3 days. Figures 8.1 through 8.3 show that during filling and loading the plot is slightly concave up for all three types of tire chips. This is most apparent for Palmer Shredding on Figure 8.2. This observation is consistent with laboratory compression tests performed by Humphrey, et al. (1992).

Further examination of Figures 8.1 through 8.3 show some scatter in data. One possible explanation for this is that the settlement plates consisted of a flat base plate and a vertical riser passing through the fill and between the surcharge blocks. Any shifting of the tire chips during filling or loading could skew the reading. This was most apparent during filling. When readings were taken it was necessary to stand next to the settlement plate. This would cause the tire chips to compress under the weight of the person taking the readings, and the riser would tilt accordingly. Although precautions were made to prevent this, its effects could not be removed completely. The measurement techniques also contributed to some scatter. The settlement readings for both the settlement grid and the settlement plates were taken with a standard tape measure and a water level. When taking readings one tried to hold the tape measure vertical, trying to prevent it from bending, and at the same time tried to hold the tube containing the water against the tape measure to read the meniscus, as discussed in Section 4.2.2.1. Although data acquisition for the settlement grid and the settlement plates was the same, it will be seen that there is less scatter for the settlement grid. The effects of scatter were less for the settlement grid because the elevation was determined as the average from 19 points, as discussed in

Section 4.2.2.2, whereas results from the settlement plates are based on readings from one point.

The vertical stress versus vertical strain for the 1.63-m (5.3-ft) settlement plate for Pine State Recycling, Palmer Shredding, F & B Enterprises are shown on Figures 8.4, 8.5, and 8.6, respectively. The plots are slightly concave up, similar to those for 3.25-m (10.7-ft) settlement plate. As with the 3.25-m (10.7-ft) settlement plate, it is most apparent for Palmer Shredding. However, it can also be seen for Pine State Recycling from the surcharges of 12.0 kPa (250 psf) to 35.9 kPa (750 psf). It is apparent that there is more scatter present in these figures than in the ones for the shallower settlement plate. One possible reason is the greater length of the riser for the deeper settlement plate. The longer riser would be affected more by shifts in the fill.

The change in strain during filling and loading for the settlement plates can be examined over three different loading increments: the strain that occurred from installation of settlement plates to completion of tire chips placement (initial to full); the change in strain that occurred from once the facility was full to the application of the first layer of surcharge blocks, 6.0 kPa (125 psf); and as the surcharge was increased from 6.0 kPa (125 psf) to 35.9 kPa (750 psf). This method of analysis allows for comparison of the settlement at the low and high stress ranges. Closer examination of Figures 8.1 and 8.4 for Pine State Recycling show abnormally low vertical strain corresponding with the single reading taken at completion of filling the facility. The reason for this can be attributed to scatter, discussed above, or measurement error. To correct for this in the following analysis, the strain at full was interpolated from the values before and after the

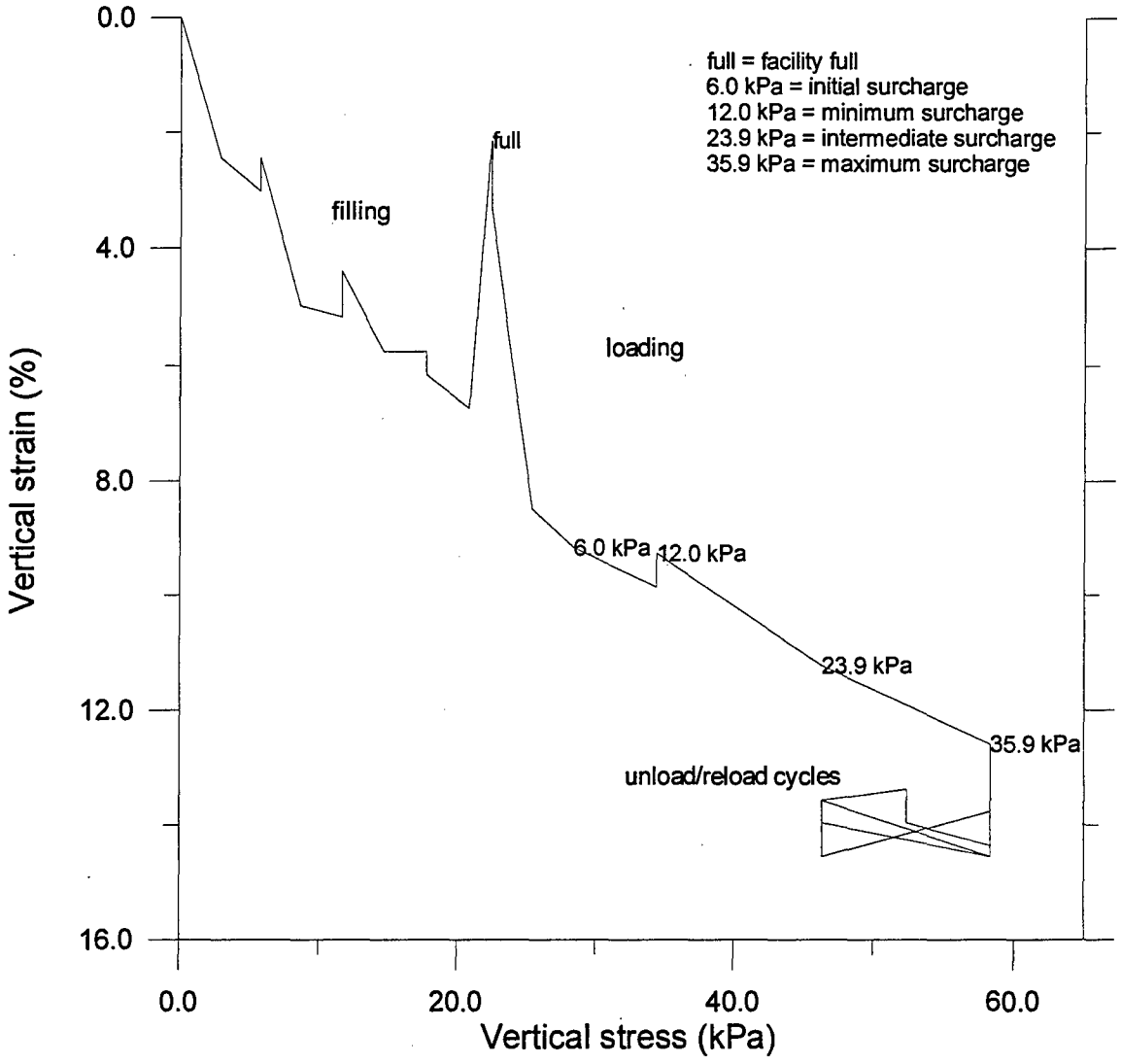

Figure 8.4 Vertical stress vs. vertical strain, Pine State Recycling, 1.63-m (5.3-ft) settlement plate

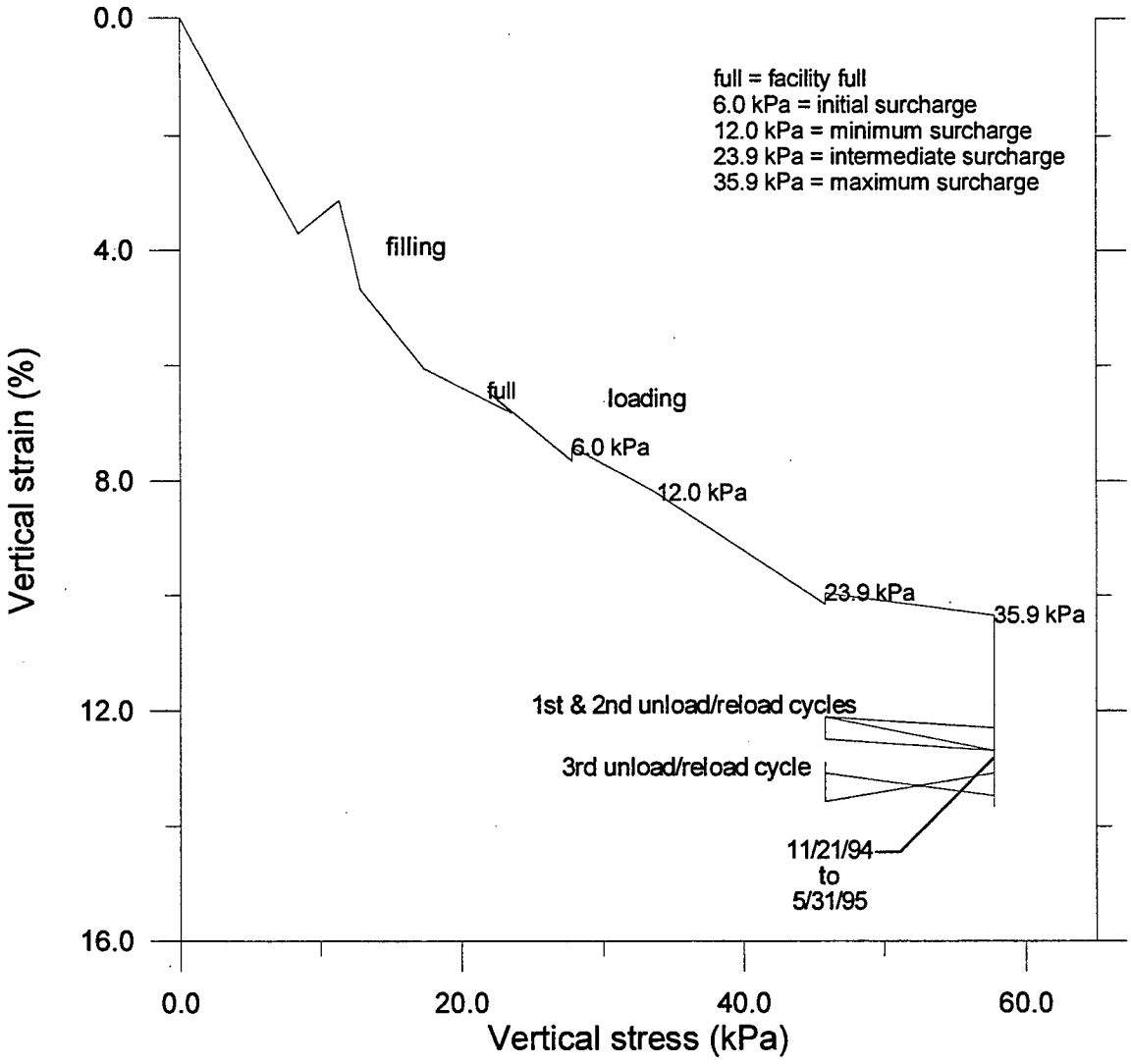

Figure 8.5 Vertical stress vs. vertical strain, Palmer Shredding, 1.63-m (5.3-ft) settlement plate

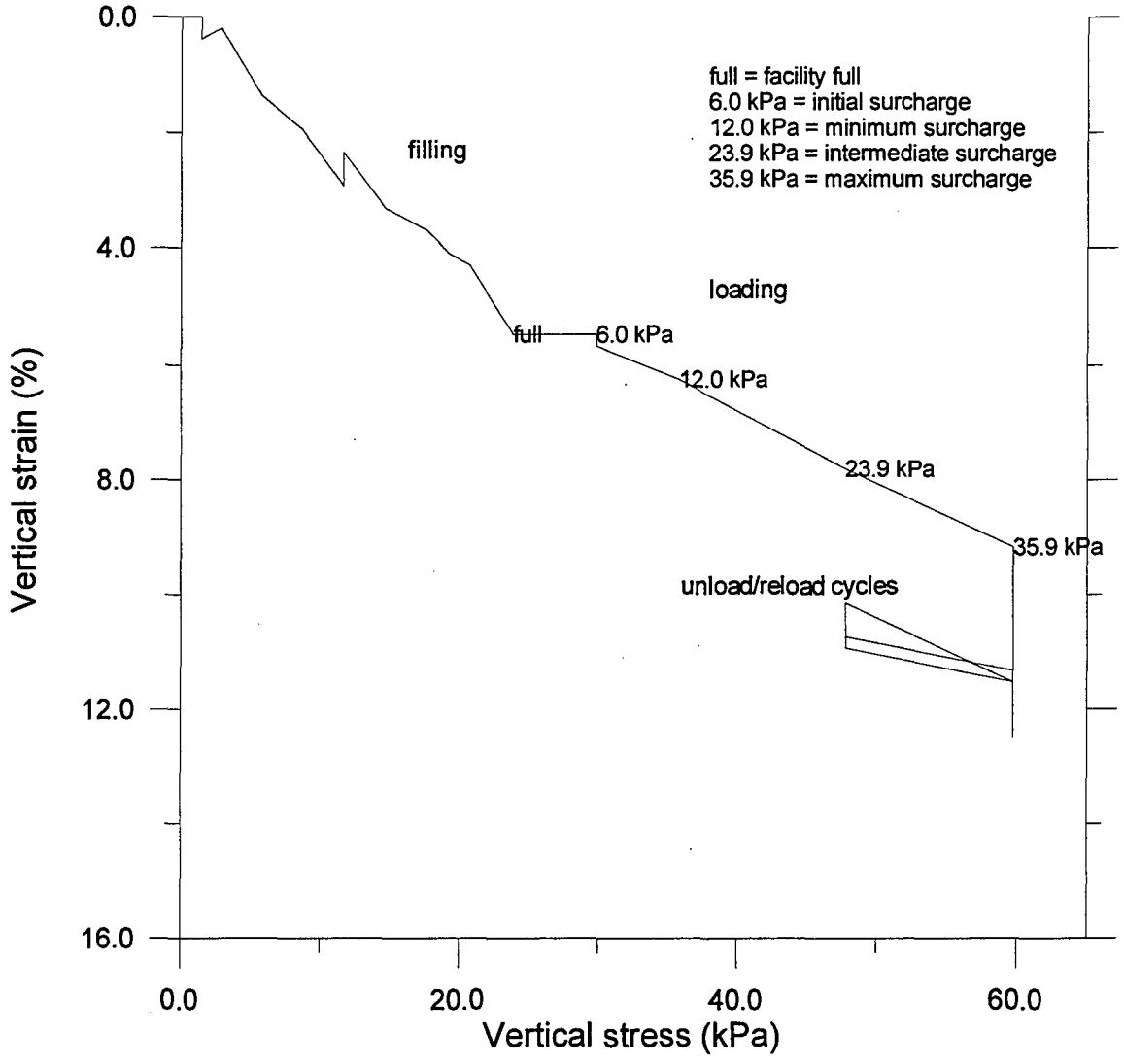

Figure 8.6 Vertical stress vs. vertical strain, F & B Enterprises, 1.63-m (5.3-ft) settlement plate

low reading. The change in vertical strain measured over each loading increment could then be compared to what was expected from laboratory compression tests by Humphrey, et al. (1992).

Humphrey, et al. (1992) performed laboratory compression tests on tire chips from the same suppliers. A typical plot of vertical strain and percent increase in density versus vertical stress is shown on Figure 6.30. A total of three trials were performed on each of the tire chips. To compare these results with the ones obtained in this study it was necessary to determine the vertical stress, using methods discussed in Section 6.5.1.1, at the midpoint between the base plate of the settlement plate and the facility floor. This was done for each of the loading conditions discussed above and shown graphically, from initial to full, on Figure 8.7. When determining the vertical stress below the settlement plates for each of the tire chip suppliers at each loading condition the values found were extremely close. So for comparison purposes the average was calculated for each loading condition, as shown on Table 8.1. These values were then used to determine a comparative change in strain from Humphrey, et al. (1992).

Examination of Table 8.1 shows that the difference in vertical stress from full to 6.0 kPa (125 psf) is 6.7 kPa (140 psf) and 7.0 kPa (146 psf) for the 3.25-m (10.7-ft) and 1.63-m (5.3-ft) settlement plates, respectively. This is greater than the actual change in vertical stress, equal to the surcharge increase of 6.0 kPa (125 psf). Similarly, the difference in vertical stress from 6.0 kPa (125 psf) to 35.9 kPa (750 psf) is 28.4 kPa (593 psf) for both settlement plates, which is slightly less than the actual change in surcharge of 29.9 kPa (625 psf). The reason for the slight difference between the calculated and

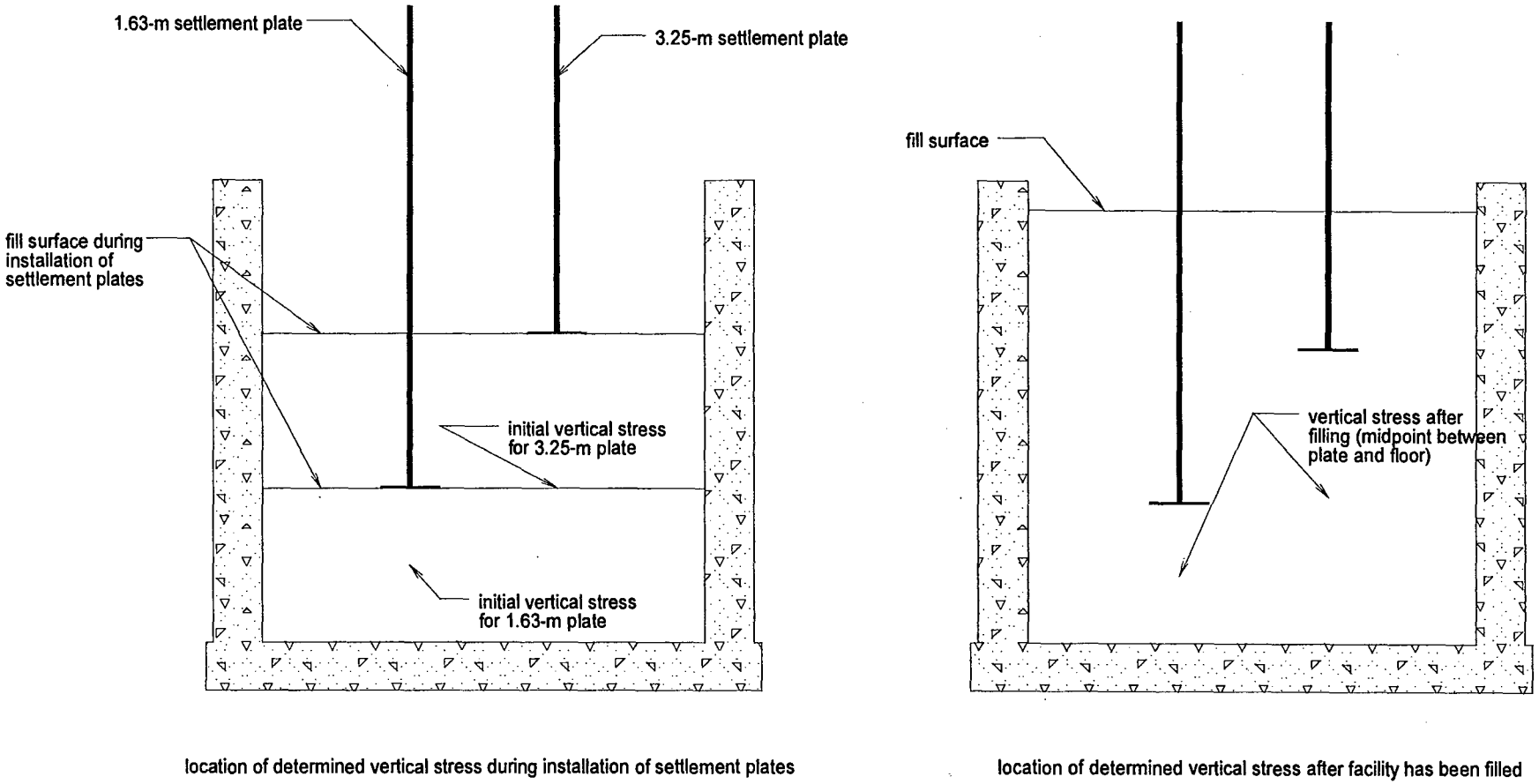

Figure 8.7 Location of vertical stress for comparison with Humphrey, et al. (1992)

Table 8.1 Average calculated vertical stress under settlement plates for each loading condition, using method in Section 6.5.1.1

Loading condition	Vertical stress under plate (kPa)	
	3.25-m plate	1.63-m plate
initial	11.7	5.5
full	24.3	30.4
6.0 kPa	31.0	37.4
35.9 kPa	59.4	65.8

actual change in stress is the method used to calculate the vertical stress. This method, as discussed in Section 6.5.1.1, approximated a portion of the vertical strain and percent increase in density versus vertical stress curves from Humphrey, et al. (1992) as a straight line. This slight difference in stress was insignificant when determining the change in vertical strain.

Once the vertical stress was determined, the change in vertical strain was found for each supplier from each of the three plots of vertical strain and percent increase in density versus vertical stress from Humphrey, et al. (1992). The change in strain from this study could then be compared to the average determined from the three plots. The measured change in strain for the different loading increments from each settlement plate along with those determined from Humphrey, et al. (1992) is shown on Table 8.2.

Table 8.2 Measured and calculated change in strain from laboratory compressibility tests by Humphrey, et al. (1992), for 3.25-m (10.7-ft) and 1.63-m (5.3-ft) settlement plates

Supplier	**Δ vertical strain (%)**			
	initial to full			
	3.25-m plate	lab*	1.63-m plate	lab*
Pine State Recycling	3.2	7.2	7.6	13.3
Palmer Shredding	3.4	7.2	6.4	14.6
F & B Enterprises	2.7	6.0	5.5	10.8
full to 6.0 kPa				
Pine State Recycling	1.4	3.0	1.6	2.2
Palmer Shredding	0.5	2.8	1.2	2.1
F & B Enterprises	0.4	2.1	0.0	1.9
6.0 kPa to 35.9 kPa				
Pine State Recycling	3.8	6.1	3.4	4.7
Palmer Shredding	5.2	7.3	2.7	6.2
F & B Enterprises	3.9	5.3	3.7	5.0

*Determined from compressibility tests by Humphrey, et al. (1992), using the vertical stresses shown on Table 8.1

The vertical compression predicted from the laboratory results is significantly larger than measured in the field. The percent difference between the lab and field values ranges from 26% to 57%, as shown in Table 8.3. The difference seems to be less for application of the surcharge than for loading from initial to full. It is felt that the difference is due mostly to the large vertical stress that is carried by interface friction

Table 8.3 Summary of percent difference between Humphrey, et al. (1992) and settlement plates.

Supplier	initial to full		full to 6.0 kPa		6.0 kPa to 35.9 kPa	
	3.25-m plate	1.63-m plate	3.25-m plate	1.63-m plate	3.25-m plate	1.63-m plate
Pine State	56%	43%	54%	30%	37%	28%
Palmer	53%	56%	82%*	43%	30%	57%
F & B	54%	49%	82%*	100%*	27%	26%
Average	54%	49%	54%	37%	31%	37%

*Could be off because of scatter caused by the method of measurement, and not included when determining the average

between the tire chips and the front wall face. This would result in the vertical stress that is carried by the tire chips being less than predicted based on the weight of the tire chips and surcharge.

The importance of wall friction can be illustrated by comparing the measured vertical interface friction force to the weight of tire chips and surcharge. This will be done for tire chips and surcharge in the 1.14-m (3.7-ft) wide strip between the settlement plates and the front wall, as shown on Figure 4.3. The plan area of this zone is thus 1.14 m (3.7 ft) by 4.57 m (15.0 ft). The latter is the side wall to side wall dimension of the facility. The weight of tire chips enclosed in this zone is approximately 185 kN (41.6 kips). The interface friction force across the entire width of the facility is found by multiplying the force measured on the center panel by three. Using the results in Figure 7.2 for Pine State Recycling, this yields a force of 99 kN (22.3 kips). This is 54% of the weight of the tire

chips between the settlement plates and the front wall. Making a similar comparison with the full surcharge applied, the friction force is 53% of the weight of the tire chips and surcharge. Thus, the friction force would substantially reduce the vertical stress carried by the tire chips at the location of the settlement plates. The result is that the change in vertical stress that was used to calculate compression based on laboratory data was too big, which caused the lab results to overpredict the vertical comparison.

Further examination of Table 8.2 shows there is general consistency between the relative compressibility of the three types from tire chips measured in the field and laboratory. This is can be seen from the loading increment of initial to full, where both settlement plates and laboratory values show that Pine State Recycling and Palmer Shredding are more compressible than F & B Enterprises. The same is true for the loading increment from full to 6.0 kPa (125 psf). For the loading increment from 6.0 kPa (125 psf) to 35.9 kPa (750 psf), the 3.25-m (10.7-ft) settlement plate and laboratory results indicate that Palmer Shredding is the most compressible with Pine State Recycling and F & B Enterprises being less compressible. However, for the 1.63-m (5.3-ft) settlement plate, Palmer Shredding exhibits less change in strain than the other two suppliers, whereas the laboratory showed that Palmer Shredding was most compressible. This lower measured change in strain may be a result of scatter, as discussed above, or measurement error. Thus, the field and laboratory settlement measurements generally agreed on the relative compressibility of the types of tire chips.

Further comparison for Pine State Recycling was made to laboratory compression tests by Nickels (1995). Nickels (1995) performed laboratory compression tests on tire

chips from Pine State Recycling with varying initial densities. To compare the results from this study to those of Nickels (1995), the Nickels (1995) test with the density closest to the average field density from this study was chosen. Nickels (1995) performed tests on dry samples. Therefore, to allow for comparison the average field density for Pine State Recycling, 0.71 Mg/m^3 (44.5 pcf), was converted into a dry density using Equation 5.2 and an assumed water content of 3%. The resulting dry density is 0.69 Mg/m^3 (43.0 pcf). Results from this study were compared to test MD1 with a density of 0.64 Mg/m^3 (40.1 pcf). Table 8.4 shows the change in strain determined from Nickels (1995) using the vertical stress values in Table 8.1 and the measured results from both settlement plates for Pine State Recycling. Comparison between the 1.63-m (5.3-ft) settlement plate and Nickels (1995) for 6.0 kPa (125 psf) to 35.9 kPa (750 psf) could not be done, because the calculated stress at a surcharge of 35.9 kPa (750 psf), as shown on Table 8.1, exceeded the maximum stress of the tests by Nickels (1995).

Table 8.4 shows that the values obtained from Nickels (1995) are consistently greater than those measured in this study by 20% to 40%. This difference is felt to be due to interface friction, as discussed previously. In addition, the initial dry density for the Nickels (1995) test used for comparison was (0.64 Mg/m^3; 40.1 pcf), whereas the calculated dry field density for this study was 0.69 Mg/m^3 (43.0 pcf). This may have also contributed to the field compression being less than the Nickels (1995) laboratory values.

Table 8.4 Measured and calculated change in strain from laboratory compressibility tests on Pine State Recycling tire chips, for 3.25-m (10.7-ft) and 1.63-m (5.3-ft) settlement plates

Supplier	Δ vertical strain (%)			
	initial to full			
	3.25-m plate	lab*	1.63-m plate	lab*
Pine State Recycling	3.2	5.4	7.6	11.4
full to 6.0 kPa				
Pine State Recycling	1.4	1.7	1.6	2.7
6.0 kPa to 35.9 kPa				
Pine State Recycling	3.8	6.4	3.4	-----

*Determined from compressibility tests by Nickels (1995) using the vertical stresses shown on Table 8.1

8.2.1.2 Settlement Grid

The initial reading for the settlement grid corresponds to the surcharge equal to one layer of surcharge blocks (6.0 kPa; 125 psf). The first layer of surcharge blocks was placed to secure wooden plates to the fill surface at the grid points. This was necessary to provide a solid surface from which to measure the elevation, as discussed in Section 4.2.2.2. The vertical stress was determined for each surcharge.

The vertical stress versus vertical strain from the settlement grid for Pine State Recycling, Palmer Shredding, and F & B Enterprises are shown on Figures 8.8, 8.9, and 8.10, respectively. Each data point is the average of the settlement recorded at the 19 grid

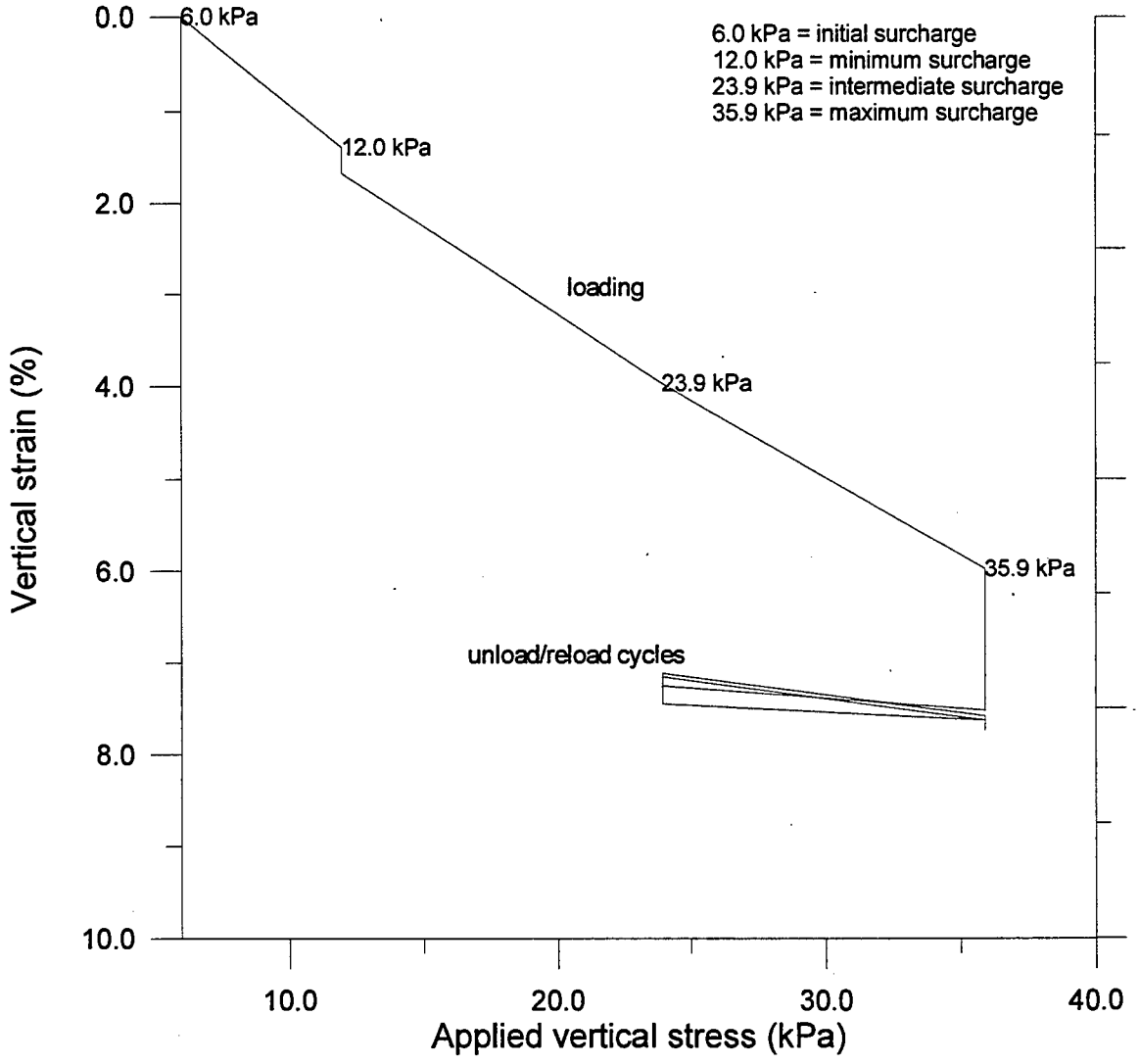

Figure 8.8 Applied vertical stress vs. vertical strain, Pine State Recycling, settlement grid

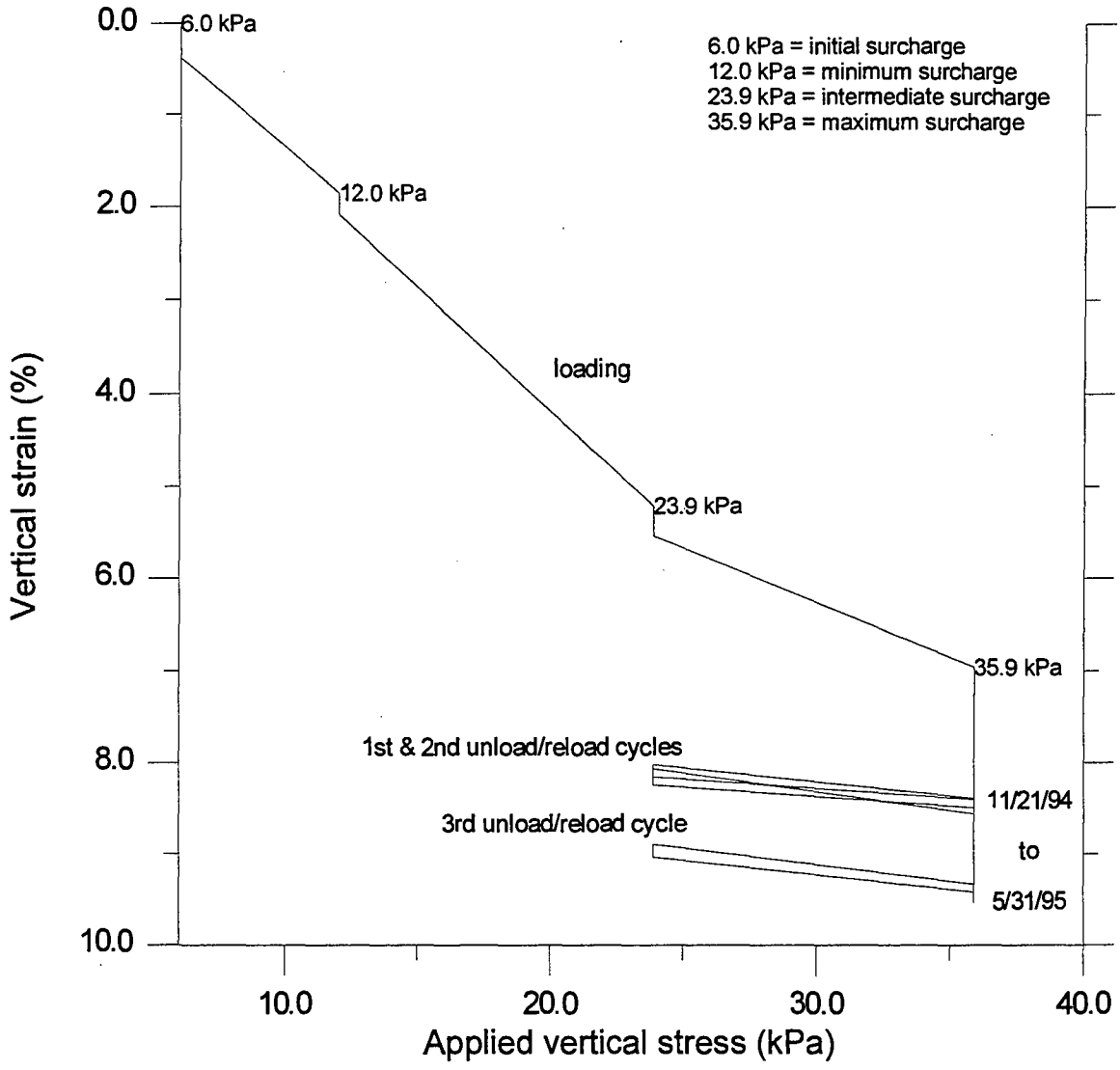

Figure 8.9 Applied vertical stress vs. vertical strain, Palmer Shredding, settlement grid

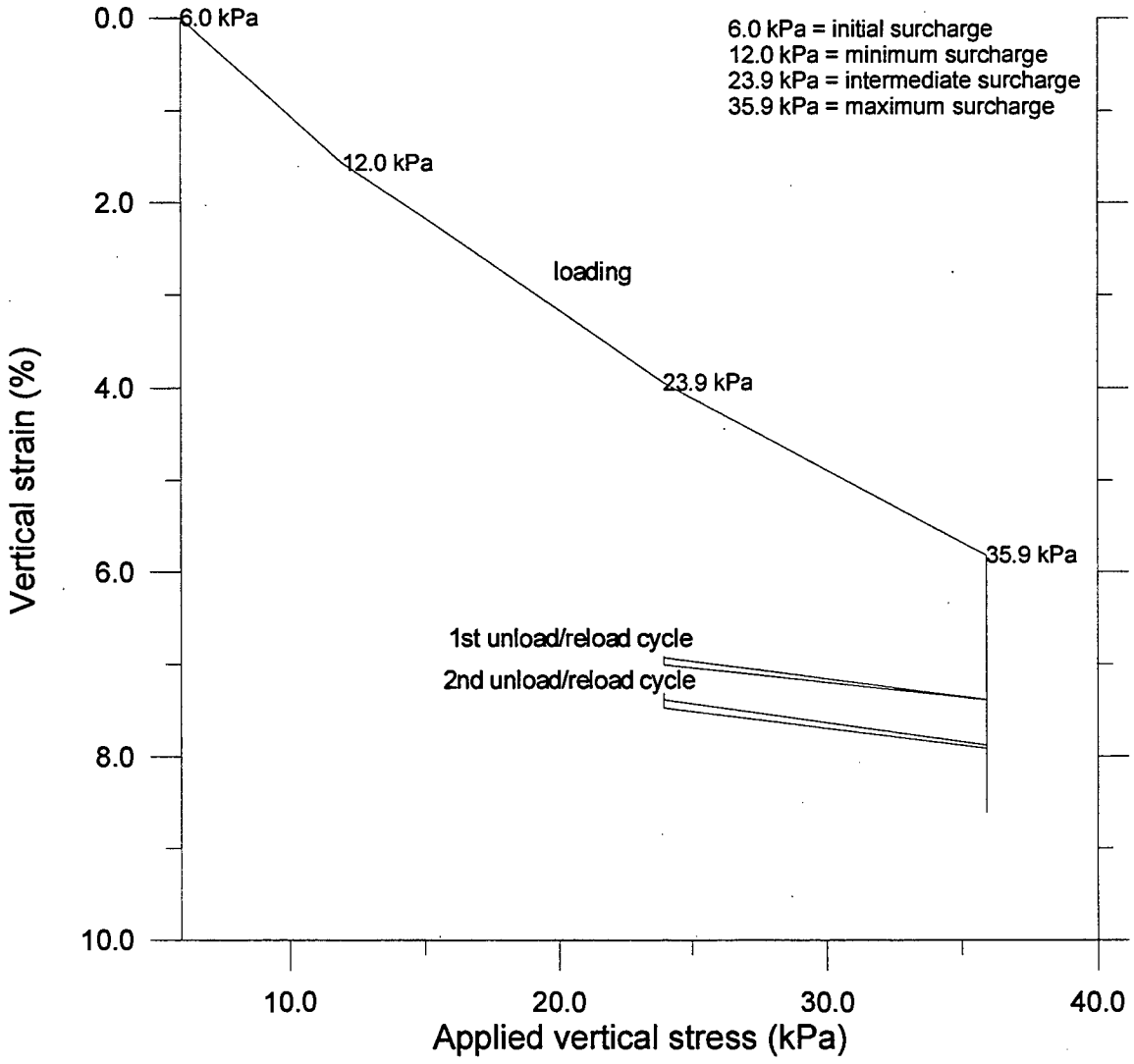

Figure 8.10 Applied vertical stress vs. vertical strain, F & B Enterprises, settlement grid

points. These show vertical line segments at some of the surcharges, this is particularly apparent on Figure 8.9 for Palmer Shredding, where it occurs for the minimum, intermediate, and maximum surcharges. This observation is consistent with the settlement plates shown on Figures 8.1 through 8.6 and are a result of time-dependent settlement, which occurred when a surcharge was left unchanged for a day or more. Figures 8.8 through 8.10 show that during loading the plot is slightly concave up for all three types of tire chips. These results are consistent with laboratory compression tests performed by Humphrey, et al. (1992) and both settlement plates, as discussed in Section 8.2.1.1. As with the settlement plates, this is most apparent for Palmer Shredding (Figure 8.9) where the three surcharges of 6.0 kPa (125 psf), 12.0 kPa (250 psf), and 23.9 kPa (500 psf) were left on for four days, one day, and three days, respectively.

Figures 8.8 through 8.10 can be further examined by looking at the change in vertical strain over the loading increment from 6.0 kPa (125 psf) to 35.9 kPa (750 psf). The change in vertical strain can be compared to the laboratory compression tests performed by Humphrey, et al. (1992), using methods similar to the settlement plates, as discussed in Section 8.2.1.1. To compare the laboratory compression tests with the settlement grid results it was necessary to determine the vertical stress, using the method given in Section 6.5.1.1, at the mid-elevation of the tire chips when the initial and the maximum surcharges were applied. The calculated vertical stress at the mid-elevation of the fill for each of the tire chip suppliers was found to be extremely close in value. Therefore, for comparison purposes, the average of the vertical stresses was used for each type of tire chip. The vertical stresses were 25.0 kPa (522 psf) for the initial surcharge and 53.8 kPa

(1120 psf) for the maximum surcharge. Thus, the calculated change in vertical stress is 28.8 kPa (602 psf). However, the actual change in vertical stress is equal to the increase in surcharge of 29.9 kPa (625 psf) or 2.0% greater than the value calculated using the method described in Section 6.5.1.1. This slight difference was insignificant when determining the change in strain. The reason for this difference is discussed in Section 8.2.1.1. The change in vertical strain for each tire chip supplier was then obtained from each of the three plots of vertical strain and percent increase in density versus vertical stress, as given by Humphrey, et al. (1992). The values obtained from the three trials were then averaged, to which the results from this study were compared. The average change in vertical strain from the three trials, as given in Humphrey, et al. (1992), along with the results from this study are shown in Table 8.5.

Table 8.5 Measured vertical strain for settlement grid compared to vertical strain calculated from laboratory compressibility tests by Humphrey, et al. (1992)

Supplier	**Δ vertical strain (%)**	
	6.0 kPa to 35.9 kPa	
	Settlement grid	**Laboratory***
Pine State Recycling	6.0	6.6
Palmer Shredding	7.0	8.0
F & B Enterprises	5.8	6.5

*Determined from compressibility tests by Humphrey, et al. (1992) using vertical stresses of 25.0 kPa (522 psf) to 53.8 kPa (1120 psf)

Table 8.5 shows that the average values from Humphrey, et al. (1992) are greater than those from the settlement grid. This is similar to comparisons with the settlement plates, although the differences are less. For Pine State Recycling the change in strain determined from Humphrey, et al. (1992) is 10% higher than that measured from the settlement grid. Similarly, the average laboratory change in strain is greater than the results measured from the settlement grid for Palmer Shredding and F & B Enterprises by 13% and 10%, respectively. The major reason for the difference is felt to be interface friction, as discussed in Section 8.2.1.1. However, the difference is less than with the settlement plates because many of the grid points are located further away from the front wall.

As with the settlement plates, the relative compressibility of the tire chip types is consistent. From both the settlement grid and laboratory data, Palmer Shredding is the most compressible, and Pine State Recycling and F & B Enterprises have similar compressibility characteristics.

Pine State results from the settlement grid can be compared to laboratory compression tests by Nickels (1995), as described in Section 8.2.1.1. Results from this study were compared to test MD1. Results from test MD1 showed a change in strain of 7.1% over the vertical stress range of 25.0 kPa (3.6 psi) to 53.8 kPa (7.8 psi). These results are greater than those in Table 8.5 from the settlement grid for Pine State Recycling by 15.8%. The reason for the difference is felt to be interface friction, as discussed above.

8.2.2 Unloading/Reloading

The unload/reload cycles were examined using the settlement grid, as shown on Figures 8.9 through 8.10. The scatter in the data from the settlement plates had more impact during the unload/reload cycles than during filling/loading, because the settlement was small relative to the magnitude scatter; so, settlement plate data is not included.

Even with the settlement grid results, scatter in the data could not be completely eliminated. As with the settlement plates, scatter had more impact on the results from the unload/reload cycles because the magnitude of the vertical movement was small.

The unload/reload cycles were examined for the settlement grid by plotting the vertical stress versus vertical strain for one or two cycles, as shown on Figures 8.11 through 8.15. This allowed for close examination of the rebound/compression behavior. Strain during periods when the surcharge was held constant appear as vertical lines on these figures. For clarity, data points were offset at the intermediate surcharge of 23.9 kPa (500 psf) and the maximum surcharge of 35.9 kPa (750 psf). The dates are also included on the figures, along with arrows, to aid in following the cycles. The solid arrows show loading and compression while the open arrows show unloading and rebound. The unload/reload cycles are discussed for each tire chip supplier.

The unload/reload cycles for Pine State Recycling are shown on Figure 8.11. This shows that when the maximum surcharge is removed for the first time on 9/20/95, the fill rebounded. The fill, now at the intermediate surcharge, was left for one day, during this time some time-dependent rebound occurred (9/21/94). When 35.9 kPa (750 psf) was

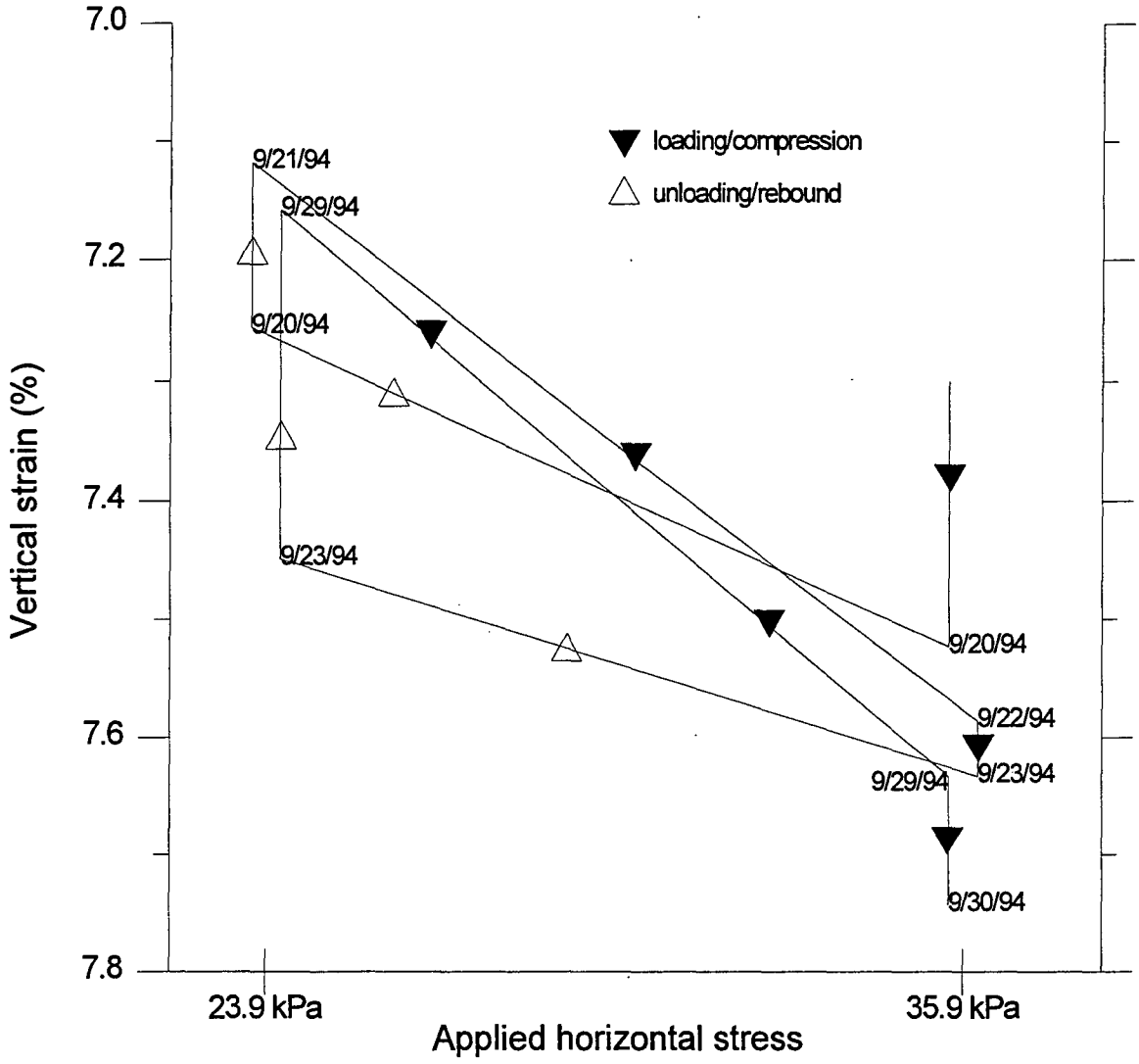

Figure 8.11 First and second unload/reload cycles, Pine State Recycling

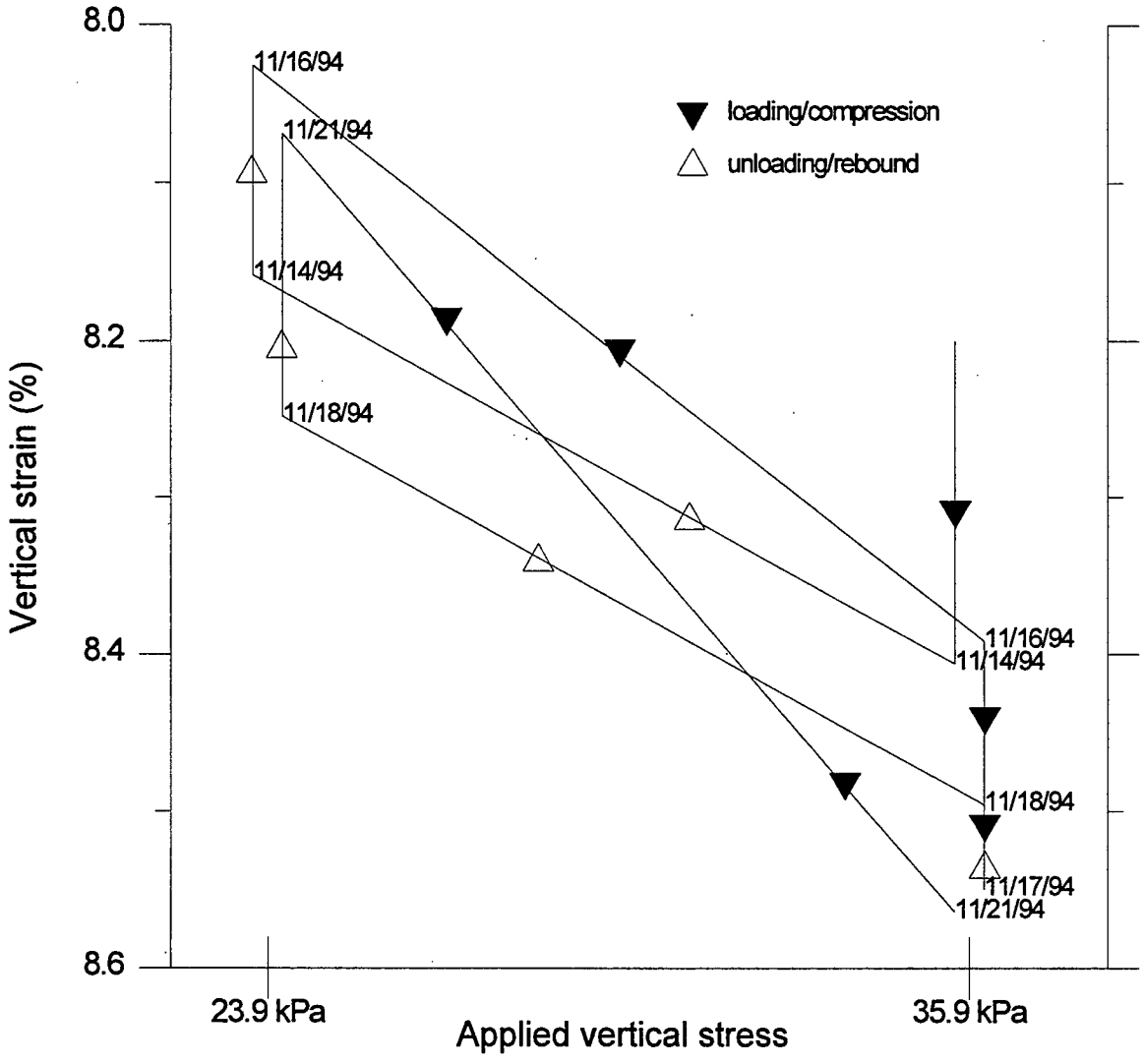

Figure 8.12 First and second unload/reload cycles, Palmer Shredding

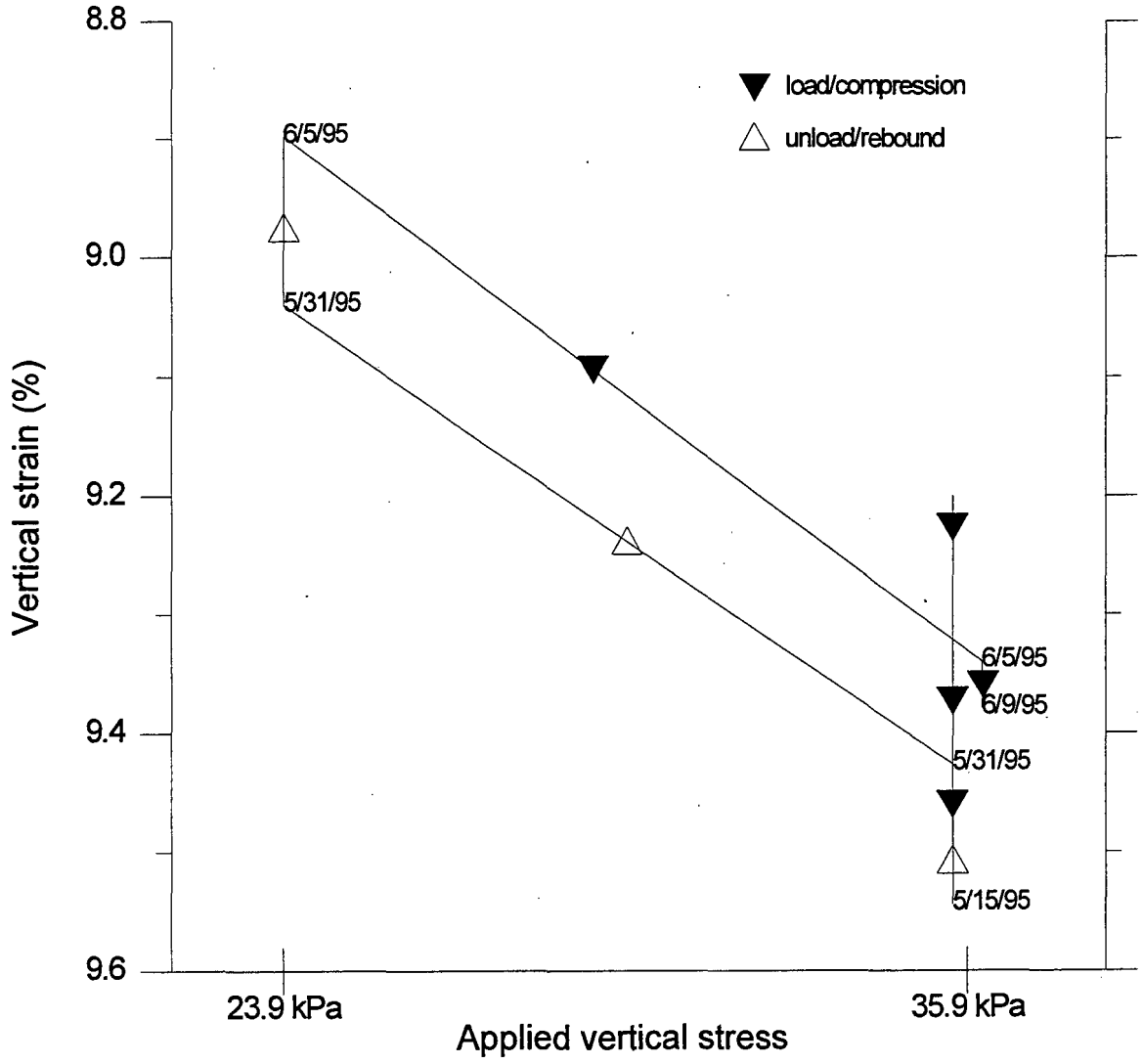

Figure 8.13 Third unload/reload cycle, Palmer Shredding

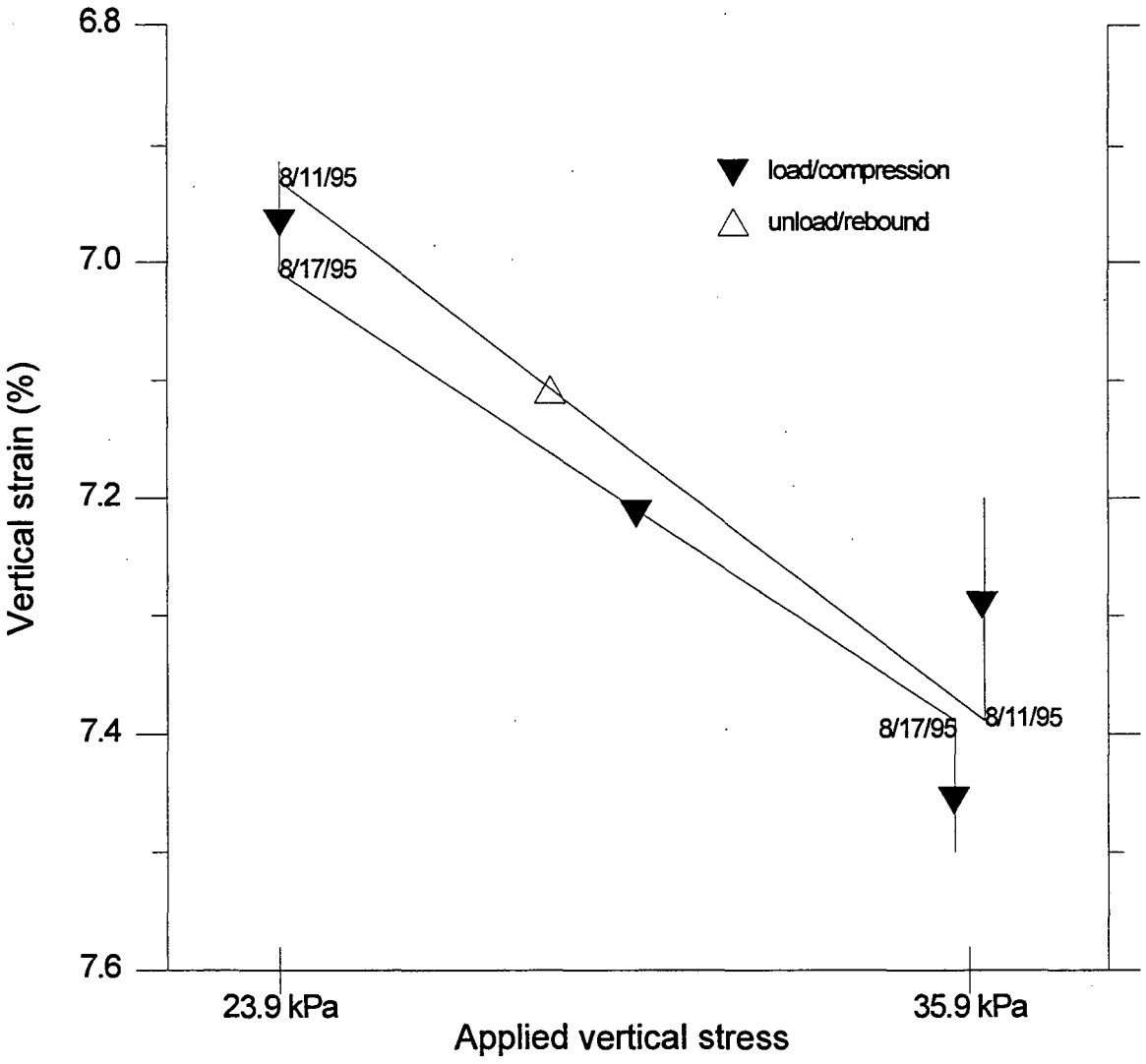

Figure 8.14 First unload/reload cycle, F & B Enterprises

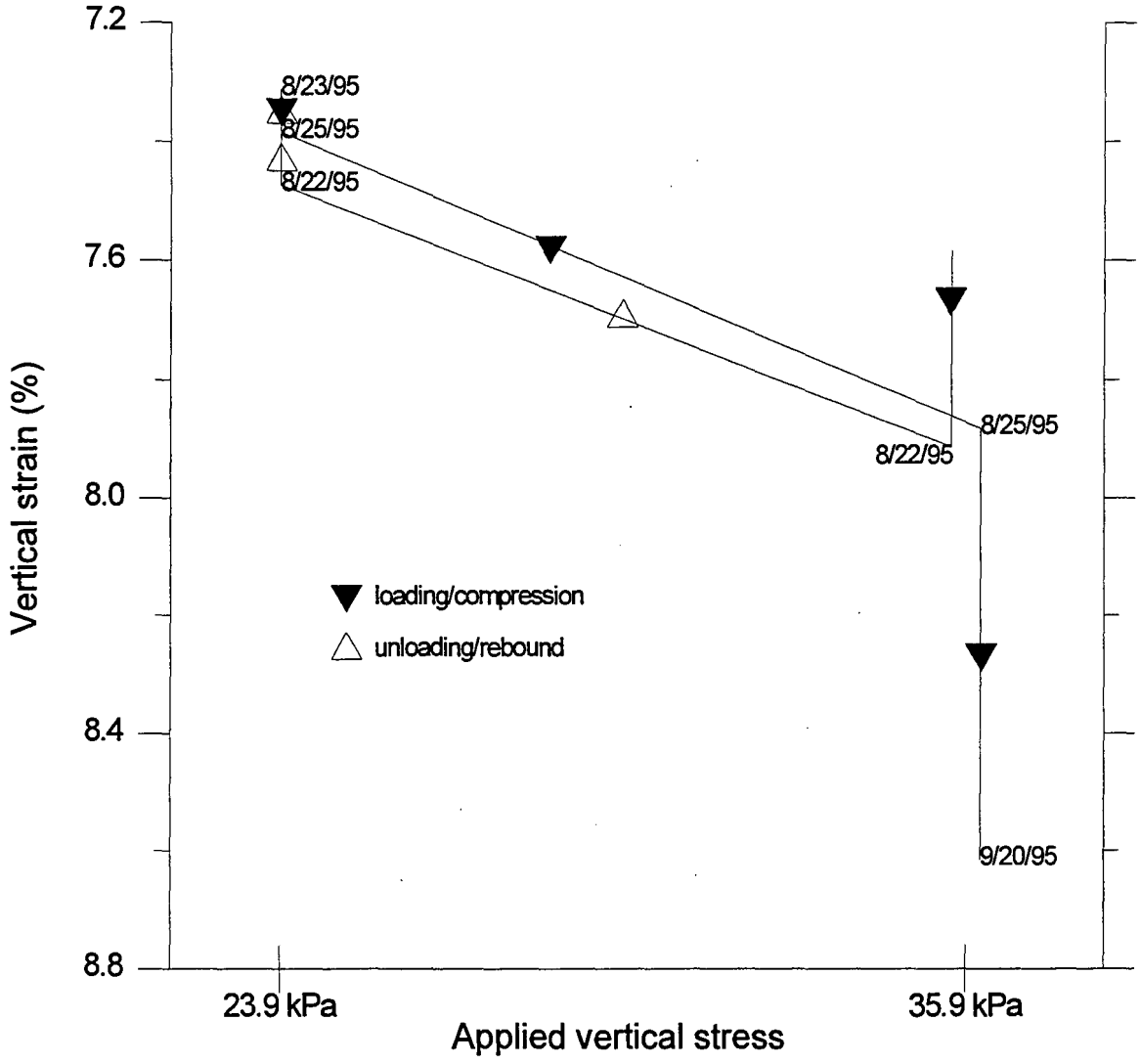

Figure 8.15 Second unload/reload cycle, F & B Enterprises

reapplied for the first time (9/22/94), the resulting strain was greater than before the unload/reload cycle had started (9/20/94). Possible explanations are that the tire chips experienced some time-dependent settlement or scatter in the data. The maximum surcharge was left on for one day, during which time a small amount of compression was measured. Once the maximum surcharge was removed for the second time, the tire chips again rebounded. With the intermediate surcharge of 23.9 kPa (500 psf) left in place for six days the tire chips rebounded an additional 3.9% (9/29/94). After the final reload to maximum surcharge (9/29/94) the tire chips compressed to a strain equal to that before the surcharge was removed the second time (9/23/94).

Palmer Shredding underwent three unload/reload cycles. The first two were performed before the Winter of 1994-95. Then the facility was left during the winter and a third cycle was performed in the spring. The first and second unload/reload cycles are shown on Figure 8.12. This shows that when the maximum surcharge was reapplied for the first time (11/16/94), the measured strain was less than just before the 35.9 kPa (750 psf) surcharge was removed the first time (11/14/94). The 35.9 kPa (750 psf) surcharge was left in place for two days, during the first day the tire chips experienced some time-dependent settlement (11/17/94). From 11/17/94 to 11/18/94 a small amount of rebound was measured. This is most likely due to scatter in the data. On 11/21/94 the maximum surcharge was reapplied for the second time, the resulting strain was slightly greater than the previous maximum strain (11/17/94).

The third unload/reload cycle for Palmer Shredding is show on Figure 8.13. The maximum surcharge was in place until 5/31/95. Just prior to unloading, between 5/15/95

and 5/31/95, some apparent rebound was measured; this was due to scatter in the data. The surcharge was reduced to the intermediate value on 5/31/95. After the third reload to 35.9 kPa (750 psf), 6/5/95, the resulting strain was less than before the unload/reload cycle began on 5/31/95.

The first unload/reload cycle for F & B Enterprises is shown on Figure 8.14. This shows that when the fill is at the intermediate surcharge for the first time a small amount of compression is observed from 8/11/95 to 8/17/95. When 35.9 kPa (750 psf) is reapplied for the first time (8/17/95) the fill was compressed to a strain about equal to when the cycle was started (8/11/95). The second unload/reload cycle is shown on Figure 8.15. This figure shows that during a second unload to 23.9 kPa (500 psf) the tire chips experience some time-dependent rebound from 8/22/95 to 8/23/95. Then a small amount of apparent compression was measured from 8/23/95 to 8/25/95. After the final reload to the maximum surcharge (8/25/95) the tire chips compressed to a strain slightly lower than when the surcharge was removed the second time on 8/22/95.

Closer examination of Figures 8.11 through 8.15 show that for all unload/reload cycles, except one, Figure 8.14, the reload curve lies above the unload curve. This type of behavior is shown by many other materials, including most fine grained soils, and is termed hysteresis.

8.3 TIME RATE OF SETTLEMENT

The relationship between time and vertical strain was determined at the maximum surcharge of 35.9 kPa (750 psf) using results from the 1.52-m (5.0-ft) and 3.05-m (10.0-

ft) settlement plates, and the settlement grid. Zero elapsed time and zero time-dependent strain were taken to be the day the maximum surcharge was applied for the first time. To find the time-dependent strain, the strain at the first day with 35.9 kPa (750 psf) surcharge was subtracted from each subsequent strain with that surcharge.

The time versus vertical strain for the 3.25-m (10.7-ft) and 1.63-m (5.3-ft) settlement plates and settlement grid are shown on Figures 8.16 through 8.18, respectively. In each figure, two plots are shown, linear and semilog. These show that under the maximum surcharge F & B Enterprises experiences more time-dependent settlement. One possible explanation for this is that F & B Enterprises was loaded faster. Loading of the surcharge blocks for Pine State Recycling and Palmer Shredding took 2 days and 8 days, respectively. During loading for Pine State, 12.0 kPa (250 psf) was left on overnight. This is evident in Figures 8.1 and 8.8. Similarly, during loading for Palmer Shredding, the surcharge of 6.0 kPa (125 psf) was left on the tire chips for 4 days, 12.0 kPa (250 psf) for 1 day, and 23.9 kPa (500 psf) for 3 days, as can be seen on Figures 8.2 and 8.9. Conversely, F & B Enterprises was loaded in one day. Therefore, it is possible that F & B Enterprises experienced less time-dependent settlement during initial loading; thus, more time-dependent settlement occurred after the maximum surcharge was placed.

The plots for the settlement plates, shown on Figures 8.16 and 8.17, show considerably more scatter than the plot for the settlement grid (Figure 8.18). This can be attributed to the reasons discussed in Section 8.2.1.1. Thus, the following discussion will concentrate on the settlement grid.

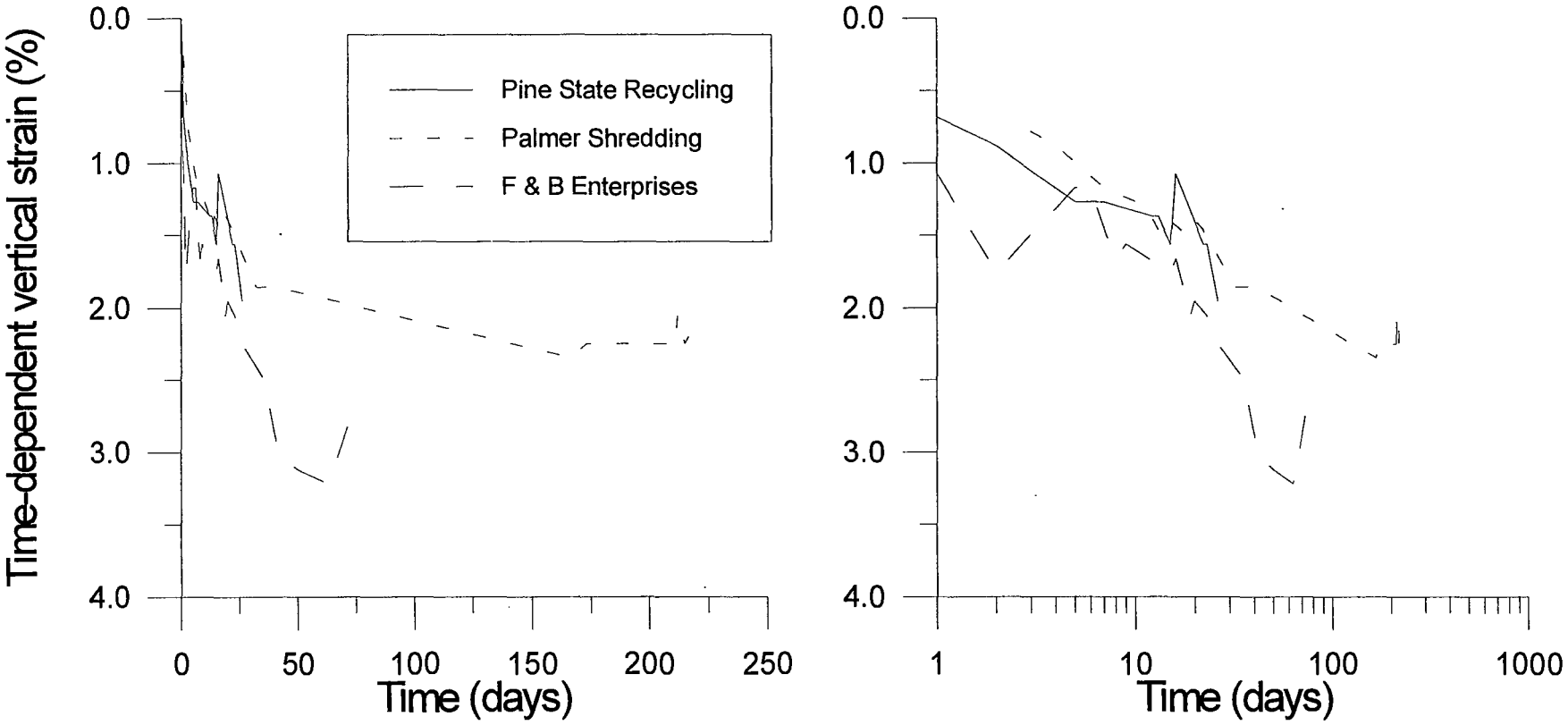

Figure 8.16 Time vs. vertical strain, 3.25-m (10.7-ft) settlement plate

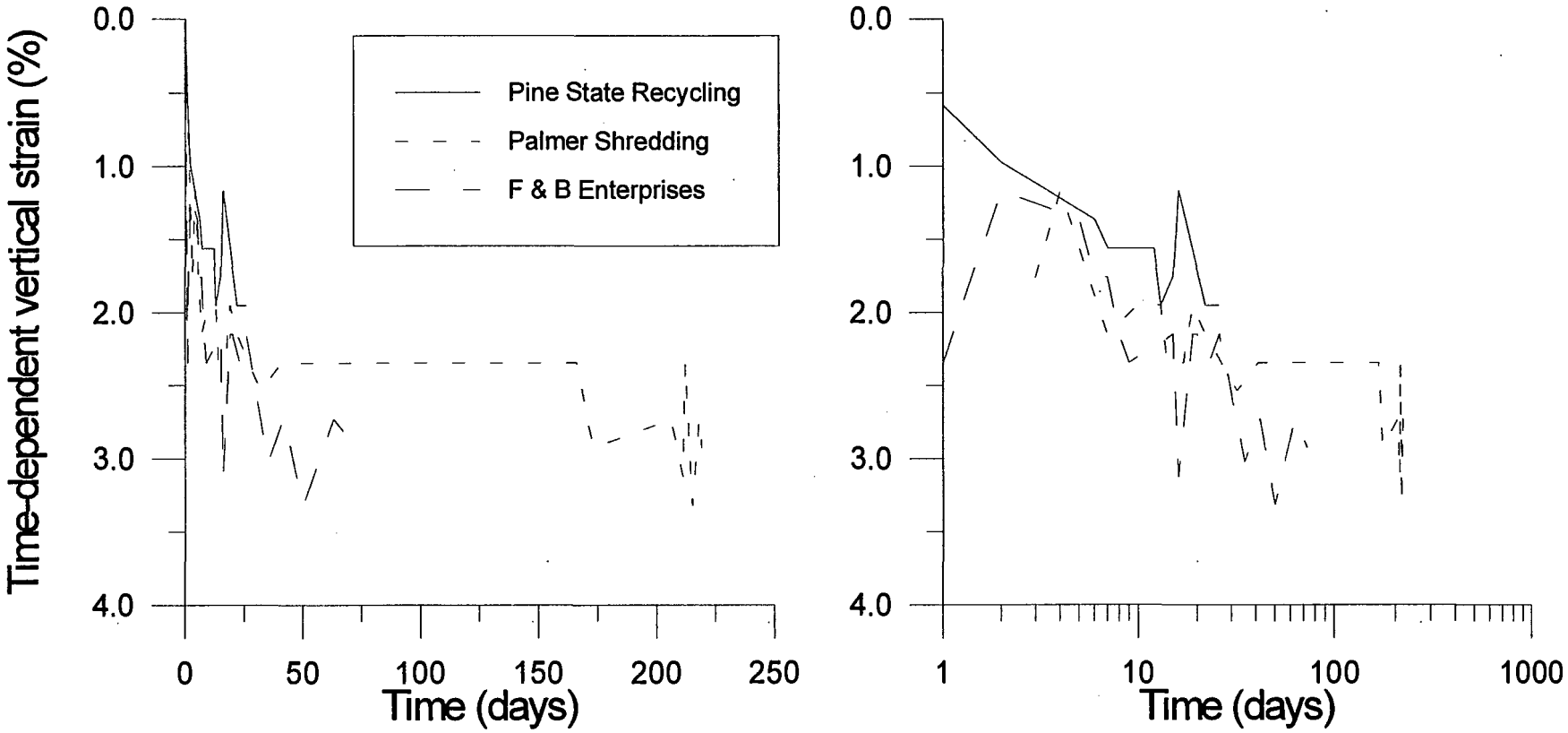

Figure 8.17 Time vs. vertical strain, 1.63-m (5.3-ft) settlement plate

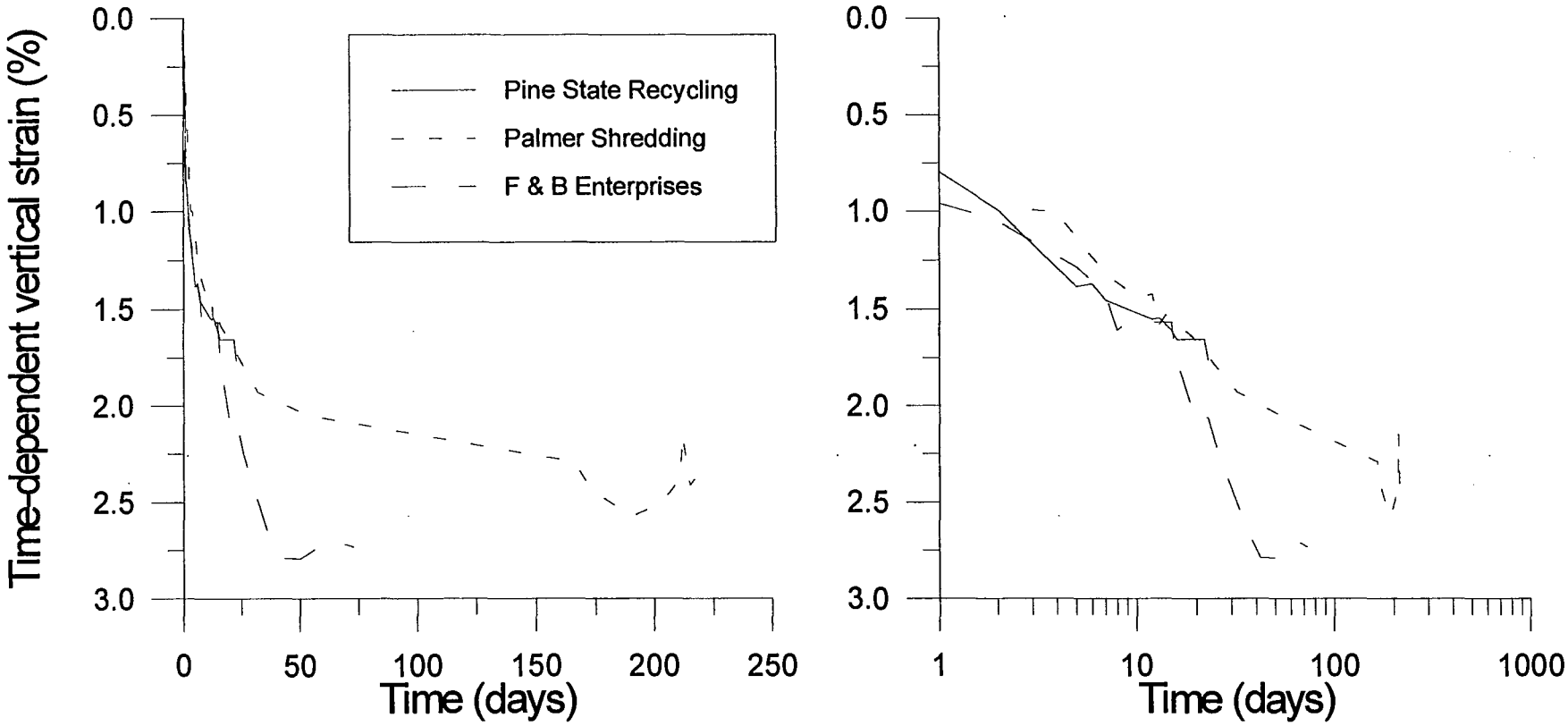

Figure 8.18 Time vs. vertical strain, settlement grid

The Pine State Recycling settlement grid data shows significant vertical strain through day 25, when the at-rest settlement measurements were completed. Examination of the Palmer Shredding settlement grid data shows significant vertical strain until approximately day 40. From the time interval of 12/28/94 (day 52) to 4/21/95 (day 166) no settlement readings were taken. After 4/21/95 settlement readings were taken at more frequent intervals. From this time until the end of the test, the measured settlement did not vary more than 15 mm (0.6 in.) from one reading to the next. As a result, it is felt that the variations can be attributed to limitations in the accuracy of the measurement techniques, as discussed in Section 8.2.1.2. The F & B Enterprises settlement grid data shows that significant vertical strain continued until approximately day 50. After day 50 the vertical strain occurred at a much slower rate. Using the data from Palmer Shredding and F & B Enterprises, it can be concluded that the majority of the time-dependent settlement for tire chips is completed in 50 days.

8.4 DESIGN CONSIDERATIONS

The following design considerations only apply to retaining walls approximately 4.57 m (15 ft) in height and with surcharges less than 35.9 kPa (750 psf). The backfill material must be tire chip fill with properties similar to those discussed in Chapter 5. The design considerations were consolidated from the results discussed above.

When using tire chips as fill material, careful consideration should be made to two important parameters, the amount of settlement during tire chip and overlaying surcharge placement, and subsequent time-dependent settlement. Examination of Figures 8.8

through 8.10 shows that as much as 7% strain can occur at the tire chip surface during surcharge placement, with an additional 3% occurring due to time-dependent settlement. As a result, the thickness of tire chips placed should be increased to accommodate settlement during and after surcharge placement. The time-dependent settlement occurs for 50 days after placement of surcharge. So, for highway applications, it is recommended that when possible the overlaying fill be in place for 60 days before settlement critical materials, such as pavement, are placed over tire chips. When long-term settlement is a concern, it is recommended that the semilog plot from the settlement grid and Palmer Shredding be used for estimating the magnitude of the settlement.

(BLANK)

CHAPTER 9. HORIZONTAL MOVEMENTS

9.1 INTRODUCTION

One aspect of this study was to monitor horizontal movements of the front wall panels and within the fill. It was necessary to measure the movement of the front wall during the at-rest case to ensure that the wall was not moving and that at-rest conditions were achieved. Horizontal movements within the fill and settlement of the fill surface measured during rotation of the front wall away from the fill made it possible to estimate the location of the active wedge.

9.2 MOVEMENT OF FRONT WALL

Horizontal movement of the front wall was determined by measuring the change in horizontal distance at six points on each of the three panels that make up the front wall. On each panel, a pair of points were located at each of three elevations. The elevation of the reference points with respect to the facility floor, are as follows: 0.38 m (1.25 ft), 2.29 m (7.50 ft), and 4.60 m (15.09 ft). The movement of the reference points was measured with respect to three reference beams. The reference beams were connected to the ends of the concrete side walls closest to the front wall at elevations corresponding to the reference points, as shown on Figure 4.8. The displacement was measured with dial calipers accurate to 0.025 mm (0.001 in.), as discussed in Section 4.2.3.2.

Figures 9.1 through 9.4 show the at-rest front wall deflections for granular fill, Pine State Recycling, Palmer Shredding, and F & B Enterprises, respectively. The deflection shown on these figures is the average of six readings taken at each elevation. Only the conditions of no surcharge and 35.9 kPa (750 psf) are shown. At no surcharge, the deflection is shown for the last measurement before the surcharge blocks were applied. For the 35.9 kPa (750 psf) surcharge, the deflection is shown for the last measurement before the wall was rotated.

Examination of Figures 9.1 through 9.4 shows that in each of the tests the front wall moved more at the top than at the bottom. The purpose of monitoring the front wall deflections was to ensure that at-rest conditions were achieved. In dense cohesionless soils the amount of horizontal movement needed to achieve active conditions is 0.001H to 0.002H (Bowles, 1988), where H is the height of the wall. For tire chips the amount of horizontal movement needed to create active conditions is considerably greater and has not yet been determined, as discussed in Section 6.4.2. The horizontal movement with respect to the wall height (H) was determined for readings taken at the 35.9 kPa (750 psf) surcharge, using the plots on Figures 9.1 through 9.4. It was found to be about 0.001H for all of the backfills tested. This amount of horizontal movement is less than required to reach active conditions in the tire chips, but the movements may have been sufficient to slightly lower the horizontal stress on the wall. For the granular fill the movement approached the lower limit of movement needed to reach active conditions. Thus, it is possible that the movements were large enough to lower pressures on the wall for the at-rest case with granular soil. However, it is unlikely that the movements were sufficient to

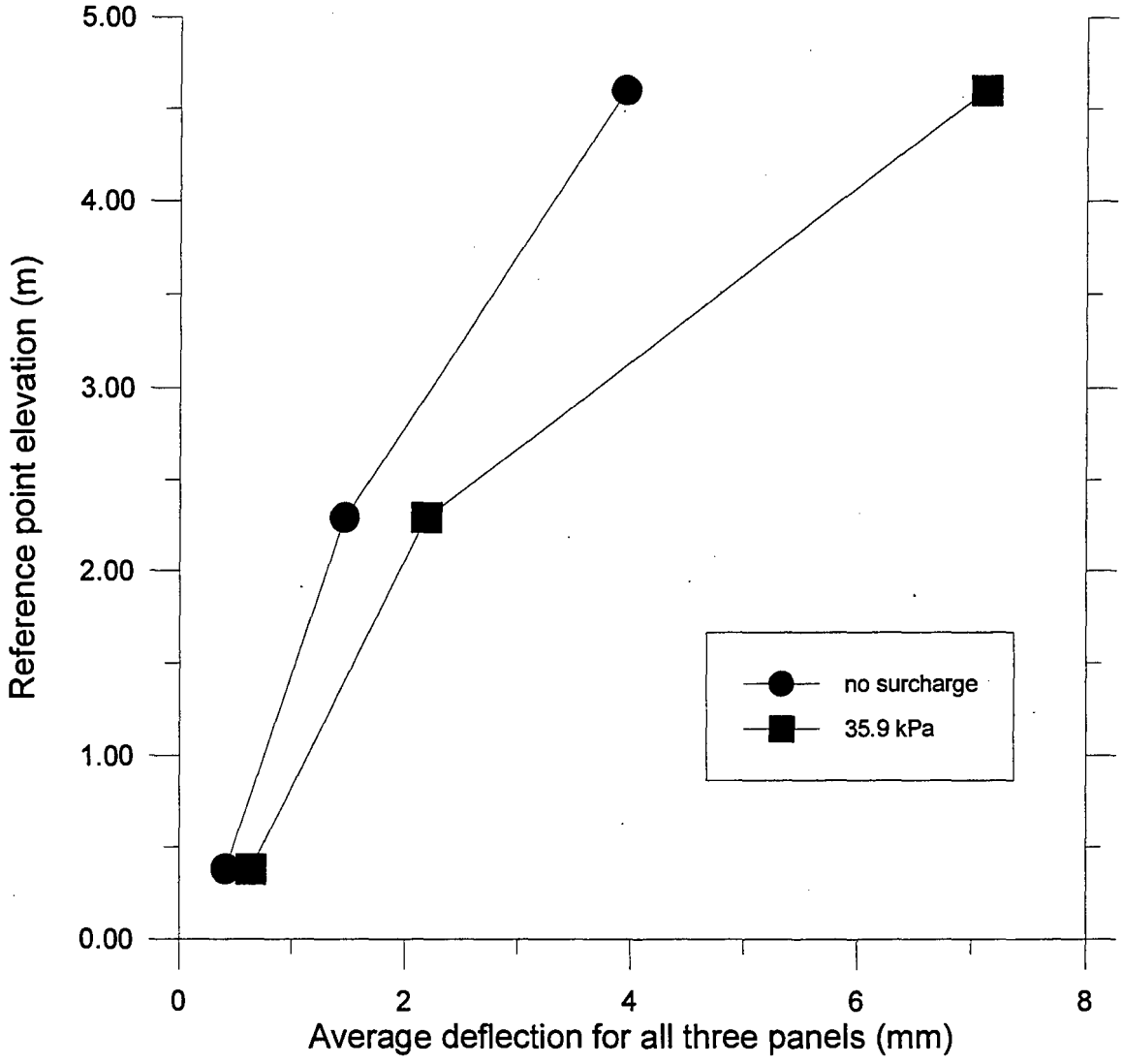

Figure 9.1 Front wall deflections, granular fill

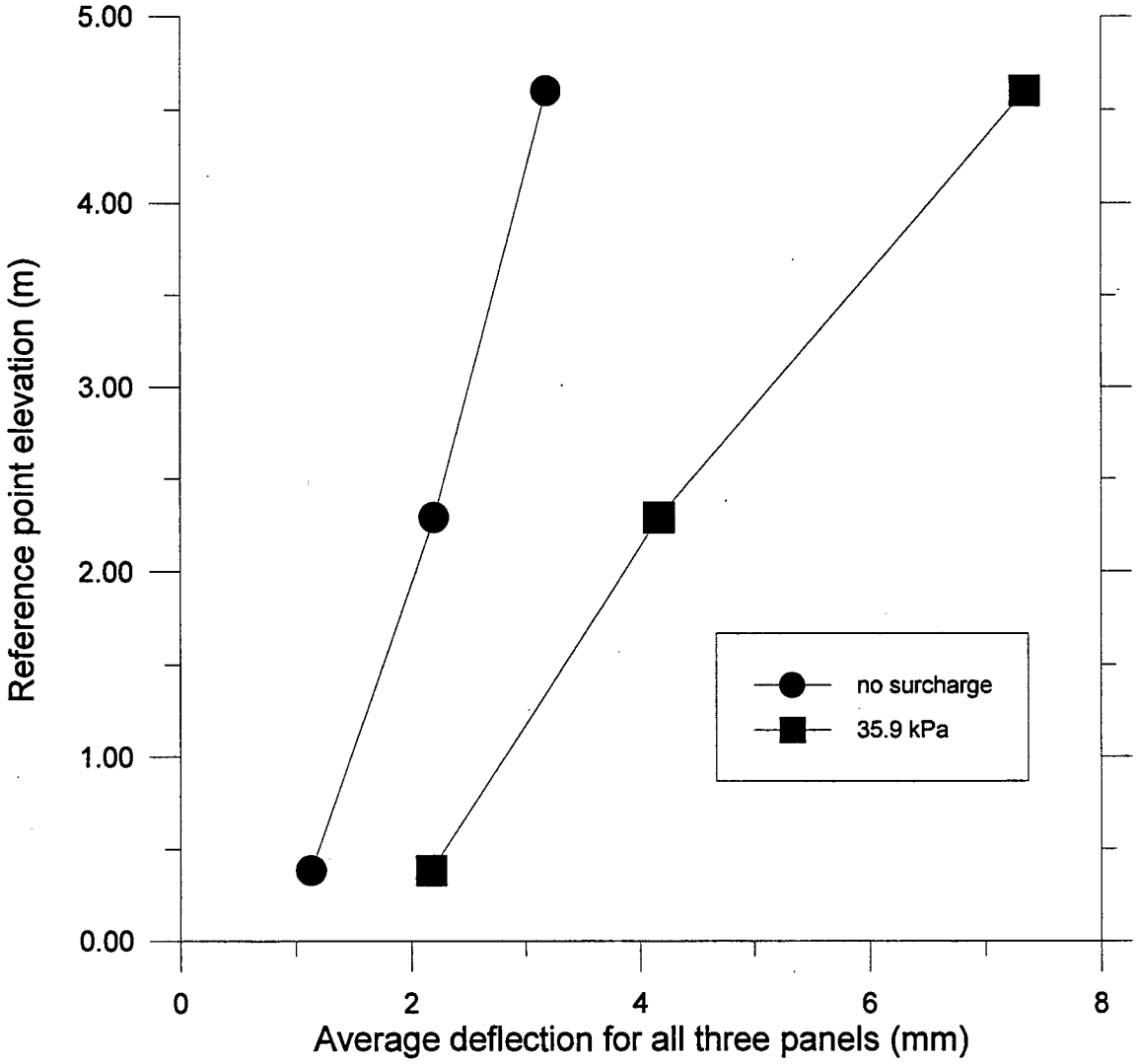

Figure 9.2 Front wall deflections, Pine State Recycling

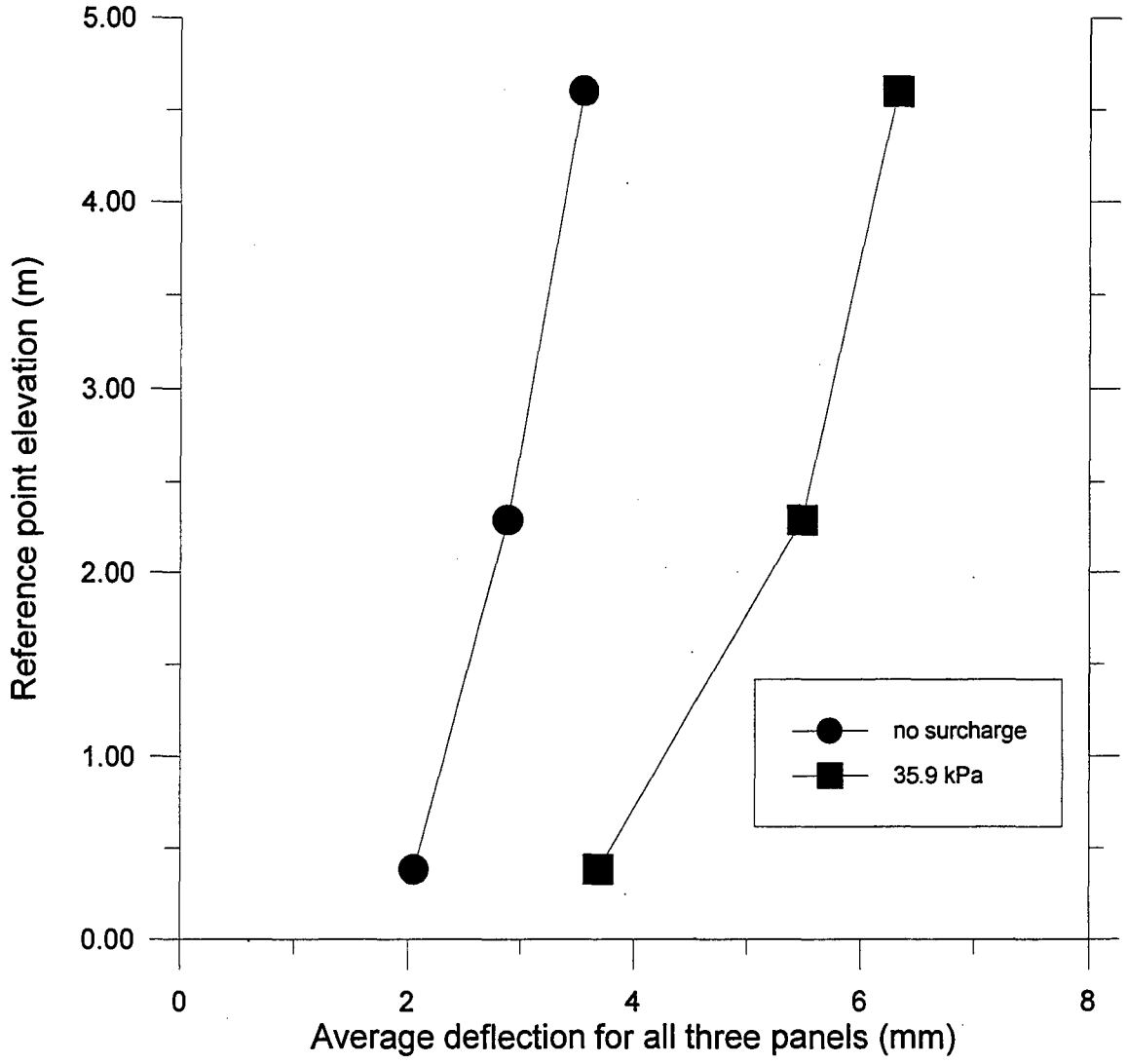

Figure 9.3 Front wall deflections, Palmer Shredding

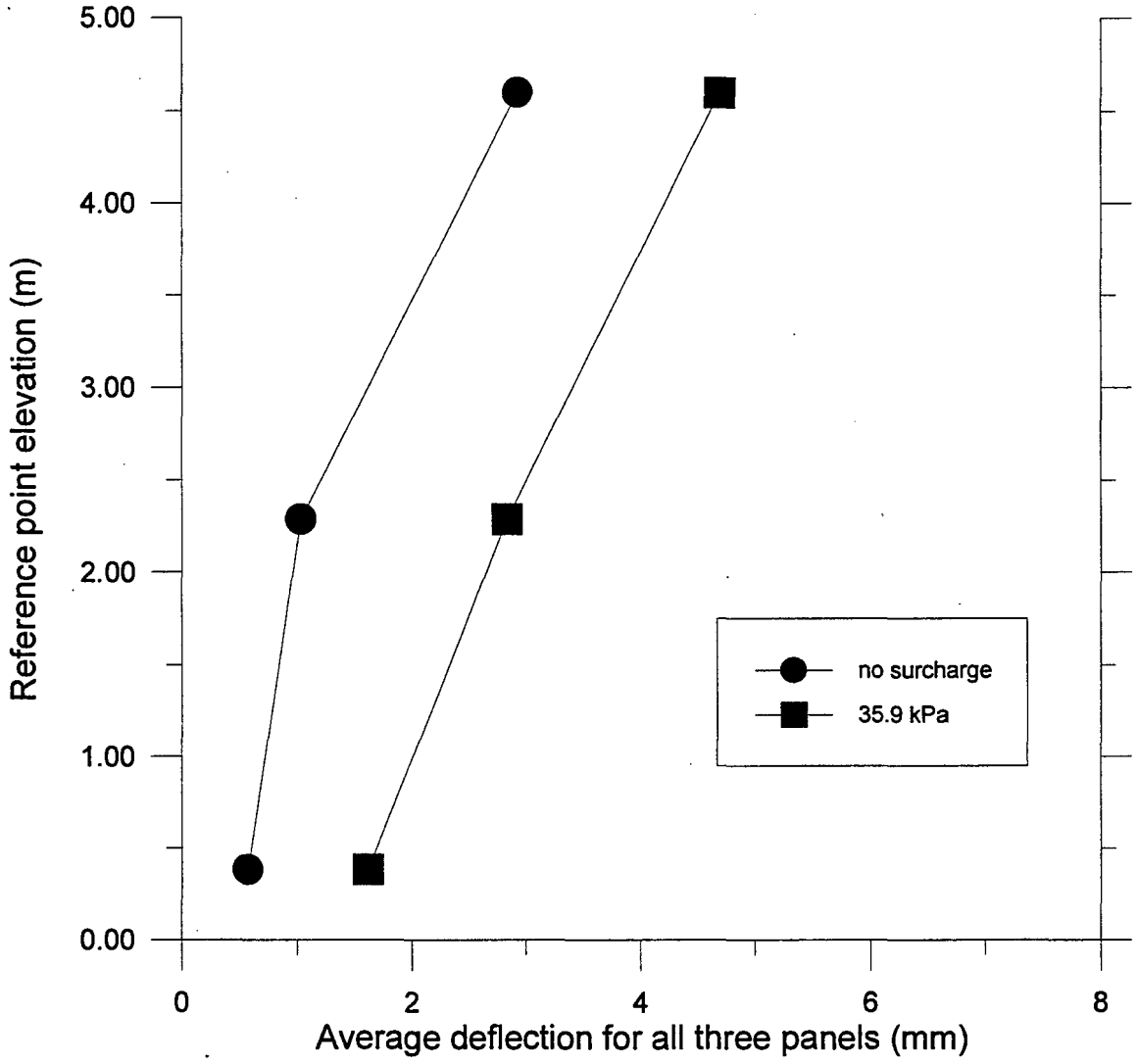

Figure 9.4 Front wall deflections, F & B Enterprises

achieve active conditions in the tire chips, as the pressures were reduced when the wall was rotated outward, as discussed in Section 6.4.1. In addition, since tire chips are less stiff than typical granular soils, with a Young's modulus for the tire chips tested here ranging from 772 to 1138 kPa (112 to 165 psi), Humphrey, et al. (1992), as shown on Table 2.4, while that of coarse sands ranges from 32400 to 45200 kPa (4700 to 6550 psi), Harr (1966), they would be less affected by wall movement.

The greater movement at the top can be explained by the configuration of the connections at the top of the wall. The front wall was supported at the bottom and the top, much like a simply supported beam, with a trapezoidal shaped stress distribution acting on the wall face. With this type of loading the maximum deflection should occur somewhere near the middle. However, each connection at the top for the center panel consisted of a hinge assembly, load cell, screw jack, and ball joint. The top connections for the two side panels had a similar configuration, less the load cell, as shown on Figure 3.8. It is theorized that once a load was applied to the front wall any gaps in this connection were taken up, resulting in a larger measured deflection. In addition, any elastic deformation of the components comprising the top connections would contribute to the larger displacement at the top.

Further examination of the measured deflections in Figures 9.1 for the granular fill shows that for no surcharge and the 35.9 kPa (750 psf) surcharge the front wall bends in at the middle toward the fill, which seems unlikely. This behavior is also seen to a lesser extent for Pine State Recycling, 35.9 kPa (750 psf), and for F & B Enterprises at no surcharge and 35.9 kPa (750 psf) surcharge. From classical structural theory the wall

should bend outward at the middle, as shown on Figure 9.3 for Palmer Shredding. The deviation from the expected shape for Figures 9.1, 9.2, and 9.4 was attributed to scatter in the data caused by limitations in the measurement method, in particular, the inability to orient the dial calipers consistently between the reference points and reference beams.

Time-dependent movement of the front walls with a constant surcharge was examined. This is shown on Figure 9.5 for Palmer Shredding, where the measured deflection was plotted after the initial application of the 23.9 kPa (500 psf) surcharge over a period of two days, from 11/2/94 to 11/4/94. This shows that the deflections are nearly identical at all measured elevations, with the greatest difference between any two points of approximately 0.5 mm (0.02 in.). Although the dial caliper used to measure the distance was accurate to 0.02 mm (0.001 in.), it is felt these differences were within the accuracy of the measurement method, as discussed above. Thus, no time-dependent movement of the front wall occurred from 11/2/94 to 11/4/94.

9.3 MOVEMENT WITHIN THE BACKFILL

Horizontal deformations within the backfill were recorded as the front wall was rotated outward away from the fill. The deformation for the granular fill, Pine State Recycling, and Palmer Shredding was determined using a Slope Indicator Co. series 200-B instrument, while a Slope Indicator model #50300940 was used for F & B Enterprises. The inclinometers worked in conjunction with inclinometer casings passing through the depth of the fill. The inclinometers casings were located at distances of 1.14 m (3.7 ft) and 2.29 m (7.5 ft) from the front wall, as shown on Figures 4.3 and 4.4. In the following

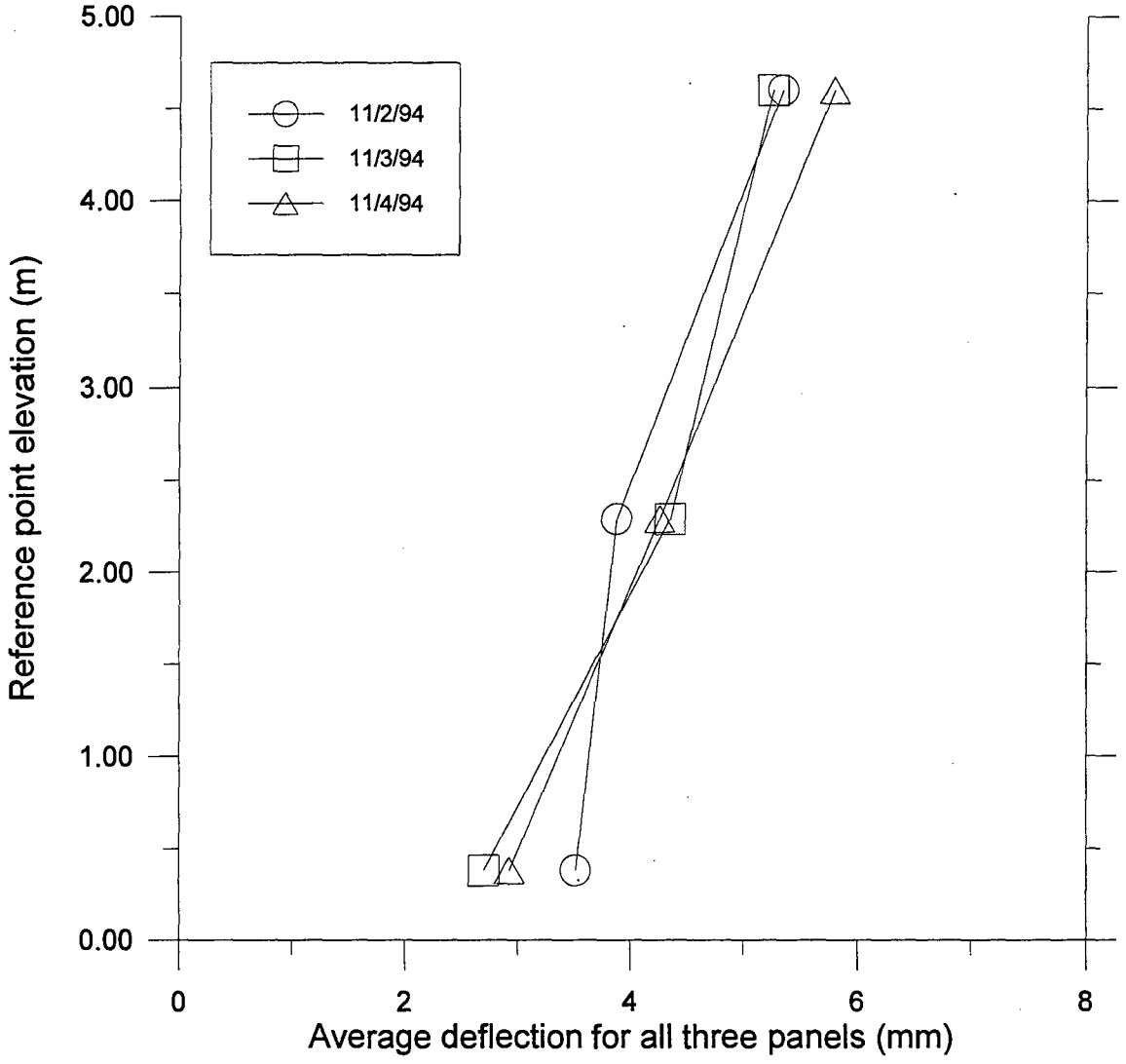

Figure 9.5 Front wall deflections on three consecutive days with 23.9 kPa (500 psf) surcharge, Palmer Shredding

text these will be referred to as the 1.14-m (3.7-ft) and the 2.29-m (7.5-ft) casings. The casings were attached to the floor of the facility, resulting in no measured horizontal deformations at the fill base. Details relevant to these measurements were discussed in Section 4.2.3.1.

The front wall was rotated outward approximately 0.01H, where H is the height of the wall. The actually rotation was 0.7 degrees for granular, 0.8 degrees Pine State Recycling, 0.8 degrees for Palmer Shredding, and 0.6 degrees for F & B Enterprises. In addition, for Pine State Recycling and Palmer Shredding, the wall was rotated further until the front row of surcharge blocks were leaning forward at an ominous angle, resulting in maximum a rotation of 2.2 degrees (0.04H) for Pine State Recycling and 1.7 degrees (0.03H) for Palmer Shredding.

9.3.1 Granular Fill

The horizontal deformation of the granular fill measured from the 1.14-m (3.7-ft) and 2.29-m (7.5-ft) casings is shown on Figure 9.6. This shows that after 0.7 degrees rotation (0.01H) a small amount of movement was measured, with maximum deflections measured from the 1.14-m (3.7-ft) and 2.29-m (7.5-ft) casings of 2.3 mm (0.09 in.) and 0.8 mm (0.03 in.), respectively. The magnitude of this movement was insignificant. Evidence will be presented later in this chapter showing fill movement in the zone closer than 1.14 m (3.7 ft) from the front wall.

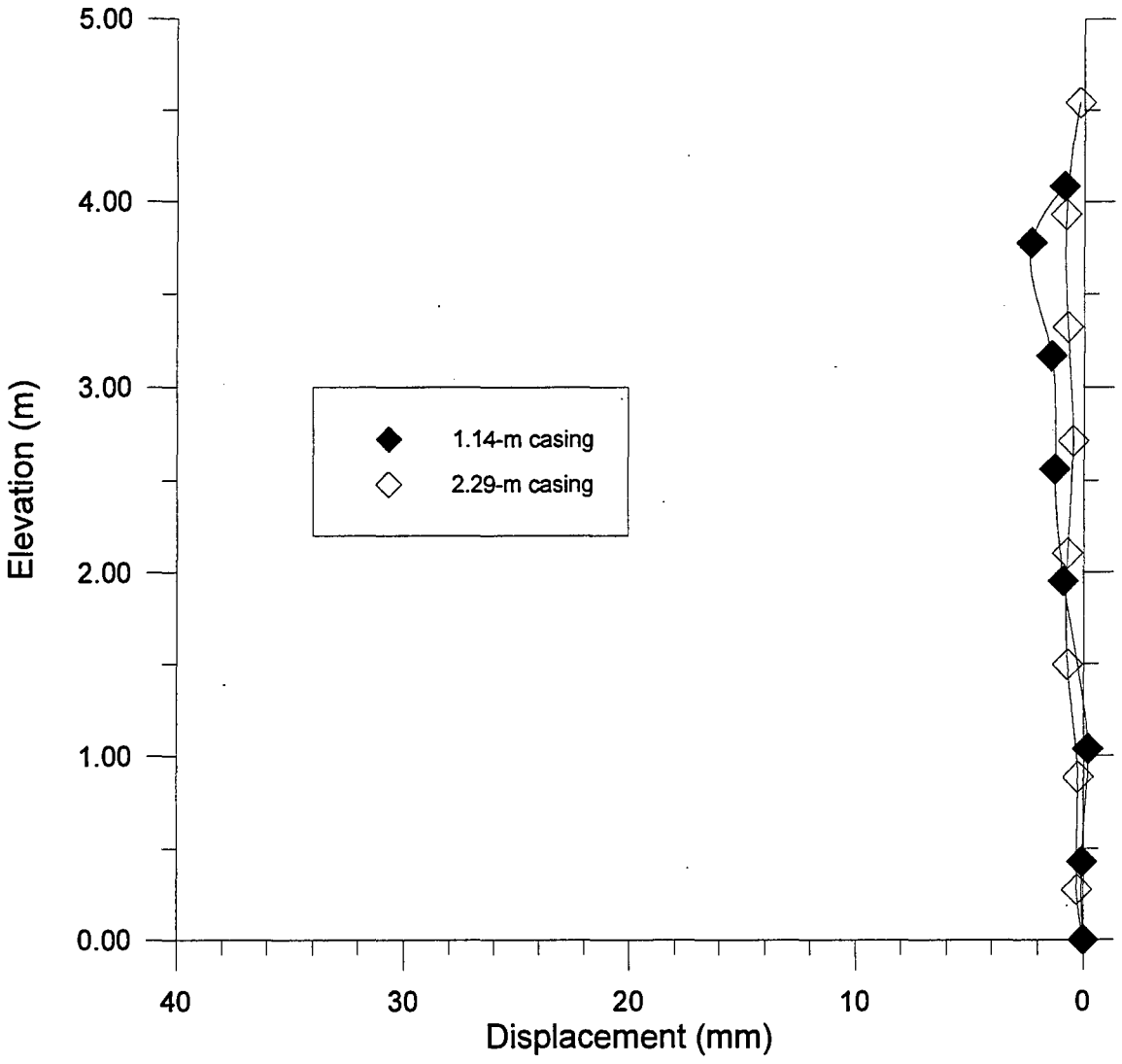

Figure 9.6 Horizontal deflection within backfill, granular fill, 1.14-m (3.7-ft) and 2.29-m (7.5-ft) casings (0.7 degrees rotation)

9.3.2 Tire Chips

The horizontal deformation of Pine State Recycling measured from the 1.14-m (3.7-ft) casing is shown on Figure 9.7. This shows that the tire chips start to move as the wall is rotated. At 0.8 degrees (0.01H), slightly more movement was noticed near the elevation of 3.0 m (9.8 ft), than at the previous two rotations. The wall was left at 0.8 degrees for two days to examine time-dependent behavior. However, no significant movement was observed, as shown on Figure 9.7. As the front wall was rotated to an angle of 2.2 degrees (0.04H) the greatest movement occurred above 3.0 m (9.8 ft), with a measured movement at 4 m (13.1 ft) of 32 mm (1.2 in.). This is significantly lower than the front wall movement at 4 m (13.1 ft) of 154 mm (6.1 in.). The horizontal deformation measured from the 2.29-m (7.5-ft) casing is shown on Figure 9.8. This shows that as front wall is rotated outward the greatest horizontal deformation, 17 mm (0.7 in.), occurred at elevation 2.5 m (8.2 ft). This bowing out corresponded with the forward movement measured from the 1.14-m (3.7-ft) casing above 3.0 m (9.8 ft). Comparison of the maximum deflections measured from each casing shows that the maximum deflection measured from the 2.29-m (7.5-ft) casing is approximately half that measured from the 1.14-m (3.7-ft) casing. Further examination of Figure 9.8 shows that the measured deformation for the second set of readings taken on 10/5/94 at 0.8 degrees is substantially larger at the elevations of 2.5 m (8.2 ft) and 3.0 m (9.8 ft) than those from readings taken before and after. Examination of the manually recorded dial readings, as discussed in Section 4.2.3.1, shows that for these two deformations the corresponding dial readings are

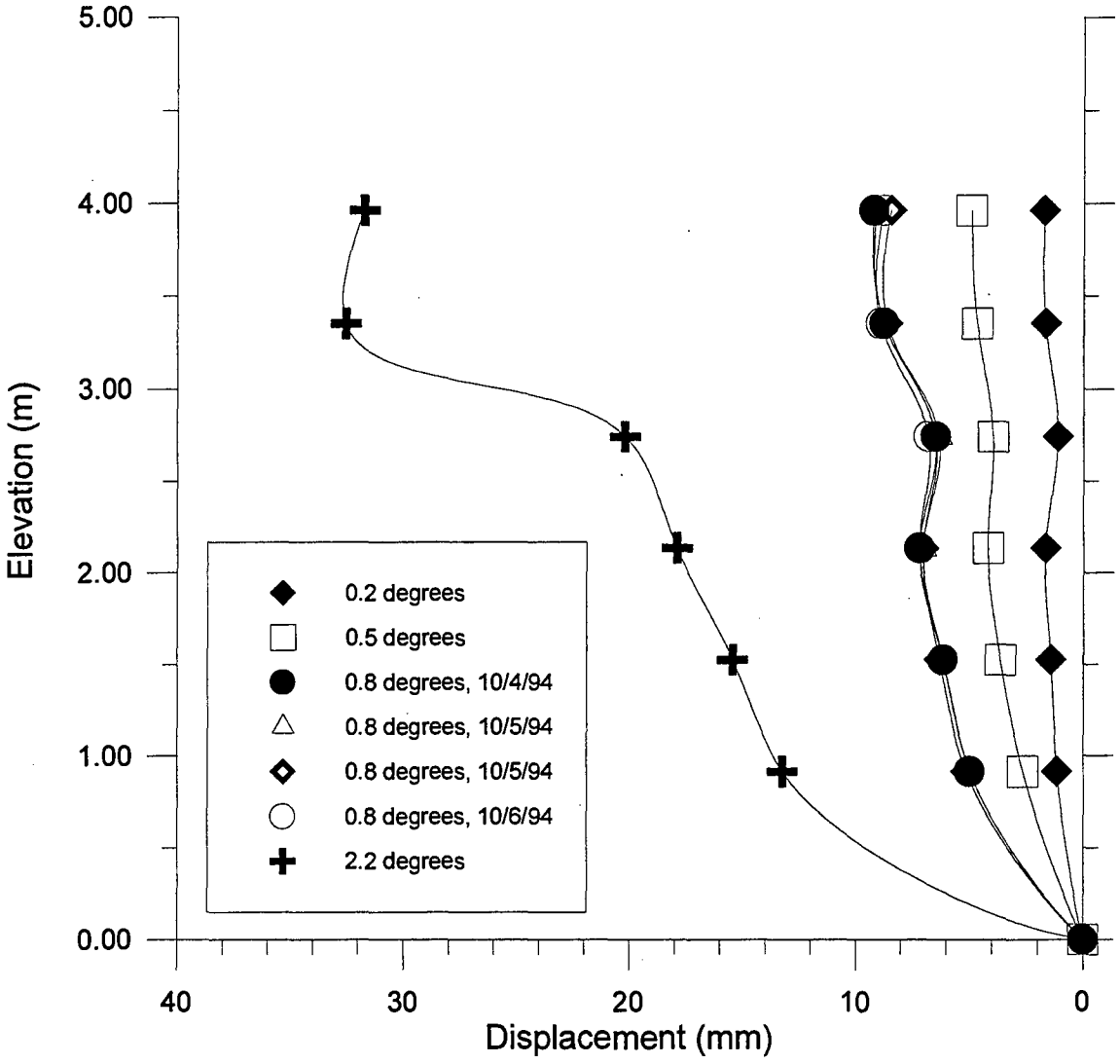

Figure 9.7 Horizontal deflection within backfill, Pine State Recycling, 1.14-m (3.7-ft) casing

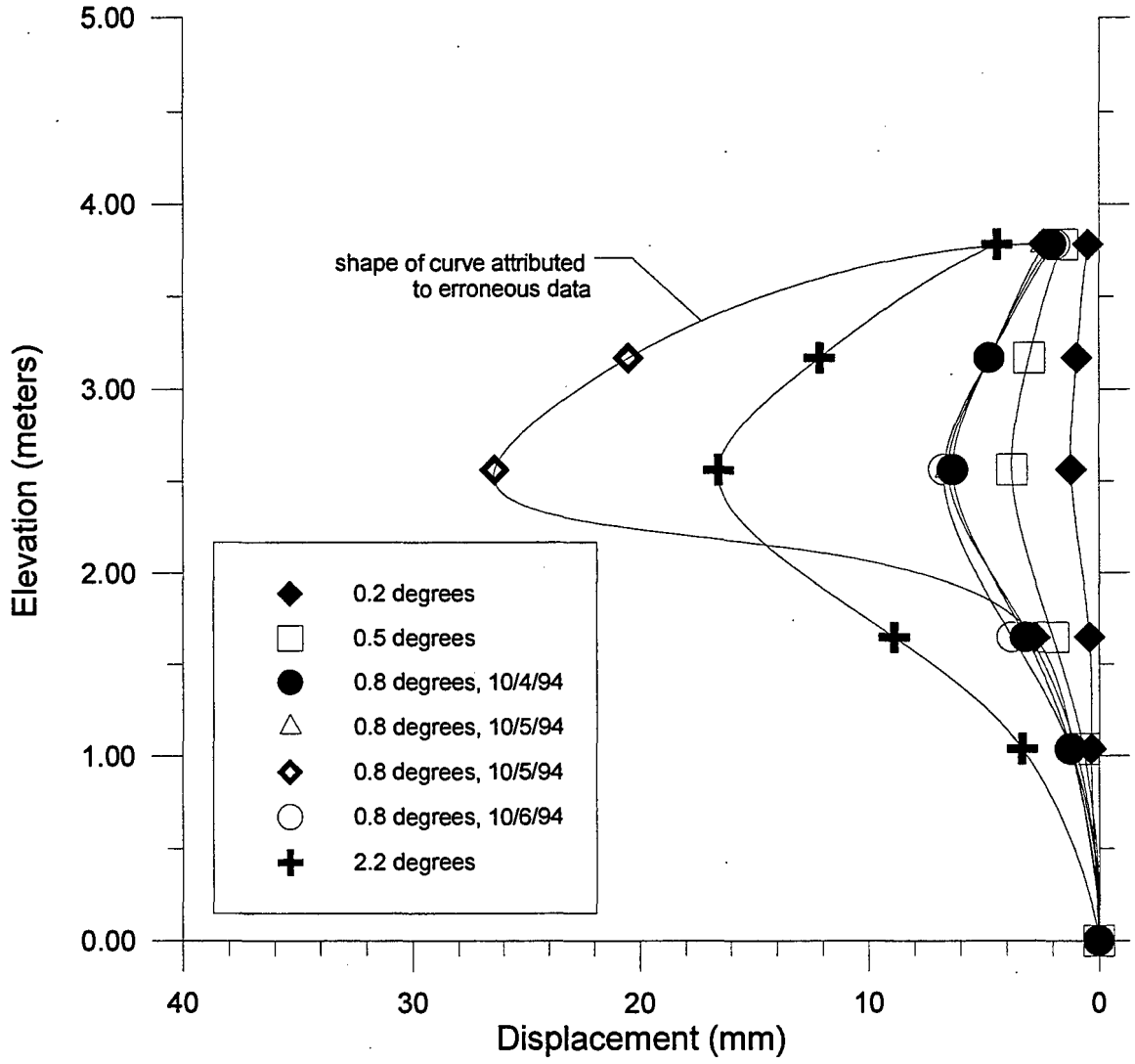

Figure 9.8 Horizontal deflection within backfill, Pine State Recycling, 2.29-m (7.5-ft) casing

100 increments greater than those recorded before or after at the same rotation. One possible explanation is that the dial readings were recorded incorrectly.

The horizontal movements within Palmer Shredding are shown on Figures 9.9 and 9.10 for the 1.14-m (3.7-ft) and 2.29-m (7.5-ft) casings, respectively. At 0.8 degrees (0.01H) readings were taken over a one day period, while at 1.7 degrees (0.03H) readings were taken immediately after rotation and two days after rotation. Figure 9.9, 1.14-m (3.7-ft) casing, shows that the tire chips start to move forward as the wall is rotated outward. At 0.8 degrees slightly greater movement is noticeable above the elevation of 2.75 m (9.0 ft). As the wall is rotated further to 1.7 degrees, the tire chips move significantly more from the mid-elevation to the top of the fill. However, the movement recorded by the 2.29-m (7.5-ft) casing for 1.7 degrees rotation, Figure 9.10, shows the that significant movement starts deeper in the fill, above 1.5 m (4.9 ft). The magnitude of the movement recorded from the 2.29-m (7.5-ft) casing near 1.5 m (4.9 ft) is half that recorded from the 1.14-m (3.7-ft) casing from the mid-elevation to the top. So when using this information to determine the location of the active wedge the larger movement detected by the 1.14-m (3.7-ft) casing is felt to be more significant.

The horizontal movements recorded by the 1.14-m (3.7-ft) and 2.29-m (7.5-ft) casings for F & B Enterprises are shown on Figure 9.11. This shows that after 0.7 degrees (0.01H) of rotation considerable movement was experienced within the fill. The magnitude at the top of the fill is 30 mm (1.2 in.) for the 1.14-m (3.7-ft) casing. This is 70% and 68% greater than the amount of horizontal movement experienced at the top for Pine State Recycling and Palmer Shredding, respectively, for the same amount of wall

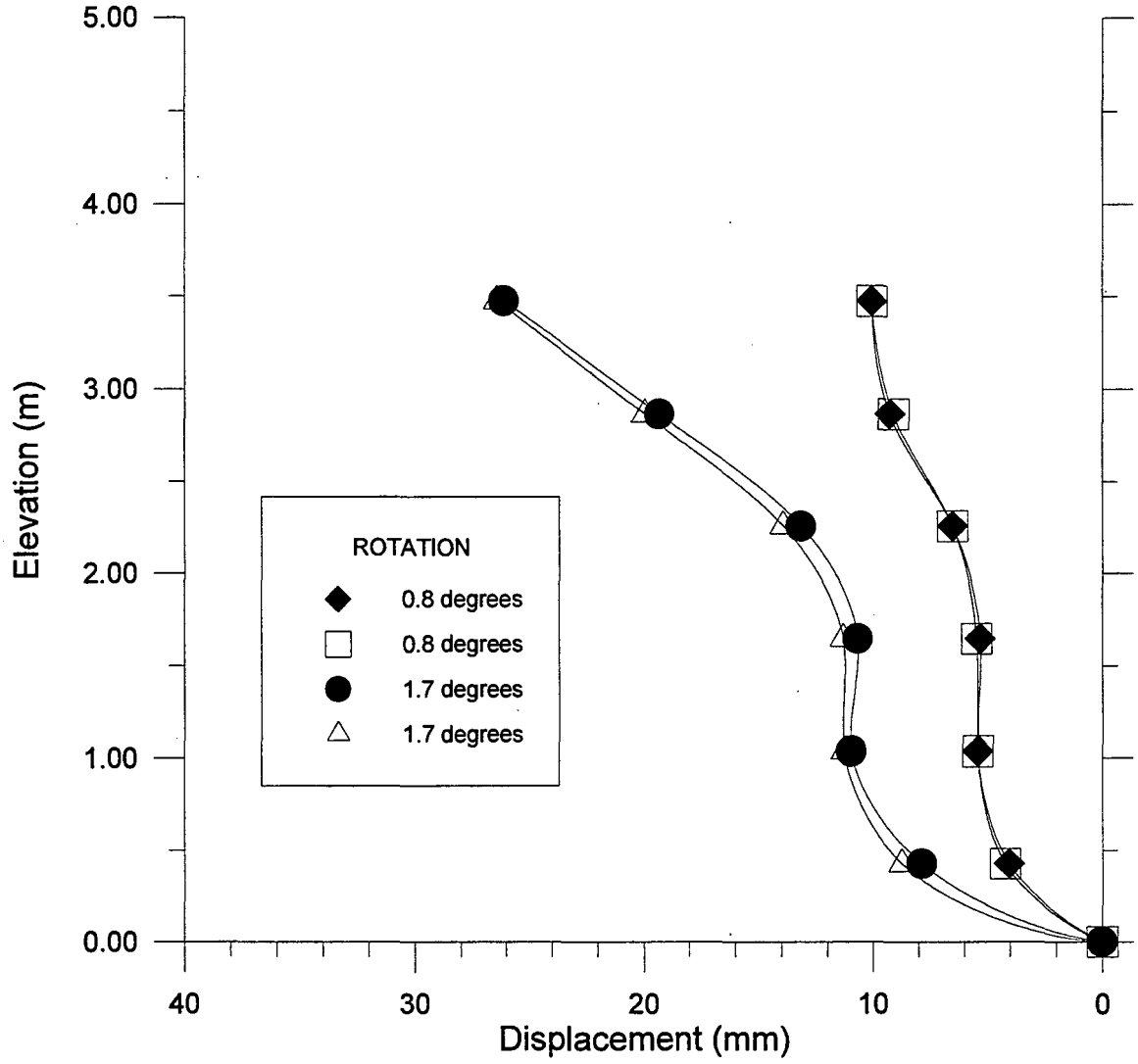

Figure 9.9 Horizontal deflection within backfill, Palmer Shredding, 1.14-m (3.7-ft) casing

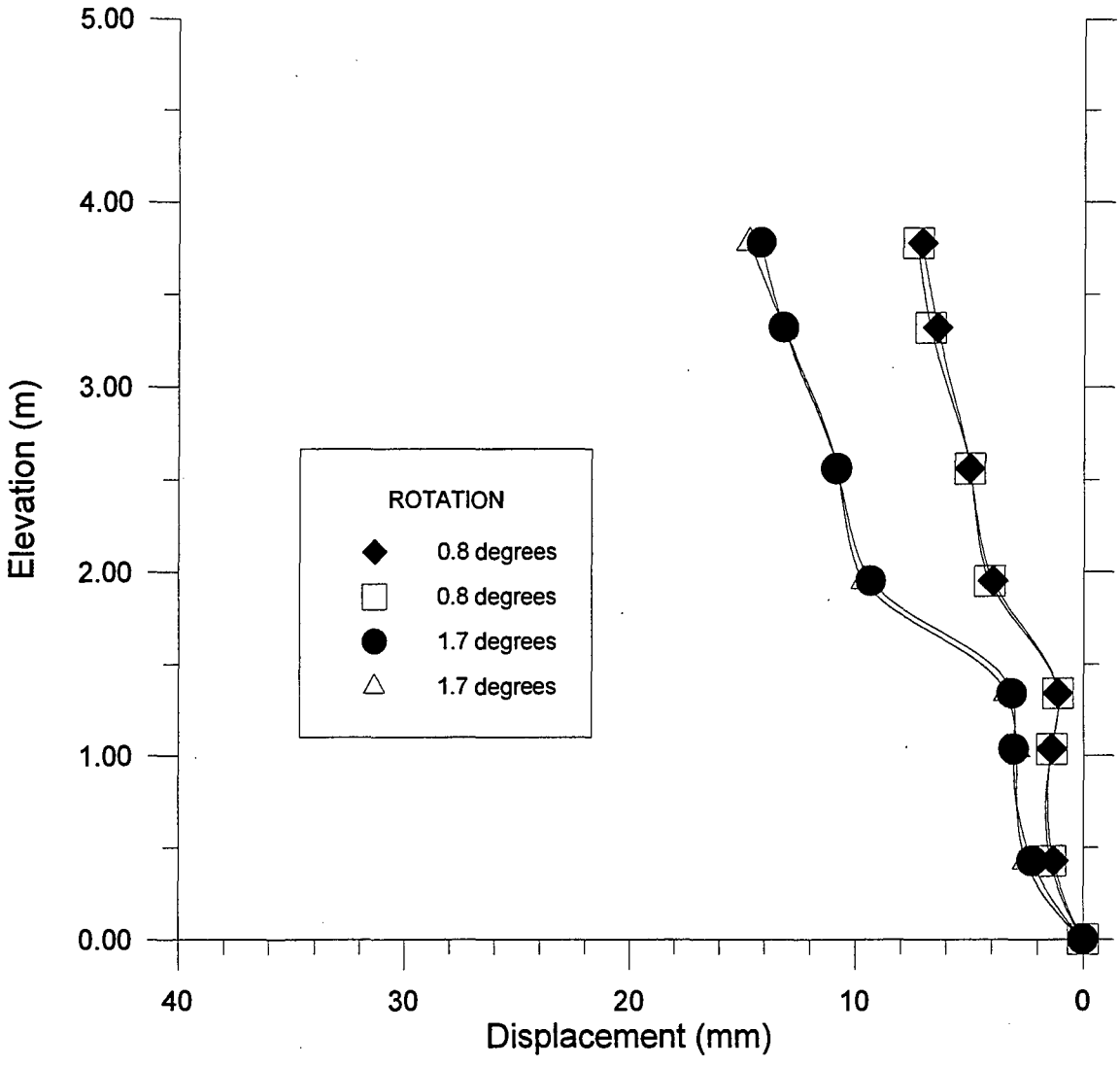

Figure 9.10 Horizontal deflection within backfill, Palmer Shredding, 2.29-m (7.5-ft) casing

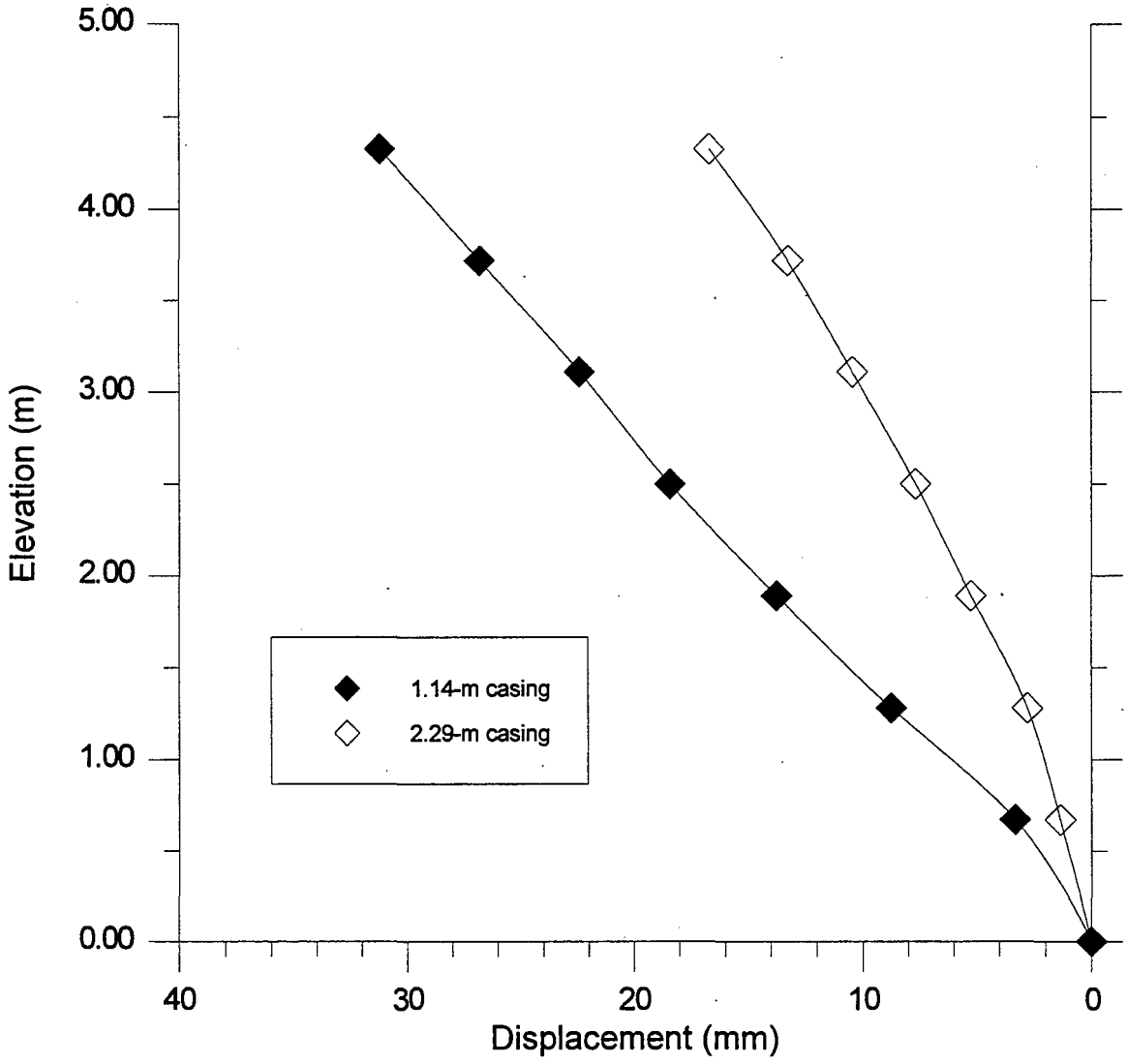

Figure 9.11 Horizontal deflection within backfill, F & B Enterprises, 1.14-m (3.7-ft) and 2.29-m (7.5-ft) casings (0.6 degrees rotation)

movement. One possible explanation for the greater amount of movement is the quantity of steel belts and the size of chips. Recall that Pine State Recycling and Palmer Shredding were 76-mm (3-in.) minus pieces, which were long and flat in shape with lots of steel belts, while F & B Enterprises was 25-mm (1-in.) minus chips, roughly equidimensional in shape with few steel belts. It is theorized that during placement and loading, tire chips from Pine State Recycling and Palmer Shredding became layered, with the flat surfaces lying against each other, as shown on Figure 6.10. This, along with interlocking between the tire chips and steel belts, made the Pine State Recycling and Palmer Shredding fills stiffer than the F & B Enterprises fill in the direction perpendicular to the layering.

9.4 ACTIVE WEDGE

The active wedge is the portion of fill that tends to move with a retaining wall as the wall moves outward away from the fill. To locate the active wedge it is necessary to find the boundary along which the fill has moved. From the information gathered in this research the location of the active wedge can be determined by three or four points. The first two points are where the fill comes into contact with the wall at the wall base and the fill surface. It is then necessary to find either one or two of the points that can isolate the plane along which the fill moved. The third point can be determined from the slope indicator readings, as indicated by a large change in horizontal movement between adjacent points. The fourth point can be determined from the settlement profile of the fill surface. A large change in the slope of the surface shows where the active wedge passes through the surface, as shown on Figure 9.12.

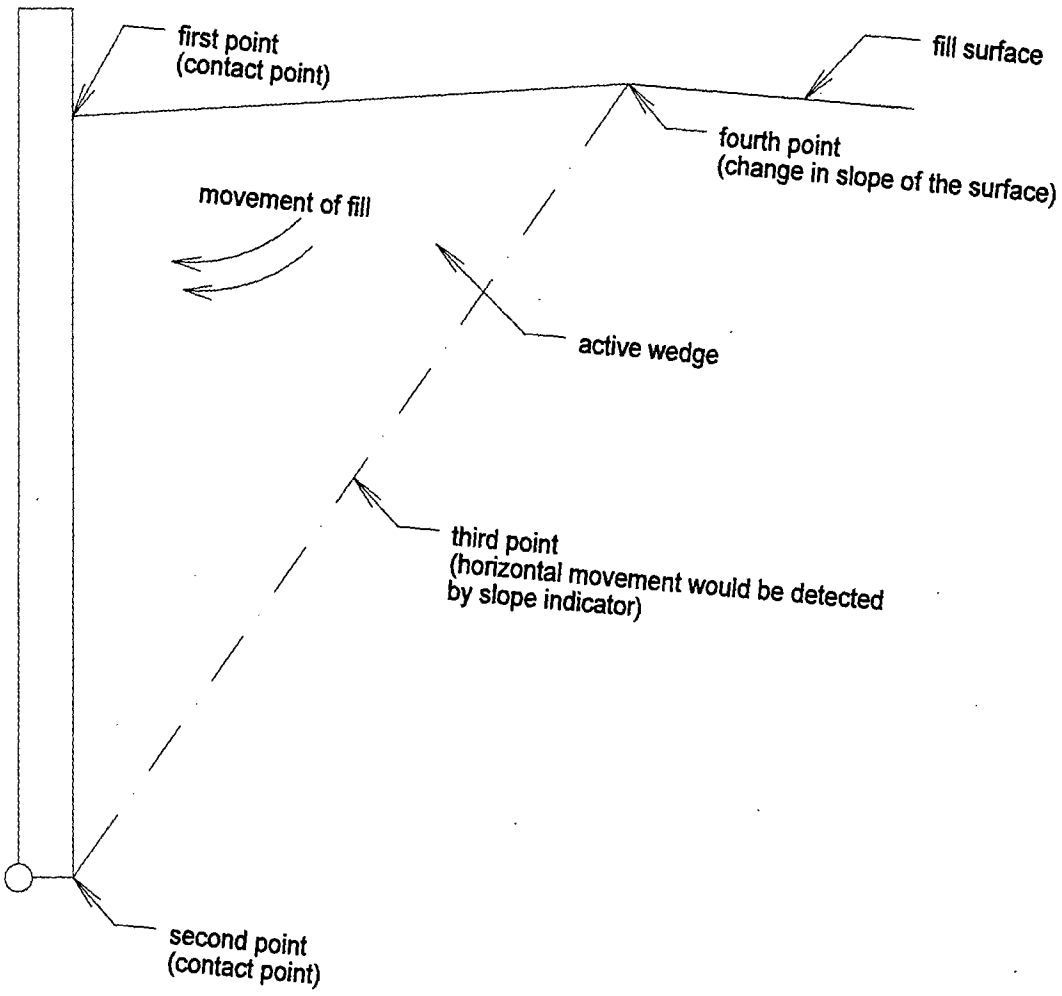

Figure 9.12 Points in locating active wedge

Settlement of the fill surface was measured using the settlement grid, as discussed in Section 4.2.2.2. The settlement grid was a system of 19 points used to measure settlement of the fill surface. Of the 19 points that make up the grid, seven of them followed the centerline of the facility, from front to back, as shown on Figure 4.6. The change in fill surface elevation caused by rotation of the font wall could then be determined by subtracting the fill elevation after rotation from the initial fill elevation. The settlement profile from front to back of the facility was determined for each test and plotted verses distance from the front wall face.

9.4.1 Granular Fill

The settlement profile for the granular fill after 0.7 degrees rotation is shown on Figure 9.13. This shows that there is a change in the slope of the surface somewhere between 1.52 m (5.0 ft) and 2.29 m (7.5 ft) from the front wall. However, no horizontal movement was recorded by either inclinometer casing, suggesting that the location of the active wedge was somewhere between the front wall and the 1.14-m (3.7-ft) casing. Examination of the backfill surface after removal of the surcharge blocks, as shown on Figure 9.14, revealed a 150-mm (6-in.) deep crack, approximately parallel to, and 0.76 m (2.5 ft) from the front wall. This indicates that the failure plane intersects the surface approximately 0.76 m (2.5 ft) from the front wall. With this information and knowing where the granular fill comes into contact with the front wall at the top and the bottom, the location of the active wedge was determined, as shown on Figure 9.15. This active wedge is much smaller than would be expected from classical earth pressure theory.

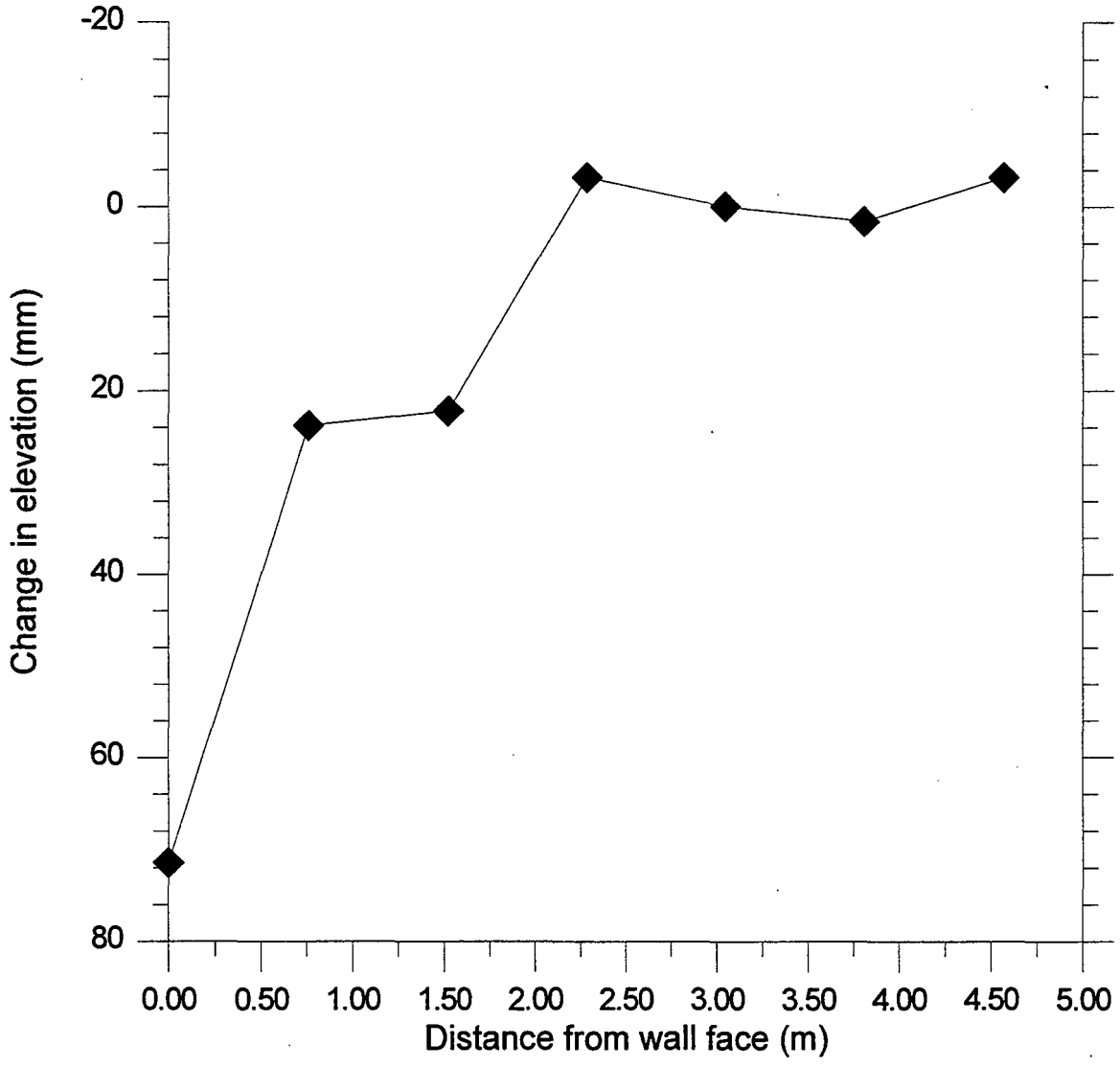

Figure 9.13 Settlement profile, granular fill (0.7 degrees rotation)

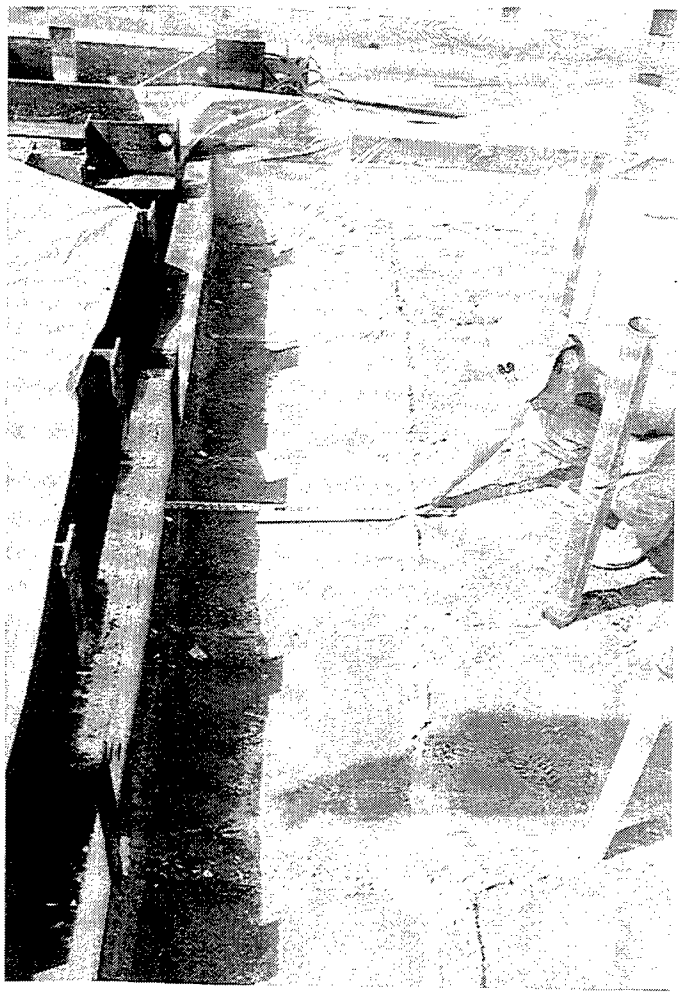

Figure 9.14 Granular backfill surface after removal of surcharge blocks

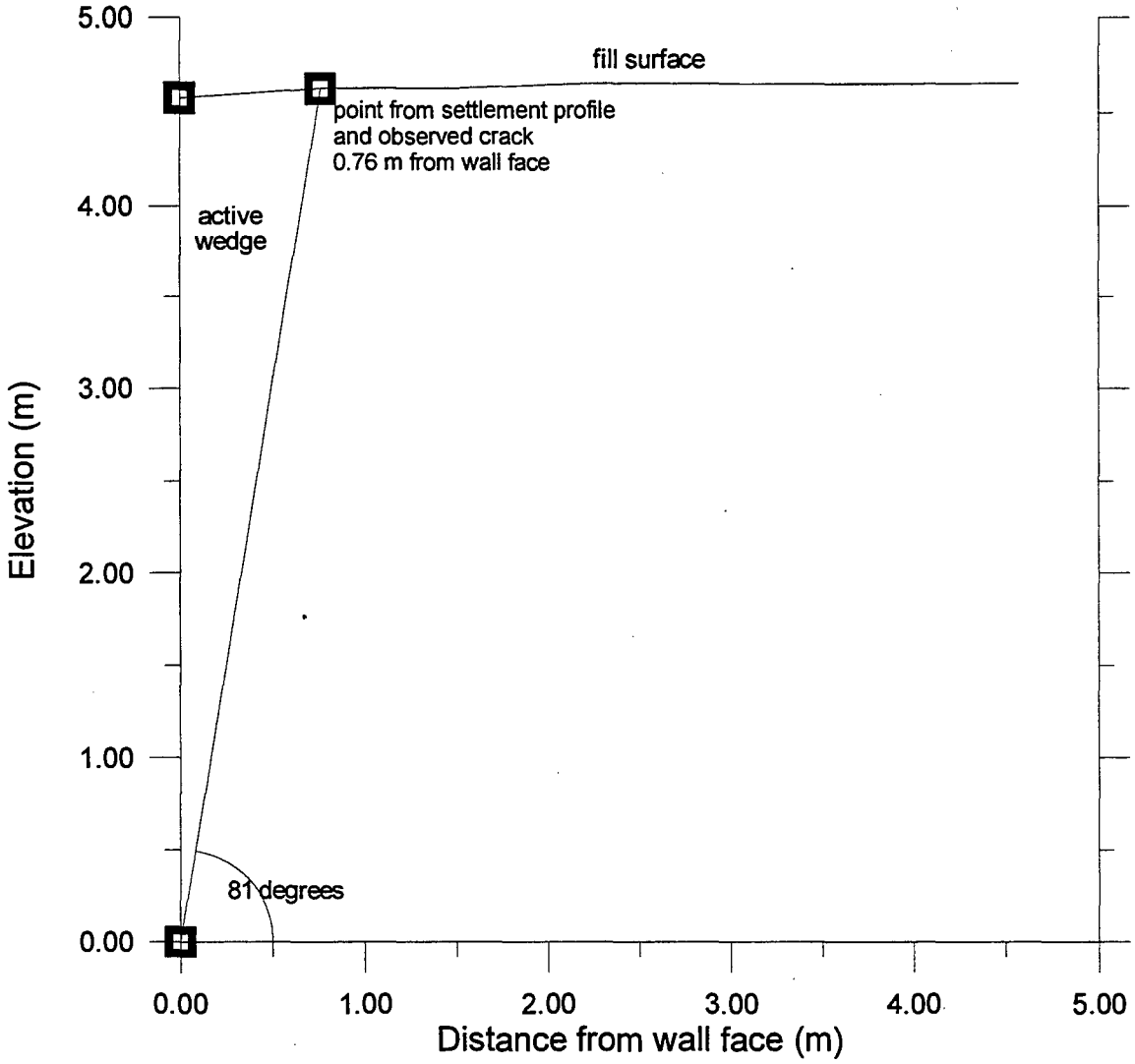

Figure 9.15 Location of active wedge, granular fill

Further examination of Figure 9.15 shows that the plane of movement is oriented 81° from the horizontal. Comparison can be made to the Rankine active state where the sliding surface is oriented at 45°+ϕ/2. Triaxial tests performed on the granular soil measured an angle of friction of 38°. Using this value, the angle with the horizontal would be 64°, which is significantly lower than what was measured in the field. One possible explanation for the small active wedge is the presence of apparent cohesion.

Apparent cohesion can occur in well graded soils and partially saturated conditions. This can be examined using Coulomb's theory of active earth pressure to analyze the active wedge. Figure 9.16 shows an analysis of the active wedge for the granular fill without apparent cohesion. The forces were calculated from the dimensions of the active wedge. The width of the sliding wedge was taken to be 1.47 m (4.82 ft), the center panel width. Figure 9.16 shows a free-body diagram of the active wedge, including the following forces: the weight of fill (W), the force due to the 35.9 kPa (750 psf) surcharge (L), the active earth force (P_A), and the friction force between the active wedge and the rest of the fill (F). The relevant angles are also shown, which include: the angle of wall fiction (δ), as discussed in Section 7.2.1; the angle of internal fiction (ϕ), determined from triaxial tests; the orientation of the active wedge with respect to the horizontal (θ); and the wall rotation (β), rounded to the nearest degree. Construction of the force polygon shows that under these conditions the active force (P_A) would be 100.8 kN (22.7 kips). However, the measured active force was 66.5 kN (14.9 kips). One possible reason for this discrepancy is the presence of apparent cohesion. Figure 9.17 shows an analysis including apparent cohesion (C_a), with the apparent cohesion shown adjacent to the

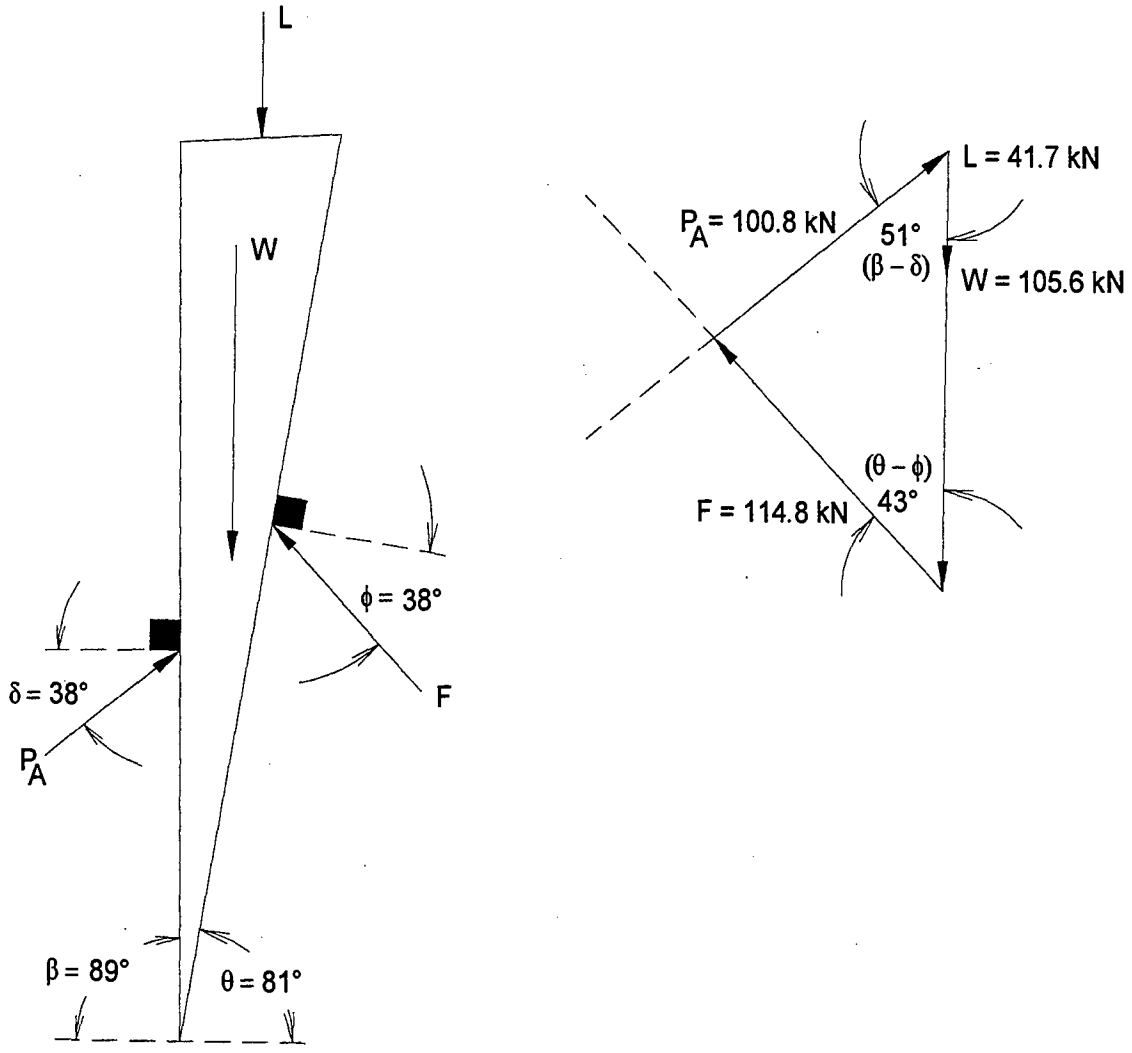

Figure 9.16 Coulomb analysis of active wedge without apparent cohesion

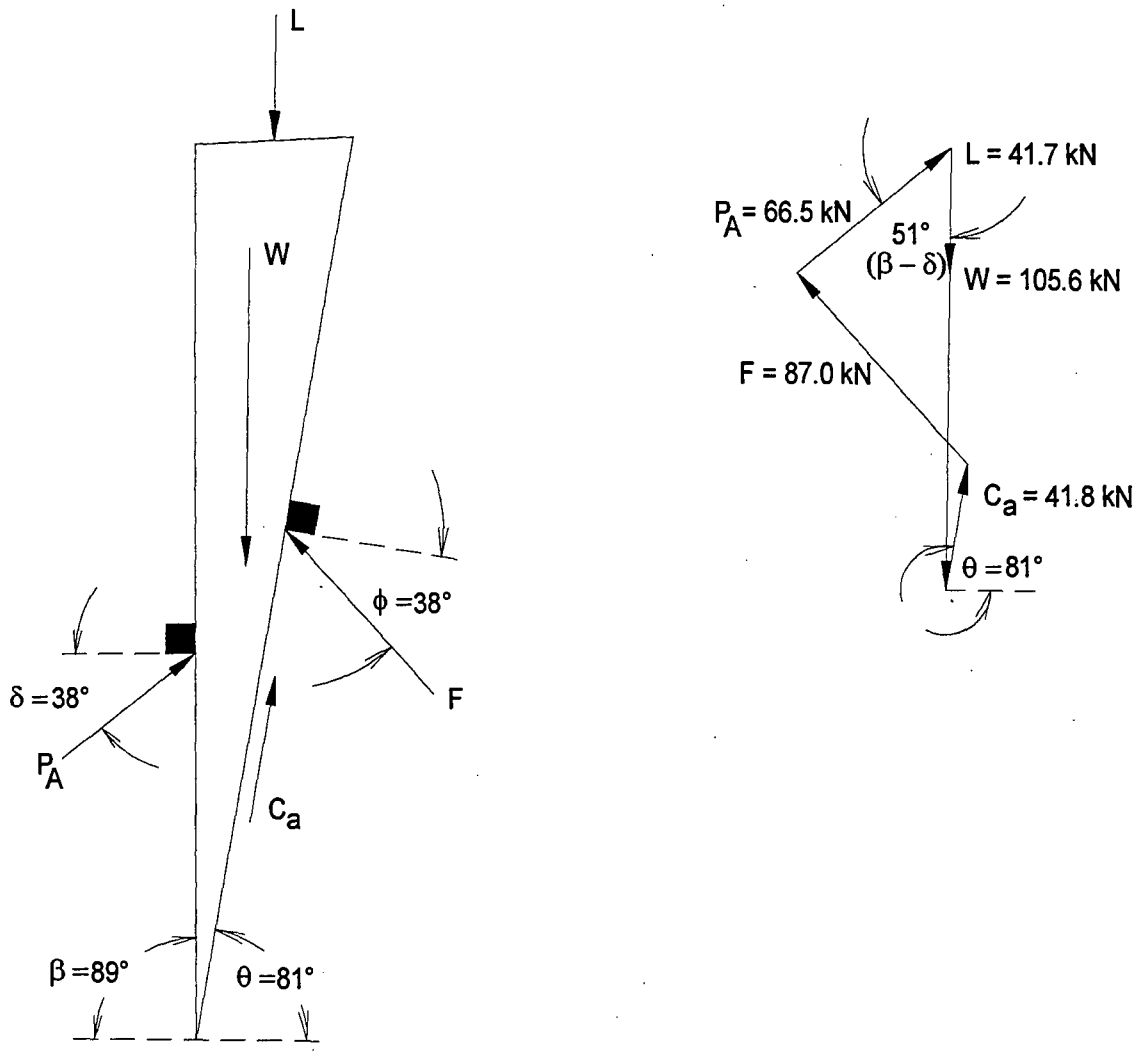

Figure 9.17 Coulomb analysis of active wedge with apparent cohesion

sliding surface of the free-body diagram for the active wedge. Construction of the force polygon using the measured active force, shows a force due to apparent cohesion of 41.8 kN (9.4 kips). In terms of stress, this is 6.1 kPa (128 psf). For comparison Lutenegger and Adams (1996) conducted in-place borehole shear tests in sand and measured an average apparent cohesion of 4.0 kPa (83.5 psf). Thus, the lower than expected horizontal stress measured for the granular fill discussed in Section 6.3.1.1, can be partially attributed to apparent cohesion. This was further supported by observing a free-standing vertical face of the granular fill when the back wall was removed upon completion of the test.

As discussed above, the failure plane was observed to pass through the fill surface at 0.76 m (2.5 ft) from the front wall. This distance also coincides with the joint between the first and second rows of surcharge blocks, as shown on Figure 4.6, suggesting that the joint between the surcharge blocks influenced the location of the failure plane.

9.4.2 Tire Chips

The settlement profile for Pine State Recycling after 2.2 degrees rotation is shown on Figure 9.18. This shows that there is an increase in the settlement between 0.76 m (2.5 ft) and 1.52 m (5.0 ft) from the front wall. This information along with that gathered from the 1.14-m (3.7-ft) casing will help locate the active wedge. The horizontal deformation within the tire chips as recorded from the 1.14-m (3.7-ft) casing after 2.2 degrees rotation is shown on Figure 9.19, with the deformation plotted with respect to distance from the front wall face. This figure shows that the plane on which the active wedge moves is

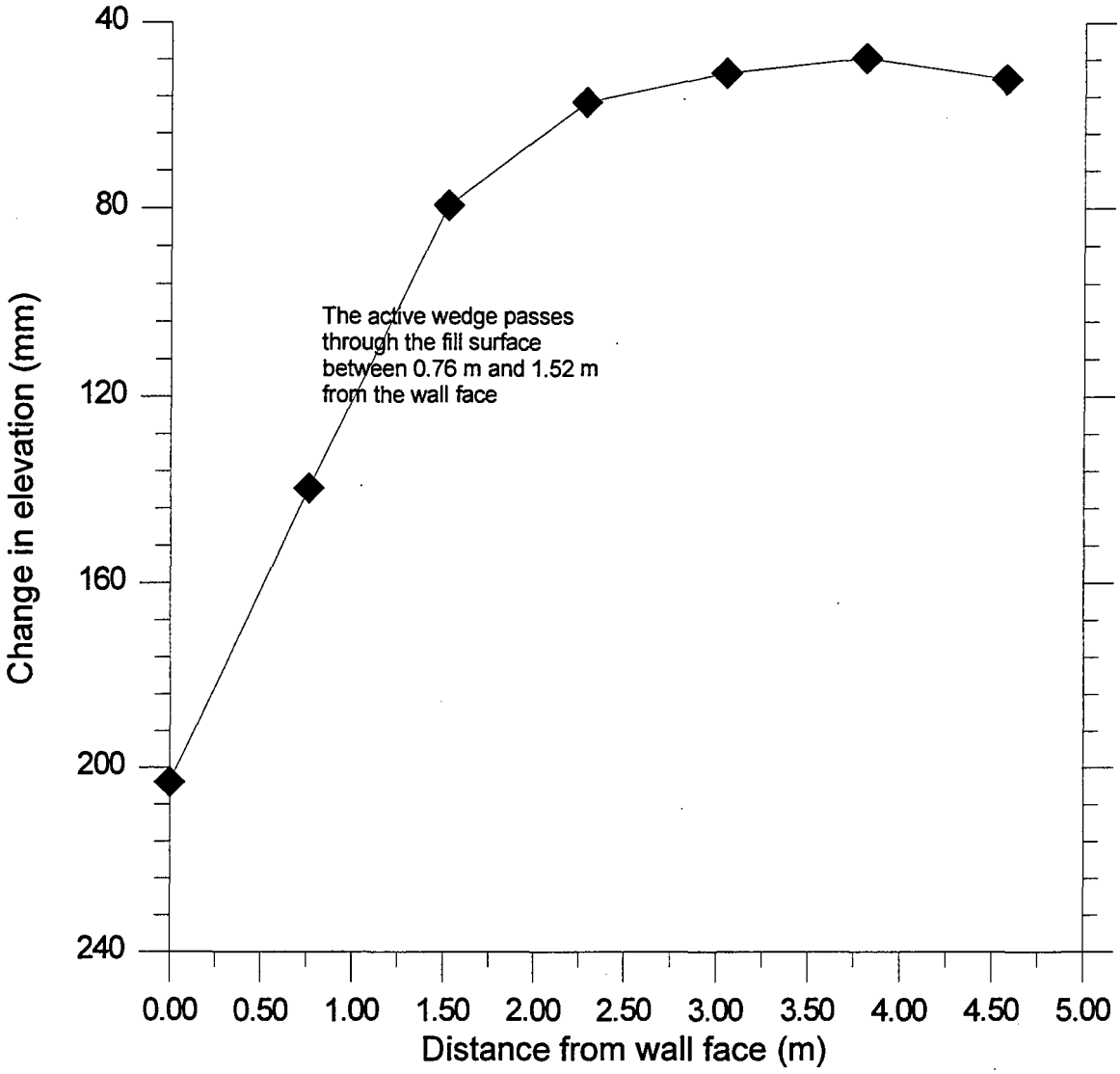

Figure 9.18 Settlement profile, Pine State Recycling (2.2 degrees rotation)

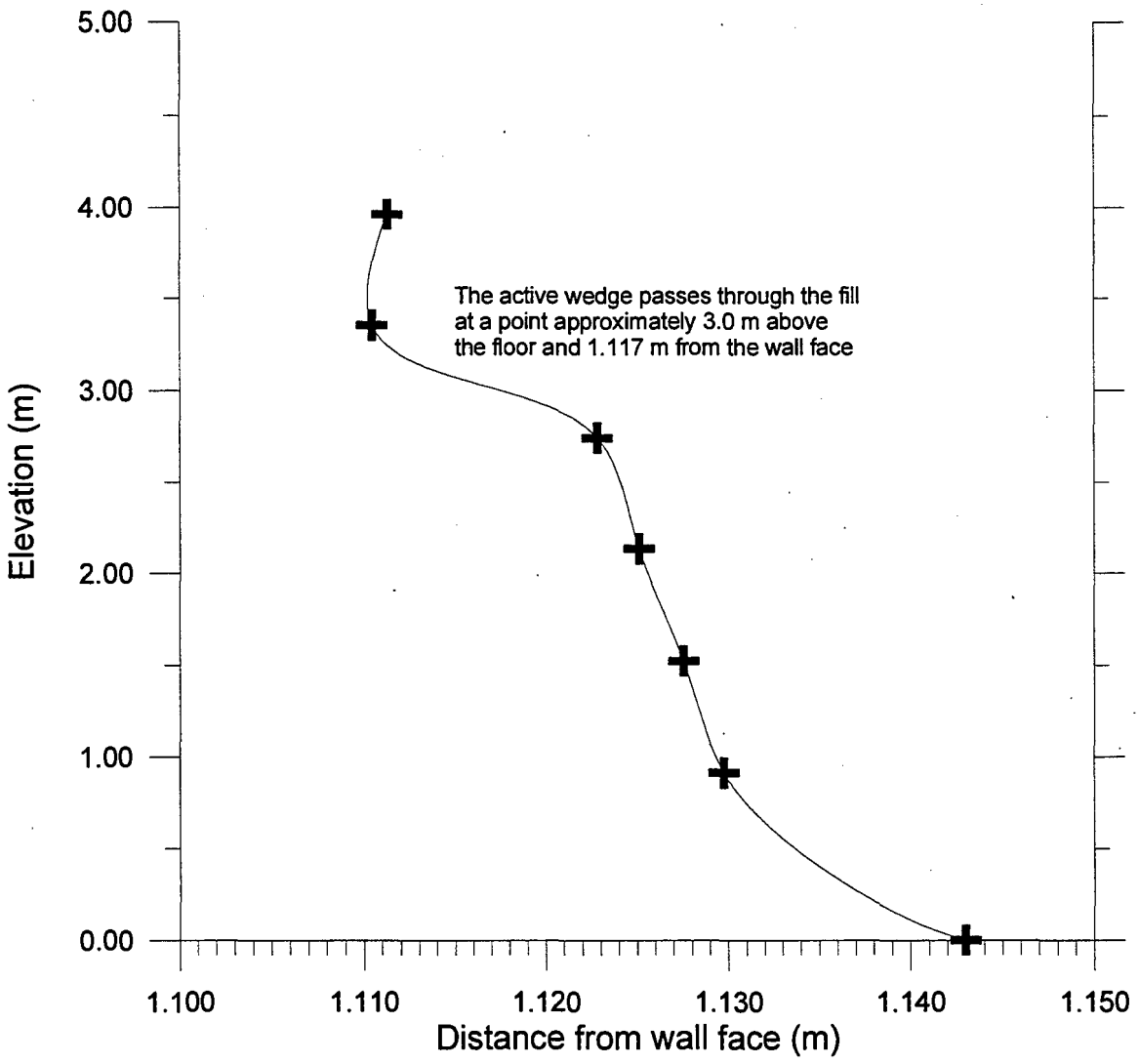

Figure 9.19 Horizontal deflection within backfill at maximum wall rotation, Pine State Recycling, 1.14-m (3.7-ft) casing (2.2 degrees rotation)

somewhere between the second and third points from the top. If the active wedge is assumed to pass somewhere between these two points at 1.117 m (3.67 ft) from the front wall and 3.0 m (9.8 ft) above the facility floor, an approximate location of the active wedge can be determined, as shown on Figure 9.20. Figure 9.20 shows that the plane of movement is oriented 70° with respect to the horizontal. This θ is smaller than that measured for the granular fill by 11 degrees.

Similarly, the location of active wedge for Palmer Shredding can be determined from the settlement profile and the horizontal movements within the fill after 1.7 degrees of rotation. The settlement profile is shown on Figure 9.21. This shows that the active wedge comes into contact with the fill surface between 2.29 m (7.5 ft) and 3.05 m (10.0 ft) from the front wall. The horizontal movement within the tire chips recorded from the 1.14-m (3.7-ft) casing plotted in respect to distance from the front wall is shown on Figure 9.22. This figure shows that the active wedge passes through the fill at approximately 2.5 m (8.2 ft) above the facility floor and 1.129 m (3.70 ft) from the front wall face. This results in the estimated active wedge location shown on Figure 9.23, with the active wedge oriented 61° with respect to the horizontal. This θ is smaller than that measured for the granular fill by 20 degrees.

Comparison of the active wedges for Pine State Recycling and Palmer Shredding, Figures 9.20 and 9.23, respectively, shows that the active wedge for Pine State Recycling is larger, with the orientation to the horizontal being 9 degrees greater.

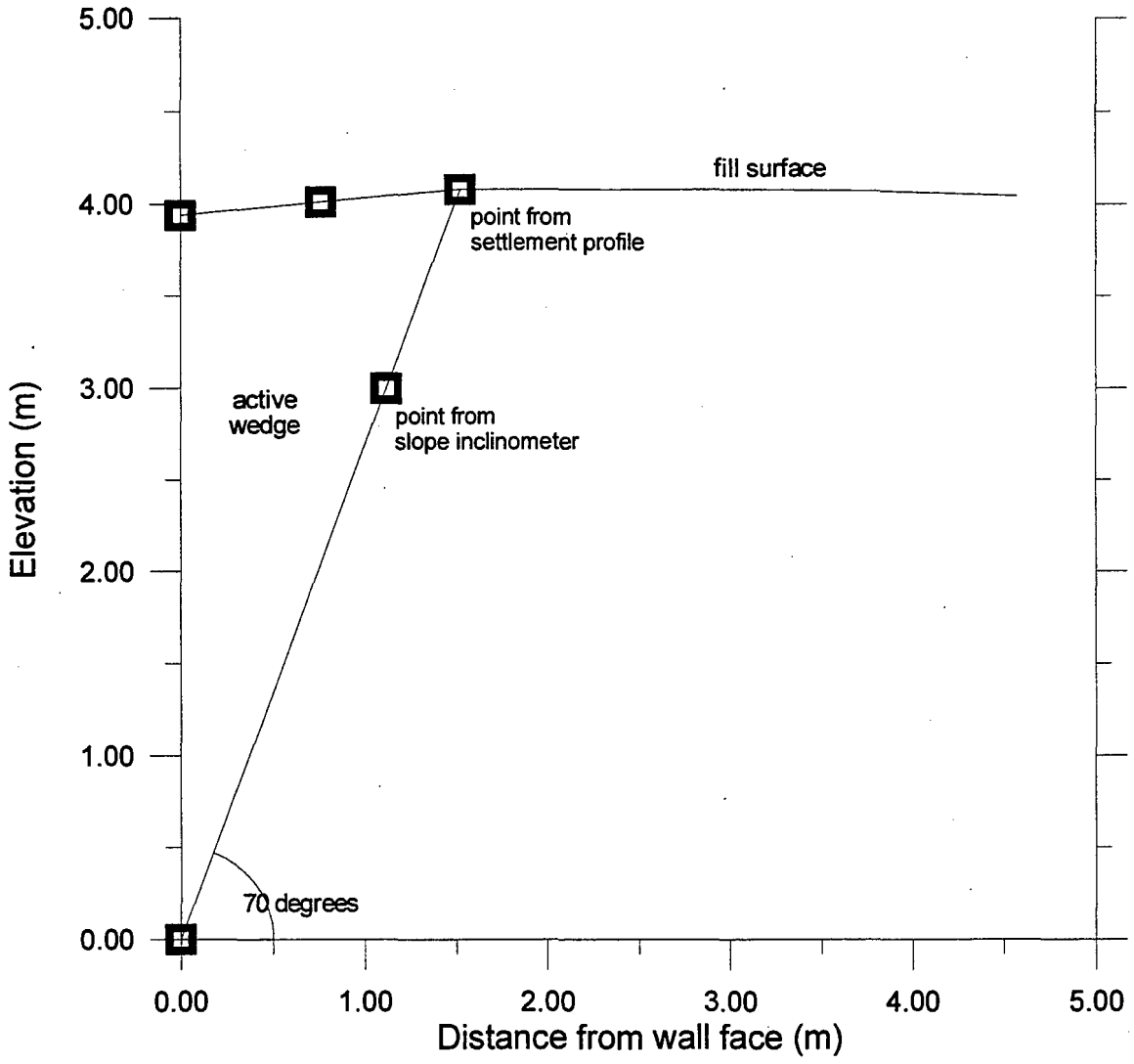

Figure 9.20 Location of active wedge, Pine State Recycling

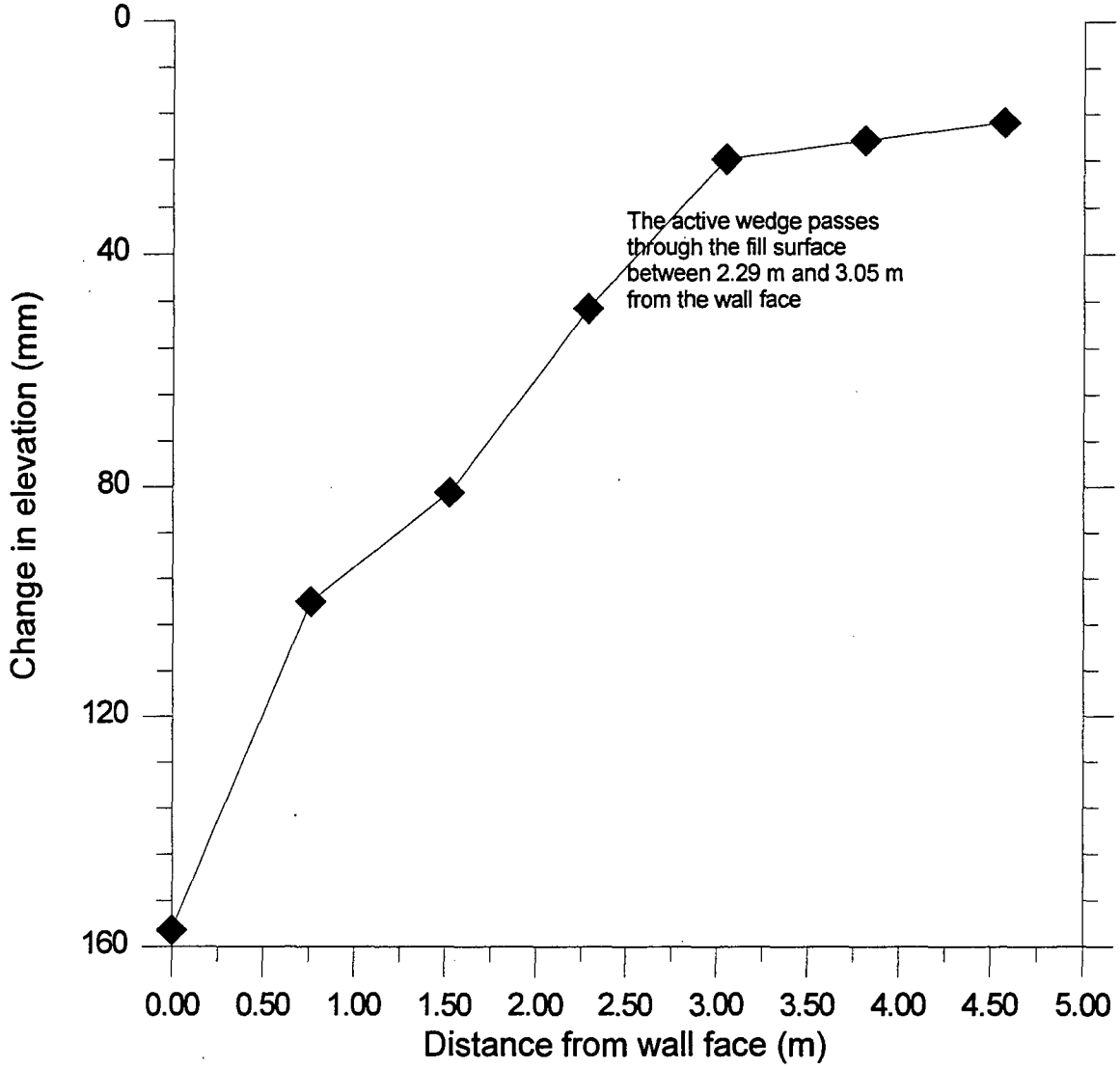

Figure 9.21 Settlement profile, Palmer Shredding (1.7 degrees rotation)

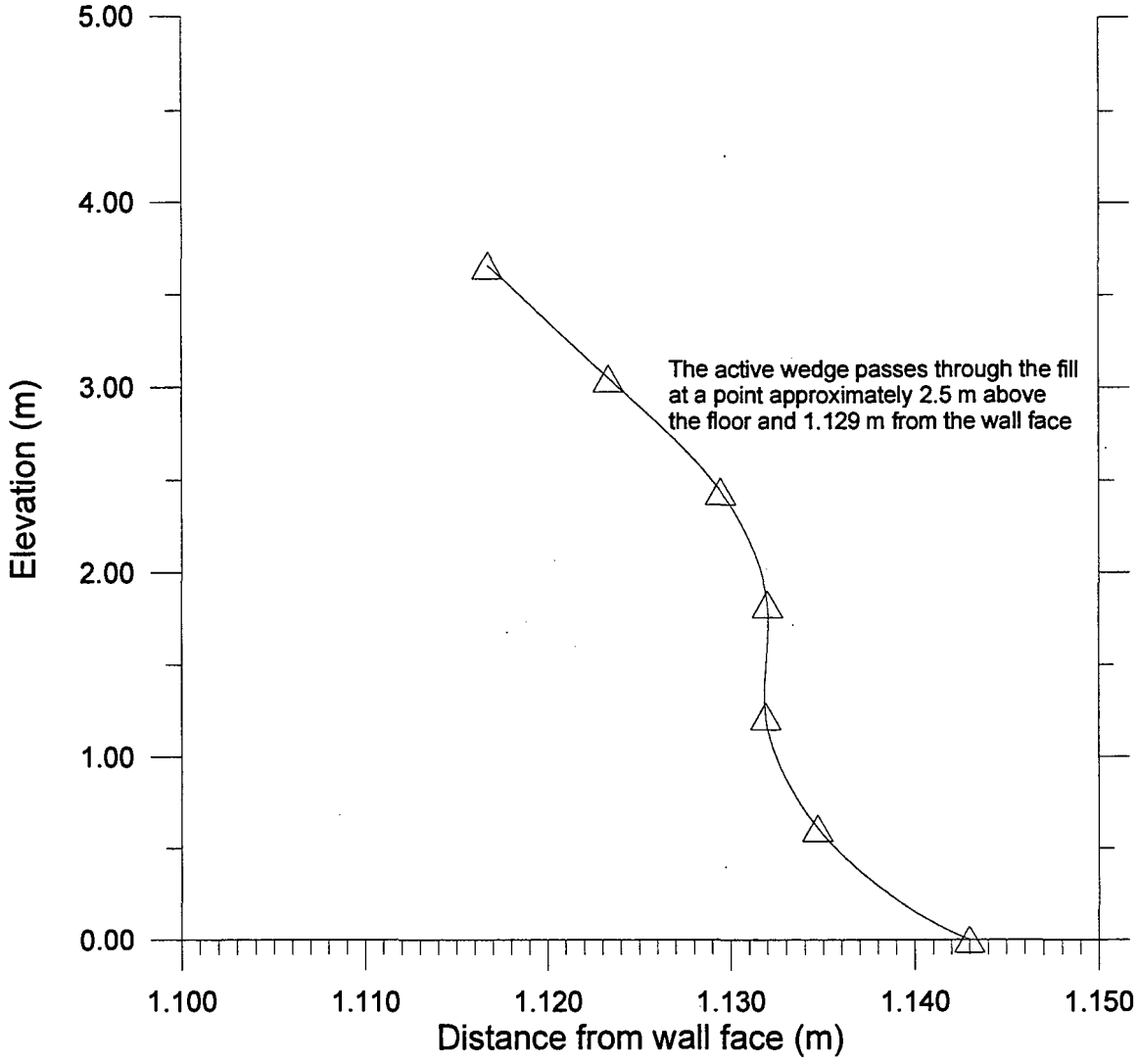

Figure 9.22 Horizontal movement within backfill at maximum wall rotation, Palmer Shredding, 1.14-m (3.7-ft) casing (1.7 degrees rotation)

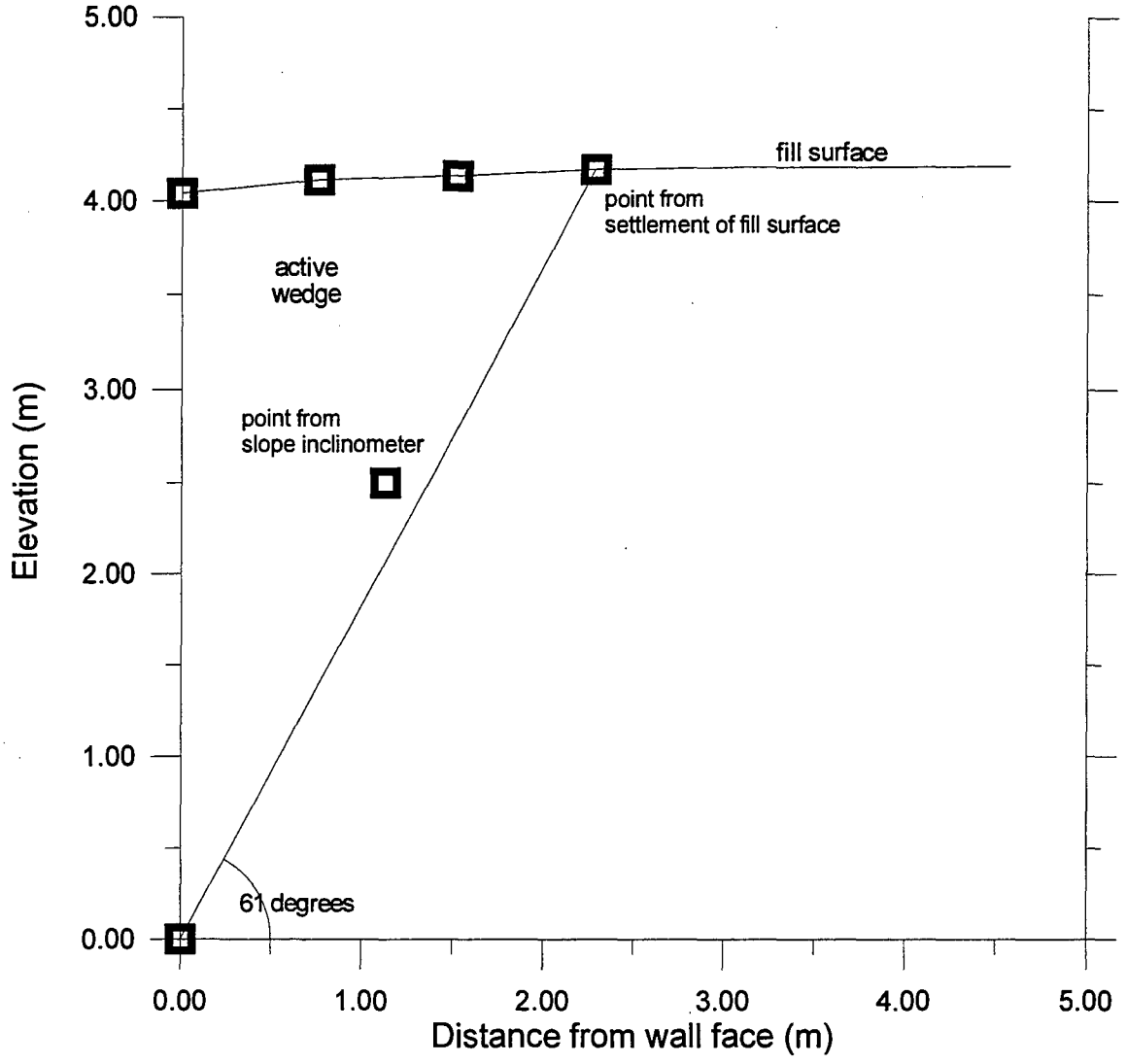

Figure 9.23 Location of active wedge, Palmer Shredding

The settlement profile for F & B Enterprises after 0.7 degrees rotation is shown on Figure 9.24. This shows that no large continuous change in elevation occurred. This, along with the horizontal deformation within the tire chips (Figure 9.11), shows that no large movements occurred between subsequent points within the fill; suggesting that more rotation of the front wall was necessary for formation of the active wedge or that this type of tire chip does not develop a distinct zone of movement.

9.5 SUMMARY

The deflection of the front wall was measured during the at-rest conditions to determine if the amount of wall movement was small enough to maintain at-rest conditions. The deflection was determined by measuring the change in distance between reference beams connected to the concrete side walls and points on the front wall panels. Dial calipers were used to measure the deflection of the front wall. The deflection was monitored at three elevations in reference to the facility floor.

Examination of the front wall deflections revealed that the maximum movement experienced by each backfill type was approximately 0.001H. This amount of movement could have lowered at-rest pressures for the granular fill. It is unlikely that the movements were sufficient to achieve active conditions, as the pressures were reduced when the wall was rotated outward, as discussed in Section 6.4.1. For the tire chips, the amount of movement needed to achieve active conditions is much greater than for granular material, as discussed in Section 6.4.2. Thus, this amount of movement probably did not significantly impact the at-rest pressures.

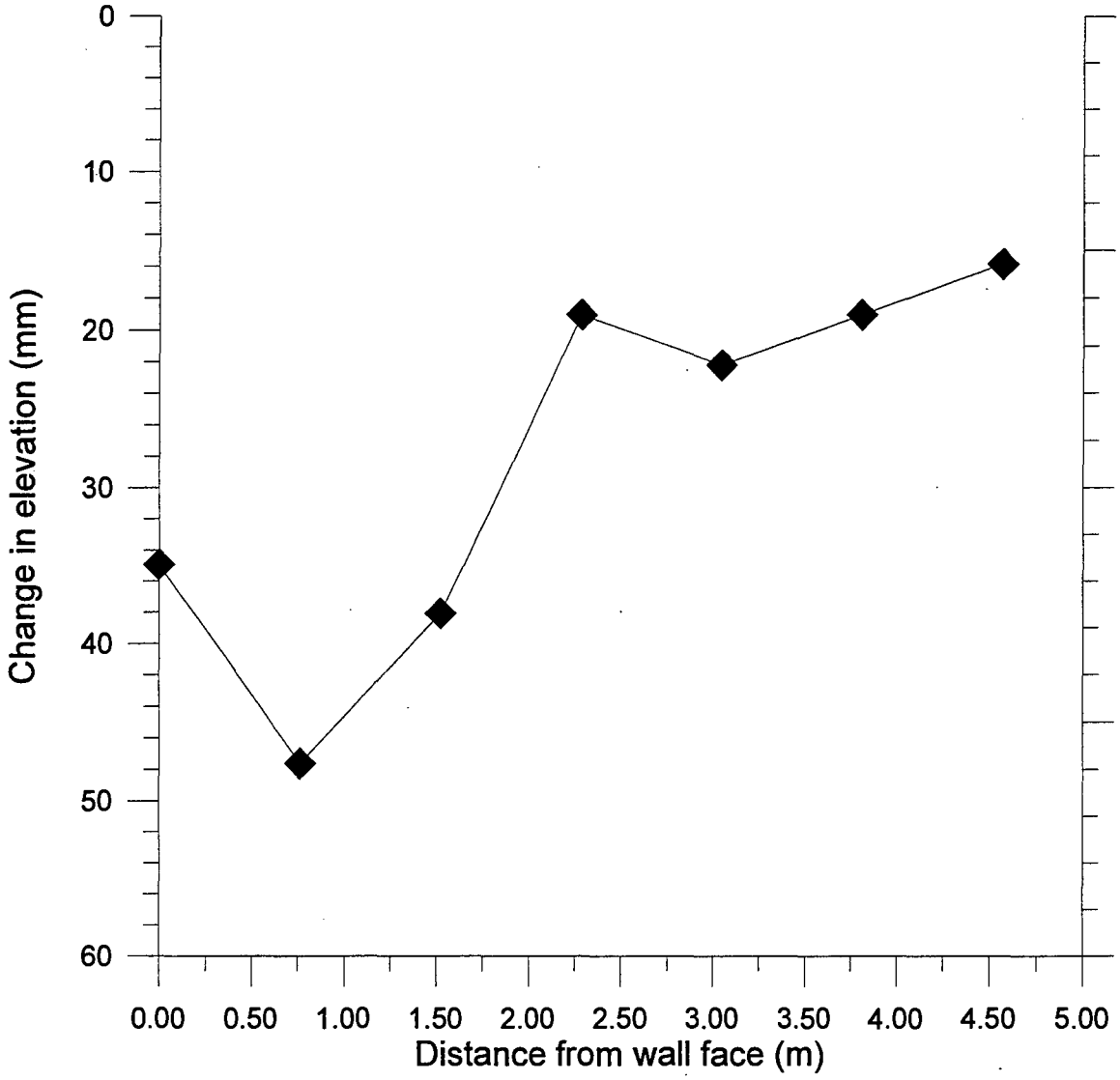

Figure 9.24 Settlement profile, F & B Enterprises (0.7 degrees rotation)

The time-dependent behavior of the front wall was examined over two days with Palmer Shredding at the 23.9 kPa (500 psf) surcharge. No time-dependent deflection was measured.

The horizontal movements within each fill was measured as the front wall was rotated outward away from the fill. The horizontal movement of the fill was determined from readings taken by an inclinometer at distances of 1.14 m (3.7 ft) and 2.29 m (7.5 ft) from the front wall. No significant movement was measured for the granular fill. Examination of the movement for the tire chips showed that for the same amount of wall rotation Pine State Recycling and Palmer Shredding moved less than F & B Enterprises. This may have been a result of the size of the tire chips and the amount of steel belts. Time-dependent movement was examined for Pine State Recycling over two days. No significant movement was measured.

The settlement profile was determined for each fill at the maximum rotation by finding the settlement at the grid points down the centerline of the facility. The horizontal movements within the fill along with the settlement profile were used to determine the approximate location of the active wedge. The active wedge was found for the granular fill, Pine State Recycling, and Palmer Shredding. However, sufficient front wall rotation was not attained to form the active wedge for F & B Enterprises, alternatively, this type of chip may not develop a distinct zone of movement.

The size of the active wedge for the granular fill was significantly smaller than what would be expected from classical earth pressure theory. This may be a result of apparent

cohesion. The active wedge for Pine State Recycling was oriented at 70° with respect to the horizontal, while Palmer Shredding was oriented at 61°. The orientation of the active wedge with respect to the horizontal was 9 degrees greater for Pine State Recycling than for Palmer Shredding.

(BLANK)

CHAPTER 10. SUMMARY, CONCLUSIONS, AND RECOMMENDATIONS

10.1 SUMMARY

An estimated 253 million tires are discarded every year in the United States, with an additional 850 million scrap tires stockpiled throughout the country. A large concentration of stockpiled scrap tires is in the New England states. In recent years, reuse of recovered tires has increased, however, disposal of scrap tires is still a problem. Whole tires occupy a significant amount of landfill space. Open scrap tire dumps present fire and health hazards, in addition to being unsightly. Using waste tires in civil engineering applications has become one of the alternatives to disposal. Using tire chips as retaining wall backfill, would provide a backfill that is coarse grained, free draining, lightweight, and a good insulator.

This study was Phase II of a previous laboratory study titled: "Tire Chips As Lightweight Backfill For Retaining Walls" (Humphrey, et al., 1992). The primary purpose of this second phase was to determine design criteria for using tire chips as backfill for retaining walls. A literature review focused on two previous studies using tire chips as backfill for retaining walls.

The design criteria was determined by testing a granular fill as a control and tire chips from three New England suppliers, for at both at-rest and active conditions. Testing was performed in a full scale retaining wall test facility. The tire chip suppliers were as

follows: Pine State Recycling, Palmer Shredding, and F & B Enterprises. For the at-rest condition, measurements were taken at the following surcharges: no surcharge, 12.0 kPa (250 psf), 23.9 kPa (500 psf), and 35.9 kPa (750 psf). The effects of unloading and reloading were investigated by removing and reapplying the maximum surcharge a minimum of two times. The measurements for the active state were taken at the 35.9 kPa (750 psf) surcharge and at different amounts of outward rotation of the wall.

The test facility can accommodate approximately 100 m^3 (130 yd^3) of backfill. It is 4.88 m (16 ft) high and 4.47 m (14.7 ft) by 4.57 m (15 ft) in plan. A surcharge of up to 35.9 kPa (750 psf) can the applied to the backfill. The facility consists of four walls and a reinforced concrete foundation. The two side walls are reinforced concrete. The front wall consists of three panels, with the center panel containing the load cells and pressure cells necessary to measure the forces and pressures. Each of the three panels are hinged at their base to allow for the outward rotation necessary to produce active conditions. The back wall is removable, which allowed the backfill to be removed after the completion of a test. The facility is equipped with an overhead crane, attached to the top of the side walls, to assist in facility construction and to hoist backfill and surcharge into the facility. Concrete blocks are used to apply the surcharge.

The instrumentation included load cells and pressure cells to measure the horizontal and vertical forces acting on the center panel of the front wall and horizontal stress produced by the backfill. Settlement plates embedded in the fill and a settlement grid located on the surface of the fill were used to measure the vertical settlement of the tire

chips. Inclinometers were installed to measure the horizontal displacement within the backfill.

The granular fill was a clean mixture of gravel and sand with no particles over 76 mm (3 in.), and between 2% and 4% passing the #200 sieve. Results from laboratory maximum dry density and field density tests taken during fill placement showed that the percent compaction was between 91% and 98%.

The properties of the tire chips from the three suppliers were determined. F & B Enterprises tire chips contained significantly fewer steel belts than those from Pine State Recycling and Palmer Shredding. In addition, tire chips from F & B Enterprises were the finest with 88% to 100% passing the 38.1-mm (1-1/2-in.) sieve. The gradation of Pine State Recycling and Palmer Shredding tire chips were similar with 25% to 40% passing the 38.1-mm (1-1/2-in.) sieve for Pine State Recycling, and 35% passing the 38.1-mm (1-1/2-in.) sieve for Palmer Shredding. The average field density at the time of placement for Pine State Recycling was 0.71 Mg/m^3 (44.3 pcf), 0.69 Mg/m^3 (43.1 pcf) for Palmer Shredding, and 0.71 Mg/m^3 (44.3 pcf) for F & B Enterprises.

The horizontal earth pressure was examined using results from the load cells and pressure cells. The at-rest and active horizontal stress distributions for the granular fill were trapezoidal in shape, with the value at the base of the fill being lower than at the top of the fill. For the at-rest condition with no surcharge, the horizontal stress at the top of the fill was 28% greater than the value at the bottom. For the other surcharges the horizontal stress at the top of the fill was larger than the bottom by 54% to 61%.

Similarly, for the active state, the value at the top of the horizontal stress distribution was twice that of the bottom. This deviates considerably from the distribution expected from classical earth pressure theory, namely, horizontal stress increasing linearly with depth. In addition, the magnitude of the horizontal stress was considerably lower than that expected for this backfill material. This may have been caused by apparent cohesion.

The at-rest horizontal stress during initial loading increases as the surcharge increases for each of the tire chip suppliers. However, the horizontal stress increases more at the backfill surface than at the base. For Pine State Recycling the value at the top of the stress distribution was 6.4 times greater at the 35.9 kPa (750 psf) than at no surcharge, while the value at the bottom was 0.8 times greater. Similarly, for Palmer Shredding, the top value of the stress distribution increased 7.4 times while increasing 0.7 times at the bottom for the same increase in surcharge. For F & B Enterprises the stress at the top was 5.5 times greater, with the bottom value being 0.6 times greater.

The at-rest horizontal stress during the unload/reload cycles for Pine State Recycling shows that for the first and second reloads to 35.9 kPa (750 psf) the horizontal stresses are 1% and 3% greater than during the initial loading with 35.9 kPa (750 psf). Conversely, the horizontal stress decreases 4% and 6% for the first and second reload cycles for Palmer Shredding. Similar to Palmer Shredding, the horizontal stress decreased 2% and 10% during reloading for F & B Enterprises. Thus, the horizontal stress does not appear to increase with repeated reloading. Time-dependent change in the at-rest horizontal stress was measured for Palmer Shredding for the period from 12/28/94 to 6/13/95. From 12/28/94 to 1/18/95 the horizontal stress increased 13%. From 1/18/95

to 6/13/95 no substantial increase in horizontal stress was measured. It appears that tire chips may experience time-dependent increases in horizontal stress that stabilized over some period of time.

The active earth pressures for Pine State Recycling decreased at each rotation up to the final maximum rotation of 2.2 degrees (0.04H). The decrease in horizontal stress from the at-rest (no rotation) to 2.2 degree rotation was 73%. This behavior is similar for the tire chips from the other two suppliers for smaller rotations, with a decrease in horizontal stress for Palmer Shredding of 70% for 1.7 degrees (0.03H) rotation and 41% for F & B Enterprises with a rotation of 0.6 degrees (0.01H). After the initial rotations, it was found that the stress increased over a period of one hour to several days. The horizontal stress increased 21% one hour after the initial rotation to 2.2 degrees for Pine State Recycling. After the initial rotation to 1.7 degrees for Palmer Shredding the horizontal stress increased 59% two days later. While, for F & B Enterprises and a rotation of 0.6 degrees, the horizontal stress 11 days after the initial rotation was 30% greater. These increases in horizontal stress over time may have been due to creep.

The coefficients of lateral earth pressure (K_o, K_a) were determined using a vertical stress calculated from laboratory compression tests by Humphrey, et al. (1992), who measured the compressibility and percent increase in density versus vertical stress for tire chips from the same suppliers used in this study. K_o for the intermediate and maximum surcharges is shown in Table 10.1.

Table 10.1 Coefficient of lateral earth pressure at rest, K_o, 23.9 kPa (500 psf) and 35.9 kPa (750 psf) surcharges

23.9 kPa surcharge			
Depth (m)	**Pine State Recycling**	**Palmer Shredding**	**F & B Enterprises**
0.0	0.46	0.51	0.44
2.0	0.32	0.27	0.32
4.0	0.26	0.17	0.26
35.9 kPa surcharge			
0.0	0.47	0.51	0.45
2.0	0.32	0.33	0.32
4.0	0.25	0.24	0.25

This shows that K_o decreases with depth for the 23.9 kPa (500 psf) and 35.9 kPa (750 psf) surcharges and the three tire chip suppliers, similar decreases were observed for no surcharge and 12.0 kPa (250 psf). Table 10.1 shows that for both surcharges at each depth the values fall within a small range for the three suppliers. This is seen for the 35.9 kPa (750 psf) surcharge, where at the fill surface K_o is slightly greater for Palmer Shredding and lowest for Pine State Recycling. At 2.0 m (6.6 ft), Palmer Shredding is again largest, with Pine State Recycling and F & B Enterprises smaller. At the 4.0-m (13.1-ft) depth, Pine State Recycling and F & B Enterprises are greater, and Palmer Shredding lowest. Similar small ranges and variations in the relative value of K_o existed for no surcharge and 12.0 kPa (250 psf).

The coefficient of active earth pressure, K_a, was determined for the three tire chip suppliers at three depths for the rotation of approximately 0.01H. The values determined for K_a fall within a very small range, from 0.22 to 0.25. At greater rotations K_a decreased. For Palmer Shredding at a rotation of approximately 0.03H, K_a ranged from 0.16 to 0.18, while for a rotation of approximately 0.04H for Pine State Recycling, K_a ranged from 0.08 to 0.12

Semiempirical designed parameters were developed for tire chips to determine the horizontal stress. The method followed that presented in Terzaghi, et al. (1996) for soils. The parameters are k_h and C. For the at-rest case with no surcharge, k_h ranged from 0.25 to 0.27 Mg/m^3 (15.6 to 16.9 pcf) for the three suppliers. A similar small range was observed for the other surcharges. k_h, for the at-rest condition, decreased with increasing surcharge, approaching 0 at the 35.9 kPa (750 psf) surcharge. For the intermediate wall rotation of 0.01H, k_h ranged from 0.17 to 0.19 Mg/m^3 (10.6 to 11.9 pcf) for the three suppliers, at larger rotations k_h ranged from 0.13 to 0.15 Mg/m^3 (8.1 to 9.4 pcf). For the at-rest case and the surcharges from 12.0 kPa (250 psf) to 35.9 kPa (750 psf), C ranged from 0.43 to 0.53 for the three suppliers. C ranged from 0.22 to 0.25 for the intermediate wall rotation of 0.01H, at larger rotations C ranged from 0.07 to 0.18.

The at-rest and active horizontal stresses from the three tire chip suppliers are approximately 45% to 35% less than that expected from granular fill. This is due, at least in part, to the density of tire chips being approximately 1/3 to 1/2 that of conventional granular backfill.

The interface friction between the tire chips and the concrete faced front wall was computed using results from the horizontal and vertical load cells. The angle of wall friction during filling/initial loading of the facility was found to be 31° for Pine State Recycling, 32° for Palmer Shredding, and 30° for F & B Enterprises.

The settlement characteristics of the tire chips was measured using the settlement plates and settlement grid. The measured settlement was compared to laboratory compression tests by Humphrey, et al. (1992). The change in vertical strain measured from the 3.25-m (10.7-ft) and 1.63-m (5.3-ft) settlement plates and that determined from laboratory compressibility tests by Humphrey, et al. (1992), for an increase in surcharge from 6.0 kPa (125 psf) to 35.9 kPa (750 psf) is shown in Table 10.2.

Table 10.2 Measured strain comparison, for 3.25-m (10.7-ft) and 1.63-m (5.3-ft) settlement plates (change in surcharge from 6.0 kPa (125 psf) to 35.9 kPa (750 psf))

Supplier	**Δ vertical strain (%)**			
	3.25-m plate	lab*	1.63-m plate	lab*
Pine State Recycling	3.8	6.1	3.4	4.7
Palmer Shredding	5.2	7.3	2.7	6.2
F & B Enterprises	3.9	5.3	3.7	5.0

*Humphrey, et al. (1992)

This shows that the laboratory compression tests predicted settlement was 26% to 57% greater than measured from both settlement plates. The major reason for the

difference is felt to be interface friction between the tire chips and the concrete faced front wall in the zone near the wall. In the zone near the front wall the friction force is as much as 54% of the weight of the tire chips. However, the settlement predicted from laboratory data was only 10% to 13% greater than settlement measured from the settlement grid. This smaller difference is reasonable since the grid points are distributed over the surface of the fill, so the influence of wall friction would be less than for the settlement plates, which are located 1.14 m (3.7 ft) from the front wall.

As much as 7% strain can occur at the tire chip surface during surcharge placement, with an additional 3% occurring due to time-dependent settlement. Time-dependent movement of the tire chips occurred at a decreasing rate for the first 50 days after placement of the maximum surcharge. After 50 days the rate of settlement was very small. The majority of the time-dependent settlement was completed within the first 50 days.

The horizontal movement within the fill was measured with inclinometers at two offsets from the face of the wall. No movement was measured within the granular backfill. Thus, movement must have occurred in the zone between the front wall and the closest inclinometer casing, 1.14 m (3.7 ft) from the wall face. At approximately 0.01H of wall rotation, the casing located 1.14 m (3.7 ft) from the wall face showed that the movement at the top of the fill for F & B Enterprises was about 70% greater than for Pine State Recycling and Palmer Shredding. One possible explanation for the greater amount of movement experienced by F & B Enterprises is that the have fewer steel belts and are smaller in size.

The approximate location of the active wedge was determined from the settlement profile of the fill surface and the horizontal movement within the fill. The active wedge for the granular fill was oriented 81° with respect to the horizontal. The size of the active wedge is considerably smaller than expected from Rankine Theory. This may have been caused by apparent cohesion. The approximate location of the active wedge was found for Pine State Recycling and Palmer Shredding. The plane of movement for Pine State Recycling was oriented 61° with respect to the horizontal, while for Palmer Shredding it was oriented at 70°. No active wedge was found for F & B Enterprises since the movement was insufficient to develop a distinct failure plane.

The presence of apparent cohesion in the granular soil would temporarily increase the shear strength of the soil, resulting in a lower than expected horizontal stress. An analysis of the active wedge for the granular fill without apparent cohesion using Coulomb's Method showed an active earth force of 100.8 kN (22.7 kips), over the 1.47-m (4.82-ft) width of the center panel. However, the measured active earth force was 66.5 kN (14.9 kips). This could be predicted using Coulomb's Method with an apparent cohesion of 6.1 kPa (128 psf). Thus, the lower measured active earth force may have been caused by apparent cohesion.

The purpose of this study was to determine design criteria for using tire chips as lightweight retaining wall backfill, this included parameters for horizontal stress, interface shear, and settlement. The recommended design values are summarized below in Table 10.3. These design parameters only apply to retaining walls approximately 4.5 meters (15 feet) in height and with surcharges of 35.9 kPa (750 psf) or less. The backfill

Table 10.3 Recommended design values

Horizontal Stress			
coefficient of lateral earth pressure			
at-rest conditions (K_o)	Surcharge (kPa)	backfill surface	backfill base
	0	0.95*	0.29
	12.0	0.55	0.27
	23.9 to 35.9	0.47	0.24
active conditions (K_a)	35.9	0.25	0.25
semiempirical design parameters			
at-rest conditions	Surcharge (kPa)	k_h (Mg/m^3)	C
	0	0.26	N/A
	12.0	0.14	0.50
	23.9	0.09	0.50
	35.9	0.00	0.50
active conditions	35.9	0.19	0.25
Interface Shear			
angle of wall friction (δ)		30°	
Settlement			
during construction		7%	
post construction		3%	
time required for most of post construction settlement to occur		60 days	

*Determined at a depth of 0.5 m (1.6 ft)

material must be tire chip fill with the properties similar to those used here. For details relevant to the use of the parameters refer to each respective chapter.

10.2 CONCLUSIONS

Several conclusions can be drawn from this research:

1. Using tire chips as backfill for retaining walls is a feasible and beneficial use for scrap tires. Their low unit weight makes them suitable for use as lightweight backfill. Tire chips produce a smaller vertical stress than conventional backfill, resulting in less settlement of compressible foundation soils. Moreover, the horizontal stress acting on the wall would be less, resulting in a more economical retaining wall design.

2. The at-rest and active stresses produced by the granular backfill were much less than expected based on classical earth pressure theory. It is felt that apparent cohesion in the partially saturated granular fill was a major factor contributing to the difference.

3. For up to two unloading/reloading cycles the at-rest horizontal stress for tire chips does not appear to change.

4. The at-rest horizontal stress may increase up to 60 days after the application of surcharge. Time-dependent increase in the active horizontal stress also occurs. It is theorized that creep of the tire chip fills is a contributing factor for time-dependent increases in horizontal stress.

5. The rotation needed to reach the active earth pressure for the tire chips is greater than 2.2 degrees (0.04H), the maximum rotation used in this study.

6. The at-rest and active horizontal stresses from the three tire chip suppliers are approximately 45% to 35% less than that expected from granular fill.

7. The coefficient of lateral earth pressure at-rest, K_o, decreases with depth and falls within a small range. At the maximum surcharge and the 2-m (6.5-ft) depth, K_o ranges from 0.32 to 0.33. K_o is not dependent on the amount of steel belts or tire chip size.

8. The coefficient of active earth pressure, K_a, is constant with depth and falls within a small range. At the rotation of 0.01H, K_a ranges from 0.22 to 0.25. K_a is not depended on the amount of steel belts or tire chip size.

9. The angle of wall friction between concrete and tire chips ranges from 30° to 32°.

10. Settlement of tire chips in the zone near the front wall appears to be greatly reduced by interface friction, which transfers some of the applied load from the tire chips to the wall.

11. Time-dependent settlement of tire chips occurs for 50 to 60 days after placement of an overlying surcharge. Therefore, on projects where tire chips are used, aspects that can be influenced by settlement, such as paving, should be delayed until at least 60 days after the application of surcharge.

12. When the wall is rotated outward, F & B Enterprises experiences more horizontal movement within the backfill than Pine State Recycling and Palmer Shredding. This could be due to the lesser quantity of steel belts and the smaller size of the F & B Enterprises chips.

10.3 RECOMMENDATIONS FOR FUTURE RESEARCH

1. A field trial should be performed where tire chips are used as backfill on an actual project. The results could then be used to validate the results obtained from this project.

2. Direct shear tests should be performed between tire chips and concrete to quantify the effect of concrete roughness on interface shear strength. The scope of the testing should include different orientations of the tire chips, with and without the cut edges of the chips bearing against the concrete.

3. The test facility should be used to test different thicknesses of tire chips used as a compressible layer between a retaining wall and granular soil used as backfill. The tire chip layer would provided drainage and insulation. In addition, the tire chip layer would allow active conditions to occur in the granular backfill.

4. Additional finite element modeling should be performed using different foundation materials and retaining wall types to better understand the interaction between the tire chip backfill, retaining wall, and foundation.

BIBLIOGRAPHY

AASHTO (1990), Standard Specifications for Transportation Materials and Methods of Sampling and Testing, Part II: Tests, 15th ed., American Association of State Highway and Transportation Officials, Washington, DC., 877 pp.

Ad Hoc Civil Engineering Committee (1997), "Interim Design Guidelines to Minimize Internal Heating of Tire Shred Fills," Scrap Tire Management Counsel, Washington D.C., 4 pp.

Ahmed, I., (1993), "Laboratory Study on Properties of Rubber Soils," Report No. FHWA/IN/JHRP-93/4, Purdue University, West Lafayette, IN.

Associated Press (1996), "A Big Pile of Tires Is a Huge Problem in a Small State," 21 Sept. 1996, p. 2.

Benda, C.C. (1995), "Engineering Properties of Scrap Tires Used in Geotechnical Applications," Report 95-1, Materials and Research Division, Vermont Agency of Transportation, Montpelier, VT.

Bressette, T. (1984), "Used Tire Material as an Alternative Permeable Aggregate," Report No. FHWA/CA/TL-84/07, Office of Transportation Laboratory, California Department of Transportation, Sacramento, CA.

Bowles, J.E. (1988), Foundation Analysis and Design, 4th ed., McGraw-Hill, New York, 1004 pp.

Cecich, V., Gonzales, L., Hoisaeter, A., Williams, J., and Krishna, K.R. (1994), "Use of Shredded Tires as a Lightweight Backfill Material for Retaining Structures," Report No. CE-GEE-94-02, University of Illinois at Chicago, Chicago, Illinois.

Cecich, V., Gonzales, L., Hoisaeter, A., Williams, J., and Reddy, K. (1996), "Use of Shredded Tires As Lightweight Backfill Material for Retaining Structures," Waste Management & Research, No. 14, pp. 433-451.

Chen, L.H. (1996), "Laboratory Measurement of Thermal Conductivity of Tire Chips," M.S. Thesis, Department of Civil and Environmental Engineering, University of Maine, Orono, Maine, 191 pp.

Cosgrove, T.A. (1995), "Interface Strength Between Tire Chips and Geomembrane for Use as a Drainage Layer in a Landfill Cover," Geosynthetics'95, Industrial Fabrics Association, St. Paul, Minnesota, Vol. 3, pp. 1157-1168.

Downs, L.A. (1996), "Water Quality Effects of Using Tire Chips Below the Ground Water Table," M.S. Thesis, Department of Civil and Environmental Engineering, University of Maine, Orono, Maine, 324 pp.

Eldin, N.N., and Senouce, A.B. (1992), "Use of Scrap Tires in Road Construction," Journal of Construction Engineering and Management, ASCE, Vol. 118, No. 3, Sept. 1992, pp. 561-576.

Federal Highway Administration (1988), CANDE-89, "Culvert ANalysis and DEsign computer program. User Manual," Musser, S.C., ed., June.

Frascoia, R.I., and Cauley, R.F. (1995), "Tire Chips in the Base Coarse of a Local Road," Proceedings of the Sixth International Conference on Low-Volume Roads, Vol. 2, Transportation Research Board, National Academy Press, Washington D.C., pp. 47-52.

Gharegrat, H. (1993), "Finite Element Analyses of Pavements Underlain by a Tire Chip Layer and of Retaining Walls with Tire Chip Backfill," M.S. Thesis, Department of Civil Engineering, University of Maine, Orono, Maine, 222 pages.

Harr, M.E. (1966), Foundations of Theoretical Soil Mechanics, McGraw-Hill, New York, 381 pp.

Humphrey, D.N. (1996), "Tire Chips -- A New Road-Building Geomaterial," TR News, No. 184, May-June, pp. 17.

Humphrey, D.N. (1996), "Investigation of Exothermic Reaction in Tire Shred Fill Located on SR 100 in Ilwaco, Washington," Report to the Federal Highway Administration, Washington, D.C., 44 pp. + appendices.

Humphrey, D.N., Chen, L.-H., and Eaton, R.A. (1997), "Laboratory and Field Measurement of the Thermal Conductivity of Tire Chips for use as Subgrade Insulation," Transportation Research Board, Washington, D.C., 14 pp.

Humphrey, D.N., and Eaton, R.A. (1993a), "Tire Chips as Insulation Beneath Gravel Surfaced Roads," Proceedings of the International Symposium on Frost in Geotechnical Engineering, Anchorage, Alaska, A.A. Balkema Publishers, Rotterdam, Netherlands, pp. 137-149.

Humphrey, D.N., and Eaton, R.A. (1993b), "Tire Chips as Subgrade Insulation - Field Trial," Proceedings of the Symposium on Recovery and Effective Reuse of Discarded Materials and By-Products for Construction of Highway Facilities, Federal Highway Administration, Denver, Colorado, pp. 5-55 to 5-68.

Humphrey, D.N., and Eaton, R.A. (1994), "Performance of Tire Chips as an Insulating Layer Beneath Gravel Surface Roads," Proceedings of the Fourth International Symposium on Cold Region Development, Espoo, Finland, pp. 125-126.

Humphrey, D.N., and Eaton, R.A. (1995), "Field Performance of Tire Chips as Subgrade Insulation for Rural Roads," Proceedings of the Sixth International Conference on Low-Volume Roads, Transportation Research Board, Washington, D.C., Vol. 2, pp. 77-86.

Humphrey, D.N., Katz, L.E., and Blumenthal, M. (1997), "Water Quality Effects of Tire Chip Fills Placed Above the Groundwater Table," Testing Soil Mixed with Waste or Recycled Materials, ASTM STP 1275, Mark A. Wasemiller and Keith B. Hoddinott, Eds., American Society for Testing and Materials, 12 pp. (in press)

Humphrey, D.N. and Manion, W.P. (1992), "Properties of Tire Chips for Lightweight Fill," Proceedings of the Conference on Grouting, Soil Improvement, and Geosynthetics, ASCE, New Orleans, Louisiana, Vol. 2, pp. 1344-1355.

Humphrey, D.N., and Nickels, W.L., Jr. (1994), "Tire Chips as Subgrade Insulation and Lightweight Fill," Proceedings of the 18th Annual Meeting of the Asphalt Recycling and Reclaiming Association, Asphalt Recycling and Reclaiming Association, Annapolis, Maryland, pp. 83-105.

Humphrey, D.N., and Nickels, W.L., Jr. (1997), "Effect of Tire Chips as Lightweight Fill on Pavement Performance," Proceedings of the Fourteenth International Conference on Soil Mechanics and Foundation Engineering, 4 pp. (in printing)

Humphrey, D.N., and Sandford, T.C. (1993), "Tire Chips as Lightweight Subgrade Fill and Retaining Wall Backfill," Proceedings of the Symposium on Recovery and Effective Reuse of Discarded Materials and By-Products for Construction of Highway Facilities, Federal Highway Administration, Denver, Colorado, pp. 5-87 to 5-99.

Humphrey, D.N., Sandford, T.C., Cribbs, M.M., Gharegrat, H.G., and Manion, W.P. (1992), "Tire Chips as Lightweight Backfill for Retaining Walls - Phase I," A Study for the New England Transportation Consortium, Department of Civil Engineering, University of Maine, Orono, Maine, 137 pp. + appendices.

Humphrey, D.N., Sandford, T.C., Cribbs, M.M., and Manion, W.P. (1993), "Shear Strength and Compressibility of Tire Chips for Use as Retaining Wall Backfill," Transportation Research Record No. 1422, Transportation Research Board, Washington, D.C., pp. 29-35.

Ingold, T.S. (1979), Retaining Wall Performance During Backfilling, Journal of the Geotechnical Engineering Division, ASCE, Vol. 105, GT5.

Jaky, J. (1948), "Pressure in Silos," Proceedings of the Second International Conference on Soil Mechanics and Foundation Engineering," Rotterdam, Vol. 1, pp. 103-107.

Lutenegger, A.J., and Adams, M. (1996), "Discussion by Alan J. Lutenegger and Michael Adams. (response to Bohdan Zadroga, Journal of Geotechnical Engineering, Vol. 120, November 1994)", Journal of Geotechnical Engineering, February 1996, Vol. 122, No. 2, pp. 168-170.

Manion, W.P., and Humphrey, D.N. (1992), "Use of Tire Chips as Lightweight and Conventional Embankment Fill, Phase I - Laboratory," Technical Paper 91-1, Technical Services Division, Maine Department of Transportation, Augusta, Maine, 151 pp. + appendices.

Mesri, G. and Hayat, T.M. (1993), "The Coefficient of Earth Pressure At Rest," Canadian Geotechnical Journal, Vol. 30, No. 4, pp. 647-666.

Mitchell, J.M. (1993), Fundamentals of Soil Behavior, 2nd ed., John Wiley & Sons, Inc., New York, 437 pp.

Nickels, W.L., Jr. (1995), "The Effect of Tire Chips As Subgrade Fill on Paved Roads," M.S. Thesis, Department of Civil and Environmental Engineering, University of Maine, Orono, Maine, 215 pp.

Pline, J.L., (1992), Traffic Engineering Handbook, 4th ed., Prentice Hall, Inglewood, NJ, p. 41

Terzaghi, K., Peck, R.B., and Mesri, G. (1996), Soil Mechanics in Engineering Practice, 3rd ed., John Wiley & Sons, Inc., New York, 549 pp.

USA Today, (1996), "Tire Battle Is Wearing on Rhode Island Town," 30 Sept. 1996, p. 23A.

Zimmer, J. (1996), "Scrap Tire Recovery: An Analysis of Alternatives," Texas Scrap Tire Market Development Conference, Texas Natural Resource Conservation Commission, Austin, Texas, pp. 63-87.

(BLANK)

APPENDIX A
INTERIM DESIGN GUIDELINES TO MINIMIZE INTERNAL HEATING OF TIRE SHRED FILLS

(BLANK)

INTERIM DESIGN GUIDELINES TO MINIMIZE INTERNAL HEATING OF TIRE SHRED FILLS (July 1997)

Background

Since 1988 more than 70 tire shred fills with a thickness less than 1 m and an additional ten fills less than 4 m thick have been constructed. In 1995 three tire shred fills with a thickness greater than 8 m experienced a catastrophic internal heating reaction. These unfavorable experiences have curtailed the use of all tire shred fills on highway projects.

Possible causes of the reaction are oxidation of the exposed steel belts and oxidation of the rubber. Microbes may have played a role in both reactions. Although details of the reaction are under study, the following factors are thought to create conditions favorable for oxidation of exposed steel and/or rubber: free access to air; free access to water, retention of heat caused by the high insulating value of tire shreds in combination with a large fill thickness; large amounts of exposed steel belts; smaller tire shred sizes and excessive amounts of granulated rubber particles; and the presence of inorganic and organic nutrients that would enhance microbial action.

The design guidelines given in the following sections were developed to minimize the possibility for heating of tire shred fills by minimizing the conditions favorable for this reaction. As more is learned about the causes of the reaction, it may be possible to ease some of the guidelines. In developing these guidelines, the insulating effect caused by increasing fill thickness and the favorable performance of projects with tire shred fills less than 4 m thick were considered. Thus, design guidelines are less stringent for projects with thinner tire shred layers. The guidelines are divided into two classes: Class I Fills with tire shred layers less than 1 m thick and Class II Fills with tire shred layers in the range of 1 m to 3 m thick. Although there have been no projects with less than 4 m of tire shred fill that have experienced a catastrophic heating reaction, to be conservative, tire shred layers greater than 3 m thick are not recommended. In addition to the guidelines given below, the designer must choose the maximum tire shred size, thickness of overlying soil cover, etc., to meet the requirements imposed by the engineering performance of the project. The guidelines are for use in designing tire shred monofills. Design of fills that are mixtures or alternating layers of tire shreds and mineral soil that is free from organic matter should be handled on a case by case basis.

General Guidelines for All Tire Shred Fills

All tires shall be shredded such that the largest shred is the lesser of one quarter circle in shape or 0.6 m in length; and at least one sidewall shall be severed from the tire shred.

The tire shreds shall be free of all contaminants such as oil, grease, gasoline, diesel fuel, etc., that could create a fire hazard. In no case shall the tire shreds contain the remains of tires that have been subjected to a fire because the heat of a fire may liberate liquid petroleum products from the tire that could create a fire hazard when the shreds are placed in a fill.

Class I Fills

Material guidelines. The tire shreds shall have a maximum of 50% (by weight) passing the 38-mm sieve and a maximum of 5% (by weight) passing the 4.75-mm sieve.

Design guidelines. No design features are required to minimize heating of Class I Fills.

Class II Fills

Material guidelines. The tire shreds shall have a maximum of 25% (by weight) passing the 38-mm sieve and a maximum of 1% (by weight) passing the 4.75-mm sieve. The tire shreds shall be free from fragments of wood, wood chips, and other fibrous organic matter. The tire shreds shall have less than 1% (by weight) of metal fragments which are not at least partially encased in rubber. Metal fragments that are partially encased in rubber shall protrude no more than 25 mm from the cut edge of the tire shred on 75% of the pieces and no more than 50 mm on 100% of the pieces.

Design guidelines. The tire shred fill shall be constructed in such a way that infiltration of water and air is minimized. Moreover, there shall be no direct contact between tire shreds and soil containing organic matter, such as topsoil. One possible way to accomplish this is to cover the top and sides of the fill with a 0.5-m thick layer of compacted mineral soil with a minimum of 30% fines. The mineral soil should be free from organic matter and should be separated from the tire shreds with a geotextile. The top of the mineral soil layer should be sloped so that water will drain away from the tire shred fill. Additional fill may be placed on top of the mineral soil layer as needed to meet the overall design of the project. If the project will be paved, it is recommended that the pavement extent to the shoulder of the embankment or that other measures be taken to minimize infiltration at the edge of the pavement.

Use of drainage features located at the bottom of the fill that could provide free access to air should be avoided. This includes, but is not limited to, open graded drainage layers daylighting on the side of the fill and drainage holes in walls. Under some conditions, it

may be possible to use a well graded granular soil as a drainage layer. The thickness of the drainage layer at the point where it daylights on the side of the fill should be minimized. For tire shreds fills placed against walls, it is recommended that the drainage holes in the wall be covered with well graded granular soil. The granular soil should be separated from the tire shreds with geotextile.

GENERAL GUIDELINES FOR ALL TIRE SHRED FILLS (July 1997)	
• All tires shall be shredded such that the largest shred is the lessor of one quarter circle in shape or 0.6 m in length; and at least one sidewall shall be severed from the tire shred	
• Tire shreds shall be free of contaminants such as oil, grease, gasoline, diesel fuel, etc., that could create a fire hazard	
• In no case shall the tire shreds contain the remains of tires that have been subjected to a fire	
CLASS I FILLS (<1 m thick)	CLASS II FILLS (1-3 m thick)
• Maximum of 50% (by weight) passing 38-mm sieve	• Maximum of 25% (by weight) passing 38-mm sieve
• Maximum of 5% (by weight) passing 4.75-mm sieve	• Maximum of 1% (by weight) passing 4.75-mm sieve
	• Tire shreds shall be free from fragments of wood, wood chips, and other fibrous organic matter
	• The tire shreds shall have less than 1% (by weight) of metal fragments that are not at least partially encased in rubber
	• Metal fragments that are partially encased in rubber shall protrude no more than 25 mm from the cut edge of the tire shred on 75% of the pieces and no more than 50 mm on 100% of the pieces
	• Infiltration of water into the tire shred fill shall be minimized
	• Infiltration of air into the tire shred fill shall be minimized
	• No direct contact between tire shreds and soil containing organic matter, such as topsoil
	• Tire chips should be separated from the surrounding soil with geotextile
	• Use of drainage features located at the bottom of the fill that could provide free access to air should be avoided

These guidelines were prepared by the Ad Hoc Civil Engineering Committee, a partnership of government and industry dealing with reuse of scrap tires for civil engineering purposes. The committee members are:

Michael Blumenthal, Executive Director, Scrap Tire Management Council
Mark Hope, Senior Vice President, Waste Recovery, Inc.
Dana Humphrey, Ph.D., Professor of Civil Engineering, University of Maine
James Powell, Federal Highway Administration
John Serumgard, Chairman, Scrap Tire Management Council
Mary Sikora, Scrap Tire Program Director, International Tire and Rubber Association
Robert Snyder, Ph.D., President, Tire Technology, Inc.
Joseph Zelibor, Ph.D., Former Science Director, Scrap Tire Management Council & Vice President, Partners in Research, Inc.

The committee can be contacted by calling the Scrap Tire Management Council at (202) 682-4880.

(BLANK)

APPENDIX B
LOAD CELL CALIBRATION

(BLANK)

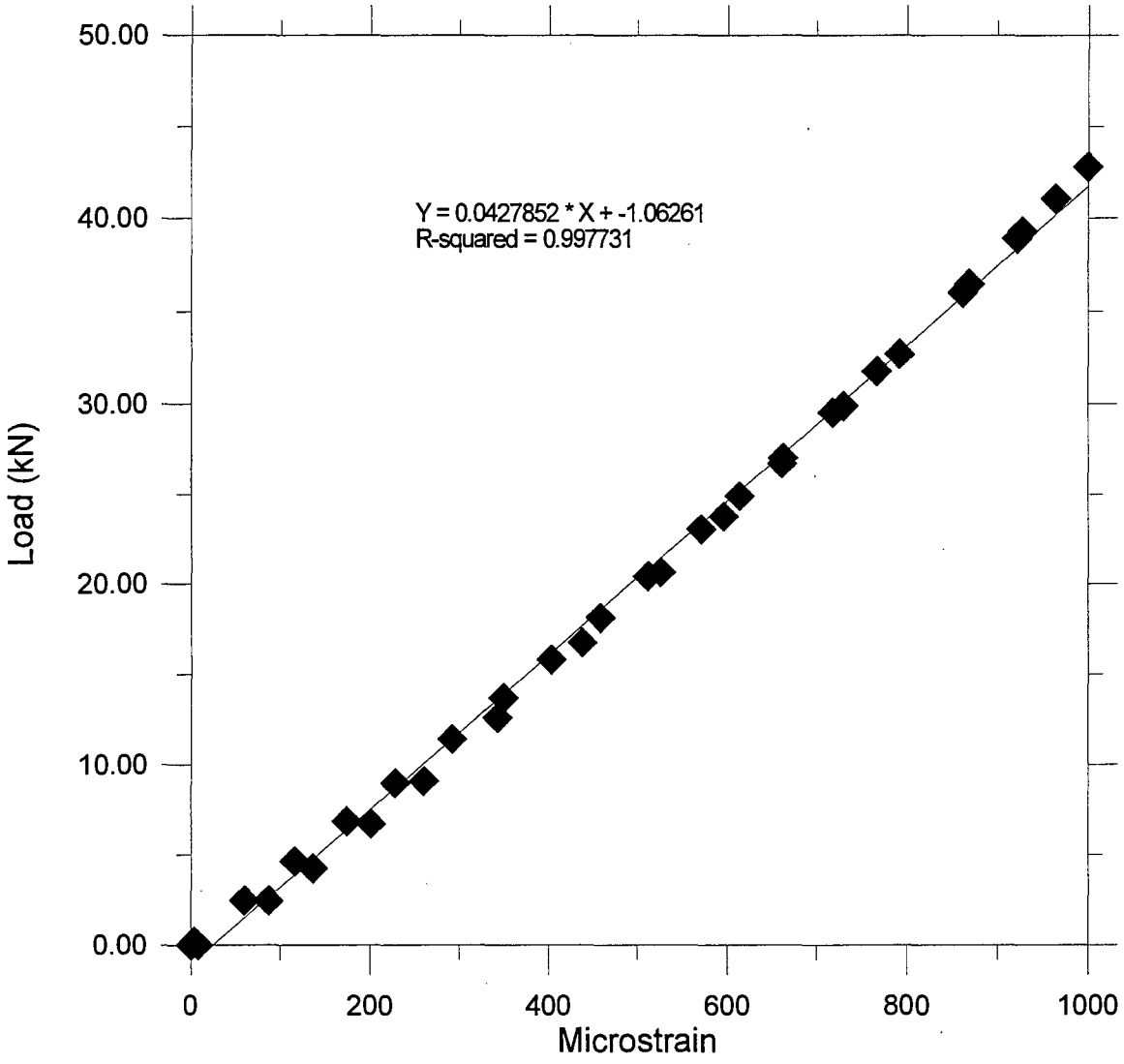

load cell #9301
calibration check #1 (after received)

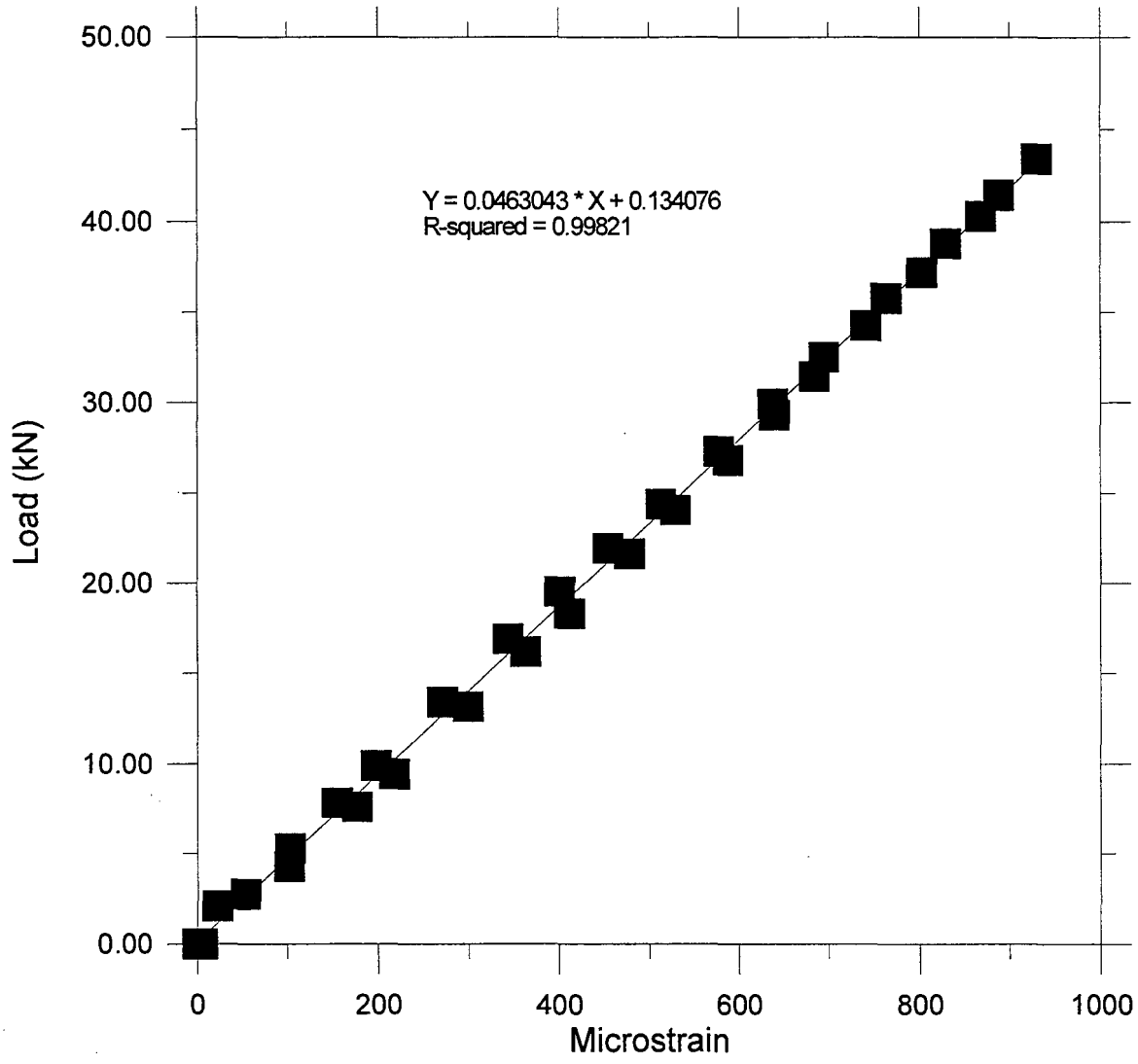

load cell #9302
calibration check #1 (after received)

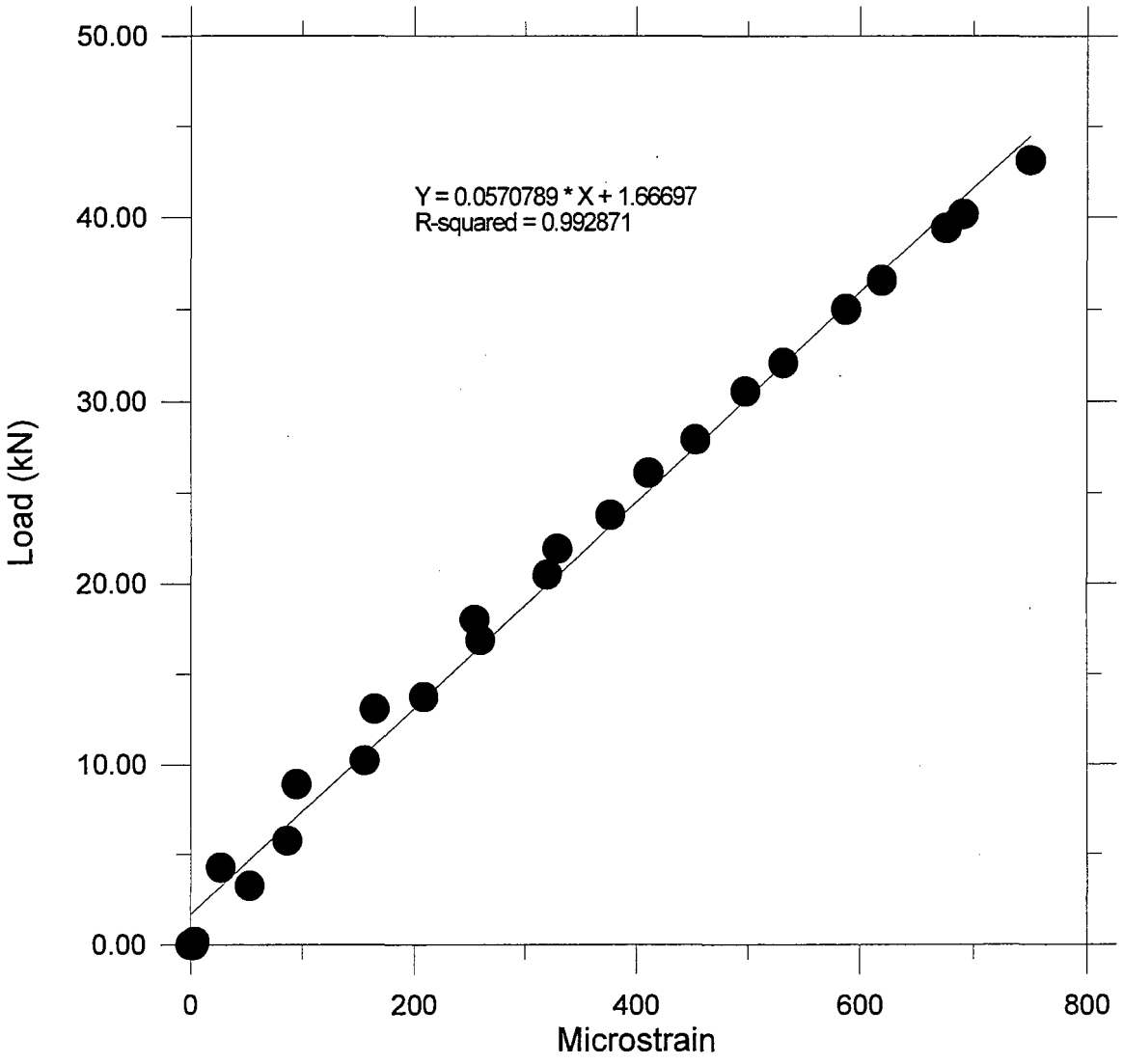

load cell #9303
calibration check #1 (after received)

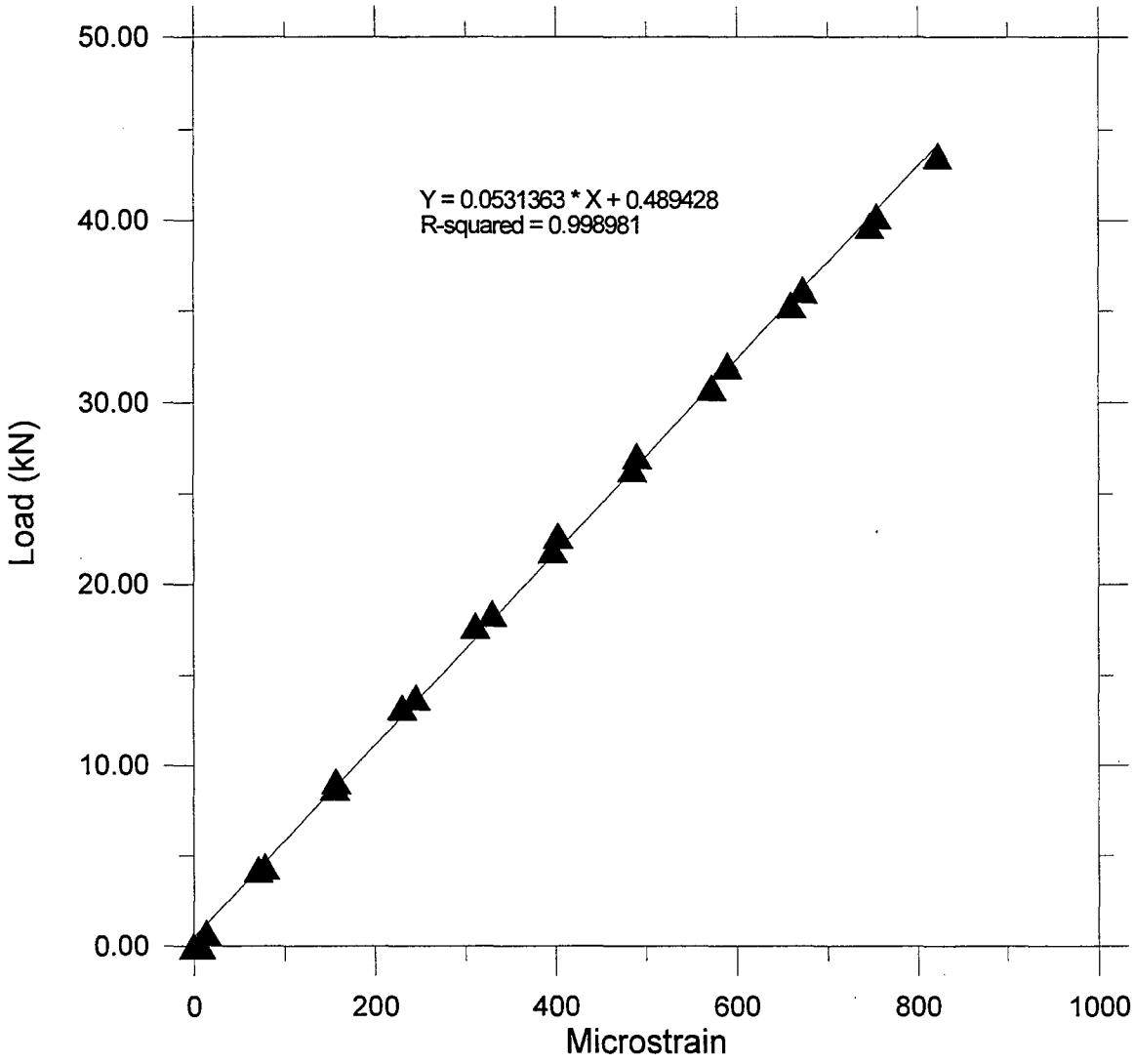

load cell #9304
calibration check #1 (after received)

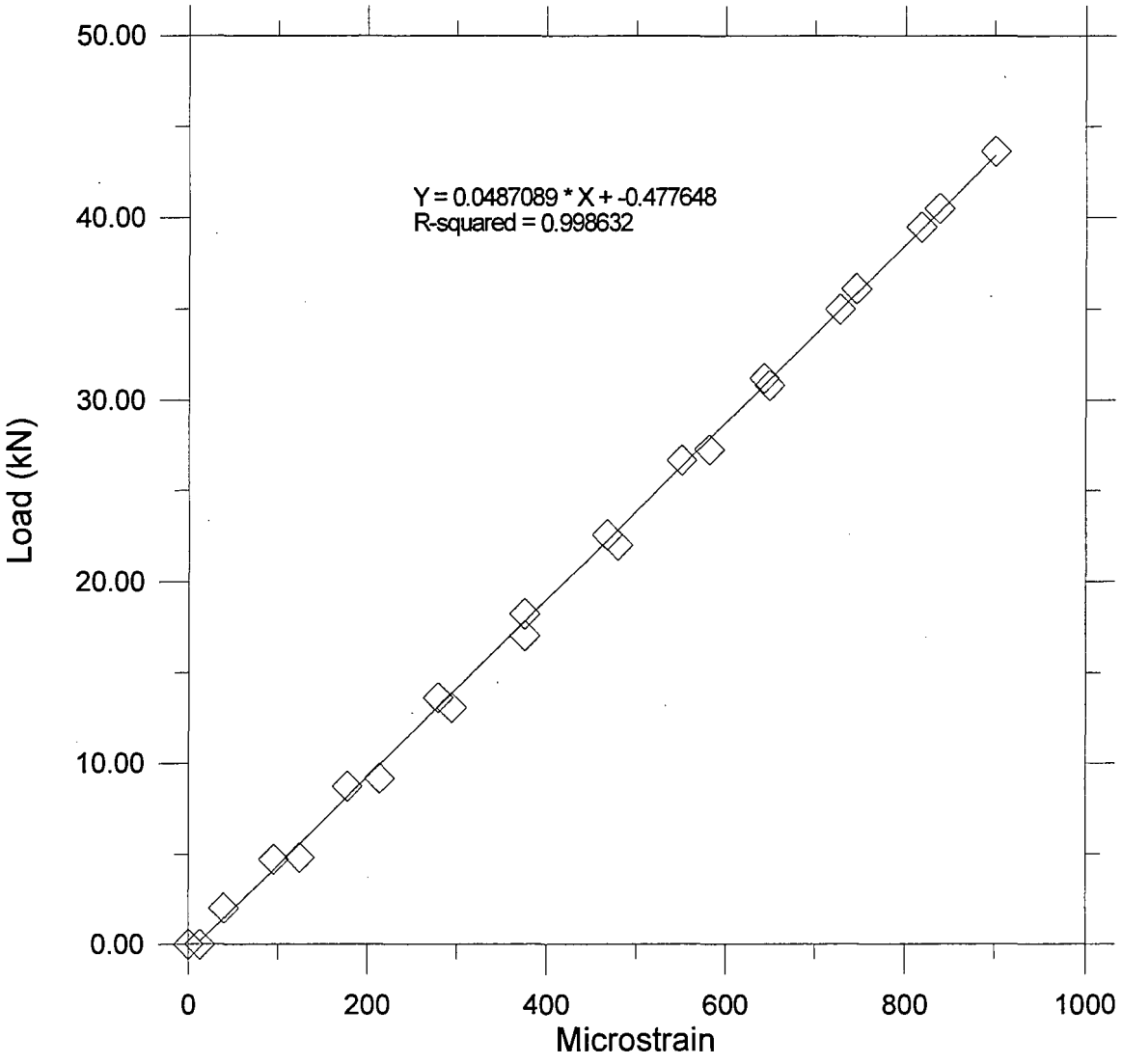

load cell #9305
calibration check #1 (after received)

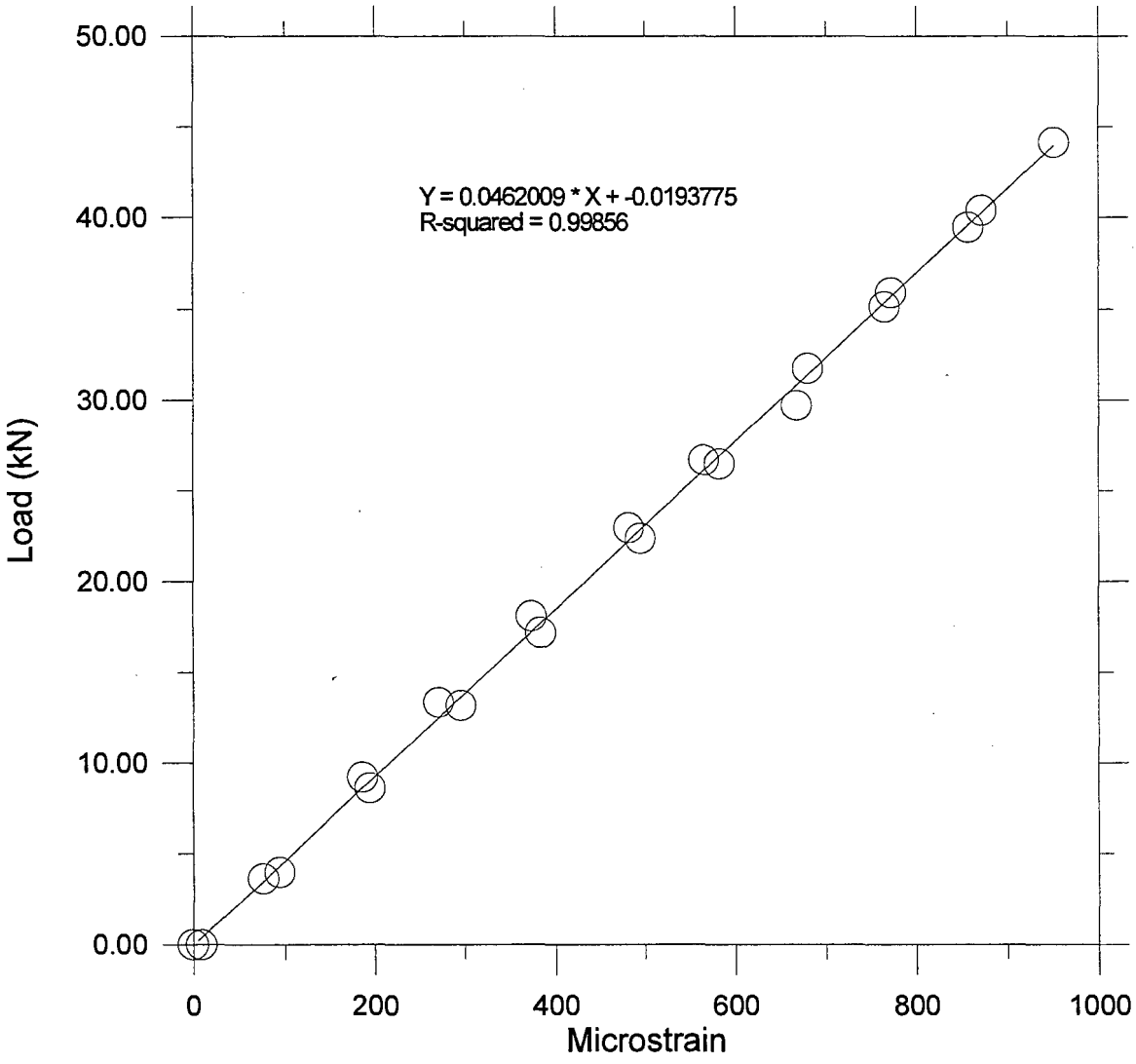

load cell #9306
calibration check #1 (after received)

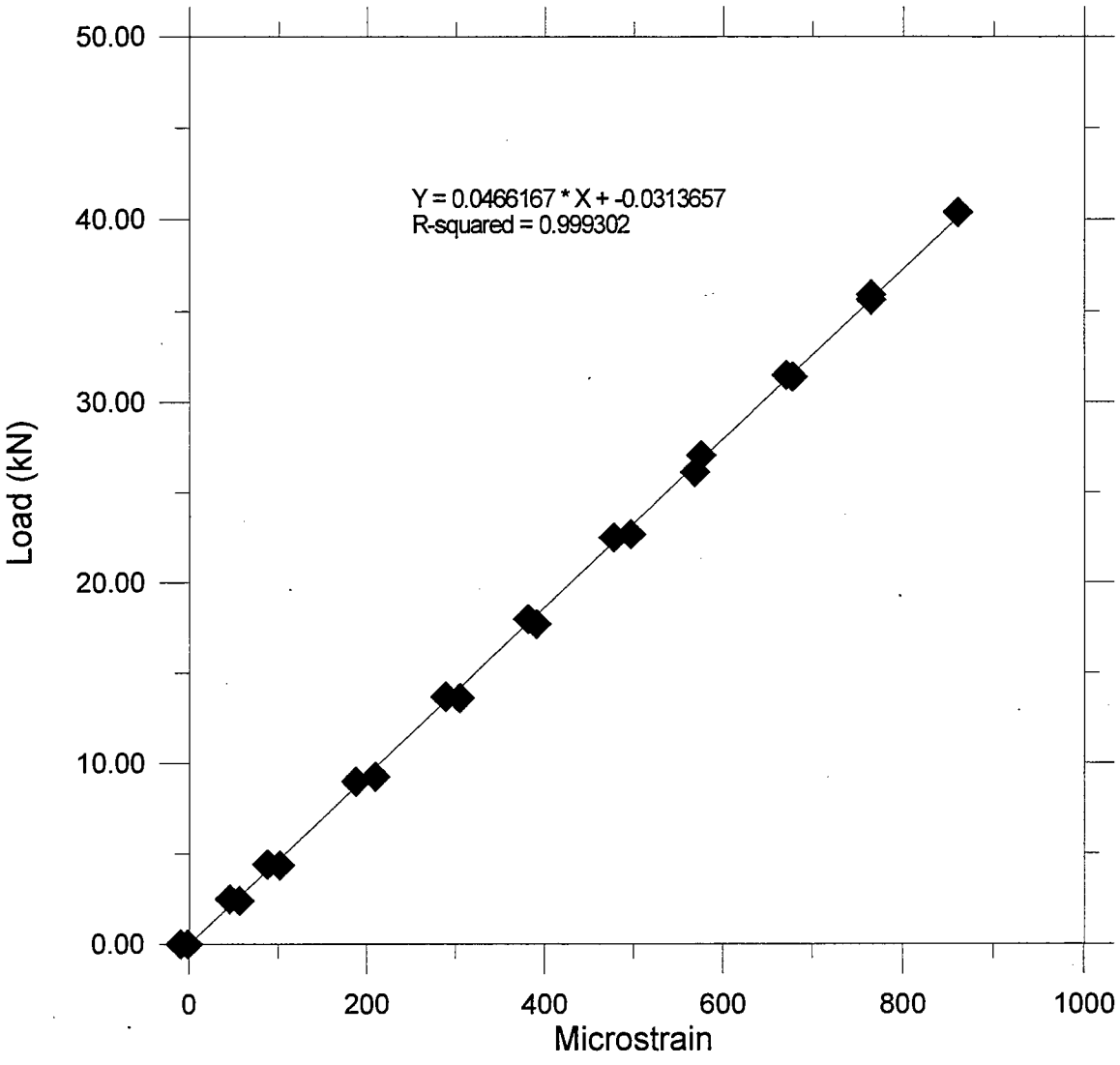

load cell #9301
calibration check #2 (after Palmer Shredding)

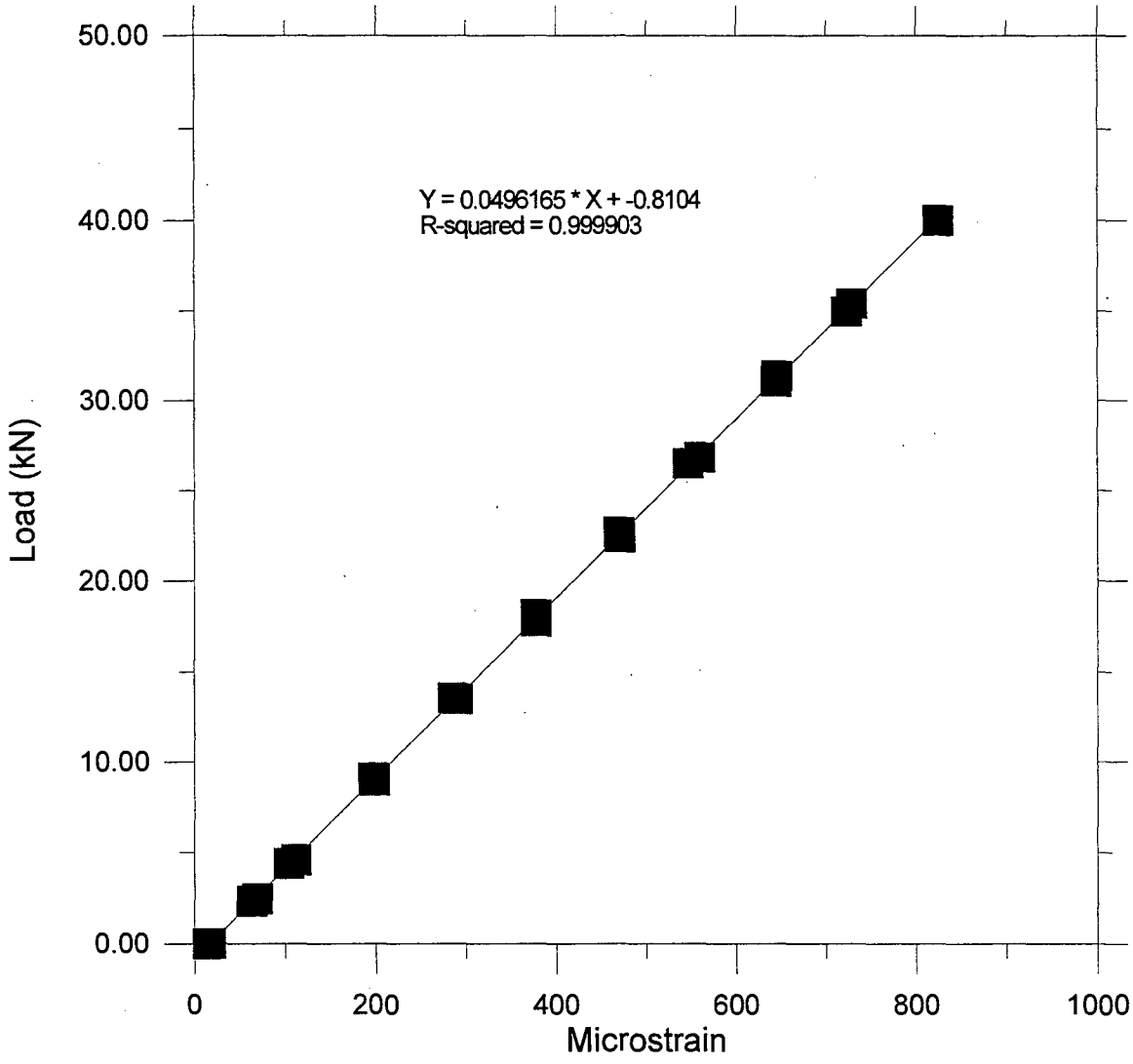

load cell #9302
calibration check #2 (after Palmer Shredding)

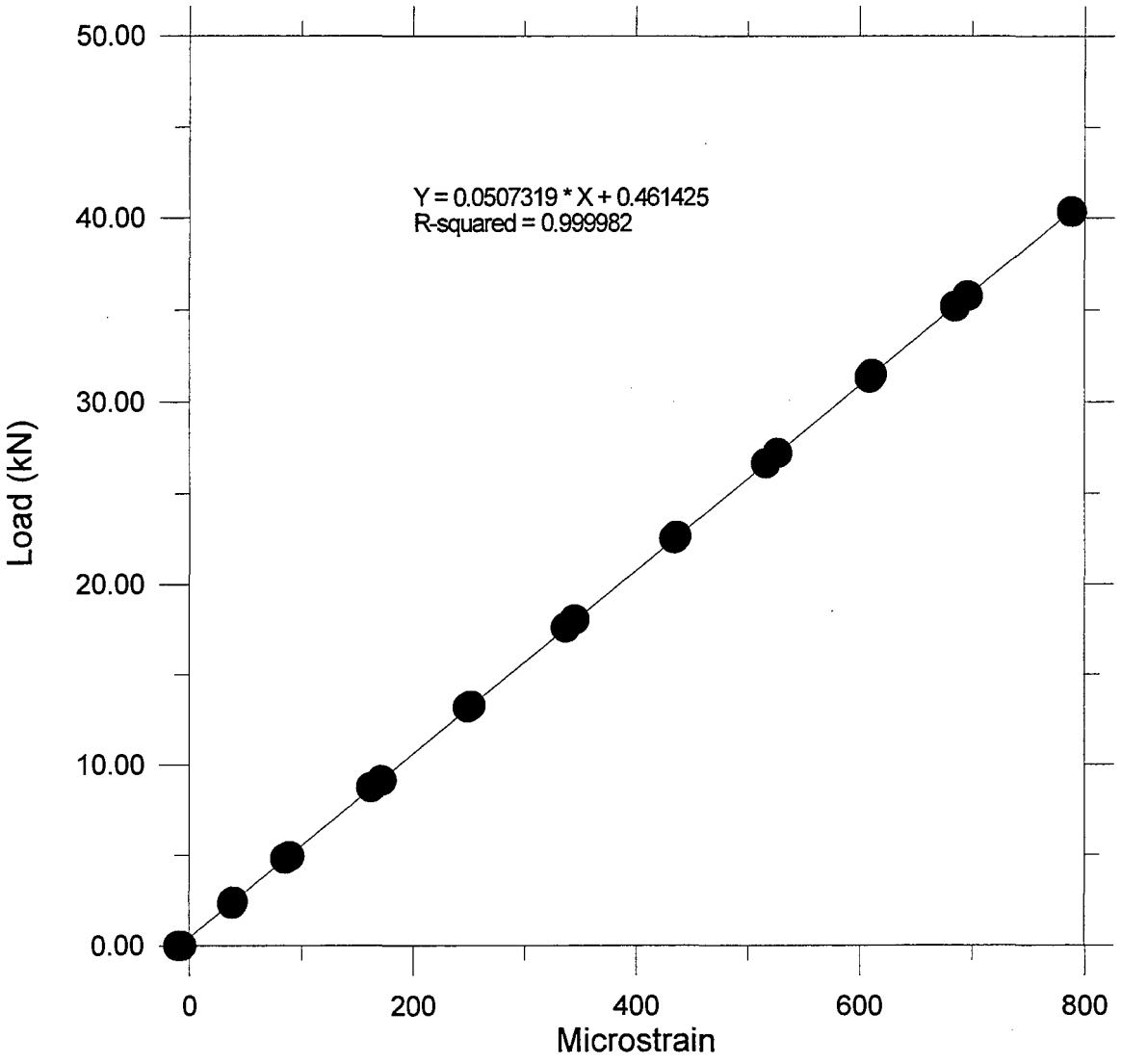

load cell #9303
calibration check #2 (after Palmer Shredding)

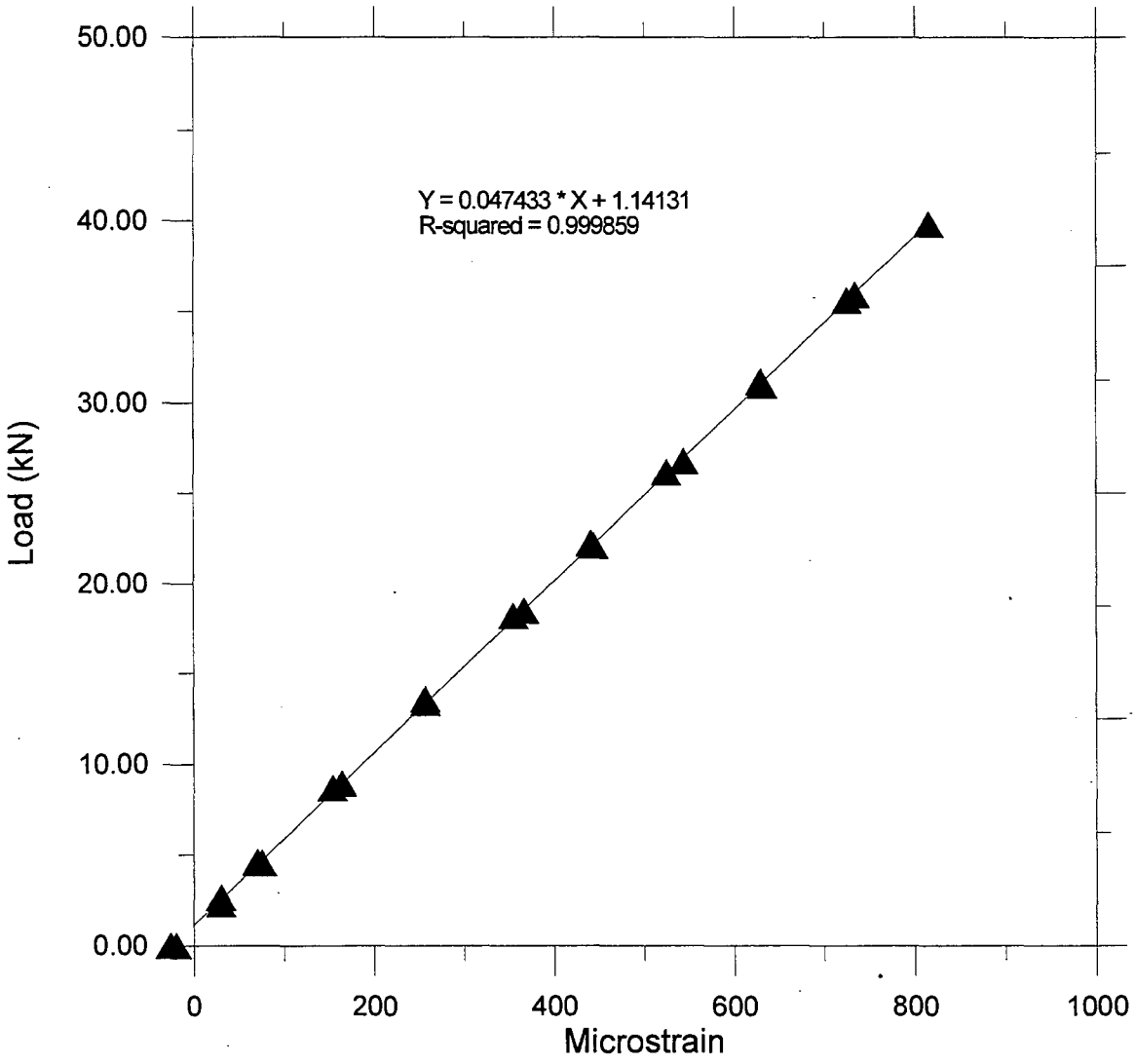

load cell #9304
calibration check #2 (after Palmer Shredding)

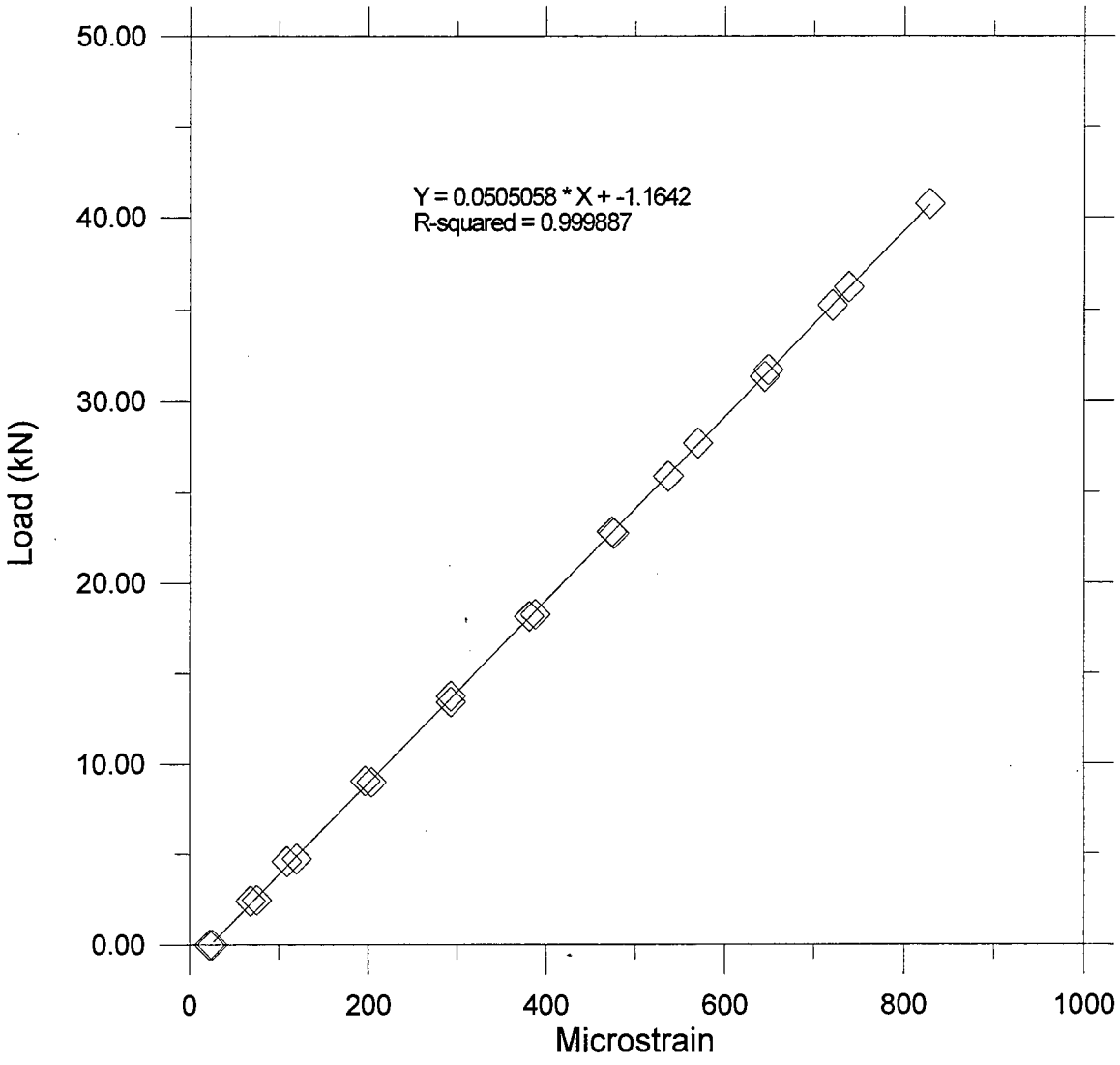

load cell #9305
calibration check #2 (after Palmer Shredding)

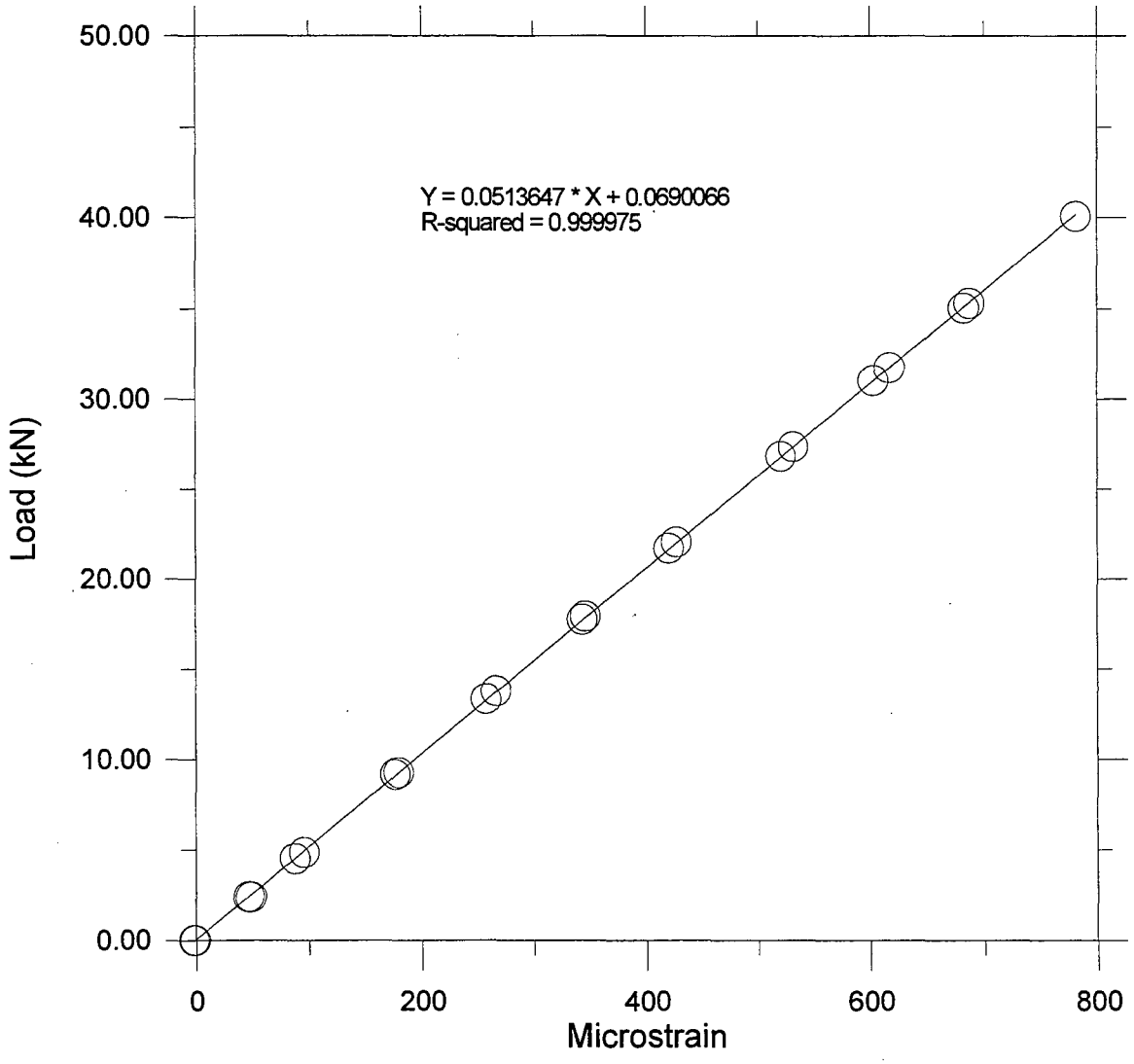

load cell #9306
calibration check #2 (after Palmer Shredding)

Summary of Load Cell Calibration Factors (CF_{lc})

load cell	CF_{lc} (kN/Microstrain)	
	calibration check #1	calibration check #2
9301	0.0428	0.0466
9302	0.0463	0.0496
9303	0.0571	0.0507
9304	0.0531	0.0474
9305	0.0487	0.0505
9306	0.0462	0.0514

(BLANK)

APPENDIX C
PRESSURE CELL CALIBRATION

(BLANK)

Summary of Pressure Cell Calibration Factors (CF_{pc})

pressure cell	CF_{ps} (kPa/L)*	
	230 mm cylinder	**1.52 m by 1.52 m box**
3026	0.2455	0.3220
3223	0.3323	0.4902
3226	0.2696	0.4364
3232	0.2889	0.8219

*CF_{ps} determined from two methods, one using a 230-mm (9-in.) diameter, 80-mm (3-in.) deep cylinder with no top or bottom. The other using a 1.52-m (5.0-ft) by 1.52-m (5.0-ft) by 0.5-m (1.6-ft) deep box with no top or bottom.

Summary of Pressure Cell Temperature Correction Factors (T_k)

pressure cell	L/°C*	CF_{ps} (kPa/L)**	
		230 mm cylinder	1.52 m by 1.52 m box
		T_k (kPa/°C)***	
3026	trial 1	-0.0602	-0.0790
	trial 2	-0.1659	-0.2177
3223	trial 1	-0.2754	-0.4063
	trial 2	-0.5687	-0.8388
3226	trial 1	-0.2814	-0.4556
	trial 2	-0.0967	-0.1565
3232	trial 1	-0.1782	-0.5068
	trial 2	-0.0614	-0.1746

*L/°C determined from two trials using a 230-mm (9-in.) diameter, 80-mm (3-in.) deep cylinder with no top or bottom

**CF_{ps} determined from two methods, one using a 230-mm (9-in.) diameter, 80-mm (3-in.) deep cylinder with no top or bottom. The other using a 1.52-m (5.0-ft) by 1.52-m (5.0-ft) by 0.5-m (1.6-ft) deep box with no top or bottom.

***T_k is product of L/°C and CF_{ps}